Australian Telecommunications Research Institute

Iterative Algorithms for Envelope-Constrained Filter Design

Chien Hsun Tseng

This thesis is presented as part of the requirements
for the award of the degree of Doctor of Philosophy
of the
Curtin University of Technology

November 1999

I hereby declare that this submission is my own work and that, to the best of my knowledge and belief, it contains no material previously published or written by another person nor material which to a substantial extent has been accepted for the award of any degree or diploma of a university or other institute of higher learning, except where due acknowledgement is made in the text.

.....

Chien Hsun Tseng

Australian Telecommunications Research Institute

November 1999

Contents

Acknowledgements

I am truly indebted to my thesis supervisor Professor Kok Lay Teo for all his help, advice, and constant source of inspiration and encouragement throughout the entire course of this research. I have benefited greatly from working with him.

I am grateful to my co-supervisor Professor Antonio Cantoni for his advice, stimulating discussions, and critical and invaluable comments and suggestions.

I would also like to thank Dr. Z. Zang and Dr. Y. H. Leung for their help, advice, and interesting discussions.

Also, I wish to thank the staff and all my friends in ATRI for their friendship, and encouragement.

I am grateful to my family for their unfailing love, constant support, and strong confidence in me.

This work was supported by the Cooperative Research Centre for Broadband Telecommunications and Networking for which I gratefully acknowledge.

List of Symbols

$\mathbf{A}, \ldots, \mathbf{Z}$	matrices
$\mathbf{a}, \ldots, \mathbf{z}$	vectors
$\mathbf{A}', \mathbf{A}^{-1}$	matrix transpose and matrix inverse
$a_{i,j}, a_i$	matrix element and vector element
$diag(\mathbf{A})$	diagonal of matrix $\mathbf{A}$
$diag(a_1, a_2 \ldots)$	diagonal matrix constructed from scalars $a_1, a_2 \ldots$
$\nabla_{\mathbf{x}}, \nabla^2_{\mathbf{x}}$	first, second derivative with respect to $\mathbf{x}$
$\Re, \Re_+$	set of real numbers (resp. real positive numbers including 0)
$\Re^n$	real n-space
$L^2([a,b])$	Hilbert space of functions consisting of all real-valued Lebesgue measurable and square integral functions on the interval $[a,b]$
ℓ^2	Hilbert space of functions consisting of all real-valued square summable functions defined on the set $\{1, 2, \ldots\}$
$C(\Omega, \Re)$	Banach space of functions consisting of all continuous functions defined on a compact set $\Omega \subset \Re$ with value on $\Re$ and equipped with the sup-norm
$M(\Omega, \Re)$	Dual space of $C(\Omega, \Re)$ consisting of all finite signed regular Borel measures on Ω with value on $\Re$
$\|\mathbf{x}\|_2$	2-norm
$\rho(\mathbf{A})$	spectral radius of matrix $\mathbf{A}$
$\eta_{max}(\mathbf{A}), \eta_{min}(\mathbf{A})$	eigenvalues of $\mathbf{A}$ with maximum (resp. minimum) modulus
$\max\{S\}, \min\{S\}$	maximum (resp. minimum) value in set S
$\overline{\lim}\ x^k$	limit superior of the sequence $\{x^k\}$
$E[\mathbf{u}\|\mathcal{F}]$	conditional expection of $\mathbf{u}$ given $\mathcal{F}$
$\sigma\{z^1, z^2 \ldots\}$	smallest σ-algebra generated by the random variables $z^1, z^2 \ldots$

Conventions Used in this Thesis

u	linear time-invariant filter impulse response
ψ	noiseless filter output response
ϵ^+, ϵ^-	upper and lower boundaries of pulse shape envelope
s,$\mathbf{S}$	noiseless input signal and the corresponding Sylvester input signal matrix
$\mathbf{n}, \mathbf{N}$	additive random noise and the corresponding matrix of noise sample
$\sigma(\mathbf{x})$	constraint robustness margin with respect to $\mathbf{x}$

List of Figures

Abstract

The design of envelope-constrained (EC) filters is considered for the time-domain synthesis of filters for signal processing problems. The objective is to achieve minimal noise enhancement where the shape of the filter output to a specified input signal is constrained to lie within prescribed upper and lower bounds. Traditionally, problems of this type were treated by using the least-square (LS) approach. However, in many practical signal processing problems, this "soft" least-square approach is unsatisfactory because large narrow excursions from the desired shape occur so that the norm of the filter can be large and the choice of an appropriate weighting function is not obvious. Moreover, the solution can be sensitive to the detailed structure of the desired pulse, and it is usually not obvious how the shape of the desired pulse should be altered in order to improve on the solution. The "hard" EC filter formulation is more relevant than the "soft" LS approach in a variety of signal processing fields such as robust antenna and filter design, communication channel equalization, and pulse compression in radar and sonar. The distinctive feature is the set of inequality constraints on the output waveform: rather than attempting to match a specific desired pulse, we deal with a whole set of allowable outputs and seek an optimal point of that set.

The EC optimal filter design problems involve a convex quadratic cost function and a number of linear inequality constraints. These EC filtering problems are classified into: discrete-time EC filtering problem, continuous-time EC filtering problem, and adaptive discrete-time EC filtering problem.

The discrete-time EC filtering problem is handled using the discrete Lagrangian duality theory in combination with the space transformation function. The optimal solution of the dual problem can be computed by finding the limiting point of an ordinary differential equation given in terms of the gradient flow. Two iterative algorithms utilizing the simple structure of the gradient flow are developed via discretizing the differential equations. Their convergence properties are derived for a deterministic environment. From the primal-dual relationship, the corresponding sequence of approximate solutions to the original discrete-time EC filtering problem is obtained.

The continuous-time EC filtering problem (semi-infinite convex programming problem) is handled using the continuous Lagrangian duality theory and Carathéodory's dimensionality theory. Several important properties are derived and discussed in relation to practical engineering requirements. These include the observation that the continuous-time optimal filter via orthonormal filters has the structure of a matched filter in cascade with another filter. Furthermore, the semi-infinite convex programming problem is converted into an equivalent finite dual

optimization problem, which can be solved by the optimization methods developed. Another issue, which relates to the continuous-time optimal filter design problem, is the design of robust optimal EC filters. The robustness issue arises because the solution of the EC filtering problem lies on the boundary of the feasible region. Thus, any disturbance in the prescribed input signal or errors in the implementation of the optimal filter are likely to result in the output constraints being violated. A detailed formulation and a corresponding design method for improving the robustness of optimal EC filters are given.

Finally, an adaptive algorithm suitable for a stochastic environment is presented. The convergence properties of the algorithm in a stochastic environment are established.

Chapter 1

Introduction

1.1 Introduction and Motivation

This thesis is concerned with the problem of designing a linear time-invariant (LTI) filter with impulse response u to process a given input signal s corrupted by an additive random noise $\mathbf{n}$ such that the noise enhancement is minimized (see Figure 1.1(a)), while the noiseless filter output ψ lies within an output pulse shape envelope (see Figure 1.1(b)).

Problems of this type are often treated by minimizing the mean square difference between the output response and some desired pulse shape known as the least mean square (LMS) approach. In many applications a "soft" least square approach is, however, unsatisfactory due to occurrence of a large narrow excursions from the desired shape. Moreover, the solution can be sensitive to the detailed structure of the desired pulse, and it is usually not obvious how the shape of the desired pulse should be altered in order to improve on the solution. With the envelope-constrained formulation, the performance requirements can be specified by using output envelope constraints. Also, the designer can avoid the difficulty of choosing a particular desired pulse. Thus, the envelope-constrained formulation has a clear advantage over the least mean square approach [12, 21, 35, 42, 60] and can be employed as an effective approach for solving a wide range of practical problems arising in signal processing and communications [1, 36, 39, 46, 70].

1.2 History and Contributions

The first results, which formulated signal processing problems as optimization problems with inequality constraints, appear to be those of McAulay [39, 41]. He considered the design of signals and filters, subject to a finite number of sidelobe inequality constraints.

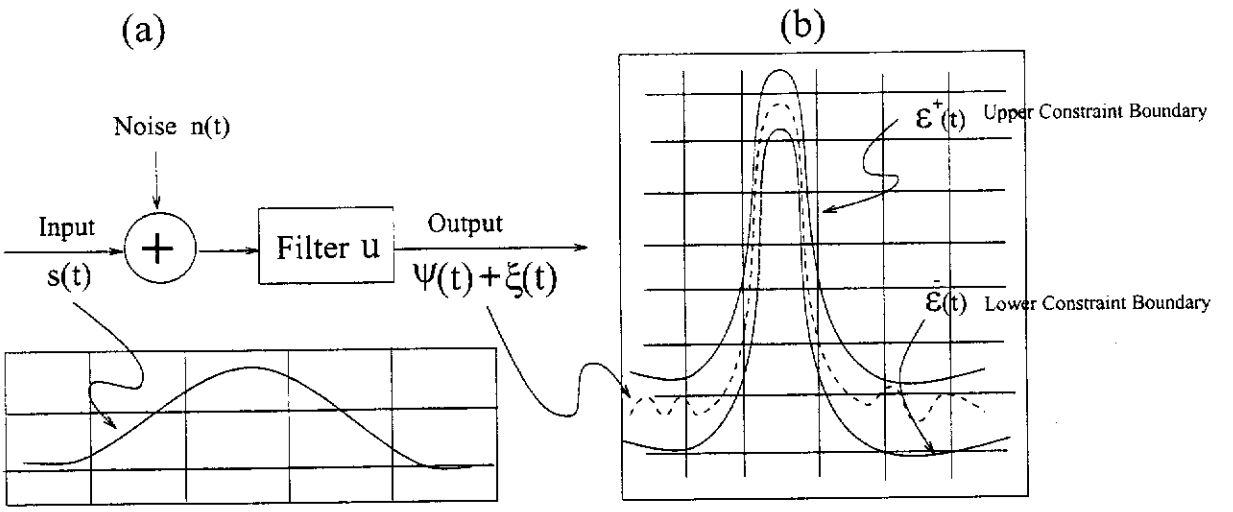

Figure 1.1: Receiver model and output mask.

Around the same time, a similar signal and filter design problem with an infinite number of sidelobe constraints was investigated by Fortmann and Athans [18]. Latter, this approach was applied and extended to time varying sidelobe constraints problem (envelope-constrained problem) by Fortmann and Evans [13, 19]. This continuous-time problem was solved by the primal-dual method, which involves transforming the constrained optimization problem into a non-smooth unconstrained dual problem [12, 13]. A steepest descent type of iterative algorithm, which is referred to as the primal-dual algorithm, was developed to tackle the non-smooth dual problem via discretizing an infinite set of constraints into a finite set of constraints.

In [12], the primal-dual algorithm was also applied to solve the discrete-time version of the envelope-constrained filtering problem with FIR model structure. The convergence properties were discussed for both deterministic and stochastic environments. However, the convergence can be quite slow, and for the case of a fixed step-size, the generated filters converge only to within a neighborhood of the optimal filter in a deterministic environment.

Since the solution of the envelope-constrained filtering problem as introduced lies on the boundary of the feasible region, any disturbance in the prescribed input signal could result in the output constraints being violated. Thus, Evans et.al. [11] addressed this problem by defining a pulse-shape envelope for the input signals. This is known as the envelope-constrained with uncertain input (ECUI) filtering problem. The EC filtering problem is a special case in which the input uncertainty is zero. The work in [72] and [73] addresses questions related to how large the input mask can be or how tight the output mask can be before there is no solution to the ECUI problem for the discrete-time case.

A related continuous-time problem to ECUI for the design of robust EC filters against errors

in the implementation of the optimal filter or any disturbance that appears in the prescribed input signal has been tackled by using the formulation known as the constraint robustness formulation (CRF) [4, 58, 62, 74].

Within this broad and existing framework in the envelope-constrained filtering, this thesis presents a detailed theoretical study of a number of problems and makes the following contributions:

- Two newly developed efficient iterative algorithms, namely the barrier-gradient algorithm and the barrier-Newton algorithm, for numerically solving the EC filtering problems are given and their convergence properties are analyzed in a deterministic environment. These algorithms are obtained by using the Lagrangian duality theory in conjunction with space transformation techniques and then discretization. We show that the sequences of filters generated by these iterative algorithms with a fixed step-size converge globally to the optimal filter.

- Based on the iterative barrier-gradient algorithm, we define an adaptive algorithm for solving the stochastic EC filtering problem in which the input signal is contaminated by additive random noise. The mean and mean square convergence properties in a stochastic environment are established for a fixed step-size. For a sequence of decreasing step-sizes, mean square and with probability one (w.p.1) convergence are also established.

- We show that the dual semi-infinite programming parameterization method associated with the barrier-Newton method can be used to solve the continuous-time EC filtering problem. A significant advantage of this approach is that the original semi-infinite optimization problem can be solved directly as an equivalent finite dimensional minimization problem. In particular, we demonstrate that a small number of active time supporting points can provide enough information to define the optimal solution such that the output response fits into the output mask. In comparison, discrete approximation methods cannot guarantee that the optimal solution obtained satisfies the continuous constraints of the original problem.

- For the continuous-time constraint robustness formulation, a newly developed simple yet efficient algorithm is proposed to solve the problem such that a constraint robustness margin is maximized. In the proposed algorithm, a smoothing technique is introduced to convert the semi-infinite constrained optimization problem into an equivalent constrained optimization problem with integral cost and strictly convex constraint. We show that allowing a larger noise gain can increase the constraint robustness margin. Furthermore,

we characterize the robustness of the optimal filter to perturbations in the input signal and to the implementation error.

These contributions have been published by the author and coauthors in [57]-[64].

1.3 Thesis Outline

Chapter 1 contains an introduction to the envelope-constrained filtering problem as well as a brief literature survey of the area.

In Chapter 2, six representative formulations of the envelope-constrained filtering problem are reviewed.

- The continuous-time envelope-constrained optimal filter design problem.
- The envelope-constrained filtering problem with L^2 orthonormal basis.
- The continuous-time constraint robustness formulation.
- The discrete-time envelope-constrained optimal filter design problem.
- The envelope-constrained filtering problem with ℓ^2 orthonormal basis.
- The discrete-time envelope-constrained filtering problem with uncertain input.

These problems have been chosen to represent a large class of practical problems and at the same time to best demonstrate the mathematical techniques developed in this thesis.

In Chapter 3, a semi-infinite constrained convex optimization technique for studying the continuous-time EC filtering problems is given. Instead of discretizing the continuous-time problem using a sampling rate sufficiently high to capture enough information for approximating the optimal solution, Carathéodory's dimensionality theorem [51] is applied to transform the dual semi-infinite programming problem into an equivalent finite dimensional optimization problem. Thus, one seeks the few crucial time supporting points for which the continuous-time constraints are active. It is shown in [59] that these active points contain enough information to ensure that the continuous-time constraints are met and the optimal solution is found. Therefore, the new approach leads to a computationally tractable method for obtaining the optimal solution meeting the constraints at all times. A practical application of the semi-infinite constrained convex optimization problem in the design of the envelope-constrained filtering problem is given in Chapter 5.

Chapter 4 presents two new iterative methods for solving a convex programming problem, subject to a finite number of linear inequality constraints. Using the dual parameterization in combination with the techniques of the space transformation [15, 16] and the gradient flow [22, 45], the optimal solution of the dual problem can be computed by finding the limiting point of ordinary differential equations (ODE's) given in terms of the gradient flow. It is shown by using the Lyapunov stability theory [14] on ODE that these system of ODE's is asymptotically stable at the equilibrium point (optimal solution point). Two iterative schemes [57, 59, 60] are developed via discretizing the differential equations. From the primal-dual relationship, the corresponding sequence of approximate solutions to the original convex programming problem is obtained. The convergence properties of these two schemes are also established in this chapter.

Chapter 5 deals with algorithms for, respectively, solving the continuous-time EC filtering problem with L^2 orthonormal basis [59] and the robustness of the optimal continuous-time EC filter design problem [58, 62]. Using the results obtained in Chapter 3 and combining them with the barrier-Newton method developed in Chapter 4, two efficient iterative algorithms are constructed for solving the finite dimensional dual optimization problem which is equivalent to the original continuous-time EC filtering problem with L^2 orthonormal basis. As for the robust optimal EC filter design problem (constraint robustness formulation problem), an efficient algorithm is developed to deal with the continuous-time constraint robustness formulation problem. By using a smoothing technique [28, 56], the relationship between the robustness margin and the noise gain for the continuous-time EC filter is established. Furthermore, the tolerance of the continuous-time EC filtering problem to input signal perturbations and implementation errors is examined. Numerical results involving the continuous-time Laguerre networks structure are given for both issues. The Laguerre networks is a special case of the continuous-time EC filtering problem with L^2 orthonormal basis.

In Chapter 6, the simple yet efficient iterative algorithms developed in Chapter 4 are applied to the discrete-time envelope-constrained filtering problem with FIR model structure and with ℓ^2 orthonormal basis. In particular, we present the filter characterization for the optimal filter (in ℓ^2 Hilbert space) of the discrete-time EC filtering problem. Furthermore, a practical application of the discrete-time Laguerre networks is devoted to the EC filtering problem with ℓ^2 orthonormal basis. Simulation results corresponding to these discrete-time EC filter design problems are obtained for several practical examples. These examples involve pulse compression [60] and channel equalization [61].

Chapter 7 is devoted to the study of an adaptive training algorithm based on the proposed iterative barrier-gradient (BG) algorithm in a stochastic environment. The convergence be-

havior is determined in mean and in mean square sense [60, 63, 64] when the step-size of the adaptive algorithm is fixed. Furthermore, the adaptive algorithm converges linearly in mean square sense and with probability one [63, 64] to the optimal filter if a sequence of decreasing step-sizes is used. The structure and convergence properties of the adaptive BG filter are compared with those of the adaptive primal-dual (PD) filter given in [12, 13], and with those of the adaptive least-mean-squares (LMS) filter given in [9, 68, 69]. Numerical results involving pulse compression and channel equalization are given to illustrate the convergence properties.

In Appendices A-D, the proofs of results presented in Chapters 3-7 are given.

Chapter 2

Problem Formulations

2.1 Introduction

The purpose of this chapter is to precisely formulate the six envelope-constrained (EC) filtering problems studied in this thesis. These problems have been chosen to represent a large class of practical problems and at the same time to best demonstrate the mathematical techniques developed in the thesis to solve them.

In Section 2.2, we focus on the continuous-time EC filtering problems, in particular, the continuous-time EC optimal filter design problem [12, 13], the EC filtering problem with L^2 orthonormal basis [59, 66] and the robustness of continuous-time EC optimal filter design problem [4, 58, 62, 74]. We formulate the continuous-time EC filtering problem in Section 2.2.1. In this problem, the output of the filter is required to fit into a prescribed output pulse shape envelope, whereas minimizing the output noise power gain. One of the attractive features of the EC filter is that the output response is guaranteed to satisfy stringent engineering requirements as specified by the envelope constraints [12, 21, 35, 42, 77]. Therefore, it has application to robust antenna, communication channel equalization, and pulse compression in radar and sonar [1, 18, 19, 36, 46, 70].

In Section 2.2.2, we study the continuous-time EC filtering problem with L^2 orthonormal basis. This problem is useful for designing data transmission channel equalizers. The use of an orthonormal basis provides an approach for approximating infinite dimensional system by finite dimensional system [40].

The robustness of continuous-time optimum EC filter design problem is the subject matter investigated in Section 2.2.3.

In Section 2.3, discrete-time EC optimal filter design problems are considered. Specifically, we deal with the discrete-time EC filtering problem using a FIR model structure [12, 60, 65, 75],

the EC filtering problem with ℓ^2 orthonormal basis [61, 76], and the discrete-time EC filtering problem with uncertain input [11, 73]. In Section 2.3.1, we formulate the discrete-time EC filtering problem which is relevant to the design of FIR equalizers for data communications channels. In this case, we assume that the input signal, filter impulse response and filter output are finite length discrete-time sequences. The problem is also considered in a stochastic environment in Chapter 7 to develop an adaptive (on-line) algorithm for solving the discrete-time EC filtering problem.

In Section 2.3.2, EC filtering problem with ℓ^2 orthonormal basis is considered. An orthonormal basis in ℓ^2 Hilbert space is used to represent the filter. Specifically, the discrete-time Laguerre functions [52, 67] forms a special case of a finite subset of an orthonormal basis. It has been shown [76] that the use of the Laguerre functions for filter representation is more robust than that of FIR filters as each of the Laguerre function contains a pole which is an adjustable parameter. In particular, the FIR filters are the special case of the Laguerre filters when the adjustable pole is chosen to be zero.

Finally, the discrete-time EC filtering problem with uncertain input is formulated in Section 2.3.3.

2.2 Continuous EC Filtering Problems

In this section, we consider the problem of finding a filter with a linear time-invariant impulse response $u(t)$ such that for a given input signal $s(t)$, the output waveform $\psi(t)$ fits into a pulse shape envelope described by the lower and upper boundaries $\varepsilon^-(t)$ and $\varepsilon^+(t)$, respectively, (see Figure 1.1). Further, since the input signal $s(t)$ is corrupted by an additive random noise $n(t)$, we define the optimal pulse shaping filter as the filter which minimizes the output noise power while satisfying the pulse shape constraints.

2.2.1 Continuous-Time EC Optimal Filter Design Problem

Let the input signal $s(t), t \in [0, \infty)$ be a continuous function of time (see Figure 1.1(a)). It is available at the receiver corrupted by an additive random noise $n(t)$. The received signal is passed through a linear time-invariant filter $u(t) \in L^2([0, \infty))$ where $L^2([0, \infty))$ denotes the Hilbert space consisting of all real-valued Lebesgue measurable and square integral functions on the semi-infinite interval $[0, \infty)$ with inner product

$$\langle f, g \rangle \triangleq \int_0^\infty f(t)g(t)dt, \text{ for any } f, g \in L^2([0, \infty)).$$

The norm of $f \in L^2([0,\infty))$ is defined by

$$\|f\|_2 = \sqrt{\langle f, f\rangle} = \sqrt{\int_0^\infty |f(t)|^2 dt}.$$

Thus, the filter output is represented as:

$$\psi(t) \;=\; \int_0^\infty u(\tau)s(t-\tau)d\tau, \quad t \in [0,\infty)$$

It was shown in [12] that additive white noise with mean zero and variance σ^2 at the filter input causes a noise component with mean zero and variance $\sigma^2\|u\|_2^2$ at the filter output. Thus, it makes sense to choose the norm square of the filter, $\|u\|_2^2$, as the objective function to be minimized. Furthermore, the noiseless output response $\psi(t)$ is required to fit into an output pulse shape envelope defined by the lower and upper boundaries $\varepsilon^-(t)$ and $\varepsilon^+(t)$, i.e,.

$$\varepsilon^-(t) \le \psi(t) \le \varepsilon^+(t), \quad t \in [0,\infty).$$

By defining the two continuous functions $d(t) \triangleq \frac{\varepsilon^+(t)+\varepsilon^-(t)}{2}$ and $\varepsilon(t) \triangleq \frac{\varepsilon^+(t)-\varepsilon^-(t)}{2}$, the continuous-time EC filtering problem can be cast as the following quadratic programming (QP) optimization problem

$$\begin{array}{ll} \min & f(u) = \|u\|_2^2, \quad u \in L^2([0,\infty)) \\ \text{subject to} & \left|\int_0^\infty u(\tau)s(t-\tau)d\tau - d(t)\right| \le \varepsilon(t), \quad t \in [0,\infty). \end{array} \tag{2.2.1}$$

In [17], it is shown that $\psi(t) \in C([0,\infty))$ when $u(t)$ is square integrable and $s(t)$ is continuous, where $C([0,\infty))$ denotes the Banach space consisting of all continuous functions defined on $[0,\infty)$ and equipped with the sup-norm.

2.2.2 EC Filtering Problem with L^2 Orthonormal Basis

Consider the continuous-time EC filtering problem (2.2.1). Since $u(t) \in L^2([0,\infty))$, it follows that if $\{\varphi_j\}_{j=0}^\infty$ is a complete orthonormal basis of $L^2([0,\infty))$ Hilbert space, then $u(t)$ can be expressed as:

$$u(t) = \sum_{j=0}^\infty x_j\varphi_j(t) \quad \text{and} \quad x_j = \langle u, \varphi_j\rangle, \tag{2.2.2}$$

where $x_j, j = 0, 1, \ldots,$ are the filter coefficients corresponding to the filter $u(t)$ and

$$\langle \varphi_i, \varphi_j\rangle = \int_0^\infty \varphi_i(t)\varphi_j(t)dt = \delta_{i,j} \triangleq \begin{cases} 1 & \text{if } i = j \\ 0 & \text{if } i \ne j. \end{cases}$$

We consider only those filters $u_n(t)$ whose impulse responses are approximated by

$$u_n(t) \;=\; \sum_{j=0}^{n-1} x_j\varphi_j(t), \quad t \in [0,\infty). \tag{2.2.3}$$

Thus, the corresponding filter output $\psi_n(t)$ to the input signal $s(t)$ is expressed as:

$$\psi_n(t) = \int_0^\infty u_n(\tau)s(t-\tau)d\tau = \Theta'(t)\mathbf{x}, \quad t \in [0,\infty) \tag{2.2.4}$$

where the filter coefficient vector $\mathbf{x} \in \Re^n$ and the input signal vector $\Theta(t) \in \Re^n$ are given as follows:

$$\mathbf{x} = [x_0, \ldots, x_{n-1}]', \quad \Theta(t) = [\theta_0(t), \ldots, \theta_{n-1}(t)]' \tag{2.2.5}$$

while

$$\theta_j(t) \;=\; \int_0^\infty \varphi_j(\tau)s(t-\tau)d\tau, \quad j = 0, \ldots, n-1. \tag{2.2.6}$$

From (2.2.3), the norm of the filter u_n can be written as:

$$\begin{aligned} \|u_n\|_2 &= \sqrt{\sum_{i=0}^{n-1}\sum_{j=0}^{n-1} x_i x_j \langle \varphi_i, \varphi_j \rangle} \\ &= \sqrt{\mathbf{x}'\mathbf{x}} = \|\mathbf{x}\|_2. \end{aligned} \tag{2.2.7}$$

From (2.2.3)-(2.2.7), the EC filtering problem with L^2 orthonormal basis is approximated as:

$$\begin{aligned} \min \quad & \|\mathbf{x}\|_2^2 = \mathbf{x}'\mathbf{x}, \quad \mathbf{x} \in \Re^n \\ \text{subject to} \quad & \varepsilon^-(t) \le \Theta'(t)\mathbf{x} \le \varepsilon^+(t), \quad \forall t \in [0,\infty). \end{aligned} \tag{2.2.8}$$

Define

$$\mathbf{A}(t) = \begin{bmatrix} \Theta'(t) \\ -\Theta'(t) \end{bmatrix}_{2\times n}, \quad \mathbf{b}(t) = \begin{bmatrix} \varepsilon^+(t) \\ -\varepsilon^-(t) \end{bmatrix}_{2\times 1} \tag{2.2.9}$$

where $\mathbf{A}(t) \in C([0,\infty), \Re^{2\times n})$ and $\mathbf{b}(t) \in C([0,\infty), \Re^2)$. Here $C([0,\infty), \Re^{2\times n})$ (respectively, $C([0,\infty), \Re^2)$) denotes the Banach space consisting of all continuous functions defined on $[0,\infty)$ with value in $\Re^{2\times n}$ (respectively, $\Re^2$). The norms of these Banach spaces are their respective sup-norms. In most practical situations, the EC filtering problem (2.2.8) is approximated with support in $[0,T]$, and accordingly cast as the following QP problem.

$$\begin{aligned} \min \quad & f(\mathbf{x}) \\ \text{subject to} \quad & \mathbf{g}(\mathbf{x},t) \le 0_2, \quad \forall t \in [0,T] \end{aligned} \tag{2.2.10}$$

where $f(\mathbf{x}) = \|\mathbf{x}\|_2^2$, and for each $\mathbf{x} \in \Re^n$, $\mathbf{g}(\mathbf{x},t) = \mathbf{A}(t)\mathbf{x} - \mathbf{b}(t) \in C([0,T], \Re^2)$.

Clearly, the QP problem (2.2.10) is a convex semi-infinite programming problem where the cost function is strictly convex and the constraints $\mathbf{g}(\cdot,t)$ are linear, and hence convex functions for each $t \in [0,T]$. If there is a feasible solution in the constraint set, the QP problem (2.2.10) admits a unique optimal solution. To avoid the trivial solution $u_n(t) = 0$ (i.e., $\mathbf{x} = 0_n$), we impose the following assumption.

Assumption 2.2.1 *There exists at least one point in the output mask at which the upper and lower mask boundaries have the same sign, i.e, there exists at least one* $t_0 \in [0, T]$ *such that* $\varepsilon^+(t_0)\varepsilon^-(t_0) > 0$.

2.2.3 Continuous-Time Constraint Robustness Formulation

In this subsection, we present a technique [4, 74] for providing a guard band on the output mask of the continuous-time EC filtering problem (2.2.8). For a given filter coefficient vector $\mathbf{x} \in \Re^n$ (which may or may not satisfy the envelope constraints in the EC filtering problem (2.2.8)), let us define, for $t \in [0, \infty)$,

$$\begin{cases} [\phi^+(\mathbf{x})](t) &= \varepsilon^+(t) - \psi_n(\mathbf{x}, t) \\ [\phi^-(\mathbf{x})](t) &= \psi_n(\mathbf{x}, t) - \varepsilon^-(t) \end{cases}$$

where $\psi_n(\mathbf{x}, t) = \Theta'(t)\mathbf{x}$. Clearly, if $\phi^-(\mathbf{x})$ and $\phi^-(\mathbf{x})$ are positive for all $t \in [0, \infty)$, then $\mathbf{x}$ satisfies the continuous-time output constraints in the EC filtering problem (2.2.8). To quantify the notion of robustness, we define the constraint robustness margin as:

$$\sigma(\mathbf{x}) \;=\; \min\left\{\min_t[\phi^+(\mathbf{x})](t), \min_t[\phi^-(\mathbf{x})](t)\right\}.$$

The feasible region of the continuous-time EC filtering problem (2.2.8) can now be expressed in terms of the robustness margin as:

$$\mathcal{F} \;=\; \{\mathbf{x} \in \Re^n : \sigma(\mathbf{x}) \geq 0\}.$$

Note that if $\sigma(\mathbf{x}) > 0$, the minimum distance between the output response $\psi_n(\mathbf{x}, t)$ and the output mask is at least equal to $\sigma(\mathbf{x})$. Specifically, if $\mathbf{x}$ is a feasible solution of the constraints of the EC filtering problem (2.2.8) such that the equality constraints are satisfied at some points in $[0, \infty)$, then $\sigma(\mathbf{x}) = 0$. Therefore, $\sigma(\mathbf{x})$ is called the constraint robustness margin corresponding to $\mathbf{x}$. In practice, it may be necessary to have a larger constraint robustness margin over certain intervals. In this case, a weighting function β can be used to achieve the purpose. More specifically, we define the weighted constraint robustness margin as follows:

$$\sigma_\beta(\mathbf{x}) \;=\; \min\left\{\min_t \frac{[\phi^+(\mathbf{x})](t)}{\beta(t)}, \min_t \frac{[\phi^-(\mathbf{x})](t)}{\beta(t)}\right\} \tag{2.2.11}$$

where β is a positive piece wise continuous weighting function which is normalized so that it attains a minimum of unity. We depict the mask for the weighted constraint robustness margin in Figure 2.1. The EC filtering problem with robustness constraint may now be formulated and

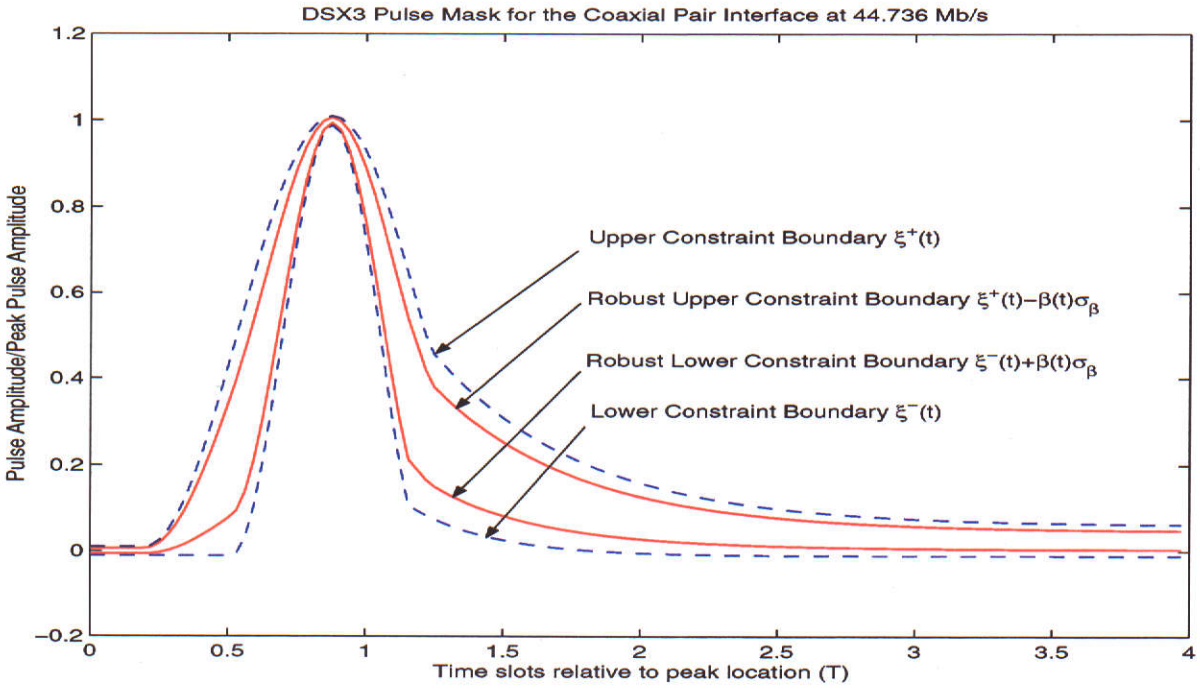

Figure 2.1: The masks of the nonrobust EC filtering and that of the robust weighted EC filtering.

approximated with support in $[0, T]$ as the following constrained optimization problem.

$$\begin{aligned} \max \quad & \sigma_\beta \\ \text{subject to} \quad & \varepsilon^-(t) + \beta(t)\sigma_\beta \le \psi_n(\mathbf{x}, t) \le \varepsilon^+(t) - \beta(t)\sigma_\beta, t \in [0, T] \\ & \|\mathbf{x}\|_2^2 \le (1+\delta)\|\mathbf{x}^*\|_2^2, \sigma_\beta \ge 0, \end{aligned} \tag{2.2.12}$$

where $\mathbf{x}^* \in \Re^n$ is the optimal filter coefficient vector, $\delta > 0$ is a constant specifying the allowable amount of increase of the output noise power.

2.3 Discrete EC Filtering Problems

In this section, we consider the discrete-time version of the EC filtering problems. We first formulate the discrete-time EC filtering problem with FIR model structure in Section 2.3.1. The EC filter design problem with approximate ℓ^2 orthonormal basis and the discrete-time EC filtering problem with uncertain input are described, respectively, in Section 2.3.2 and Section 2.3.3.

2.3.1 Discrete-Time EC Optimal FIR Filter Design Problem

Consider the continuous-time EC filtering problem (2.2.1) with support in $[0, T]$. Then the discrete-time version of the EC filtering problem (2.2.1) consists of breaking the time interval

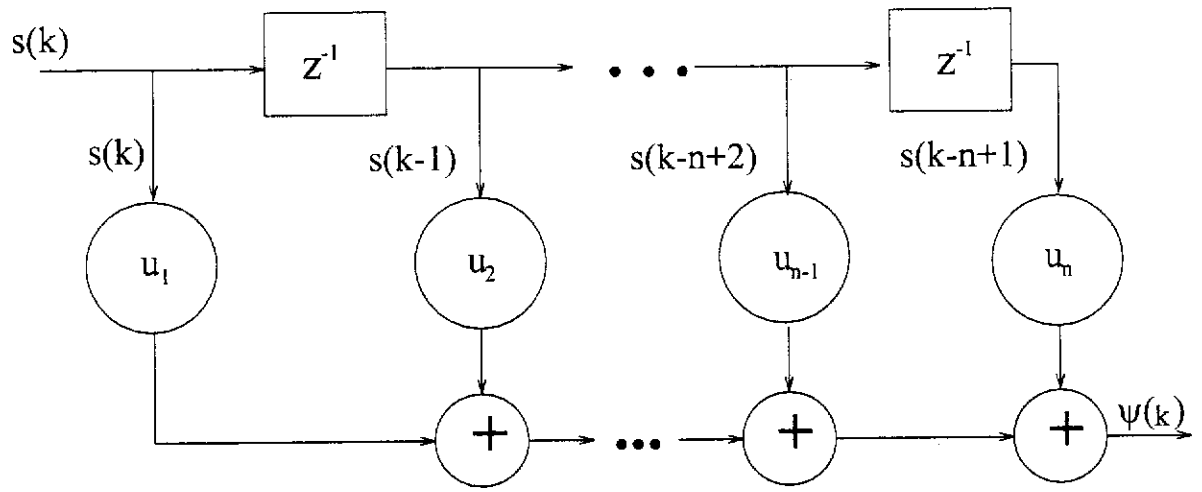

Figure 2.2: Tapped delay line FIR filter

$[0,T]$ into $N = m+n-1$ subintervals, and approximating the input signal $\mathbf{s} \triangleq [s_1,\ldots,s_m]' \in \Re^m$, the filter impulse response $\mathbf{u} \triangleq [u_1,\ldots,u_n]' \in \Re^n$, and the output response $\psi \triangleq [\psi_1,\ldots,\psi_N]' = \mathbf{S}\mathbf{u} \in \Re^N$, where the $N \times n$ Sylvester input signal matrix $\mathbf{S}$ is defined by

$$\mathbf{S} = \begin{bmatrix} s_1 & 0 & \cdots & 0 \\ \vdots & s_1 & \ddots & \vdots \\ s_m & \vdots & \ddots & 0 \\ 0 & s_m & & s_1 \\ \vdots & \ddots & \ddots & \vdots \\ 0 & \cdots & 0 & s_m \end{bmatrix}. \tag{2.3.1}$$

Thus, the discrete-time EC filtering problem is formulated as follows:

$$\begin{aligned} \min \quad & f(\mathbf{u}) = \|\mathbf{u}\|_2^2, \quad \mathbf{u} \in \Re^n \\ \text{subject to} \quad & \mathbf{d} - \varepsilon \le \psi \le \mathbf{d} + \varepsilon \end{aligned} \tag{2.3.2}$$

where the constraint functions $\mathbf{d} \in \Re^N$ and $\varepsilon \in \Re^N$ are, respectively, given by

$$\begin{cases} \mathbf{d} \triangleq [d_1,\ldots,d_N]' = \frac{\varepsilon^+ + \varepsilon^-}{2} \\ \varepsilon \triangleq [\varepsilon_1,\ldots,\varepsilon_N]' = \frac{\varepsilon^+ - \varepsilon^-}{2} \end{cases} \quad \text{with} \quad \begin{cases} \varepsilon^+ \triangleq [\varepsilon_1^+,\ldots,\varepsilon_N^+]' \in \Re^N \\ \varepsilon^- \triangleq [\varepsilon_1^-,\ldots,\varepsilon_N^-]' \in \Re^N. \end{cases} \tag{2.3.3}$$

We note that this problem is important for designing tapped delay line equalizers as shown in Figure 2.2, where z^{-1} is the unit delay operator and n is the order of the filter, for data communication channels and it will be discussed in Section 6.2.

Define

$$\mathbf{A} = \begin{bmatrix} \mathbf{S} \\ -\mathbf{S} \end{bmatrix} \in \Re^{2N \times n}, \quad \mathbf{b} = \begin{bmatrix} \varepsilon^+ \\ -\varepsilon^- \end{bmatrix} \in \Re^{2N}. \tag{2.3.4}$$

The EC filtering problem (2.3.2) is rewritten as the following QP problem:

$$\begin{aligned} \min \quad & f(\mathbf{u}) = \|\mathbf{u}\|_2^2, \quad \mathbf{u} \in \Re^n \\ \text{subject to} \quad & \mathbf{A}\mathbf{u} \leq \mathbf{b}. \end{aligned} \tag{2.3.5}$$

Note that the problem (2.3.5) consists of a strictly convex cost function and a finite number of linear constraints. Clearly, if the set of constraints admits a feasible solution, then the problem (2.3.5) has a unique optimal solution. Thus, similar to Assumption 2.2.1 so as to exclude the trivial solution where the zero output response lies within the prescribed output mask, there must exist at least one $i \in \{1, 2, \ldots, N\}$ such that $\varepsilon_i^+ \varepsilon_i^- > 0$ where ε_i^- and ε_i^- are, respectively, the ith elements of ε^+ and ε^-.

2.3.2 EC Filtering Problem with ℓ^2 Orthonormal Basis

In this subsection, the EC filter design problem with an approximate orthonormal basis is formulated in the Hilbert space ℓ^2. The necessary mathematical background ans notation for norms and inner products are provided for completeness.

Orthonormal basis on ℓ^2

Let ℓ^2 denote the Hilbert space consisting of all real-valued square summable functions defined on the set $\{1, 2, \ldots\}$ with inner product given by

$$\langle f, g \rangle \triangleq \sum_{i=1}^{\infty} f_i g_i, \quad \text{for any } f, g \in \ell^2 \text{ and } f_i, g_i \in \Re.$$

The norm of $f \in \ell^2$ is defined by

$$\|f\|_2 \triangleq \sqrt{\langle f, f \rangle} = \sqrt{\sum_{i=1}^{\infty} |f_i|^2}. \tag{2.3.6}$$

By the completeness of ℓ^2, there exists a complete orthonormal basis $\{\varphi_i\}_{i=0}^{\infty}$ such that any $f \in \ell^2$ can be expressed as:

$$f = \sum_{i=0}^{\infty} x_i \varphi_i \tag{2.3.7}$$

where $x_i = \langle f, \varphi_i \rangle, i = 0, 1, \ldots$, and $\langle \varphi_i, \varphi_j \rangle = \delta_{i,j}$.

Envelope-Constrained Filtering Problem

Let $s(k)$ denote the present value of the input signal, and $s(k-1), s(k-2), \ldots, s(0)$ denote the k past values of the input signal. Let $u(k)$ and $\psi(k)$ represent the present value of the

filter impulse response and that of the corresponding output response, respectively. From the input-output relation of the filter, we may then describe the present values of the filter impulse response $u(k) \in \ell^2$ as follows:

$$u(k) = \sum_{j=0}^{\infty} x_j \varphi_j(k), \quad k = 0, 1, \ldots,$$

where $\{\varphi_j\}_{j=0}^{\infty}$ is a complete orthonormal basis of ℓ^2, and x_j is the filter coefficient given by $x_j = \langle u, \varphi_j \rangle$. The corresponding present value of the output response $\psi(k)$ is thus given by

$$\psi(k) = \sum_{j=0}^{\infty} u(j) s(k-j), \quad k = 0, 1, \ldots$$

Then, the discrete-time EC filtering problem with ℓ^2 orthonormal basis can be posed as follows:

$$\begin{aligned} \min \quad & \|u\|_2^2, \quad u \in \ell^2 \\ \text{subject to} \quad & \varepsilon^-(k) \le \psi(k) \le \varepsilon^+(k), \quad k = 0, 1, \ldots \end{aligned}$$

where $\varepsilon^-(k)$ and $\varepsilon^+(k)$ are, respectively, the present values of the lower and upper boundaries of the output mask. Let us consider only those filters $u_n(k)$ whose impulse responses are approximated by

$$u_n(k) = \sum_{j=0}^{n-1} x_j \varphi_j(k), \quad k = 0, 1, \ldots. \tag{2.3.8}$$

The corresponding present values of the output response to the input signal $s(k)$ are given by

$$\begin{aligned} \psi_n(k) &= \sum_{j=0}^{\infty} u_n(j) s(k-j) \\ &= \sum_{i=0}^{n-1} \theta_i(k) x_i, \quad k = 0, 1, \ldots, \end{aligned} \tag{2.3.9}$$

where

$$\theta_i(k) = \sum_{j=0}^{\infty} \varphi_i(j) s(k-j), \quad i = 0, 1, \ldots, n-1. \tag{2.3.10}$$

By the definition of the norm in ℓ^2 Hilbert space given by (2.3.6), the norm of the filter u_n can be written as:

$$\begin{aligned} \|u_n\|_2 &= \sqrt{\sum_{j=0}^{n-1} \sum_{k=0}^{n-1} x_j x_k \langle \varphi_j, \varphi_k \rangle} \\ &= \sqrt{\mathbf{x}'\mathbf{x}} = \|\mathbf{x}\|_2 \end{aligned} \tag{2.3.11}$$

where $\mathbf{x} = [x_0, x_1, \ldots, x_{n-1}]' \in \Re^n$ is the filter coefficient vector and $\langle \varphi_j, \varphi_k \rangle = \delta_{j,k}$.

From (2.3.8)-(2.3.11), the discrete-time EC filtering problem with ℓ^2 orthonormal basis is approximated as:

$$\begin{aligned} \min \quad & f(\mathbf{x}) = \mathbf{x}'\mathbf{x}, \quad \mathbf{x} \in \Re^n \\ \text{subject to} \quad & \varepsilon^- \leq \psi_n(\mathbf{x}) \leq \varepsilon^+ \end{aligned} \tag{2.3.12}$$

where $\psi_n(\mathbf{x}) \triangleq \mathbf{S}_o\mathbf{x} \in \Re^N$ is the output response vector. The input signal matrix $\mathbf{S}_o \in \Re^{N\times n}$, the lower output mask $\varepsilon^- \in \Re^N$ and the upper output mask $\varepsilon^+ \in \Re^N$ are, respectively, given by

$$\mathbf{S}_o \triangleq \begin{bmatrix} \theta_0(0) & \theta_1(0) & \dots & \theta_{n-1}(0) \\ \theta_0(1) & \theta_1(1) & \dots & \theta_{n-1}(1) \\ \vdots & \vdots & \dots & \vdots \\ \theta_0(N-1) & \theta_1(N-1) & \dots & \theta_{n-1}(N-1) \end{bmatrix} \tag{2.3.13}$$

$$\varepsilon^- \triangleq \begin{bmatrix} \varepsilon^-(0) \\ \varepsilon^-(1) \\ \vdots \\ \varepsilon^-(N-1) \end{bmatrix}, \quad \varepsilon^+ \triangleq \begin{bmatrix} \varepsilon^+(0) \\ \varepsilon^+(1) \\ \vdots \\ \varepsilon^+(N-1) \end{bmatrix}. \tag{2.3.14}$$

Remark 2.3.1 *Combining with (2.3.8) and (2.3.10), the output response vector $\psi_n(\mathbf{x})$ is transformed into $\psi_n(\mathbf{u}_n) \triangleq \mathbf{S}\mathbf{u}_n$ where $\mathbf{u}_n \in \Re^n$ is the filter impulse response vector, $\mathbf{S} \in \Re^{N\times n}$ is a Sylvester input signal matrix given by (2.3.1), and $N = n + m - 1$.*

Let $\mathbf{d} \triangleq \frac{\varepsilon^+ + \varepsilon^-}{2} \in \Re^N$ and $\varepsilon \triangleq \frac{\varepsilon^+ - \varepsilon^-}{2} \in \Re^N$. Then, the set of feasible points for the problem (2.3.12) can be characterized by the following set:

$$\mathcal{X} = \{\mathbf{x} \in \Re^n : \mathbf{d} - \varepsilon \leq \mathbf{S}_o\mathbf{x} \leq \mathbf{d} + \varepsilon\} = \{\mathbf{x} \in \Re^n : \mathbf{A}_o\mathbf{x} \leq \mathbf{b}_o\} \tag{2.3.15}$$

where $\mathbf{A}_o \in \Re^{2N\times n}$ and $\mathbf{b}_o \in \Re^{2N}$ are defined analogously to (2.3.4). By (2.3.15), the EC filtering problem (2.3.12) can now be rewritten as a QP problem:

$$\begin{aligned} \min \quad & f(\mathbf{x}) = \mathbf{x}'\mathbf{x}, \quad \mathbf{x} \in \Re^n \\ \text{subject to} \quad & \mathbf{A}_o\mathbf{x} \leq \mathbf{b}_o. \end{aligned} \tag{2.3.16}$$

Note that the QP problem (2.3.16) has a strictly convex cost function and linear constraints in $\mathbf{x}$. If the constraint set admits a feasible solution, then the problem has a unique optimal solution by assuming that there exists at least one $k \in \{0, 1, \dots, N-1\}$ such that $\varepsilon^+(k)\varepsilon^-(k) > 0$ where $\varepsilon^+(k)$ and $\varepsilon^-(k)$ are, respectively, the kth elements of ε^+ and ε^-.

2.3.3 Discrete-Time EC Filtering Problem with Uncertain Input

In EC filtering problem, the filter is optimized subject to the requirement that the output response to a given input signal lies within a specified envelope or mask. EC filters with uncertain input (ECUI) [11] arises when the EC filtering problem is faced with the robustness requirements. These requirements are real practical issues, as the input signal may not be precisely the ideal shape but is known to be within a specified mask. The optimal solution to the EC filtering problem can be de-sensitized with respect to uncertainty in the prescribed input signal by assuming that the input signal lies within an input envelope described, respectively, by upper and lower boundaries $\mathbf{s}^+ \in \Re^m$ and $\mathbf{s}^- \in \Re^m$. The objective of ECUI is to minimize $\|\mathbf{u}\|_2^2$ under the requirement that every input signal $\mathbf{s} \in \Re^m$ within the input envelope evokes an output response that lies in the output envelope:

$$\begin{aligned} \min \quad & \|\mathbf{u}\|_2^2, \quad \mathbf{u} \in \Re^n \\ \text{subject to} \quad & \psi \in \Psi, \quad \forall \mathbf{s} \in \mathbf{S_s} \end{aligned}$$

where the set of all outputs within the output mask and the set of all inputs within the input mask are given, respectively, by

$$\begin{aligned} \Psi &\triangleq \{\psi \in \Re^N : \mathbf{d} - \varepsilon \le \psi \le \mathbf{d} + \varepsilon\} \\ \mathbf{S_s} &\triangleq \{\mathbf{s} \in \Re^m : \mathbf{c} - \theta \le \mathbf{s} \le \mathbf{c} + \theta\}, \end{aligned}$$

while $\mathbf{d}$ and ε are defined by (2.3.3), and $\mathbf{c} \triangleq \frac{\mathbf{s}^+ + \mathbf{s}^-}{2} \in \Re^m$, $\theta \triangleq \frac{\mathbf{s}^+ - \mathbf{s}^-}{2} \in \Re^m$. Note that $\mathbf{d}$ represents the center of the output mask, whereas ε stands for a scaling vector of the size of the output mask. Similarly, $\mathbf{c}$ represents the center of the input mask, whereas θ stands for a scaling vector of the size of the input mask.

The set of all linear time-invariant FIR filters, which will take any and every signal $\mathbf{s} \in \mathbf{S_s}$ and map it into an element $\psi \in \Psi$ is given by

$$\mathcal{U} = \{\mathbf{u} \in \Re^n : \mathbf{d} - \varepsilon \le \mathbf{S}\mathbf{u} \le \mathbf{d} + \varepsilon, \quad \forall \mathbf{S_s} : \mathbf{C} - \Theta \le \mathbf{S_s} \le \mathbf{C} + \Theta\} \qquad (2.3.17)$$

where the matrices $\mathbf{C} \in \Re^{N \times n}$ and $\Theta \in \Re^{N \times n}$ are defined analogously to $\mathbf{S}$ in terms of $\mathbf{c}$ and θ. Since the set, $\mathcal{U}$, of feasible filters is not suitable for optimization analysis in its present form, it has been shown in [11] that the set (2.3.17) is equivalent to

$$\mathcal{U} = \{\mathbf{u} \in \Re^n : [|\mathbf{C}\mathbf{u} - \mathbf{d}| + \Theta|\mathbf{u}|]_i \le \varepsilon_i, i = 1, 2, \ldots N\} \subseteq \Re^n,$$

and the optimal filter is found by solving

$$\begin{aligned} \min \quad & \|\mathbf{u}\|_2^2 = \mathbf{u}'\mathbf{u}, \quad \mathbf{u} \in \Re^n \\ \text{subject to} \quad & \begin{cases} \mathbf{C}\mathbf{u} - \mathbf{d} + \Theta|\mathbf{u}| \leq \varepsilon \\ -\mathbf{C}\mathbf{u} + \mathbf{d} + \Theta|\mathbf{u}| \leq \varepsilon, \end{cases} \end{aligned} \tag{2.3.18}$$

where $|\mathbf{u}|$ is defined by $|\mathbf{u}| \triangleq [|u_1|, |u_2|, \ldots, |u_n|]'$. It is worth noting that the problem (2.3.18) is a nonsmooth optimization problem. To overcome the difficulties caused, it is shown in [55] that by introducing the coordinate vector $\mathbf{z} \in \Re^{2n}$ partitioned as: $\mathbf{z} \triangleq [\mathbf{z}_+', \mathbf{z}_-']'$ where $\mathbf{z}_+, \mathbf{z}_- \in \Re^n$, the ECUI problem (2.3.18) is equivalent to the following quadratic programming problem

$$\begin{aligned} \min \quad & \|\mathbf{z}\|_2^2, \quad \mathbf{z} \in \Re^{2n} \\ \text{subject to} \quad & \mathcal{Q}\mathbf{z} \leq \mathbf{e} \end{aligned} \tag{2.3.19}$$

where

$$\mathcal{Q} \triangleq \begin{bmatrix} \mathbf{C}+\Theta & -\mathbf{C}+\Theta \\ -\mathbf{C}+\Theta & \mathbf{C}+\Theta \end{bmatrix} \in \Re^{2N \times 2n}, \quad \mathbf{e} \triangleq \begin{bmatrix} \varepsilon + \mathbf{d} \\ \varepsilon - \mathbf{d} \end{bmatrix} \in \Re^{2N},$$

and $\mathbf{u}^* = \mathbf{z}_+^* - \mathbf{z}_-^*$ is an optimal solution to the ECUI problem (2.3.18) if and only if $\mathbf{z}^*$ is an optimal solution to the problem (2.3.19).

Note that the EC filtering problem with uncertain input has been extensively studied in [11, 55]. The work in [72, 73] addresses questions related to how large the input mask can be or how tight the output mask can be before there is no solution to the ECUI problem.

Chapter 3

Semi-infinite Constrained Convex Quadratic Programming Problem

3.1 Introduction

In this chapter, we investigate in a general framework, the problem of minimizing a convex cost function over a convex set defined by continuous linear inequality constraints. This problem is known as the semi-infinite constrained convex programming problem.

The semi-infinite programming problem arises in a number of applications, and it was from these that the first attempts to extend the finite-dimensional theory arose. The semi-infinite constrained linear programming problem has been well documented in [3, 25]. The main objective of this chapter is to present a semi-infinite constrained convex quadratic programming (QP) problem which contains the class of the continuous-time EC filtering problems formulated in Section 2.2. The theory of the quadratic programming in semi-infinite-dimensional spaces is both elegant and complete with the Lagrangian duality theory [2, 34] and Carathéodory's dimensionality theory [51]. Using the Lagrangian duality theory in combination with Carathéodory's dimensionality theory, the semi-infinite QP problem is converted into an equivalent finite dimensional optimization problem which is solvable by any finite optimization method.

Instead of discretizing the semi-infinite problem and solving the discretized problem to obtain an approximate optimal solution, our approach directly handle the semi-infinite problem by seeking only a few crucial time supporting points for which the continuous constraints are active. We show that these active supporting points and the corresponding dual variables carry enough information to obtain the optimal solution such that the continuous constraints are met. The results presented in this chapter are obtained by extending those reported in [30, 59].

This chapter is organized as follows: In Section 3.2, a semi-infinite constrained convex quadratic programming problem is stated. Section 3.3 deals with the Lagrangian duality theory associated with the semi-infinite convex QP problem with inequality constraints. This leads to a dual semi-infinite QP problem with only simple nonnegativity constraints on the dual variables. Finally, by using Carathéodory's dimensionality theory, the dual semi-infinite programming problem is reduced to an equivalent finite dimensional optimization problem. This result is presented in Section 3.4.

The main references for this chapter are [2, 34, 51]

3.2 Problem Formulation

Consider the convex semi-infinite QP problem as follows:

$$\begin{aligned} \min \quad & f(\mathbf{x}), \quad \mathbf{x} \in \Re^n \\ \text{subject to} \quad & \mathbf{g}(\mathbf{x}, t) \leq 0_m, \quad \text{for all } t \in \Omega. \end{aligned} \tag{3.2.1}$$

The objective function $f : \Re^n \to \Re$ and the constraint function $\mathbf{g} : \Re^n \times \Omega \to \Re^m$ are, respectively, defined by

$$\begin{aligned} f(\mathbf{x}) &\triangleq \frac{1}{2}\mathbf{x}'\mathbf{Q}\mathbf{x} + \mathbf{c}'\mathbf{x} + d \\ \mathbf{g}(\mathbf{x}, t) &\triangleq \mathbf{A}(t)\mathbf{x} - \mathbf{b}(t) \end{aligned} \tag{3.2.2}$$

where $\mathbf{Q} \in \Re^{n \times n}$ is a symmetric positive definite matrix, $\mathbf{c} \in \Re^n$, $d \in \Re$, $\Omega \subset \Re$ is a compact set, $\mathbf{A}(t) \in C(\Omega, \Re^{m \times n})$ and $\mathbf{b}(t) \in C(\Omega, \Re^m)$, while $C(\Omega, \Re^{m \times n})$ and $C(\Omega, \Re^m)$ denote, respectively, the Banach spaces consisting of all continuous functions defined on Ω with value on $\Re^{m \times n}$ and $\Re^m$. The norms of these Banach spaces are their respective sup-norms. In addition, it is assumed that for each $\mathbf{x} \in \Re^n$, $\mathbf{g}(\mathbf{x}, t) \in C(\Omega, \Re^m)$.

Since the Hessian matrix $\mathbf{Q}$ is symmetric positive definite, the cost function $f(\mathbf{x})$ is strictly convex, i.e, the contour of the values for the function f in any two-dimensional subspace are ellipses (the vector $\mathbf{c}$ merely shifts the center of the ellipse, and the scalar d merely shifts the minimum value achieved). Clearly, $\mathbf{g}(\cdot, t)$ is a linear, and hence convex function for each $t \in \Omega$. Thus, if the constraints of the QP problem (3.2.1) admit a feasible solution, then the problem has a unique solution [34].

In the subsequent sections, the dual parameterization technique, together with Carathéodory's dimensionality theory will be used to convert the semi-infinite convex QP problem into an equivalent finite dimensional optimization problem.

3.3 Continuous Dual Parameterization

In this section, we use the Lagrangian duality theory to convert the semi-infinite convex QP problem (3.2.1) with continuous inequality constraints into a dual semi-infinite programming problem with simple nonnegativity constraints.

Consider the QP problem (3.2.1) and define the Lagrangian function as follows:

$$\begin{aligned}\mathcal{L}(\mathbf{x},\lambda) &\triangleq f(\mathbf{x}) + \langle \mathbf{g}(\mathbf{x},t), \lambda(t)\rangle \\ &= \frac{1}{2}\mathbf{x}'\mathbf{Q}\mathbf{x} + \mathbf{c}'\mathbf{x} + d + \langle \mathbf{A}(t)\mathbf{x} - \mathbf{b}(t), \lambda(t)\rangle\end{aligned}$$

where $\mathcal{L} : \Re^n \times M(\Omega, \Re^m) \longrightarrow \Re$, and $\lambda(t) = [\lambda_1(t), \ldots, \lambda_m(t)]' \in M(\Omega, \Re^m)$ is the Lagrange multiplier vector with $0 \leq \lambda_i(t) \in M(\Omega, \Re), i = 1, 2, \ldots, m$, while $M(\Omega, \Re)$ is the dual space of $C(\Omega, \Re)$. It consists of all finite signed regular Borel measures on Ω, and $\langle \cdot, \cdot \rangle$ denotes the inner product defined by

$$\langle y(t), \lambda(t)\rangle = \int_\Omega y(t) d\lambda(t).$$

Clearly,

$$\langle \mathbf{A}(t)\mathbf{x}, \lambda(t)\rangle = \mathbf{x}' \int_\Omega \mathbf{A}'(t) d\lambda(t).$$

Thus,

$$\mathcal{L}(\mathbf{x},\lambda) = \frac{1}{2}\mathbf{x}'\mathbf{Q}\mathbf{x} + \mathbf{c}'\mathbf{x} - \int_\Omega \mathbf{b}(t) d\lambda(t) + \mathbf{x}' \int_\Omega \mathbf{A}'(t) d\lambda(t) + d$$

Since the Lagrange multiplier vector $\lambda(t)$ do not always exist for constrained minimization problems, it becomes necessary to add some additional assumptions on the nature of the constraint equations. Slater's constraint qualification condition [49] is suitable for a constrained minimization problem with a convex set of inequality constraints. In fact, it ensures the existence of $\lambda_i(t), i = 1, \ldots, m$, not all zero so that the following equations hold:

$$\begin{cases} \nabla_{\mathbf{x}} \mathcal{L}(\mathbf{x}^*, \lambda(t)) = 0_n \\ \langle \mathbf{g}(\mathbf{x}^*, t), \lambda(t)\rangle = 0 \\ \lambda(t) \geq 0_m, \quad t \in \Omega \end{cases}$$

where $\mathbf{x}^*$ is the optimal solution to the primal problem (3.2.1). Thus, we proceed to consider the primal problem (3.2.1) under Slater's constraint qualification condition.

Assumption 3.3.1 *{Slater's constraint qualification(CQ)} [49]*
There exists an $\mathbf{x}^0 \in \Re^n$ *such that* $\mathbf{g}(\mathbf{x}^0, t) < 0_m$ *for all* $t \in \Omega$.

Since the Lagrangian function is convex in $\mathbf{x}$ and concave in λ, by Assumption 3.3.1, we obtain the following Lagrangian duality theorem for the QP problem (3.2.1).

Theorem 3.3.1 *{Lagrangian Duality} [2, 34]*
Let Assumption 3.3.1 be satisfied. If the optimal solution of the primal problem (3.2.1) is achieved at $\mathbf{x}^* \in \Re^n$, then there exists a solution $\lambda^*(t) = [\lambda_1^*(t), \ldots, \lambda_m^*(t)]' \in M(\Omega, \Re_+^m)$ with $\lambda_i^*(t) \in M(\Omega, \Re_+)$, such that

$$f(\mathbf{x}^*) = \max_{\substack{\lambda(t) \geq 0_m \\ t \in \Omega}} \min_{\mathbf{x}} \mathcal{L}(\mathbf{x}, \lambda) = \min_{\mathbf{x}} \mathcal{L}(\mathbf{x}, \lambda^*) \tag{3.3.1}$$
$$\langle \mathbf{g}(\mathbf{x}^*, t), \lambda^*(t) \rangle = 0$$

From (3.3.1), we note that the minimization over $\mathbf{x}$ is unconstrained. Thus,

$$\nabla_{\mathbf{x}} \mathcal{L}(\mathbf{x}, \lambda) = \mathbf{Q}\mathbf{x} + \mathbf{c} + \int_\Omega \mathbf{A}'(t) d\lambda(t) = 0_n.$$

The above equation immediately yields

$$\mathbf{x}(t, \lambda(t)) \;=\; -\mathbf{Q}^{-1} \left(\int_\Omega \mathbf{A}'(t) d\lambda(t) + \mathbf{c} \right). \tag{3.3.2}$$

Substituting (3.3.2) into the problem (3.3.1), we obtain the following dual semi-infinite QP problem corresponding to the primal problem (3.2.1):

$$\begin{array}{ll} \min_{(t, \lambda(t))} & \phi(t, \lambda) \\ \text{subject to} & \lambda(t) \geq 0_m, \quad t \in \Omega, \end{array} \tag{3.3.3}$$

where the dual cost function $\phi(t, \lambda)$ is given by

$$\phi(t, \lambda) \;=\; \frac{1}{2} \left(\int_\Omega \mathbf{A}'(t) d\lambda(t) + \mathbf{c} \right)' \mathbf{Q}^{-1} \left(\int_\Omega \mathbf{A}'(t) d\lambda(t) + \mathbf{c} \right) + \int_\Omega \mathbf{b}'(t) d\lambda(t) - d.$$

Note that the dual problem is easier to solve than the primal problem, as the constraint set is much simpler.

3.4 An Equivalent Finite Optimization Problem

In this section, we transform the dual semi-infinite QP problem (3.3.3) into an equivalent finite dimensional optimization problem by using the Karush-Kuhn-Tucker (KKT) conditions [2, 34] and Carathéodory's dimensionality theory [51].

Note that the cost function $f(\mathbf{x})$ given by (3.2.2) is differentiable in $\mathbf{x} \in \Re^n$. Furthermore, the constraint function $\mathbf{g}(\mathbf{x}, t)$ is continuous in t for each $\mathbf{x} \in \Re^n$, and it is convex and continuously differentiable in $\mathbf{x}$ for each $t \in \Omega$. By [2, 34], the KKT optimality conditions for the primal QP problem (3.2.1) are obtained in the following.

Lemma 3.4.1 *{KKT conditions} [2, 34]*

Let Assumption 3.3.1 be satisfied. The optimal solution of the QP problem (3.2.1) is achieved at $\mathbf{x}^* \in \Re^n$ *if and only if* $\mathbf{x}^*$ *is feasible and there exists a* $\lambda^*(t) \in M(\Omega, \Re^m_+)$ *such that*

$$\begin{cases} \nabla_{\mathbf{x}}\mathcal{L}(\mathbf{x}^*, \lambda^*(t)) = \nabla f(\mathbf{x}^*) + \int_\Omega \nabla_{\mathbf{x}}\mathbf{g}'(\mathbf{x}^*, t)d\lambda^*(t) = 0_n, \\ \int_\Omega \mathbf{g}'(\mathbf{x}^*, t)d\lambda^*(t) = 0, \\ \lambda^*(t) \geq 0_m, \quad (\lambda^*(t) \text{ is a regular Borel measure}). \end{cases} \tag{3.4.1}$$

In the next two lemmas, we extend the results [30, 59] from $\Re^2$ to $\Re^m$. The new results are then used in combination with Carathéodory's dimensionality theorem to obtain a necessary condition for which the set of the Lagrangian multiplier vector $\{\lambda(t) \in \Re^m_+, t \in \Omega\}$ satisfying the KKT conditions (3.4.1) includes a measure with finite support at no more than mn points. This result is presented in Theorem 3.4.2. Consequently, we obtain in Theorem 3.4.3 that the optimal solution $\lambda^*(t)$ to the dual QP problem (3.3.3) always includes a measure with finite support at no more than mn points.

Lemma 3.4.2 *Let Assumption 3.3.1 be satisfied. Assume that the optimal solution of the primal QP problem (3.2.1) is achieved at* $\mathbf{x}^* \in \Re^n$. *Then the set of multipliers satisfying the KKT conditions (3.4.1) coincides with the optimal solution to the dual QP problem (3.3.3).*

Proof: See Appendix A.1. ∎

Lemma 3.4.3 *Let* $\bar{\Omega}(\mathbf{x}^*) \triangleq \{t \in \Omega | \mathbf{g}(\mathbf{x}^*, t) = 0_m\}$. *For each* $i = 1, \ldots m$, *let*

$$\begin{aligned} \mathbf{X}_{1,i} &= \left\{ \int_{\bar{\Omega}(\mathbf{x}^*)} \nabla_{\mathbf{x}}\mathbf{g}_i(\mathbf{x}^*, t)d\lambda_i(t) \middle| 0 \leq \lambda_i(t) \in M(\Omega, \Re) \right\} \\ \mathbf{X}_{2,i} &= \left\{ \nabla_{\mathbf{x}}\mathbf{g}_i(\mathbf{x}^*, t) \middle| t \in \bar{\Omega}(\mathbf{x}^*) \right\}. \end{aligned}$$

Define

$$\mathbf{X}_1 = \sum_{i=1}^m \mathbf{X}_{1,i}, \quad \mathbf{X}_2 = \sum_{i=1}^m cone\mathbf{X}_{2,i}.$$

Then, $\mathbf{X}_1 = \mathbf{X}_2$.

Proof: See Appendix A.2. ∎

Carathéodory's dimensionality theorem given below will be needed in the proofs of the subsequent theorems.

Theorem 3.4.1 *{Carathéodory's dimensionality theorem} [51]*

Let $\{\mathbf{X}_i | i \in I\}$ *be an arbitrary collection of non-empty convex sets in* $\Re^n$, *and* K *be the convex*

cone generated by the union of the collection. Then every non-zero vector of K can be expressed as a non-negative linear combination of n or fewer linearly independent vectors, each belonging to a different $\mathbf{X}_i$.

By using the results obtained from Lemma 3.4.3 and Carathéodory's dimensionality theorem, we attain the following necessary condition for transforming the dual semi-infinite convex QP problem (3.3.3) into an equivalent finite dimensional optimization problem.

Theorem 3.4.2 *Let Assumption 3.3.1 be satisfied and assume that the optimal solution of the primal QP problem (3.2.1) is achieved at $\mathbf{x}^* \in \Re^n$. Then the set of multipliers satisfying the KKT conditions (3.4.1) necessarily includes a measure with finite support at no more than mn points.*

Proof: See Appendix A.3. ∎

The result obtained in Theorem 3.4.2 yields the following classical result [31].

Corollary 3.4.1 *Let Assumptions 3.3.1 be satisfied. The optimal solution of the primal problem (3.2.1) is achieved at $\mathbf{x}^* \in \Re^n$ if and only if $\mathbf{x}^*$ is feasible and there exist positive $\lambda^*_{i,j}$ for all $i = 1, \ldots, k$, and $j = 1, \ldots, m$, such that*

$$-\nabla f(\mathbf{x}^*) = \sum_{j=1}^{m} \sum_{i=1}^{k_j} \nabla_{\mathbf{x}} \mathbf{g}_j(\mathbf{x}^*, t_{j,i}) \lambda^*_{i,j}, \text{ for some } t_{j,i} \in \bar{\Omega}(\mathbf{x}^*) \tag{3.4.2}$$

$$\sum_{j=1}^{m} \sum_{i=1}^{k_j} \mathbf{g}_j(\mathbf{x}^*, t_{j,i}) \lambda^*_{i,j} = 0, \quad \lambda^*_{i,j} \geq 0, \tag{3.4.3}$$

where for $i = 1, \ldots, k_j$, $\lambda^*_{i,j}$ is the jth component of $\lambda^*_i \triangleq [\lambda^*_{i,1}, \ldots, \lambda^*_{i,m}]' \in \Re^m_+$ and $k_j \leq n$.

Associated with Lemma 3.4.2 and Theorem 3.4.2, the set of solutions to the dual QP problem (3.3.3) always includes a measure with finite support at no more than mn points.

Theorem 3.4.3 *Let Assumption 3.3.1 be satisfied. Assume that the optimal solution of the primal QP problem (3.2.1) is achieved at $\mathbf{x}^* \in \Re^n$. Then the optimal solution to the dual QP problem (3.3.3) always includes a measure with finite support at no more than mn points.*

By Corollary 3.4.1 and Theorem 3.4.3, we are able to find a dual solution in a subset of $M(\Omega, \Re^m_+)$ whose elements are characterized by the location of a finite number of supporting points and the associated measures are concentrated only on these points. More specifically, for each $j = 1, \ldots, m$, there are $k_j \leq n$ points for the constraint $\mathbf{g}_j(\mathbf{x}^*, t) \leq 0$. Let $k = \sum_{j=1}^{m} k_j \leq mn$.

Now, we add in, for each $j = 1, \ldots, m$, $\sum_{\substack{i=1 \\ i \neq j}}^{m} k_i$ points for the constraint $g_j(\mathbf{x}^*, t) \leq 0$, giving k supporting points. In view of (3.4.2)-(3.4.3), these k supporting points are written as:

$$\Gamma = \left\{ (t_{1,1}, \ldots, t_{1,k_1}), (t_{2,1}, \ldots, t_{2,k_2}), \ldots, (t_{m,1}, \ldots, t_{m,k_m}) \right\}$$

in which the k supporting points are denoted by the corresponding t_j with $t_j \in \Gamma$. Consequently, for $\lambda^*_{i,j} \in \{\lambda^*_{i,1}, \ldots, \lambda^*_{i,m}\}$ with $\lambda^*_i = [\lambda^*_{i,1}, \ldots, \lambda^*_{i,m}]'$, (3.4.2) is reduced to

$$-\nabla f(\mathbf{x}^*) = \sum_{i=1}^{k} \sum_{j=1}^{m} \nabla_{\mathbf{x}} \mathbf{g}_j(\mathbf{x}^*, t_i) \lambda^*_{i,j}, \quad \text{for some } t_i \in \bar{\Omega}(\mathbf{x}^*) \tag{3.4.4}$$

where $\Lambda^* \triangleq [\lambda^{*'}_1, \ldots, \lambda^{*'}_k]' \in \Re^{mk}_+$. Then, solving the dual semi-infinite QP problem (3.3.3) is equivalent to solving the following finite dimensional optimization problem.

$$\begin{array}{ll} \min_{(\lambda(t_i), t_i)} & \phi(\mathbf{t}, \Lambda(\mathbf{t})) \\ \text{subject to} & \Lambda(\mathbf{t}) \geq 0_{mk} \end{array} \tag{3.4.5}$$

where the cost function $\phi(\mathbf{t}, \Lambda(\mathbf{t}))$ is given by

$$\phi(\mathbf{t}, \Lambda(\mathbf{t})) = \frac{1}{2} \left(\mathbf{A}'(\mathbf{t})\Lambda(\mathbf{t}) + \mathbf{c} \right)' \mathbf{Q}^{-1} \left(\mathbf{A}'(\mathbf{t})\Lambda(\mathbf{t}) + \mathbf{c} \right) + \mathbf{b}'(\mathbf{t})\Lambda(\mathbf{t}) - d.$$

Here $\mathbf{t} \in \Re^k_+$, $\Lambda(\mathbf{t}) \in \Re^{mk}_+$, $\mathbf{A}(\mathbf{t}) \in \Re^{mk \times n}$, and $\mathbf{b}(\mathbf{t}) \in \Re^{mk}$, are given, respectively, as follows:

$$\mathbf{t} = [t_1, \ldots, t_k]', \qquad \Lambda(\mathbf{t}) = [\lambda'(t_1), \ldots, \lambda'(t_k)]' \tag{3.4.6}$$

$$\mathbf{A}(\mathbf{t}) = [\mathbf{A}'(t_1), \ldots, \mathbf{A}'(t_k)]', \qquad \mathbf{b}(\mathbf{t}) = [\mathbf{b}'(t_1), \ldots, \mathbf{b}'(t_k)]' \tag{3.4.7}$$

where $t_i \in \Omega$, $\mathbf{A}(t_i) \in \Re^{m \times n}$, $\mathbf{b}(t_i) \in \Re^m$, and $\lambda(t_i) = [\lambda_{i,1}, \ldots, \lambda_{i,m}]' \in \Re^m_+$, $i = 1, \ldots, k$. Once $\mathbf{t}$ and the corresponding $\Lambda(\mathbf{t})$ are obtained, the original (primal) QP problem (3.2.1) with strictly convex cost function is readily obtained from the primal-dual relationship as follows:

$$\mathbf{x}(\mathbf{t}, \Lambda(\mathbf{t})) = -\mathbf{Q}^{-1} \left(\mathbf{A}'(\mathbf{t})\Lambda(\mathbf{t}) + \mathbf{c} \right).$$

Chapter 4

Finite Convex Quadratic Programming Problem

4.1 Introduction

In this chapter, we present two new iterative methods for solving a convex QP problem with a finite number of linear inequality constraints. The main idea behind these methods is to convert the constrained convex QP problem into a dual problem with simple constraints by applying the concept of the Lagrangian duality theory. We note that the dual problem remains unchanged as a QP problem. By means of the space transformation function [15, 16] in combination with the gradient flow technique [22, 45], the dual QP problem is transformed into a Cauchy problem (differential equation). As a result of the space transformation, the right-hand side of the differential equation appears as the multiplication of the gradient of the cost function with an appropriate diagonal matrix. This diagonal matrix is to prevent the trajectories from crossing the boundary of the feasible set. Euler method is then applied to discretize the Cauchy problem leading to two simple yet efficient new gradient-type numerical methods for solving the dual QP problem. We note that since the diagonal matrix plays the role of barrier, the resulting methods are called the barrier-gradient (BG) and barrier-Newton (BN) methods [57, 59, 60]. From the primal-dual relationship, the solution of the original (primal) QP problem is readily obtained.

As can be noted that the term "barrier" used in this thesis is different from the one used as a penalty function described in the books [20, 22, 14]. Numerical methods based on penalty functions are inherently unstable and expensive since the penalty parameter is usually required to be sufficiently large to ensure feasibility. Moreover, it is difficult to locate the minimizer due

to ill-conditioning and large gradients. In contrast, the unconventional multiplicative barriers, which we use, do not tend to infinity as the current point approaches the boundary of the feasible set. In our algorithms, the barrier functions are continuous and equal to zero on the boundary. These barriers ensure the feasibility of the trajectories without the need of any penalty coefficient.

This chapter is divided into four sections. In Section 4.2, the general format of a convex QP problem is addressed. In Section 4.3, the discrete dual parameterization technique is used to convert the original (primal) problem into a corresponding dual problem which is also a QP problem. The dual QP problem is easier to solve than the primal QP problem since the constraint set is much simpler.

In Section 4.4.1, the space transformation technique is used to convert the dual QP problem with simple constraints into an unconstrained optimization problem. By applying the gradient flow technique to the unconstrained optimization problem yields an ordinary differential equation (ODE)- an initial value problem. The limiting solution of the ODE solves the dual QP problem. Integrating the ODE numerically by using Euler method, we obtain an iterative BG scheme for solving the dual QP problem. The simple iterative BG scheme is suitable for on-line (adaptive) applications in a stochastic setting. A practical on-line application based on the iterative BG scheme in the design of the adaptive FIR envelope-constrained filtering problem in a stochastic environment is given in Chapter 7.

In Section 4.4.2, a Jacobian matrix and its inverse are introduced to the left-hand side of the differential equation. This leads to a new ODE, which is usually referred to as the continuous analog of Newton's method. The optimal solution of the dual QP problem can also be obtained by finding the limiting point of the specified ODE. Since the Jacobian matrix is nonsingular at the optimal dual vector, we can integrate the ODE numerically in a neighborhood of the optimal dual vector by using Euler method to obtain an iterative scheme. This scheme is called BN scheme.

Finally, we make use of the Lyapunov stability theory [14] in Section 4.4 to establish the stability and convergence properties of solutions of the above two ODE's and their corresponding algorithms. These results are extended from those reported in [57, 59, 60]. They are applicable to any finite dimensional constrained convex optimization problem.

The main references for this chapter are [14, 15, 16, 22, 45, 57, 59, 60].

4.2 Problem Formulation

Consider a convex QP problem of the form

$$\begin{array}{ll} \min & f(\mathbf{x}) = \frac{1}{2}\mathbf{x}'\mathbf{Q}\mathbf{x} + \mathbf{c}'\mathbf{x} + d, \quad \mathbf{x} \in \Re^n \\ \text{subject to} & \mathbf{A}\mathbf{x} \leq \mathbf{b} \end{array} \tag{4.2.1}$$

where $f : \Re^n \longrightarrow \Re$ is a strictly convex quadratic function consisting of the symmetric positive definite Hessian matrix $\mathbf{Q} \in \Re^{n \times n}$, $\mathbf{c} \in \Re^n$, and $d \in \Re$. The constraint matrix $\mathbf{A} \in \Re^{m \times n}$ and vector $\mathbf{b} \in \Re^m$ are given, and $\mathbf{x} \in \Re^n$ is a decision vector to be determined. It is assumed that $m \geq n$, i.e., there are more constraints than variables.

In view of the QP problem (4.2.1), we note that the cost function $f(\mathbf{x})$ is strictly convex and the constraint set is convex. Thus, any point $\mathbf{x}^*$ satisfying the KKT conditions is the global maximizer.

4.3 Discrete Dual Parameterization

Define the Lagrangian function for the convex QP problem (4.2.1) as follows:

$$\mathcal{L}(\mathbf{x}, \lambda) \;=\; \frac{1}{2}\mathbf{x}'\mathbf{Q}\mathbf{x} + \mathbf{c}'\mathbf{x} + \lambda'(\mathbf{A}\mathbf{x} - \mathbf{b}) + d$$

where $\lambda = [\lambda_1, \ldots, \lambda_m]' \in \Re_+^m$ is the Lagrange multiplier vector with the property that $\lambda_i \geq 0$, $i = 1, \ldots, m$. Then, it is easily seen that the gradients of the Lagrange function with respect to $\mathbf{x}$ and λ are:

$$\left\{ \begin{array}{lcl} \nabla_{\mathbf{x}}\mathcal{L}(\mathbf{x}, \lambda) & = & \mathbf{Q}\mathbf{x} + \mathbf{c} + \mathbf{A}'\lambda \\ \nabla_{\lambda}\mathcal{L}(\mathbf{x}, \lambda) & = & \mathbf{A}\mathbf{x} - \mathbf{b}. \end{array} \right. \tag{4.3.1}$$

Assumption 4.3.1 *There exists an* $\mathbf{x}^0 \in \Re^n$ *satisfying* $\mathbf{A}\mathbf{x}^0 < \mathbf{b}$.

By the Lagrangian duality theory [34] and Assumption 4.3.1, it follows that the convex QP problem (4.2.1) is equivalent to

$$\max_{\lambda \geq 0_m} \min_{\mathbf{x}} \mathcal{L}(\mathbf{x}, \lambda). \tag{4.3.2}$$

Since the minimization over $\mathbf{x}$ is unconstrained in (4.3.2), it follows from (4.3.1) that

$$\mathbf{x}(\lambda) \;=\; -\mathbf{Q}^{-1}(\mathbf{A}'\lambda + \mathbf{c}). \tag{4.3.3}$$

Substituting (4.3.3) into the problem (4.3.2) gives rise to the following dual optimization problem with respect to the primal problem (4.2.1):

$$\max_{\lambda \geq 0_m} \left\{ -\frac{1}{2}(\mathbf{A}'\lambda + \mathbf{c})'\mathbf{Q}^{-1}(\mathbf{A}'\lambda + \mathbf{c}) - \lambda'\mathbf{b} + d \right\}$$

or equivalently,

$$\min_{\lambda \geq 0_m} \left\{ \frac{1}{2} \lambda' \bar{\mathbf{A}} \lambda + \lambda' \bar{\mathbf{c}} + \bar{\mathbf{d}} \right\}, \tag{4.3.4}$$

where

$$\bar{\mathbf{A}} \triangleq \mathbf{A}\mathbf{Q}^{-1}\mathbf{A}', \quad \bar{\mathbf{c}} \triangleq \mathbf{b} + \mathbf{A}\mathbf{Q}^{-1}\mathbf{c}, \quad \bar{\mathbf{d}} \triangleq \frac{1}{2}\mathbf{c}'\mathbf{Q}^{-1}\mathbf{c} - d. \tag{4.3.5}$$

Clearly, the dual problem is also a QP problem. If the matrix $\bar{\mathbf{A}}$ is positive definite (respectively, positive semi-definite), then the dual cost function is strictly convex (respectively, convex). From (4.3.3), the optimal solution of the primal convex QP problem (4.2.1) can be readily obtained.

4.4 Solution Techniques

In this section, two gradient-based optimization methods will be developed for solving the convex QP problem (4.3.4) by using the techniques of the space transformation [15, 16] and the gradient flow [22, 45]. These methods are: the barrier-gradient method and the barrier-Newton method. To establish the stability and convergence properties, Lyapunov stability theory [14] is applied to the above two methods and their corresponding schemes. The resulting properties are extended from those reported in [57, 59, 60]. They are applicable to any finite dimensional constrained convex optimization problem.

4.4.1 Barrier-Gradient Method

Let the cost function of the dual QP problem (4.3.4) be written as:

$$\phi(\lambda) \triangleq \frac{1}{2} \lambda' \bar{\mathbf{A}} \lambda + \lambda' \bar{\mathbf{c}} + \bar{\mathbf{d}}. \tag{4.4.1}$$

Consider a $m-$dimensional space with the coordinate vector $\mathbf{y} \in \Re^m$ given by

$$\mathbf{y} = [y_1, \ldots, y_m]'. \tag{4.4.2}$$

We then introduce the following quadratic component-wise space transformation function:

$$\lambda = \xi(\mathbf{y}) = [\xi_1(y_1), \ldots, \xi_m(y_m)]' \in \Re_+^m, \tag{4.4.3}$$

where

$$\lambda_i = \xi_i(y_i) = \frac{1}{4} y_i^2, \quad 1 \leq i \leq m. \tag{4.4.4}$$

We now construct a new unconstrained optimization problem based on the space transformation function as follows:

$$\min_{\lambda \in \Re^m_+} \phi(\lambda) = \min_{\mathbf{y} \in \Re^m} \phi(\xi(\mathbf{y})) = \min_{\mathbf{y} \in \Re^m} \widehat{\phi}(\mathbf{y}) \tag{4.4.5}$$

where the cost function $\widehat{\phi}(\mathbf{y}) = \phi(\xi(\mathbf{y}))$ is a differentiable function of $\mathbf{y}$.

Since the right-hand side of (4.4.5) is an unconstrained minimization problem, the gradient of the cost function $\widehat{\phi}(\mathbf{y})$ with respect to $\mathbf{y}$, denoted as $\nabla\widehat{\phi}(\mathbf{y})$, can be expressed in terms of the gradient of the dual cost function, denoted as $\nabla\phi(\lambda)$, as follows:

$$\begin{aligned} \nabla\widehat{\phi}(\mathbf{y}) &= \frac{\partial\phi(\xi(\mathbf{y}))}{\partial\mathbf{y}} = \left\langle \frac{\partial\phi(\lambda)}{\partial\lambda}, \frac{\partial\lambda}{\partial\mathbf{y}} \right\rangle \\ &= \left\langle \nabla\phi(\lambda), \widehat{\mathbf{J}}(\mathbf{y}) \right\rangle \end{aligned} \tag{4.4.6}$$

where the gradient $\nabla\widehat{\phi}(\mathbf{y})$ is to be realized as a column vector, the gradient $\nabla\phi(\lambda)$ and the Jacobian matrix $\widehat{\mathbf{J}}(\mathbf{y})$ of the transformation $\lambda = \xi(\mathbf{y})$ with respect to $\mathbf{y}$ are, respectively, given by

$$\begin{aligned} \nabla\phi(\lambda) &= \frac{\partial\phi}{\partial\lambda} = \bar{\mathbf{A}}\lambda + \bar{\mathbf{c}} \\ \widehat{J}(\mathbf{y}) &= \frac{\partial\xi(\mathbf{y})}{\partial\mathbf{y}}. \end{aligned} \tag{4.4.7}$$

Making use of the quadratic component-wise transformation function given in (4.4.3)-(4.4.4), it is clear from (4.4.7) that the Jacobian matrix of the mapping $\xi(\mathbf{y})$ yields

$$\widehat{\mathbf{J}}(\mathbf{y}) = \frac{1}{2}\mathbf{D}(\mathbf{y}) \tag{4.4.8}$$

where $\mathbf{D}(\mathbf{y}) \triangleq diag(y_1, \ldots, y_m) \in \Re^{m\times m}$ is a diagonal matrix containing only components of the vector $\mathbf{y}$ defined in (4.4.2). Substituting $y_i = \pm 2\sqrt{\lambda_i}$, $i = 1, \ldots, m$, into (4.4.8), we obtain the matrix $\widehat{\mathbf{J}}(\mathbf{y})$ in terms of λ-function as follows:

$$\widehat{\mathbf{J}}(\mathbf{y}) = \mathbf{D}(\pm\sqrt{\lambda}) \tag{4.4.9}$$

where $\mathbf{D}(\pm\sqrt{\lambda}) \triangleq diag(\pm\sqrt{\lambda_1}, \ldots, \pm\sqrt{\lambda_m}) \in \Re^{m\times m}$. Combining (4.4.6) with (4.4.9), the gradient of $\widehat{\phi}(\mathbf{y})$ can be rewritten in terms of λ-function as:

$$\nabla\widehat{\phi}(\mathbf{y}) = \left\langle \nabla\phi(\lambda), \widehat{\mathbf{J}}(\mathbf{y}) \right\rangle = \mathbf{D}(\pm\sqrt{\lambda})\nabla\phi(\lambda). \tag{4.4.10}$$

Let the gradient flow associated with the unconstrained problem (4.4.5) be expressed as

$$\frac{d\mathbf{y}}{dt} = -\nabla\widehat{\phi}(\mathbf{y}). \tag{4.4.11}$$

Based on the transformation function, the dual QP problem (4.3.4) is equivalent to the unconstrained problem (4.4.5). We note from the system (4.4.11) that

$$\frac{d\widehat{\phi}(\mathbf{y})}{dt} = \left\langle \nabla\widehat{\phi}(\mathbf{y}), \frac{d\mathbf{y}}{dt} \right\rangle = -\|\nabla\widehat{\phi}(\mathbf{y})\|_2^2 \leq 0. \tag{4.4.12}$$

Furthermore, following from the system (4.4.11), $\mathbf{y}(t)$ converges to the following singleton set

$$\left\{\mathbf{y} \in \Re^m | \nabla\widehat{\phi}(\mathbf{y}) = 0_m\right\}.$$

Now by differentiating $\xi(\mathbf{y})$ with respect to $\mathbf{y}$, we obtain the following ordinary differential equations associated with the dual QP problem (4.3.4) as:

$$\frac{d\lambda}{dt} = \left\langle \frac{\partial\xi(\mathbf{y})}{\partial\mathbf{y}}, \frac{d\mathbf{y}}{dt} \right\rangle, \quad \lambda(0;\lambda^0) = \lambda^0 \in \Re_+^m. \tag{4.4.13}$$

By (4.4.7) and (4.4.9), we obtain

$$\frac{\partial\xi(\mathbf{y})}{\partial\mathbf{y}} = \mathbf{D}(\pm\sqrt{\lambda}).$$

Combining the systems (4.4.11) and (4.4.13) yields the following Cauchy problem:

$$\begin{aligned} \frac{d\lambda}{dt} &= \left\langle \frac{\partial\xi(\mathbf{y})}{\partial\mathbf{y}}, \frac{d\mathbf{y}}{dt} \right\rangle = \mathbf{D}(\pm\sqrt{\lambda})\frac{d\mathbf{y}}{dt} \\ &= -\mathbf{D}(\pm\sqrt{\lambda})\nabla\widehat{\phi}(\mathbf{y}). \end{aligned} \tag{4.4.14}$$

Substituting (4.4.10) into the system (4.4.14), we obtain

$$\begin{aligned} \frac{d\lambda}{dt} &= -\mathbf{D}(\pm\sqrt{\lambda})[\mathbf{D}(\pm\sqrt{\lambda})\nabla\phi(\lambda)] = -\mathbf{D}(\lambda)\nabla\phi(\lambda) \\ &= -\mathbf{F}(\lambda), \quad \lambda(0;\lambda^0) = \lambda^0 \in \Re_+^m \end{aligned} \tag{4.4.15}$$

where $\mathbf{F}(\lambda) \triangleq \mathbf{D}(\lambda)\nabla\phi(\lambda)$ is a continuous barrier function and $\lambda = \lambda(t;\lambda^0)$.

Remark 4.4.1

1) For any $i \in \{1,\ldots,m\}$, if there exists a $\hat{t}$ such that $\lambda_i(\hat{t};\lambda^0) = 0$, then $\mathbf{D}_{ii}(\lambda(t;\lambda^0)) = 0$ for all $t \geq \hat{t}$ and hence, $\frac{d\lambda_i(\hat{t};\lambda^0)}{dt} = 0$ for all $t \geq \hat{t}$. This simply implies that the trajectory $\lambda(t;\lambda^0)$ of the system (4.4.15) cannot cross the boundary $\lambda_i = 0$. In other words, if a starting point is feasible then the subsequent trajectories remain in the feasible set, i.e, the feasibility of the dual constraints is preserved.

2) By differentiating the dual cost function $\phi(\lambda(t;\lambda^0))$ with respect to t, we obtain

$$\begin{aligned} \frac{d\phi(\lambda)}{dt} &= \left\langle \frac{\partial\phi(\lambda)}{\partial\lambda}, \frac{d\lambda}{dt} \right\rangle = -\nabla\phi'(\lambda)\mathbf{D}(\lambda)\nabla\phi(\lambda) \\ &= -\|\mathbf{D}(\pm\sqrt{\lambda})\nabla\phi(\lambda)\|_2^2 = -\|\nabla\widehat{\phi}(\mathbf{y})\|_2^2 \leq 0, \text{ for all } \lambda \geq 0_m. \end{aligned}$$

Thus, it is clear that the dual cost function $\phi\left(t;\lambda(\lambda^0)\right)$ is monotonically decreasing and bounded along the trajectory $\lambda\left(t;\lambda^0\right)$ without leaving the feasible set $\Re_+^m$.
3) Along the descent search direction $-\mathbf{F}(\lambda) \leq 0_m$, we find that $\lambda(t)$ converges to the singleton set $\left\{\lambda \in \Re_+^m | \mathbf{F}(\lambda) = 0_m\right\}$.

Definition 4.4.1 *If $\lambda^* \in \Re_+^m$ satisfies the following condition*

$$\mathbf{F}(\lambda^*) = \mathbf{D}(\lambda^*)\nabla\phi(\lambda^*) = 0_m, \tag{4.4.16}$$

then it is said to be a local minimizer of the dual QP problem (4.3.4).

Integrating the Cauchy equation (4.4.15) numerically by using Euler method, we obtain an iterative scheme for solving the dual QP problem (4.3.4):

$$\lambda^{k+1} = \lambda^k - h_k\mathbf{F}(\lambda^k) \tag{4.4.17}$$

where $\lambda^k \triangleq \lambda(t_k)$, $t_{k+1} = t_k + h_k$, and h_k is an appropriate step-size.

Substituting (4.4.17) into $\mathbf{x}(\lambda)$ in (4.3.3) yields the following simple iterative BG scheme for solving the original convex QP problem (4.2.1)

$$\begin{cases} \mathbf{F}(\lambda^k) = \mathbf{D}(\lambda^k)\nabla\phi(\lambda^k) \\ \lambda^{k+1} = \lambda^k - h_k\mathbf{F}(\lambda^k) \\ \mathbf{x}^{k+1} = -\mathbf{Q}^{-1}\left(\mathbf{A}'\lambda^{k+1} + \mathbf{c}\right). \end{cases} \tag{4.4.18}$$

Definition 4.4.2 *$\lambda^* = [\lambda_1^*, \ldots, \lambda_m^*]' \in \Re_+^m$ is said to satisfy the strict complementary condition (SCC) if for all $i \in \{1, \ldots, m\}$, either $\lambda_i^* > 0$ and $\nabla_i\phi(\lambda^*) = 0$ or $\lambda_i^* = 0$ and $\nabla_i\phi(\lambda^*) > 0$.*

Lemma 4.4.1 *Assume SCC holds and let the Hessian matrix $\bar{\mathbf{A}}$ defined in (4.3.5) be symmetric positive semi-definite. Since $\lambda^* \in \Re_+^m$ satisfies (4.4.16), the Jacobian matrix of the mapping $\mathbf{F}(\lambda)$ at λ^* defined by*

$$\nabla\mathbf{F}(\lambda^*) = \mathbf{D}(\nabla\phi(\lambda^*)) + \mathbf{D}(\lambda^*)\bar{\mathbf{A}} \tag{4.4.19}$$

is symmetric positive definite.

Proof: See Appendix B.1. ∎

In the remaining part of this section, we shall make use of the Lyapunov stability theory [14] on differential equations to establish the stability and convergence properties of solutions of the Cauchy equation (4.4.15) and the corresponding BG scheme (4.4.18).

We say that a point $\hat{\lambda}$ is an equilibrium point of the system (4.4.15) if the right-hand side of the system (4.4.15) evaluated at $\hat{\lambda}$ is a zero vector. From (4.4.16), the optimal point λ^* is clearly an equilibrium point of the system (4.4.15).

Definition 4.4.3 *Let $\lambda(t;\lambda^0)$ be the solution of the system (4.4.15) corresponding to the initial condition $\lambda(0;\lambda^0) = \lambda^0$. An equilibrium point $\lambda^* \in \Re_+^m$ is said to be asymptotically stable if for any $\nu > 0$, there exists a $\sigma = \sigma(\nu)$, such that for any λ^0 satisfying $\|\lambda^0 - \lambda^*\|_2 < \nu$, the following conditions hold:*

(i): $\|\lambda(t;\lambda^0) - \lambda^*\|_2 < \sigma$, for all $t \in [0,\infty)$;

(ii): $\|\lambda(t;\lambda^0) - \lambda^*\|_2 \to 0$ as $t \to \infty$.

Theorem 4.4.1 *Let the conditions in Lemma 4.4.1 be satisfied. Then, the system (4.4.15) is asymptotically stable at the global solution point λ^*. Furthermore, there exists a number $h^* = \frac{2}{\eta_{max}}$ where η_{max} is the largest eigenvalue of the Jacobian matrix $\nabla\mathbf{F}(\lambda^*)$ defined in (4.4.19) such that for a fixed step-size $h_k = h$ for all k satisfying $0 < h < h^*$, the sequences $\{\lambda^k\}_{k=0}^{\infty}$ and $\{\mathbf{x}^k\}_{k=0}^{\infty}$ generated by the BG scheme (4.4.18) converge, respectively, to the optimum λ^* and $\mathbf{x}^*$, both globally and at a linear rate.*

Proof: See Appendix B.2. ∎

4.4.2 Barrier-Newton Method

We present another gradient-type approach for solving the dual QP problem (4.3.4). This approach is called the barrier-Newton method, and it possesses a quadratic rate of convergence.

Motivated by the system (4.4.15), we consider the following initial value problem.

$$\nabla\mathbf{F}(\lambda)\frac{d\lambda}{dt} = -\mathbf{D}(\alpha)\mathbf{F}(\lambda), \quad \lambda(\lambda^0,t) = \lambda^0 \in \Re_+^m \tag{4.4.20}$$

where $\mathbf{D}(\alpha) \triangleq diag\,(\alpha_1,\ldots,\alpha_m)$ is a diagonal matrix containing a positive scaling vector $\alpha \triangleq [\alpha_1,\ldots,\alpha_m]' \in \Re_+^m$ and $\nabla\mathbf{F}(\lambda)$ defined by (4.4.19) is the Jacobian matrix of the mapping $\mathbf{F}(\lambda)$. The initial value problem (4.4.20) is known as the continuous analog of Newton's method.

From Lemma 4.4.1, it follows that all eigenvalues of $\nabla\mathbf{F}(\lambda)$ at λ^* are real and positive. This implies that $\nabla\mathbf{F}(\lambda^*)$ is a positive definite matrix and hence nonsingular. Combining with the convexity of the dual cost function $\phi(\lambda)$ defined by (4.4.1) and taking into account of the fact that the Jacobian matrix is nonsingular at λ^*, the stability and convergence properties of solutions of the system (4.4.20) are obtained via Lyapunov stability theory and Newton method in the following theorem.

Theorem 4.4.2 *Let the conditions in Lemma 4.4.1 be satisfied. Then, for any scaling vector $\alpha > 0_m$, the system (4.4.20) is asymptotically stable at the equilibrium point λ^* which is an isolated global minimizer of the dual QP problem (4.3.4). For $\lambda^k \triangleq \lambda(t_k)$ and $t_{k+1} = t_k + h_k$, in*

a neighborhood $N(\lambda^*)$ of the solution λ^* of the system (4.4.20), the sequence $\{\lambda^k\}_{k=0}^{\infty}$ generated by the following iterative scheme

$$\lambda^{k+1} = \lambda^k - h_k \nabla \mathbf{F}^{-1}(\lambda^k)\mathbf{D}(\alpha)\mathbf{F}(\lambda^k) \tag{4.4.21}$$

converges globally to the point λ^* with at least linear rate if the step size $h_k = h$ is chosen such that $0 < h < \frac{2}{\alpha^*}$ for every k where $\alpha^* = \max_i[\alpha_i]$. Furthermore, if there exists a constant $\ell > 0$ such that the Jacobian matrix $\nabla\mathbf{F}(\lambda)$ satisfies a Lipschitz condition in the neighborhood of the point λ^*, i.e., $\|\nabla\mathbf{F}(\lambda) - \nabla\mathbf{F}(\lambda^*)\|_2 \leq \ell\|\lambda - \lambda^*\|_2 \ \forall\lambda \in N(\lambda^*)$, and $\alpha_i = e \simeq 2.71828$, $\forall i = 1, \ldots, m$, then the sequence $\{\lambda^k\}_{k=0}^{\infty}$ and the corresponding sequence $\{\mathbf{x}^k\}_{k=0}^{\infty}$ globally converge to the optimum λ^* and $\mathbf{x}^*$, respectively, at a quadratic rate.

Proof: See Appendix B.3. ∎

Remark 4.4.2

1) In view of Remark 4.4.1(1), we see that the trajectory of the system (4.4.20) starting at a point $\lambda^0 \geq 0$ does not leave the feasible set $\Re_+^m$.

2) To analyze the convergence property of the system (4.4.20) and to determine the step-size for the BN scheme (4.4.21), the system (4.4.20) is linearized in a neighborhood of the point λ^*

$$\Delta\dot{\lambda}(t) = -\mathbf{H}(\lambda^*)\Delta\lambda(t), \quad \lambda(\lambda^0, t) = \lambda^0$$

where $\Delta\lambda \triangleq \lambda - \lambda^*$, $\Delta\dot{\lambda}(t) \triangleq \frac{d\Delta\lambda(t)}{dt}$, and

$$\mathbf{H}(\lambda^*) \triangleq \nabla\mathbf{F}^{-1}(\lambda^*)\mathbf{D}(\alpha)\nabla\mathbf{F}(\lambda^*). \tag{4.4.22}$$

Since the matrix $\mathbf{H}(\lambda^*)$ is a similarity transform of the diagonal matrix $\mathbf{D}(\alpha)$ consisting of the scaling vector $\alpha \in \Re_+^m$, they have the same eigenvalues. Thus, for a specified $\alpha_i = \bar{\alpha}, i = 1, \ldots, m$, the matrix $\mathbf{H}(\lambda^*) = \bar{\alpha}\mathbf{I}_m$. Accordingly, the step-size $h_k = h, \forall k$, depends on $\bar{\alpha} > 0$, i.e, the largest eigenvalue of the matrix $\mathbf{H}(\lambda^*)$. Therefore, a bigger step-size combined with a smaller scaling parameter $\bar{\alpha}$ can create a faster convergent algorithm.

Chapter 5

Application Algorithms: Continuous-Time EC Filtering Problems

5.1 Introduction

The continuous-time EC filtering problems consist of two major classes: continuous-time EC filtering problem with L^2 orthonormal basis; and the robustness of the continuous-time EC optimal filter design problem in L^2 Hilbert space. In this chapter, we give an approach for solving both types of continuous-time EC filtering problem in L^2 Hilbert basis without resorting to the discretization of any of the functions. More specifically, using the Lagrangian duality theory in combination with Carathéodory's dimensionality theory, the continuous-time EC filtering problem with L^2 orthonormal basis (semi-infinite programming problem) is reduced to an equivalent finite dual optimization problem discussed in Section 5.2.

In Section 5.3, the robust continuous-time EC optimal filter design problem in L^2 Hilbert space is considered. Using the smoothing technique [28, 56], the semi-infinite constrained optimization problem is converted into an equivalent constrained optimization problem with integral cost and strictly convex constraint. It is shown in [56, 62] that solving the semi-infinite constrained optimization problem is equivalent to solving a sequence of finite constrained optimization problems with integral cost. Numerical examples involving the orthonormal Laguerre series are solved for both classes of continuous-time EC filtering problem in Section 5.4.

The main references for this chapter are [58, 57, 59, 62].

5.2 EC Filtering Problem with L^2 Orthonormal Basis

The EC filtering problems was initially posed in the continuous-time domain as a constrained L^2 space optimization problem [12]. However, only the discretized version has been solved using various approaches, e.g., [12, 66]. The EC filtering problem considered in [12] is formulated in terms of discrete-time versions of the input signal, the filter and the output response and as such can only be an approximation to the continuous-time problem. In [66], the EC filtering problem is formulated in terms of a continuous-time filter and input signal. However, only a discrete-time version of the filter output and the output mask is considered.

With the help of the general frame work of the semi-infinite constrained convex QP problem discussed in Chapter 3, we can handle the same class of continuous-time EC filtering problem as in [66] in this section without resorting to the discretization of any of the functions. Carathéodory's dimensional theorem [51] is used together with the semi-infinite constrained convex programming problem to obtain a dual finite dimensional optimization problem. The dual problem is equivalent to the original continuous-time EC filtering problem. Two algorithms based on the space transformation and the gradient flow techniques [15, 16, 57] are developed for solving the dual optimization problem. Instead of discretizing the continuous-time problem using a sampling rate sufficiently high to capture enough information to approximate the optimal solution, our approach seeks only a few crucial time points at which the envelope constraints are active. It is shown that these active points provide enough information for finding the optimal filter such that the corresponding output response fits into the output mask. Therefore, the new approach leads to a computationally tractable method for obtaining the optimal filter with a guarantee that the solution meets the constraints. In contrast, a problem with methods that employ discrete-time approximations is that there is no guarantee that the output mask constraints will be met.

5.2.1 Dual Semi-infinite EC Filtering Problem

In developing the characterization of the continuous-time EC optimal filter, we first convert the continuous-time EC filtering problem with inequality constraints into a dual semi-infinite programming problem with simple constraints by utilizing the Lagrangian duality theory.

5.2.1.1 Continuous Dual Parameterization

Consider the continuous-time EC filtering problem (2.2.10). Assume that there exists a $\mathbf{x}^0 \in \Re^n$ such that Slater's constraint qualification given in Assumption 3.3.1 holds, i.e, $\mathbf{g}(\mathbf{x}^0, t) < 0_2$,

for all $t \in [0,T]$. By Theorem 3.3.1, we obtain the filter coefficient vector

$$\mathbf{x}(t,\lambda(t)) \;=\; -\frac{1}{2}\int_0^T \mathbf{A}'(t)d\lambda(t). \tag{5.2.1}$$

where $\lambda(t) = [\lambda_1(t), \lambda_2(t)]'$ is the Lagrange multiplier vector with $\lambda_i \in M([0,T],\Re_+), i = 1,2$. Substituting (5.2.1) into the objective function $f(\mathbf{x}) = \mathbf{x}'\mathbf{x}$, we obtain the following dual semi-infinite QP problem:

$$\begin{array}{ll} \min_{(t,\lambda(t))} & \phi(t,\lambda) \\ \text{subject to} & \lambda(t) \geq 0, \;\; t \in [0,T], \end{array} \tag{5.2.2}$$

where the dual cost function $\phi(t,\lambda(t))$ is given by

$$\phi(t,\lambda) \;=\; \frac{1}{4}\left\|\int_0^T \mathbf{A}'(t)d\lambda(t)\right\|_2^2 + \int_0^T \mathbf{b}'(t)d\lambda(t).$$

5.2.1.2 Characterization of Continuous Optimal Filter

To characterize the continuous EC optimal filter, we consider the filter coefficient vector $\mathbf{x} \in \Re^n$. Substituting the matrix $\mathbf{A}(t)$ given by (2.2.9) into (5.2.1) and associating with (2.2.2) and (2.2.6), the $(j+1)$th component of the filter coefficient vector is given by

$$\begin{aligned} x_j(t,\lambda) \;&=\; -\frac{1}{2}\int_0^T \theta_j(t)d\Delta\lambda(t) = -\frac{1}{2}\int_0^T \left(\int_0^\infty \varphi_j(\tau)s(t-\tau)d\tau\right) d\Delta\lambda(t) \\ &=\; \int_0^\infty \left(-\frac{1}{2}\int_0^T s(t-\tau)d\Delta\lambda(t)\right)\varphi_j(\tau)d\tau = \int_0^\infty u_n(\tau)\varphi_j(\tau)d\tau \end{aligned}$$

where $\Delta\lambda(t) = \lambda_1(t) - \lambda_2(t)$. Thus, the optimal filter u_n^* can be expressed in terms of the optimal Lagrange multiplier vector $\lambda^*(t) = [\lambda_1^*(t), \lambda_2^*(t)]'$, which is the solution of the semi-infinite dual problem (5.2.2), as follows:

$$u_n^*(\tau) = -\frac{1}{2}\int_0^T s(t-\tau)d\Delta\lambda^*(t), \quad \tau \in [0,\infty) \tag{5.2.3}$$

where $\Delta\lambda^*(t) = \lambda_1^*(t) - \lambda_2^*(t), t \in [0,T]$. We note from (5.2.3) that the optimal filter can be interpreted as consisting of a filter matched to the input signal followed by an equalizer determined by the optimal Lagrange multiplier vector $\lambda^*(t), t \in [0,T]$.

5.2.2 An Equivalent Finite EC Filtering Problem

Applying the results obtained in Section 3.4, the dual semi-infinite EC filtering problem (5.2.2) is converted into an equivalent finite dual optimization problem without discretization on any continuous function. Making use of Theorem 3.4.3 to the primal EC filtering problem (2.2.10), we obtain the following theorem which points out that the optimal solution to the dual problem (5.2.2) always includes a measure of finite support at no more than $2n$ points.

Theorem 5.2.1 *Let Slater's constraint qualification be satisfied. Assume that the optimal solution of the primal EC filtering problem (2.2.10) is achieved at* $\mathbf{x}^* \in \Re^n$. *Then the optimal solution to the corresponding dual problem (5.2.2) always includes a measure of finite support at no more than* $2n$ *points.*

In view of Theorem 5.2.1, (3.4.4) is reduced to

$$-\nabla f(\mathbf{x}^*) = \sum_{i=1}^{k}\sum_{j=1}^{2} \nabla_{\mathbf{x}} \mathbf{g}_j(\mathbf{x}^*, t_i)\lambda_{i,j}^*, \quad \text{for some } t_i \in \bar{\Omega}(\mathbf{x}^*)$$

where $k \leq 2n$, $\bar{\Omega}(\mathbf{x}^*) \triangleq \{t \in [0,T] | \mathbf{g}(\mathbf{x}^*, t) = 0_2\}$, and

$$\Lambda^{*'} = \left[\lambda_1^{*'}, \ldots, \lambda_k^{*'}\right] \in \Re_+^{2k} \text{ with } \lambda_i^{*'} = \left[\lambda_{i,1}^*, \lambda_{i,2}^*\right] \in \Re_+^2.$$

Accordingly, the dual semi-infinite EC filtering problem (5.2.2) can be converted into the following equivalent finite dimensional optimization problem.

$$\begin{array}{ll} \min\limits_{(\lambda(t_i), t_i)} & \phi(\mathbf{t}, \Lambda(\mathbf{t})) \\ \text{subject to} & \Lambda(\mathbf{t}) \geq 0_{2k} \end{array} \tag{5.2.4}$$

where these k, $k \leq 2n$, active time supporting points are denoted collectively by $\mathbf{t} \triangleq [t_1, \ldots, t_k]' \in \Re_+^k$, and the finite dual cost function is given by

$$\phi(\mathbf{t}, \Lambda(\mathbf{t})) = \frac{1}{4}\|\mathbf{A}'(\mathbf{t})\Lambda(\mathbf{t})\|_2^2 + \mathbf{b}'(\mathbf{t})\Lambda(\mathbf{t}). \tag{5.2.5}$$

Here $\Lambda(\mathbf{t}) \in \Re_+^{2k}$ with $\lambda(t_i) = [\lambda_{i,1}, \lambda_{i,2}]' \in \Re_+^2, i = 1, \ldots, k$, is given in (3.4.6), and $\mathbf{A}(\mathbf{t}) \in \Re^{2k \times n}$ and $\mathbf{b}(\mathbf{t}) \in \Re^{2k}$, with $\mathbf{b}(t_i) \in \Re^2$, $\forall i = 1, \ldots, k$, are given in (3.4.7).

Once $\mathbf{t}$ and the corresponding $\Lambda(\mathbf{t})$ are obtained, the filter coefficient vector $\mathbf{x}(\mathbf{t}, \Lambda(\mathbf{t}))$ and the noiseless output response defined by (2.2.4) can be constructed, respectively, as follows:

$$\mathbf{x}(\mathbf{t}, \Lambda(\mathbf{t})) = -\frac{1}{2}\mathbf{A}'(\mathbf{t})\Lambda(\mathbf{t}) \tag{5.2.6}$$

$$\psi_n(\mathbf{t}) = \Theta'(\mathbf{t})x, \tag{5.2.7}$$

where $\psi_n(\mathbf{t}) \in \Re^k$, $\Theta(\mathbf{t}) \in \Re^{n \times k}$ and $\Theta(t_i) \in \Re^n$ are, respectively, given by

$$\psi_n(\mathbf{t}) = \begin{bmatrix} \psi_n(t_1) \\ \vdots \\ \psi_n(t_k) \end{bmatrix}, \quad \Theta'(\mathbf{t}) = \begin{bmatrix} \Theta'(t_1) \\ \vdots \\ \Theta'(t_k) \end{bmatrix}, \quad \Theta(t_i) = \begin{bmatrix} \theta_0(t_i) \\ \vdots \\ \theta_{n-1}(t_i) \end{bmatrix},$$

while $\theta_j(t_i)$ is given by (2.2.6), for $i = 1, \ldots, k$ and $j = 0, \ldots, n-1$.

5.2.2.1 Characterization of Equivalent Discrete Optimal Filter

Following the steps used to establish the equivalent finite dimensional optimization problem (5.2.4), we are able to characterize the equivalent discrete optimal filter. First, we note that the filter coefficient vector given in (5.2.6) can be written as:

$$\mathbf{x}(\mathbf{t}, \Lambda(\mathbf{t})) = -\frac{1}{2}\sum_{i=1}^{k} \mathbf{A}'(t_i)\lambda(t_i) = -\frac{1}{2}\sum_{i=1}^{k} \Theta(t_i)\Delta\lambda_i.$$

where $\Delta\lambda_i \triangleq \lambda_{i,1} - \lambda_{i,2}$. Then, by combining it with (2.2.2) and (2.2.6), it follows that the $(j+1)$th component of the discrete filter coefficient vector is:

$$\begin{aligned} x_j &= -\frac{1}{2}\sum_{i=1}^{k} \theta_j(t_i)\Delta\lambda_i = -\frac{1}{2}\sum_{i=1}^{k} \left(\int_0^\infty \varphi_j(\tau)s(t_i-\tau)d\tau\right)\Delta\lambda_i \\ &= \int_0^\infty \left(-\frac{1}{2}\sum_{i=1}^{k} s(t_i-\tau)\Delta\lambda_i\right)\varphi_j(\tau)d\tau = \int_0^\infty u_n(\tau)\varphi_j(\tau)d\tau, \quad j = 0, \ldots n-1. \end{aligned}$$

Thus, the equivalent discrete optimal filter corresponding to the continuous optimal filter (5.2.3) can be expressed as:

$$u_n^*(\tau) = -\frac{1}{2}\sum_{i=1}^{k} s(t_i-\tau)\Delta\lambda_i^*, \quad \tau \in [0,\infty) \tag{5.2.8}$$

It is worth noting that the discrete optimal filter (5.2.8) consists of a matched filter followed by an equalizer whose weights are the elements of the Lagrange multiplier vector Λ^*. Furthermore, the equalizer has tap positions determined by the set of the time supporting points $\{t_i\}_{i=1}^k$.

5.2.3 Iterative Algorithms

In this subsection, we develop two iterative algorithms based on the BN method constructed in Section 4.5 for solving the equivalent finite dimensional dual problem (5.2.4).

Let $\eta = [\mathbf{t}', \Lambda']' \in \Re_+^{3k}$ and consider the quadratic component-wise space transformation function (4.4.3) with the coordinate vector vector $\mathbf{y} = [y_1, \ldots, y_{3k}]' \in \Re^{3k}$. Following the BN method developed in Section 4.5, we obtain the following iterative scheme

$$\eta^{j+1} = \eta^j - h_j \nabla\mathbf{F}^{-1}(\eta^j)\mathbf{D}(\alpha)\mathbf{F}(\eta^j) \tag{5.2.9}$$

where $\mathbf{D}(\alpha) \triangleq diag\,(\alpha_1, \ldots, \alpha_{3k}) \in \Re_+^{3k\times 3k}$ is a diagonal matrix containing components of a scaling vector $\alpha \triangleq [\alpha_1, \ldots, \alpha_{3k}]' \in \Re_+^{3k}$, the barrier function $\mathbf{F}(\eta) \in \Re^{3k}$, and the Jacobian matrix $\nabla\mathbf{F}(\eta) \in \Re^{3k\times 3k}$ are, respectively, defined by

$$\mathbf{F}(\eta) = \mathbf{D}(\eta)\nabla\phi(\eta) = \begin{bmatrix} \mathbf{D}(\mathbf{t})\nabla_{\mathbf{t}}\phi(\mathbf{t},\Lambda) \\ \mathbf{D}(\Lambda)\nabla_{\Lambda}\phi(\mathbf{t},\Lambda) \end{bmatrix}, \tag{5.2.10}$$

$$\nabla \mathbf{F}(\eta) = \mathbf{D}(\nabla\phi(\eta)) + \mathbf{D}(\eta)\nabla^2\phi(\eta) \tag{5.2.11}$$
$$= \begin{bmatrix} \mathbf{D}(\nabla_{\mathbf{t}}\phi(\mathbf{t},\Lambda)) + \mathbf{D}(\mathbf{t})\nabla^2_{\mathbf{t}}\phi(\mathbf{t},\Lambda) & \mathbf{D}(\mathbf{t})\nabla^2_{(\mathbf{t},\Lambda)}\phi(\mathbf{t},\Lambda) \\ \mathbf{D}(\Lambda)\nabla^2_{(\Lambda,\mathbf{t})}\phi(\mathbf{t},\Lambda) & \mathbf{D}(\nabla_{\Lambda}\phi(\mathbf{t},\Lambda)) + \mathbf{D}(\Lambda)\nabla^2_{\Lambda}\phi(\mathbf{t},\Lambda) \end{bmatrix},$$

while $\nabla_{\mathbf{t}}\phi(\mathbf{t},\Lambda)$, $\nabla_{\Lambda}\phi(\mathbf{t},\Lambda)$, $\nabla^2_{\mathbf{t}}\phi(\mathbf{t},\Lambda)$, $\nabla^2_{(\mathbf{t},\Lambda)}\phi(\mathbf{t},\Lambda)$, $\nabla^2_{(\Lambda,\mathbf{t})}\phi(\mathbf{t},\Lambda)$ and $\nabla^2_{\Lambda}\phi(\mathbf{t},\Lambda)$ are all defined in Appendix C. Substituting η^{j+1} in (5.2.9) into $\mathbf{x}^{j+1}$ given by (5.2.6), we obtain the following simple iterative algorithm for solving the continuous-time EC filtering problem (2.2.10).

Algorithm 5.2.1 *Set $j = 0$. Choose an initial point $\eta^0 \in \Re^{3k}_+$, a stopping criterion ϵ_η, and a proper step-size h_j.*

1. *Let $\mathbf{d}^j = \nabla\mathbf{F}^{-1}(\eta^j)\mathbf{D}(\alpha)\mathbf{F}(\eta^j)$ be a search direction where the matrices $\mathbf{F}(\eta^j)$ and $\nabla\mathbf{F}(\eta^j)$ are, respectively, given by (5.2.10) and (5.2.11).*

   Calculate the following scheme

$$\eta^{j+1} = \eta^j - h_j\mathbf{d}^j \tag{5.2.12}$$

   in which the step-size h_j is chosen such that

$$\nabla\phi'(\eta^j)\mathbf{d}^j < 0 \quad \textit{and} \quad \eta^j > 0_{3k} \tag{5.2.13}$$

2. *Use η^{j+1} to obtain $\mathbf{x}^{j+1}$ and f^{j+1} as follows:*

$$\mathbf{x}^{j+1} = -\frac{1}{2}\mathbf{A}'(\mathbf{t}^{j+1})\Lambda^{i+1}$$
$$f^{j+1} = f(\mathbf{x}^{j+1}).$$

   If $\mathbf{x}^{j+1}$ satisfies the continuous constraints of the EC filtering problem (2.2.10) and the stopping criterion $\|\mathbf{d}^{j+1}\|_2 < \epsilon_\eta$ is satisfied, then terminate; otherwise return to Step 1 with j replaced by $j+1$.

Remark 5.2.1

1) In Step 1, there exists, by Theorem 4.4.2, a fixed step-size $0 < h_j = h < \frac{2}{\max\{\alpha_i : 1 \le i \le 3k\}}$ such that conditions (5.2.13) are satisfied for all j. Furthermore, if the Jacobian matrix $\nabla\mathbf{F}(\eta)$ satisfies a Lipschitz condition in a neighborhood of η^* and $\alpha_i = e \simeq 2.71828$, $\forall i = 1, \ldots, 3k$, then the sequence $\{\eta^j\}_{j=0}^{\infty}$ generated by the scheme (5.2.9) converges to η^* locally and at a quadratic rate.

2) Many simulation studies have been carried out by using Algorithm 5.2.1 for various EC filter design problems. Our experience indicates that minimizing the time supporting point t_i and the corresponding dual variable λ_i, $\forall i = 1, \ldots, k$, simultaneously may cause numerical problems. It is due to two causes:

- *The equivalent finite optimization problem is nonconvex with respect to the time supporting point* $t_i, i = 1, \ldots, k$.

- *A large error is accumulated in the computation of the second derivatives involving the dual vector* Λ.

The second cause is more severe for the example considered in this chapter. To alleviate this difficulty, we propose an alternative algorithm to solve the continuous-time EC filtering problem (2.2.10).

Define

$$\begin{cases} \mathbf{G}(\mathbf{t}) &= \mathbf{D}(\mathbf{t})\nabla_{\mathbf{t}}\phi(\mathbf{t},\Lambda) \in \Re^{k}, \\ \mathbf{G}(\Lambda) &= \mathbf{D}(\Lambda)\nabla_{\Lambda}\phi(\mathbf{t},\Lambda) \in \Re^{2k} \end{cases}$$

and

$$\begin{cases} \nabla_{\mathbf{t}}\mathbf{G}(\mathbf{t}) &= \mathbf{D}\left(\nabla_{\mathbf{t}}\phi(\mathbf{t},\Lambda)\right) + \mathbf{D}(\mathbf{t})\nabla^2_{\mathbf{t}}\phi(\mathbf{t},\Lambda) \in \Re^{k\times k}, \\ \nabla_{\Lambda}\mathbf{G}(\Lambda) &= \mathbf{D}\left(\nabla_{\Lambda}\phi(\mathbf{t},\Lambda)\right) + \mathbf{D}(\Lambda)\nabla^2_{\Lambda}\phi(\mathbf{t},\Lambda) \in \Re^{2k\times 2k}. \end{cases}$$

Algorithm 5.2.2 *Set* $i = j = 0$. *Let* $\mathbf{D}(\alpha) = \mathbf{D}(e) \in \Re^{2k\times 2k}_{+}$, *and* $\mathbf{D}(\beta) = \mathbf{D}(e) \in \Re^{k\times k}_{+}$ *where* $e \simeq 2.71828$. *Choose two initial points* $\mathbf{t}^0 \in \Re^{k}_{+}$ *and* $\Lambda^0 \in \Re^{2k}_{+}$, *two proper step-sizes* $h^i_{\mathbf{t}}$ *and* h^j_{Λ}, *and three stopping criteria* ϵ_f, $\epsilon_{\mathbf{t}}$, *and* ϵ_{Λ}.

1. *Fix* $\Lambda^i_* = \Lambda$ *and let* $\mathbf{d}^i_{\mathbf{t}} = \nabla_{\mathbf{t}}\mathbf{G}^{-1}(\mathbf{t}^i)\mathbf{D}(\beta)\mathbf{G}(\mathbf{t}^i)$ *be a search direction.*
   Calculate the following scheme

$$\mathbf{t}^{i+1} \;=\; \mathbf{t}^i - h^i_{\mathbf{t}}\mathbf{d}^i_{\mathbf{t}}$$

   in which the step-size $h^i_{\mathbf{t}}$ *is chosen such that*

$$\nabla_{\mathbf{t}}\phi'(\mathbf{t}^{i+1},\Lambda)\mathbf{d}^{i+1}_{\mathbf{t}} \;<\; 0. \tag{5.2.14}$$

2. *Fix* $\mathbf{t}^{i+1} = \mathbf{t}$ *and complete Steps (a) and (b).*
   (a) Let $\mathbf{d}^j_{\Lambda} = \nabla_{\Lambda}\mathbf{G}^{-1}(\Lambda^j)\mathbf{D}(\alpha)\mathbf{G}(\Lambda^j)$ *be an another search direction and perform the following scheme to obtain the optimum* Λ^{i+1}_*:

$$\Lambda^{j+1} \;=\; \Lambda^j - h^j_{\Lambda}\mathbf{d}^j_{\Lambda}, \tag{5.2.15}$$

   where the step-size h^j_{Λ} *is chosen such that*

$$\nabla_{\Lambda}\phi'(\mathbf{t},\Lambda^{j+1})\mathbf{d}^{j+1}_{\Lambda} < 0 \quad \textit{and} \quad \Lambda^{j+1} \geq 0_{2k}. \tag{5.2.16}$$

   (b) If $\Lambda^{j+1} \geq 0_{2k}$ *and the stopping criterion* $\|\mathbf{d}^{j+1}_{\Lambda}\|_2 \leq \epsilon_{\Lambda}$ *is satisfied, then stop and set* $\Lambda^{i+1}_* = \Lambda^{j+1}$; *otherwise return to Step (a) with* j *replaced by* $j+1$.

3. Use $(\mathbf{t}^{i+1}, \Lambda_*^{i+1})$ *to obtain* $\mathbf{x}^{i+1}$ *and* f^{i+1} *as follows:*

$$\begin{aligned} \mathbf{x}^{i+1} &= -\frac{1}{2}\mathbf{A}'(\mathbf{t}^{i+1})\Lambda_*^{i+1}, \\ f^{i+1} &= f(\mathbf{x}^{i+1}). \end{aligned} \tag{5.2.17}$$

If $\mathbf{x}^{i+1}$ *satisfies the continuous constraints of the EC filtering problem (2.2.10) and the stopping criteria* $|f^{i+1}| \leq \epsilon_f$ *and* $\|\mathbf{d}_{\mathbf{t}}^{i+1}\|_2 \leq \epsilon_{\mathbf{t}}$ *are satisfied, then stop; otherwise return to Step 1 with* i *replaced by* $i+1$.

Remark 5.2.2

1) By Theorem 4.4.2, there exist fixed step-sizes $h_{\mathbf{t}}^i = h_{\mathbf{t}}$ *and* $h_\Lambda^j = h_\Lambda$ *such that conditons in (5.2.14) and (5.2.16) are, respectively, satisfied for all* i *and* j.

2) There are two important issues in the implementation of the above algorithm:

(a) The choice of a good initial time supporting point $\mathbf{t}^0$.

To obtain a good initial point $\mathbf{t}^0$, *we first discretize the time interval* $[0, T]$, *such that the dual problem (5.2.2) has a finite number of constraints. We then use Step 2 of Algorithm 5.2.2 to obtain the dual vector* Λ_*^0 *corresponding to the initial supporting point vector* $\mathbf{t}^0 = [t_1^0, \ldots, t_k^0]'$. *Clearly, each* Λ_{*j}^0, *where* $\Lambda_{*j}^0 = [\lambda_{j,1}^0, \lambda_{j,2}^0]'$, *corresponds to a time supporting point* $t_j^0 \in [0, T]$ *such that the active time supporting point of the output constraint is achieved at* $t_j^0 \in \{t_1^0, \ldots, t_k^0\}$ *if either* $\lambda_{j,1}^0$ *or* $\lambda_{j,2}^0$ *is nonzero. This simple test enables us not only to select a good initial supporting point vector* $\mathbf{t}^0$, *but also to estimate the dimension of* $\mathbf{t}^i$ *at the* i*th iteration in terms of the number of the active supporting points.*

(b) The determination of dimension of the supporting points $\mathbf{t}^i$ *at the* i*th iteration.*

In view of results obtained in Theorem 5.2.1, the dimension of the supporting points $\mathbf{t}^i$ *is* $k \leq 2n$. *However, extensive simulation experience indicates that* k *is usually much smaller than* $2n$.

In view of Remark 5.2.2, we present Algorithm 5.2.2 as flowcharts in Figure 5.1 where initialization, processing module 1, and processing module 2 are designed as modules. More specifically, the initialization module is used to determine a good initial point $\mathbf{t}^0$ and the dimension of active supporting points $\mathbf{t}$ at each iteration. Furthermore, for a fixed $\Lambda = \Lambda_*^i$, where i denotes the ith iteration, the processing module 1 is designed to search for a new active supporting point vector $\mathbf{t}^{i+1}$, whereas the design of processing module 2 is for finding an optimum Λ_*^{i+1} with the supporting point vector $\mathbf{t}^{i+1}$ obtained from the previous processing taken as a fixed parameter.

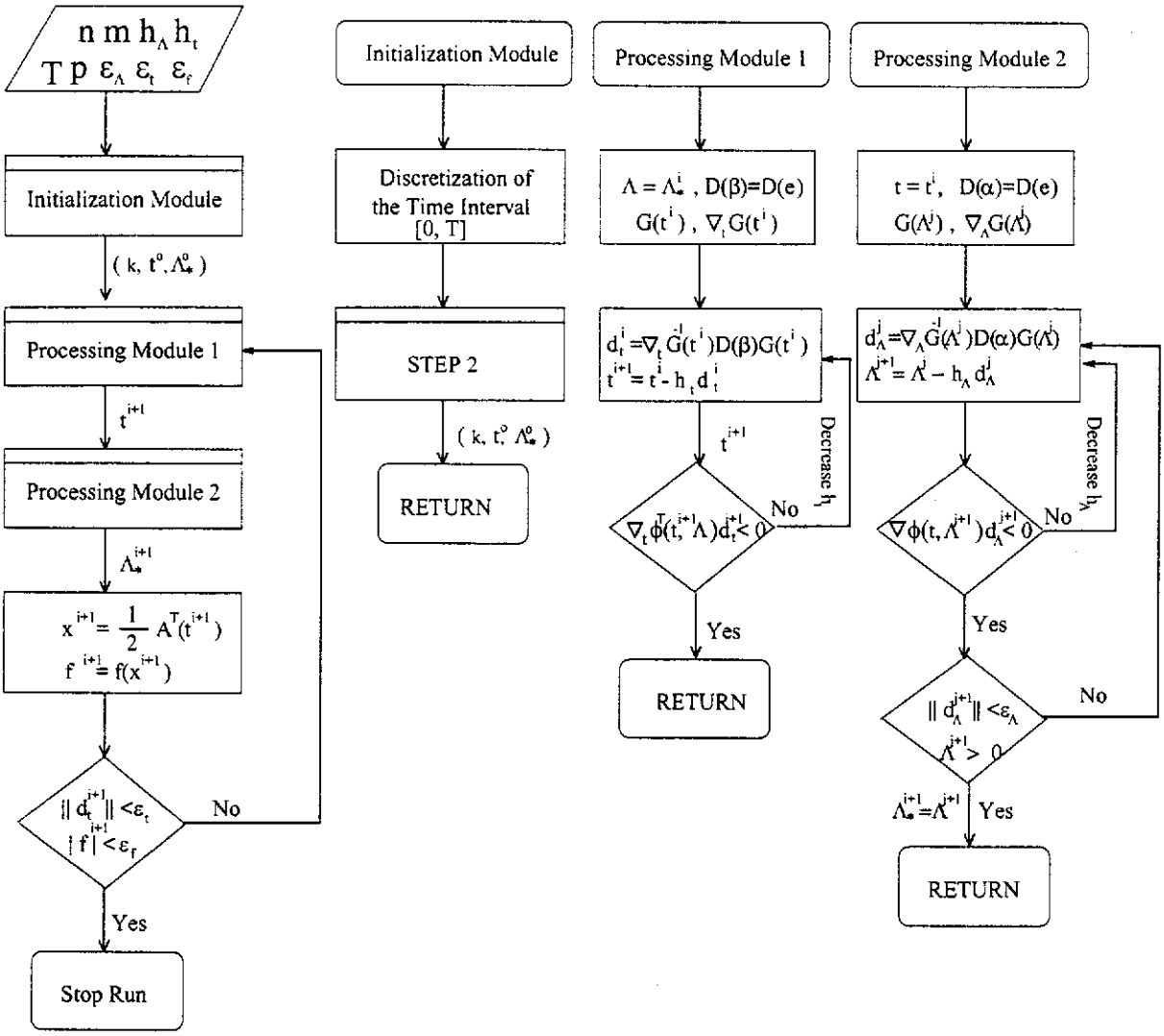

Figure 5.1: Flowcharts for Algorithm 5.2.2.

For a specific active point vector $\mathbf{t^i}$, the schemes (5.2.15) and (5.2.17) are equivalent to the following dual finite dimensional minimization problem.

$$\begin{aligned} \min \quad & \phi\left(\Lambda(\mathbf{t^i})\right) \\ \text{subject to} \quad & \Lambda(\mathbf{t^i}) \geq 0_{2k} \end{aligned} \tag{5.2.18}$$

where the cost function is given by

$$\phi(\Lambda(\mathbf{t^i})) \;=\; \frac{1}{4} \left\| \mathbf{A}'(\mathbf{t^i}) \Lambda(\mathbf{t^i}) \right\|_2^2 + \Lambda'(\mathbf{t^i}) \mathbf{b}(\mathbf{t^i}),$$

while $\mathbf{A}(\mathbf{t}^i) \in \Re^{2k\times n}$ and $\mathbf{b}(\mathbf{t}^i) \in \Re^{2k}$ are, respectivly, given by

$$\mathbf{A}(\mathbf{t}^i) = \begin{bmatrix} \mathbf{A}(t_1^i) \\ \vdots \\ \mathbf{A}(t_k^i) \end{bmatrix} \text{ with } \mathbf{A}(t_j^i) = \begin{bmatrix} \Theta'(t_j^i) \\ -\Theta'(t_j^i) \end{bmatrix} \in \Re^{2\times n}, \text{ and } \Theta(t_j^i) = \begin{bmatrix} \theta_0(t_j^i) \\ \vdots \\ \theta_{n-1}(t_j^i) \end{bmatrix} \in \Re^n$$

and

$$\mathbf{b}'(\mathbf{t}^i) = \left[\mathbf{b}'(t_1^i), \ldots, \mathbf{b}'(t_k^i)\right] \text{ with } \mathbf{b}(t_j^i) = \begin{bmatrix} \varepsilon^+(t_j^i) \\ \varepsilon^-(t_j^i) \end{bmatrix} \in \Re^2, \forall j = 1, \ldots, k.$$

The corresponding primal finite convex programming problem can also be obtained:

$$\begin{aligned} \min \quad & f(\mathbf{x}) \\ \text{subject to} \quad & \mathbf{g}(\mathbf{x}, \mathbf{t}^i) = \mathbf{A}(\mathbf{t}^i)\mathbf{x} - \mathbf{b}(\mathbf{t}^i) \leq 0_{2k} \end{aligned} \tag{5.2.19}$$

where $\mathbf{g}(\mathbf{x}, \mathbf{t}^i) = [\mathbf{g}'(\mathbf{x}, t_1^i), \ldots, \mathbf{g}'(\mathbf{x}, t_k^i)]' \in \Re^{2k}$, while $\mathbf{g}(\mathbf{x}, t_j^i) \in \Re^2$, $\forall j = 1, \ldots, k$.

Define two feasible solution sets corresponding to the primal semi-infinite EC filtering problem (2.2.10) and the primal equivalent finite EC filtering problem (5.2.19), respectively, as follows:

$$\begin{aligned} \mathbf{X}_1 &\triangleq \{\mathbf{x} \in \Re^n : \mathbf{g}(\mathbf{x}, t) \leq 0_2, \forall t \in [0, T]\} \\ \mathbf{X}_2 &\triangleq \{\mathbf{x} \in \Re^n : \mathbf{g}(\mathbf{x}, t_j) \leq 0_2, j = 1, \ldots, k\}. \end{aligned}$$

Theorem 5.2.2 *Let the optimal solutions $\bar{\mathbf{x}} \in \mathbf{X}_2$ and $\mathbf{x}^* \in \mathbf{X}_1$. If $\bar{\mathbf{x}} \in \mathbf{X}_1$, then $\bar{\mathbf{x}} = \mathbf{x}^*$.*

Proof: Trivially, $\mathbf{X}_1 \subseteq \mathbf{X}_2$. Let $\mathbf{x}^* \triangleq \arg\min\{f(\mathbf{x}) : \mathbf{x} \in \mathbf{X}_1\}$ and $\bar{\mathbf{x}} \triangleq \arg\min\{f(\mathbf{x}) : \mathbf{x} \in \mathbf{X}_2\}$. It is clear that $f(\bar{\mathbf{x}}) \leq f(\mathbf{x}^*)$. If $\bar{\mathbf{x}} \in \mathbf{X}_1$, then $\bar{\mathbf{x}}$ is an optimal solution of the primal semi-infinite EC filtering problem (2.2.10), i.e., $f(\bar{\mathbf{x}}) = f(\mathbf{x}^*)$. Since f is strictly convex in $\mathbf{x}$, we conclude that $\bar{\mathbf{x}} = \mathbf{x}^*$. ∎

Remark 5.2.3 *If Algorithm 5.2.2 is terminated at $\mathbf{x}^i = \bar{\mathbf{x}}$ because the continuous constraints of the EC filtering problem (2.2.10) is satisfied, then $\bar{\mathbf{x}} \in \mathbf{X}_1$ which implies $f(\bar{\mathbf{x}}) \geq f(\mathbf{x}^*)$. By Theorem 5.2.2, we conclude that $\bar{\mathbf{x}} = \mathbf{x}^*$. However, the algorithm may fail to find an $\bar{\mathbf{x}}$ such that $\bar{\mathbf{x}} \in \mathbf{X}_1$ if the initial supporting points $\mathbf{t}^0$ are badly chosen.*

5.3 Robust Optimal EC Filtering Problem

For the EC filtering problem introduced in the previous sections, the output response of the optimum filter to the prescribed input signal touches the output boundaries at some points.

Consequently, any disturbance in the prescribed input signal or errors in the implementation of the optimal filter could result in the output constraints being violated. Clearly, it is practically important to design filters which are robust against such disturbances.

One approach for dealing with this problem is to maximize the minimum distance between the output response and the output envelope constraints, subject to a specified allowable increase in the optimal noise power gain. This formulation, which is called constraint robustness formulation (CRF), was first proposed in [4, 74] as a semi-infinite constrained optimization problem. However, only a discrete-time version of the time-domain constraints is considered. In this section, we handle directly the same class of the semi-infinite constrained optimization problem without resorting to the discretization of any of the functions involved. Using a smoothing technique reported in [28, 56], the semi-infinite constrained problem is converted into an equivalent constrained optimization problem with integral cost and strictly convex constraint. It is shown in [56, 62] that solving the semi-infinite constrained optimization problem is equivalent to solving a sequence of finite constrained optimization problems with integral cost.

5.3.1 Robust Envelope-Constrained Filter

Consider the constraint robustness formulation (CRF) of the problem (2.2.12) with support in $[0, T]$. For a given weighted constrained robustness margin σ_β defined in (2.2.11), we define the feasible region of the CRF problem in $\mathbf{x}$ as follows:

$$\mathcal{F}_{\sigma_\beta}(\mathbf{x}) = \left\{\mathbf{x} \in \Re^n : |\psi_n(\mathbf{x}, t) - d(t)| \leq \varepsilon(t) - \beta(t)\sigma_\beta, t \in [0, T], \|\mathbf{x}\|_2^2 \leq (1+\delta)\|\mathbf{x}^*\|_2^2\right\}$$

where $d(t)$ is a desired pulse shape, and $\varepsilon(t)$ is an error tolerance band about $d(t)$.

We characterize the sensitivity of the feasible point in the set $\mathcal{F}_{\sigma_\beta}$ with different values of σ_β in the following proposition.

Proposition 5.3.1 *Let σ_β^1 and σ_β^2 be such that $\mathbf{x}_{\sigma_\beta^1} \in \mathcal{F}_{\sigma_\beta^1}(\mathbf{x})$ and $\mathbf{x}_{\sigma_\beta^2} \in \mathcal{F}_{\sigma_\beta^2}(\mathbf{x})$. If $0 < \sigma_\beta^1 \leq \sigma_\beta^2$, then*

$$\mathcal{F}_{\sigma_\beta^2}(\mathbf{x}) \subseteq \mathcal{F}_{\sigma_\beta^1}(\mathbf{x}) \quad \textit{and} \quad \|\mathbf{x}_{\sigma_\beta^1}\|_2 \leq \|\mathbf{x}_{\sigma_\beta^2}\|_2. \tag{5.3.1}$$

Proof: Clearly, $|\psi_n(\mathbf{x}, t) - d(t)| \leq \varepsilon(t) - \beta(t)\sigma_\beta^2 \leq \varepsilon(t) - \beta(t)\sigma_\beta^1, \quad t \in [0, T]$. ∎

Remark 5.3.1

1) Proposition 5.3.1 indicates that the optimum σ_β^* must be a bounded positive constant. Otherwise, there is no solution to the CRF problem (2.2.12) for any finite σ_β. In addition, a feasible point with a bigger constraint robustness margin can be found at the expense of the increased

noise gain $\|\mathbf{x}\|^2$.

2) By (5.3.1), it is clear that finding the maximum σ_β *by solving the CRF problem (2.2.12) is equivalent to finding the maximum* σ_β *for which the set* $\mathcal{F}_{\sigma_\beta}(\mathbf{x})$ *remains non-empty. Thus, for a given weighting function* $\beta > 0$*, we can begin with a* $\sigma_\beta \geq 0$ *and check if the corresponding set* $\mathcal{F}_{\sigma_\beta}(\mathbf{x})$ *remains nonempty. If it does, we can increase the value of* σ_β *and repeat the process. On the other hand, if the set* $\mathcal{F}_{\sigma_\beta}(\mathbf{x})$ *becomes empty for a given* σ_β*, it follows from Proposition 5.3.1 that the value of* σ_β *needs to be reduced.*

In view of Remark 5.3.1, we see that the golden section search method [44] can be applied to locate the maximum value of σ_β to within a required interval of uncertainty. To check the feasibility of the set $\mathcal{F}_{\sigma_\beta}(\mathbf{x})$ for a given σ_β, we use the idea reported in [28] to handle the continuous inequality constraints.

Let the weighted constraints in the CRF problem (2.2.12) be defined as:

$$\begin{cases} g_1(\mathbf{x}, t|\sigma_\beta) & \triangleq & \beta(t)\sigma_\beta - \psi_n(\mathbf{x}, t) + \varepsilon^-(t) \\ g_2(\mathbf{x}, t|\sigma_\beta) & \triangleq & \beta(t)\sigma_\beta + \psi_n(\mathbf{x}, t) - \varepsilon^+(t). \end{cases}$$

Clearly, for a given $\sigma_\beta \geq 0$, $g_1(\mathbf{x}, t|\sigma_\beta)$ and $g_2(\mathbf{x}, t|\sigma_\beta)$ satisfy the following conditions:
1) $g_j(\mathbf{x}, t|\sigma_\beta)$, $j = 1, 2$, are continuous in $t \in [0, T]$, and for each $\mathbf{x}$, $\frac{\partial g_j(\mathbf{x}, t|\sigma_\beta)}{\partial t}$ is piecewise continuous in $t \in [0, T]$.
2) $g_j(\mathbf{x}, t|\sigma_\beta)$, $j = 1, 2$ are continuously differentiable with respect to $\mathbf{x}$ for almost all $t \in [0, T]$.
Then, for a given σ_β, we construct the following optimization problem which contains a strictly convex constraint. This optimization problem is used to check the feasibility of the constraints of the CRF problem (2.2.12) corresponding to the given σ_β.

$$\begin{array}{rl} \min & J_\epsilon(\mathbf{x}|\sigma_\beta), \quad \mathbf{x} \in \Re^n \\ \text{subject to} & \|\mathbf{x}\|_2^2 \leq (1+\delta)\|\mathbf{x}^*\|_2^2 \end{array} \tag{5.3.2}$$

where $\epsilon > 0$ is an accuracy parameter, and the integral cost function J_ϵ is given by

$$J_\epsilon(\mathbf{x}|\sigma_\beta) = \int_0^T \Big(\Phi_\epsilon(g_1(\mathbf{x}, t|\sigma_\beta)) + \Phi_\epsilon(g_2(\mathbf{x}, t|\sigma_\beta)) \Big) dt,$$

while the smoothing constraint transcription $\Phi_\epsilon(\cdot)$ is differentiable and defined by

$$\Phi_\epsilon(g_j) = \begin{cases} 0 & \text{if } g_j < -\epsilon \\ \frac{(g_j+\epsilon)^2}{4\epsilon} & \text{if } -\epsilon \leq g_j \leq \epsilon \\ g_j & \text{if } g_j > \epsilon. \end{cases}$$

Remark 5.3.2

1) $\Phi_\epsilon(g_j), j = 1, 2$*, possess the following properties:*

- $\Phi_\epsilon(g_j)$ *is once continuously differentiable and piece-wise twice continuously differentiable.*
- $\Phi_\epsilon(g_j)$ *is convex and monotonically non-decreasing.*

2) The accuracy parameter in the problem (5.3.2) is required to be positive but not necessarily be small. In fact, if the feasible space is sufficiently large, a larger ϵ *may be chosen so as to enhance the convergence characteristic of the algorithm. Otherwise, a smaller* ϵ *should be chosen.*

The next two propositions contain, respectively, necessary and sufficient conditions for feasibility of the set $\mathcal{F}_{\sigma_\beta}(\mathbf{x})$ for a given σ_β (for details, see [28]).

Proposition 5.3.2 {*Necessary condition*}
For a given $\sigma_\beta \geq 0$ *and a given* $\epsilon > 0$, *let* $\bar{\mathbf{x}} \in \mathcal{F}_{\sigma_\beta}(\mathbf{x})$. *If* $\mathcal{F}_{\sigma_\beta}(\mathbf{x}) \neq \emptyset$, *then*

$$J_\epsilon(\bar{\mathbf{x}}|\sigma_\beta) \leq \frac{\epsilon T}{2}. \tag{5.3.3}$$

Proposition 5.3.3 {*Sufficient condition*}
Let $\bar{\mathbf{x}}$ *be such that*

$$J_\epsilon(\bar{\mathbf{x}}|\sigma_\beta) \leq \frac{\epsilon}{8}\min\left\{\frac{\epsilon}{4M}, T\right\} \tag{5.3.4}$$

where

$$M = \max\left\{\left|\frac{\partial g_j(\bar{\mathbf{x}}, t|\sigma_\beta)}{\partial t}\right| : t \in [0,T], j = 1,2\right\}.$$

Then $\bar{\mathbf{x}} \in \mathcal{F}_{\sigma_\beta}(\mathbf{x})$.

Associated with Propositions 5.3.2- 5.3.3, we can determine whether an $\mathbf{x}$ is such that $\mathcal{F}_{\sigma_\beta}(\mathbf{x}) \neq \emptyset$ for a given σ_β by solving the constrained minimization problem (5.3.2).

Remark 5.3.3 *The constrained minimization problem (5.3.2) is solvable by gradient-based quasi-Newton methods. We note that for quasi-Newton methods, the cost and constraint function values and their gradients need to be calculated. The gradient of the cost function* $J_\epsilon(\mathbf{x}|\sigma_\beta)$ *with respect to* $\mathbf{x}$ *is given by*

$$\nabla J_\epsilon(\mathbf{x}|\sigma_\beta) = \int_0^T \left(\frac{\partial \Phi_\epsilon(g_1(\mathbf{x}, t|\sigma_\beta))}{\partial \mathbf{x}} + \frac{\partial \Phi_\epsilon(g_2(\mathbf{x}, t|\sigma_\beta))}{\partial \mathbf{x}}\right) dt,$$

where $\frac{\partial \Phi_\epsilon(g_j(\mathbf{x},t|\sigma_\beta))}{\partial \mathbf{x}} \in \Re^N, j = 1,2,$ *are defined as*

$$\frac{\partial \Phi_\epsilon(g_j(\mathbf{x}, t|\sigma_\beta))}{\partial \mathbf{x}} = \begin{cases} 0 & \text{if } g_j(\mathbf{x}, t|\sigma_\beta) < -\epsilon \\ \left(\frac{g_j(\mathbf{x},t|\sigma_\beta)+\epsilon}{2\epsilon}\right)\frac{\partial g_j(\mathbf{x},t|\sigma_\beta)}{\partial \mathbf{x}} & \text{if } -\epsilon \leq g_j(\mathbf{x}, t|\sigma_\beta) \leq \epsilon \\ \frac{\partial g_j(\mathbf{x},t|\sigma_\beta)}{\partial \mathbf{x}} & \text{if } g_j(\mathbf{x}, t|\sigma_\beta) > \epsilon. \end{cases}$$

5.3.2 Iterative Algorithms

Let the cost function $J_\epsilon(\mathbf{x}|\sigma_\beta)$, that is piece-wise twice continuously differentiable with respect to $\mathbf{x}$ at the iterate $\mathbf{x}^k$, be expressed as the following convex quadratic model

$$J_\epsilon(\mathbf{x}^k + \mathbf{d}|\sigma_\beta) \;=\; J_\epsilon(\mathbf{x}^k|\sigma_\beta) + \mathbf{d}'\nabla J_\epsilon(\mathbf{x}^k|\sigma_\beta) + \frac{1}{2}\mathbf{d}'\nabla^2 J_\epsilon(\mathbf{x}^k|\sigma_\beta)\mathbf{d} \tag{5.3.5}$$

Clearly, (5.3.5) produces a search direction $\mathbf{d}^k$ given by

$$\mathbf{d}^k \;=\; -\mathbf{H}^k\nabla J_\epsilon(\mathbf{x}^k|\sigma_\beta)$$

where $\mathbf{H}^k$ is constructed sequentially to approximate the inverse Hessian $\nabla^2 J_\epsilon^{-1}(\mathbf{x}^k|\sigma_\beta)$. Accordingly, quasi-Newton method is discussed in terms of updating $\mathbf{H}^k$ in the following algorithm that is used to determine whether a given σ_β is feasible when a feasible solution of the constrained minimization problem (5.3.2) is obtained. To efficiently update the matrix $\mathbf{H}^k$, the Broyden-Fletcher-Goldfarb-Shanno (BFGS) update formula [14] is applied to the following algorithm.

Algorithm 5.3.1 *Set $k = 0$ and $\mathbf{H}^0 = \mathbf{I}$. Given a weighted constraint robustness margin $\sigma_\beta \geq 0$ with weighting function $\beta > 0$, an accuracy paramter $\epsilon > 0$, and an appropriate step-size h_k.*

1. *Calculate the gradient $\nabla J_\epsilon(\mathbf{x}^k|\sigma_\beta)$ and the search direction $\mathbf{d}^k = -\mathbf{H}^k\nabla J_\epsilon(\mathbf{x}^k|\sigma_\beta)$. Perform the following iterative scheme to find a new point*

   $$\mathbf{x}^{k+1} \;=\; \mathbf{x}^k + h_k\mathbf{d}^k$$

   in which the step-size h_k is chosen such that

   $$\nabla J_\epsilon'(\mathbf{x}^k|\sigma_\beta)\mathbf{d}^k \;<\; 0.$$

2. *If $J_\epsilon(\mathbf{x}^k|\sigma_\beta) > \frac{\epsilon T}{2}$ then go to Step 4; otherwise, go to Step 3.*

3. *Check if the constraints of the CRF problem (2.2.12) are satisfied. If so, go to Step 5; otherwise, go to Step 4.*

4. *Update the gradient to obtain a new search direction $\mathbf{d}^{k+1} = -\mathbf{H}^{k+1}\nabla J_\epsilon(\mathbf{x}^{k+1}|\sigma_\beta)$ where the BFGS update formula for $\mathbf{H}^{k+1}$ is given by*

$$\mathbf{H}^{k+1} \;=\; \mathbf{H}^k + \frac{\left(\Delta\mathbf{x}^k - \mathbf{H}^k\Delta\mathbf{g}^k\right)\Delta\mathbf{x}^{k'} + \Delta\mathbf{x}^k\left(\Delta\mathbf{x}^k - \mathbf{H}^k\Delta\mathbf{g}^k\right)'}{\langle\Delta\mathbf{x}^k, \Delta\mathbf{g}^k\rangle} - \frac{\left\langle\Delta\mathbf{x}^k - \mathbf{H}^k\Delta\mathbf{g}^k, \Delta\mathbf{g}^k\right\rangle}{\langle\Delta\mathbf{x}^k, \Delta\mathbf{g}^k\rangle^2}\Delta\mathbf{x}^k\Delta\mathbf{x}^{k'}$$

where $\Delta \mathbf{x}^k = \mathbf{x}^{k+1} - \mathbf{x}^k$ *and* $\Delta \mathbf{g}^k = \nabla J_\epsilon(\mathbf{x}^{k+1}|\sigma_\beta) - \nabla J_\epsilon(\mathbf{x}^k|\sigma_\beta)$. *Set* $k = k+1$, *and go to Step 1.*

5. *Stop.* $\mathbf{x}^k$ *is a feasible point in* $\mathcal{F}_{\sigma_\beta}(\mathbf{x})$.

Remark 5.3.4 *If* $\mathbf{H}^0$ *is positive definite matrix and* $J_\epsilon(\mathbf{x}|\sigma_\beta)$ *is strictly convex, then each of the subsequent* $\mathbf{H}^k$ *obtained by the quasi-Newton update formula is positive definite. Furthermore, if the gradient* $\nabla J_\epsilon(\mathbf{x}^k|\sigma_\beta) \neq 0$, $\mathbf{d}^k$ *is a descent search direction. Thus, a line search can produce a step-size* h_k *such that* $J_\epsilon(\mathbf{x}^{k+1}|\sigma_\beta) < J_\epsilon(\mathbf{x}^k|\sigma_\beta)$.

In view of Algorithm 5.3.1, the CRF problem (2.2.12) can be solved by using a combination of the golden section search method and a quasi-Newton method as follows:

Algorithm 5.3.2 *Set* $k = 0$ *and* $\sigma_{\beta 0} = 0$, *choose a* $\sigma_{\beta t} > 0$, *and assign the accuracy parameters* $\gamma_1 > 0$ *and* $\gamma_2 > 0$ *for* σ_β *and* $(1+\delta)\|\mathbf{x}^*\|_2^2 - \|\mathbf{x}^k\|_2^2$, *respectively.*

1. *Determine if* $\mathcal{F}_{\sigma_{\beta t}}(\mathbf{x}_t^k) = \emptyset$ *by using Algorithm 5.3.1.*

2. *If so, go to Step 3; otherwise, set* $\sigma_{\beta 0} = \sigma_{\beta t}$ *and* $\sigma_{\beta t} = 2\sigma_{\beta t}$, *and then go to Step 1.*

3. *Set* $\bar{\sigma}_{\beta 0} = \sigma_{\beta 0} + (1-\lambda)(\sigma_{\beta t} - \sigma_{\beta 0})$; $\bar{\sigma}_{\beta t} = \sigma_{\beta 0} + \lambda(\sigma_{\beta t} - \sigma_{\beta 0})$ *where* $\lambda \simeq 0.618$ *is the golden section ratio.*

4. *If* $\mathcal{F}_{\bar{\sigma}_{\beta 0}}(\bar{\mathbf{x}}_0^k) = \emptyset$, *set* $\sigma_{\beta t} = \bar{\sigma}_{\beta 0}$, $\mathbf{x}^k = \mathbf{x}_0^k$ *and go to Step 6; otherwise, set* $\sigma_{\beta 0} = \bar{\sigma}_{\beta 0}$, $\mathbf{x}_0^k = \bar{\mathbf{x}}_0^k$ *and go to Step 5.*

5. *If* $\mathcal{F}_{\bar{\sigma}_{\beta t}}(\bar{\mathbf{x}}_t^k) = \emptyset$, *set* $\sigma_{\beta t} = \bar{\sigma}_{\beta t}$, $\mathbf{x}^k = \mathbf{x}_0^k$ *and go to Step 6; otherwise, set* $\sigma_{\beta 0} = \bar{\sigma}_{\beta t}$, $\mathbf{x}^k = \bar{\mathbf{x}}_t^k$ *and go to Step 6.*

6. *If* $\sigma_{\beta t} - \sigma_{\beta 0} \leq \gamma_1$ *and* $(1+\delta)\|\mathbf{x}^*\|_2^2 - \|\mathbf{x}^k\|_2^2 \leq \gamma_2$, *set* $\sigma_\beta(\mathbf{x}_r^*) = \sigma_{\beta 0}$, $\mathbf{x}_r^* = \mathbf{x}^k$ *and stop; otherwise, go to Step 3 and replace* k *by* $k+1$.

Algorithm 5.3.2 can be presented in the form of a Flowchart 5.2. More specifically, the module of initialization is designed to determine the feasibility of the constraint robustness formulation problem in $\mathbf{x}$ for a given σ_β via solving the constrained minimization problem (5.3.2) using a quasi-Newton method. The processing module is used to locate the optimal solution $\sigma_\beta(\mathbf{x}_r^*)$ with the robust optimal filter coefficient vector $\mathbf{x}_r^*$ by using the golden section search method.

Theorem 5.3.1 *Algorithm 5.3.2 is guaranteed to locate the optimal solution* $\sigma_\beta(\mathbf{x}_r^*)$ *of the problem (2.2.12) with the robust optimal filter coefficient vector* $\mathbf{x}_r^*$ *to within a given interval of uncertainty in a finite number of iterations.*

Proof: See Appendix C.3. ∎

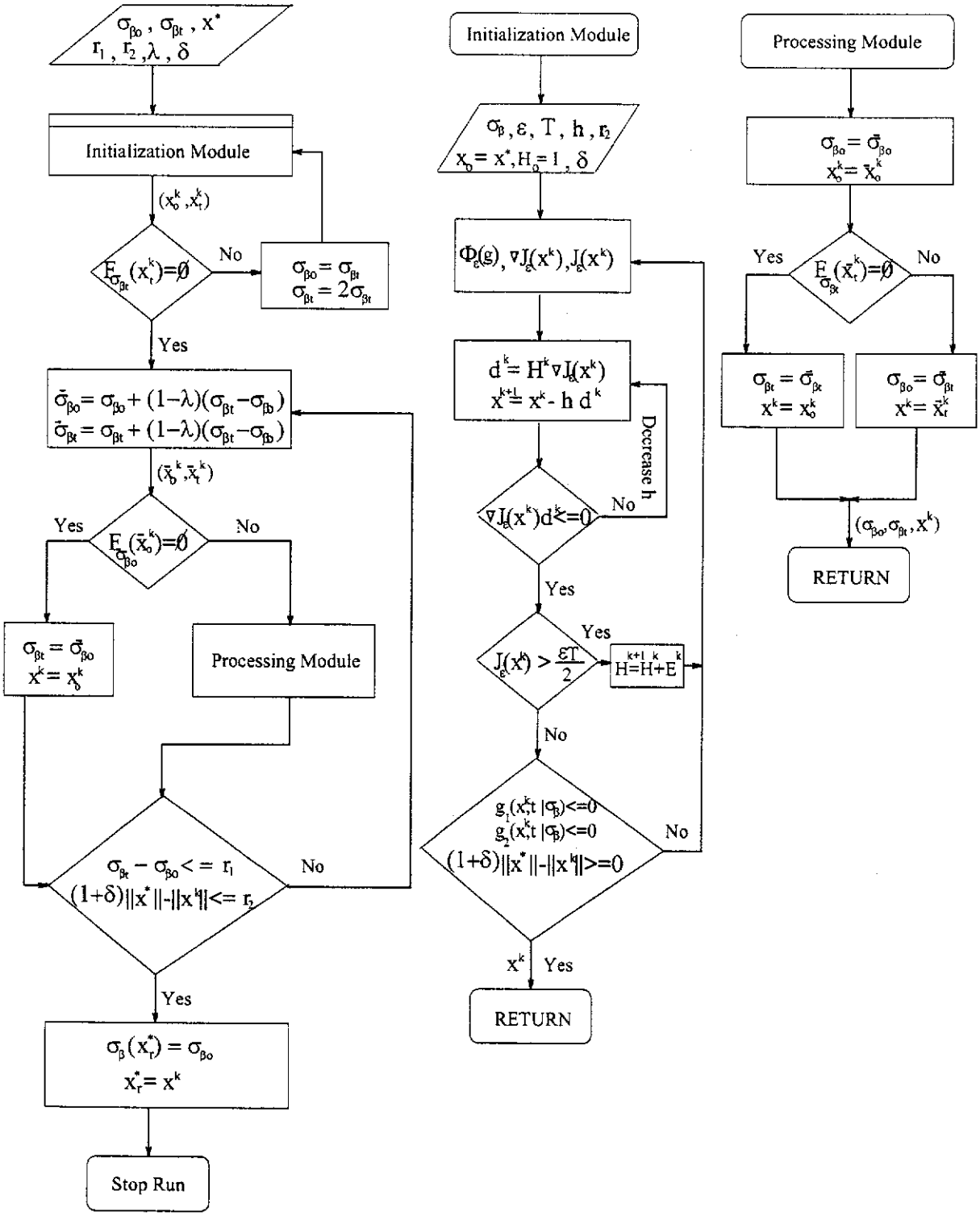

Figure 5.2: Flowcharts for Algorithm 5.3.2.

5.3.3 Behavior of Optimal Filter with Perturbations

In this subsection, we consider two perturbation cases, namely perturbation in the implementation of the optimal filter, and perturbation in the prescribed input signal. Without the robustness constraints, these two types of perturbation will result in the output constraints being violated.

5.3.3.1 Perturbation in the Implementation of Optimal Filter

Let $\tilde{u}_n^*(t)$ denote the perturbed EC optimal filter that results due to error in the implementation of the nonrobust EC optimal filter $u_n^*(t)$. $\tilde{u}_n^*(t)$ is given by

$$\tilde{u}_n^*(t) \;=\; \sum_{j=0}^{n-1} \tilde{x}_j^* \varphi_j(t), \quad t \in [0,\infty)$$

where $\tilde{\mathbf{x}}^* \triangleq [\tilde{x}_0^*, \ldots, \tilde{x}_{n-1}^*]' \in \Re^n$ denotes the perturbed optimal filter coefficient vector resulting from the implementation error. The corresponding output response of the perturbed optimal filter to the input signal $s(t)$ is

$$\psi_n(\tilde{u}_n^*, t) = \int_0^\infty \tilde{u}_n^*(\tau) s(t-\tau) d\tau = \psi_n(\tilde{\mathbf{x}}^*, t), t \in [0,\infty), \tag{5.3.6}$$

where $\psi_n(\tilde{\mathbf{x}}^*, t) = \Theta'(t)\tilde{\mathbf{x}}^*$ and $\Theta(t)$ is defined by (2.2.5). By the definition of the weighted constraint robustness margin defined in (2.2.11), it follows from (5.3.6) that the weighted constraint margin $\sigma_\beta(\tilde{\mathbf{x}}^*) \in \Re$ of the perturbed normal EC optimal filter coefficient vector is:

$$\sigma_\beta(\tilde{\mathbf{x}}^*) \;=\; \min\left\{ \min_t \left[\frac{\varepsilon^+(t) - \psi_n(\tilde{\mathbf{x}}^*, t)}{\beta(t)} \right], \min_t \left[\frac{\psi_n(\tilde{\mathbf{x}}^*, t) - \varepsilon^-(t)}{\beta(t)} \right] \right\}. \tag{5.3.7}$$

Let us define the perturbed robust EC optimal filter coefficient vector $\tilde{\mathbf{x}}_r^*$. Similar to (5.3.7), we also obtain the weighted constraint margin $\sigma_\beta(\tilde{\mathbf{x}}_r^*) \in \Re$ of the perturbed robust EC optimal filter coefficient vector as:

$$\sigma_\beta(\tilde{\mathbf{x}}_r^*) \;=\; \min\left\{ \min_t \left[\frac{\varepsilon^+(t) - \psi_n(\tilde{\mathbf{x}}_r^*, t)}{\beta(t)} \right], \min_t \left[\frac{\psi_n(\tilde{\mathbf{x}}_r^*, t) - \varepsilon^-(t)}{\beta(t)} \right] \right\}. \tag{5.3.8}$$

Theorem 5.3.2 *Let the weighted constraint margins $\sigma_\beta(\tilde{\mathbf{x}}^*)$ and $\sigma_\beta(\tilde{\mathbf{x}}_r^*)$ be, respectively, defined in (5.3.7)-(5.3.8) where $\tilde{\mathbf{x}}^* \triangleq \mathbf{x}^* + \alpha_f \Delta\mathbf{x} \|\mathbf{x}^*\|_2$ and $\tilde{\mathbf{x}}_r^* \triangleq \mathbf{x}_r^* + \alpha_f \Delta\mathbf{x} \|\mathbf{x}_r^*\|_2$, while $\mathbf{x}^*$ and $\mathbf{x}_r^*$ are, respectively, the nonrobust optimal filter coefficient vector and the robust optimal filter coefficient vector, $\alpha_f > 0$ is the perturbation scaling parameter and $\Delta\mathbf{x}$ is an error vector due to an error in the implementation of the optimal filter. Assume that $\|\Theta(t)\|_2 \le C, t \in [0,\infty)$ and $\|\Delta\mathbf{x}\|_2 \le \bar{\eta}$ hold. Then there exists a number $\alpha_f^* = \frac{\beta^* \sigma_\beta(\mathbf{x}_r^*)}{M_\mathbf{x}}$, where $M_\mathbf{x} = \sqrt{(1+\delta)} C \bar{\eta} \|\mathbf{x}^*\|_2$ and $\beta^* = \max_t[\beta(t)]$, such that for α_f satisfying $0 < \alpha_f \le \alpha_f^*$, $\sigma_\beta(\tilde{\mathbf{x}}_r^*) \ge 0 > \sigma_\beta(\tilde{\mathbf{x}}^*)$.*

Proof: See Appendix C.4. ∎

Remark 5.3.5

1) If the error vector $\Delta\mathbf{x}$ is normalized to achieve $\|\Delta\mathbf{x}\|_2 = 1$, then the perturbation scaling parameter α_f is a measure of the norm of the error in the implementation of the optimal filter as a fraction of the optimal filter norm.

2) Theorem 5.3.2 indicates that if the error vector is bounded within a certain interval, then the output response of the perturbed robust EC optimal filter remains within the prescribed upper and lower boundaries. However, the same bounded error vector introduced on the normal EC optimal filter results in the output constraints being violated and its weighted constraint margin $\sigma_\beta(\tilde{\mathbf{x}}^*)$ will become negative.

5.3.3.2 Perturbation in the Prescribed Input Signal

Let $\tilde{s}(t)$ denote the input signal contaminated by perturbation. By the expression of the filter impulse response $u_n(t)$ in (2.2.3), the corresponding perturbed output response of the nonrobust EC optimal filter $u_n^*(t)$ is obtained as:

$$\begin{aligned}\tilde{\psi}_n(u_n^*, t) &= \int_0^\infty u_n^*(\tau)\tilde{s}(t-\tau) = \sum_{j=0}^{n-1} \tilde{\theta}_j(t) x_j^* \\ &= \tilde{\psi}_n(\mathbf{x}^*, t), \quad t \in [0, \infty)\end{aligned} \tag{5.3.9}$$

where $\tilde{\psi}_n(\mathbf{x}^*, t) = \tilde{\Theta}'(t)\mathbf{x}^*$, $\tilde{\Theta}'(t) \triangleq [\tilde{\theta}_0(t), \ldots, \tilde{\theta}_{n-1}(t)]$ is the vector representing the perturbation input signal, and

$$\tilde{\theta}_j(t) = \int_0^\infty \varphi_j(\tau)\tilde{s}(t-\tau)d\tau, \quad j = 0, \ldots, n-1. \tag{5.3.10}$$

By (2.2.11), we obtain the weighted constraint margin $\tilde{\sigma}_\beta(\mathbf{x}^*) \in \Re$ of the nonrobust EC optimal filter coefficient vector for the perturbed input signal as:

$$\tilde{\sigma}_\beta(\mathbf{x}^*) = \min\left\{\min_t\left[\frac{\varepsilon^+(t) - \tilde{\psi}_n(\mathbf{x}^*, t)}{\beta(t)}\right], \min_t\left[\frac{\tilde{\psi}_n(\mathbf{x}^*, t) - \varepsilon^-(t)}{\beta(t)}\right]\right\}. \tag{5.3.11}$$

Similar to (5.3.9), the output response of the robust EC optimal filter with the perturbed input signal is given by

$$\tilde{\psi}_n(\mathbf{x}_r^*, t) = \tilde{\Theta}'(t)\mathbf{x}_r^*, \quad t \in [0, \infty). \tag{5.3.12}$$

Using (5.3.12), we also obtain the weighted constraint margin $\tilde{\sigma}_\beta(\mathbf{x}_r^*) \in \Re$ of the robust EC optimal filter coefficient vector for the perturbed input signal as:

$$\tilde{\sigma}_\beta(\mathbf{x}_r^*) = \min\left\{\min_t\left[\frac{\varepsilon^+(t) - \tilde{\psi}_n(\mathbf{x}_r^*, t)}{\beta(t)}\right], \min_t\left[\frac{\tilde{\psi}_n(\mathbf{x}_r^*, t) - \varepsilon^-(t)}{\beta(t)}\right]\right\}. \tag{5.3.13}$$

By (5.3.11) and (5.3.13), we obtain a similar result as Theorem 5.3.2 in the following.

Theorem 5.3.3 *Define the perturbed input signal as* $\tilde{s}(t) \triangleq s(t) + \alpha_s \Delta s(t) s^*, t \in [0, \infty)$, *where* $\alpha_s > 0$ *is the perturbation scaling parameter,* $\Delta s(t)$ *is a perturbation on the input signal, and* $s^* = max_t[|s(t)|]$. *Let* $\tilde{\sigma}_\beta(\mathbf{x}^*)$ *and* $\tilde{\sigma}_\beta(\mathbf{x}_r^*)$ *be, respectively, defined in (5.3.11) and (5.3.13). Assume that* $|\Delta s(t)| \leq \bar{\gamma}$ *holds. Then there exists a number* $\alpha_s^* = \frac{\beta^* \sigma_\beta(\mathbf{x}_r^*)}{M_s s^*}$, *where* $\beta^* = \max_t[\beta(t)]$ *and* $M_s = \sqrt{n(1+\delta)}\bar{\gamma}\|\mathbf{x}^*\|_2$, *while* $\delta > 0$ *is defined in the CRF problem (2.2.12) such that for* α_s *satisfying* $0 < \alpha_s \leq \alpha_s^*$, $\tilde{\sigma}_\beta(\mathbf{x}_r^*) \geq 0 > \tilde{\sigma}_\beta(\mathbf{x})$.

Proof: See Appendix C.5. ∎

Remark 5.3.6

1) For the numerical examples to be considered in Section 5.4.3.2, the input signal $s(t)$ *and the perturbation* $\Delta s(t)$ *will be approximated by the time interval* $[0, T]$, *and* $[0, T]$ *is divided into* m *subintervals. These signal sequences are represented as vectors denoted by* $\mathbf{s} \in \Re^m$ *and* $\Delta\mathbf{s} \in \Re^m$, *respectively. Then, the approximate perturbed input signal* $\tilde{\mathbf{s}} \in \Re^m$ *becomes* $\tilde{\mathbf{s}} = \mathbf{s} + \alpha_s \Delta\mathbf{s} \|\mathbf{s}\|_\infty$. *By choosing* $0 < \alpha_s \leq \alpha_s^*$, *where* $\alpha_s^* = \frac{\beta^* \sigma_\beta(\mathbf{x}_r^*)}{M_s \|\mathbf{s}\|_\infty}$, *we have the results of Theorem 5.3.3. Furthermore, when* $\|\Delta\mathbf{s}\|_\infty = 1$, *the scaling parameter* α_s *is a measure of the norm of the perturbation as a fraction of the signal norm.*

2) Theorem 5.3.3 shows that if the perturbation on the input signal is bounded within a certain interval, then the output response of the robust EC optimal filter to the perturbed input signal remains in the region defined by the output boundaries. On the other hand, with the same bounded perturbation on the input signal, the corresponding output response of the normal EC optimal filter will violate the output envelope constraints and the weighted constrained margin $\tilde{\sigma}_\beta(\mathbf{x}^*)$ *will become negative.*

5.4 Numerical Results with Laguerre Networks

To illustrate the performance of the algorithm derived in the previous section, we consider the Laguerre basis functions which have been used as examples in the previous work on the EC filtering problems. These functions can be implemented as cascaded filters with a single real pole. The use of Laguerre functions for signal representation and filter synthesis has been well documented [52, 40]. Other filter structures could also be used. For example, Legendre functions correspond to cascade filters with real non-identical poles, [37], and Kautz filters consist of cascaded all-pass filter sections with a pair of complex conjugate non-identical poles, [33]. In comparison, the structure of Laguerre filters is easier to implement.

In what follows, we briefly introduce the orthonormal Laguerre basis and then apply it to

a practical EC filter design example involving the channel equalization of a data communications [33].

5.4.1 Laguerre Basis of $L^2([0,\infty))$

Let $\mathcal{L}_j^p(t), t \in [0,\infty)$ be the Laguerre function with a scale factor $p > 0$ defined by

$$\mathcal{L}_j^p(t) = \sqrt{2p}e^{-pt}\ell_j(2pt), \quad j = 0,1,2,\ldots \tag{5.4.14}$$

where $\ell_j(t)$ is the classical Laguerre polynominal given by

$$\begin{aligned}\ell_j(t) &= \frac{e^t}{j!}\frac{d^j}{dt^j}\left(e^{-t}t^j\right) \\ &= \sum_{i=0}^{j}\begin{pmatrix} j \\ j-i \end{pmatrix}\frac{(-t)^i}{i!}, \quad j = 0,1,2,\ldots\end{aligned}$$

Taking the Laplace transform of $L_j^p(t)$, we obtain

$$H_j^p(s) = \frac{\sqrt{2p}}{s+p}\left(\frac{s-p}{s+p}\right)^j, \quad j = 0,1,2,\ldots$$

For each $j = 0,1,2,\ldots$, the function $H_j^p(s)$ consists of the first-order low-pass term and the jth-order all-pass factor. These functions are the classical Laguerre functions in frequency domain. It is known that the Laguerre sequence $\{\mathcal{L}_j^p\}_{j=0}^{\infty}$ forms a uniformly bounded orthonormal basis for the Hilbert space $L^2([0,\infty))$ (cf. [52, 40]).

Since $\{\mathcal{L}_j^p\}_{j=0}^{\infty}$ is an orthonormal basis of $L^2([0,\infty))$, any $u(t) \in L^2([0,\infty))$ can be represented as:

$$u(t) = \sum_{j=0}^{\infty} x_j\mathcal{L}_j^p(t), \quad t \in [0,\infty)$$

where $x_j = \left\langle u, L_j^p \right\rangle$, $j = 0,1,\ldots$ are known as the Laguerre-Fourier coefficients. Define the Laguerre filter of order n as:

$$u_n(t) = \sum_{j=0}^{n-1} x_j\mathcal{L}_j^p(t), \quad t \in [0,\infty). \tag{5.4.15}$$

Let $U_n(s)$ denote the Laplace transform of $u_n(t)$. Then, $U_n(s)$ can be expressed as:

$$U_n(s) = \sum_{j=0}^{n-1} x_j H_j^p(s). \tag{5.4.16}$$

From (5.4.14)-(5.4.16), the continuous-time EC filtering system with Laguerre orthonormal basis is realized and shown in Figure 5.3, where $s(t)$ and $\psi_n(t), t \in [0,\infty)$ denote, respectively, the input and output pulses.

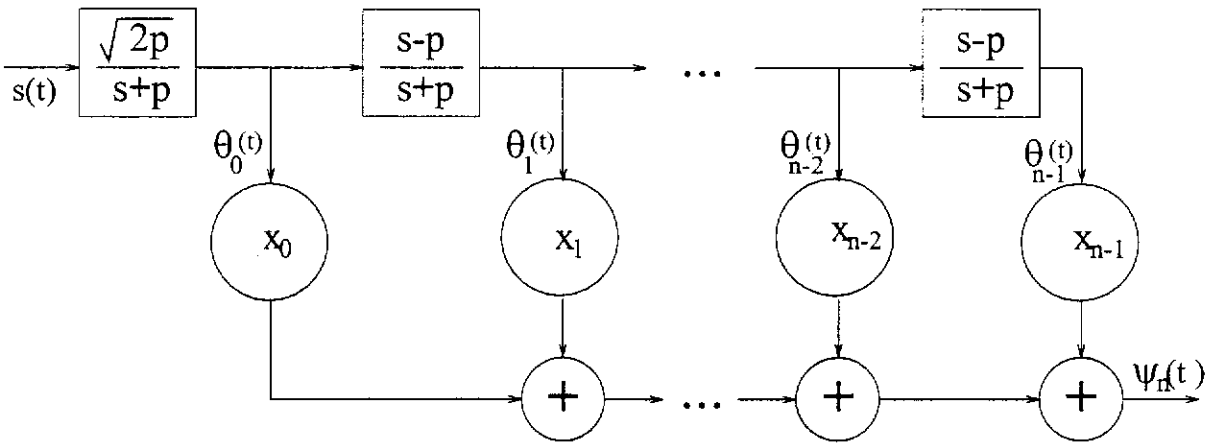

Figure 5.3: Block diagram of implementation of the continuous-time EC filter with Laguerre basis.

Remark 5.4.1 *It is possible to include the scale factor p as a variable of the optimization problem. However, we have chosen to fix it due to the following consideration:*
1) For many real systems, the bandwidth of the channel to be equalized is often known at least approximately. In this case, the scale factor p in the Laguerre filter can often be chosen off-line from a priori information about the channel impulse response.
2) Including p in the optimization problem may complicate the presentation without providing any additional insight into the proposed method which is the primary focus of this chapter. Moreover, the optimization of p for impulse inputs and any well-behaved input can be achieved by the methods reported such as in [6, 10, 53, 54].

5.4.2 Test 1: EC Filter with Continuous Laguerre Networks

We consider the equalization of a digital transmission channel involving a coaxial cable operating at the DSX3 rate (44.736 Mb/s) [5]. The coaxial cable has a 30 dB attenuation at a normalized frequency of $1/\bar{\beta}$ where $\bar{\beta}$ is the baud interval ($22.35 \times 10^{-9} s$).

The design objective is to find an equalizing filter shaping the impulse response of the coaxial cable so that the output response of the filter fits into the envelope given by the DSX3 pulse template. The input signal and the output pulse mask are given in continuous-time domain with support in $[0, T]$ in Appendix C.

To have a good representation of the continuous input signal, the analog input signal is sampled every $\frac{\bar{\beta}}{32}$ time unit over $[0, T]$ where $T = 32\bar{\beta}$. To display the designed results, we further discretize the input signal, the output mask and the filter output in (5.2.7) into 1024 points. This gives a reasonably fine partition over the interval. However, we note that the

approach presented in Section 5.2 for obtaining the optimal solution does not require any discretization of input signal, the output mask, and the filter output.

Solving the discretized problem, we first obtain a good initial guess Λ_*^0 needed in Step 2 of Algorithm 5.2.2. Then, $\mathbf{t}^0$ can be chosen accordingly. In this example, we note that it is only required to use $m = 3$ points although $n = 8$ Laguerre coefficients are used in this example. From Λ_*^0, we choose $\mathbf{t}^0 = [0.2, 0.875, 1.1]'$ as the initial guess. We further choose $h_t = h_\Lambda = 10^{-3}$ as the fixed step-sizes for Step 1 and Step 2 of Algorithm 5.2.2, the scale factor $p = 14/32\bar{\beta}$. The simulation results are depicted in Figure 5.4 and Figure 5.5. From Figure 5.4, it is clear that the output response fits into the output envelope mask. Figure 5.5 shows that all convergence conditions are satisfied. The optimal cost value obtained using Algorithm 5.2.2 is 59.3968.

5.4.3 Test 2: Robust Optimal EC Filter with Continuous Laguerre Networks

In this test, we consider two examples: without perturbations; and with perturbations for the design of the robust EC optimum filter with the continuous-time Laguerre networks.

5.4.3.1 Example 1: Without Perturbations

For the first test, we assume that there is no disturbance in the prescribed input signal nor implementation error. The noiseless output response of the normal EC optimal filter fits into the envelope constraints as shown in Figure 5.4 and the optimal cost value $\|\mathbf{x}^*\|_2^2$ is obtained in Section 5.4.2. The robust EC filtering problem is combined with a weighting function $\beta(t) = \frac{\varepsilon^+(t)-\varepsilon^-(t)}{2}$, where $\varepsilon^+(t)$ and $\varepsilon^-(t)$ are defined in Section 2.2.1 with support in $[0, 32\bar{\beta}]$. $\beta(t)$ is a tolerance band about the desired pulse shape $d(t)$.

For Algorithm 5.3.2, we begin the simulation with $\sigma_{\beta 0} = 0$, $\sigma_{\beta t} = 0.1$, $\mathbf{x}_0 = \mathbf{x}^*$ and specify the iteration accuracy parameter $\gamma_1 = 10^{-15}$, and $\gamma_2 = 10^{-4}$. For the improved robustness in the CRF problem (2.2.12), we are prepared to accept an additional 100% increase in the output noise power gain, i.e, $\delta = 1.0$. The accuracy parameter in Algorithm 5.3.1 is set at $\epsilon = 10^{-3}$. The simulation results are depicted in Figures 5.6- 5.7. Figure 5.6(a) shows the convergence of Algorithm 5.3.2 where the golden section search method is used to locate σ_{β_0} and σ_{β_t}. Figure 5.6(b) depicts the convergence of the robust filters to meet the noise gain constraint in a finite number of iterations. This is consistent with Theorem 5.3.1. Figure 5.7 shows a comparison between the nonrobust EC optimal output response and the robust optimal output response. Clearly, the robust optimal output response is farther from the boundaries of the output mask when compared with the nonrobust optimal output response.

5.4.3.2 Example 2: With Perturbations

To illustrate the improved tolerance of the robust optimal filter to the perturbations discussed in Section 5.3.3, we consider the performance of the optimal filter in the presence of perturbations in the prescribed input signal, and errors in the implementation of the optimal filter.

The output response of the implemented optimal filter will depend on the actual implementation error and the actual perturbation on the input signal. To obtain an idea on the effect of different input signal perturbations, the responses of the robust optimal filter to fifty input signals with random perturbations were determined. In the numerical examples, the input signal is represented by a discrete sequence comprised of 1024 samples over its support interval $[0, 32\bar{\beta}]$. Each of the fifty input signal perturbation sequence, $\{\Delta \mathbf{s}^i \in \Re^m\}_{i=1}^{50}$, is generated by producing $m = 1024$ independent zero mean random numbers from a uniform distribution over the interval $[-1.0, 1.0]$. Since the perturbation is generated on the interval $[-1.0, 1.0]$, we have that $\|\Delta \mathbf{s}^i\|_\infty = 1, \forall i = 1, \ldots, 50$.

Similarly, to gauge the effect of implementation errors, the response of fifty different implementations of robust optimal filter were determined. The fifty different implementations were produced by adding a perturbation vector, $\{\Delta \mathbf{x}^i \in \Re^N\}_{i=1}^{50}$, to the optimal filter vector. The components of each perturbation vector were zero mean independent random numbers from a uniform distribution over the interval $[-1.0, 1.0]$. The perturbation vectors were normalized to have unit norm, that is, $\|\Delta \mathbf{x}^i\|_2 = 1, i = 1, \ldots, 50$.

Figure 5.8(a) shows that the nonrobust optimal filter has zero tolerance to implementation errors since the weighted constraint margin becomes negative at the presence of any implementation error. On the other hand, Figure 5.8(b) shows that the robust optimal filter is highly tolerant to implementation errors since for a wide range of implementation errors the output has a positive margin.

Figure 5.9(a) shows that the nonrobust optimal filter has zero tolerance to input signal perturbations since the weighted constraint margin becomes negative at the presence of any input perturbation. From Figure 5.9(b), we see that the robust optimal filter is highly tolerant to implementation errors since for a wide range of input signal perturbations the output has a positive margin.

The numerical results obtained for the above two types of perturbation example are consistent with Theorem 5.3.2 and Theorem 5.3.3, and illustrate the improved tolerance of the robust optimal filter with respect to input signal perturbations and implementation errors.

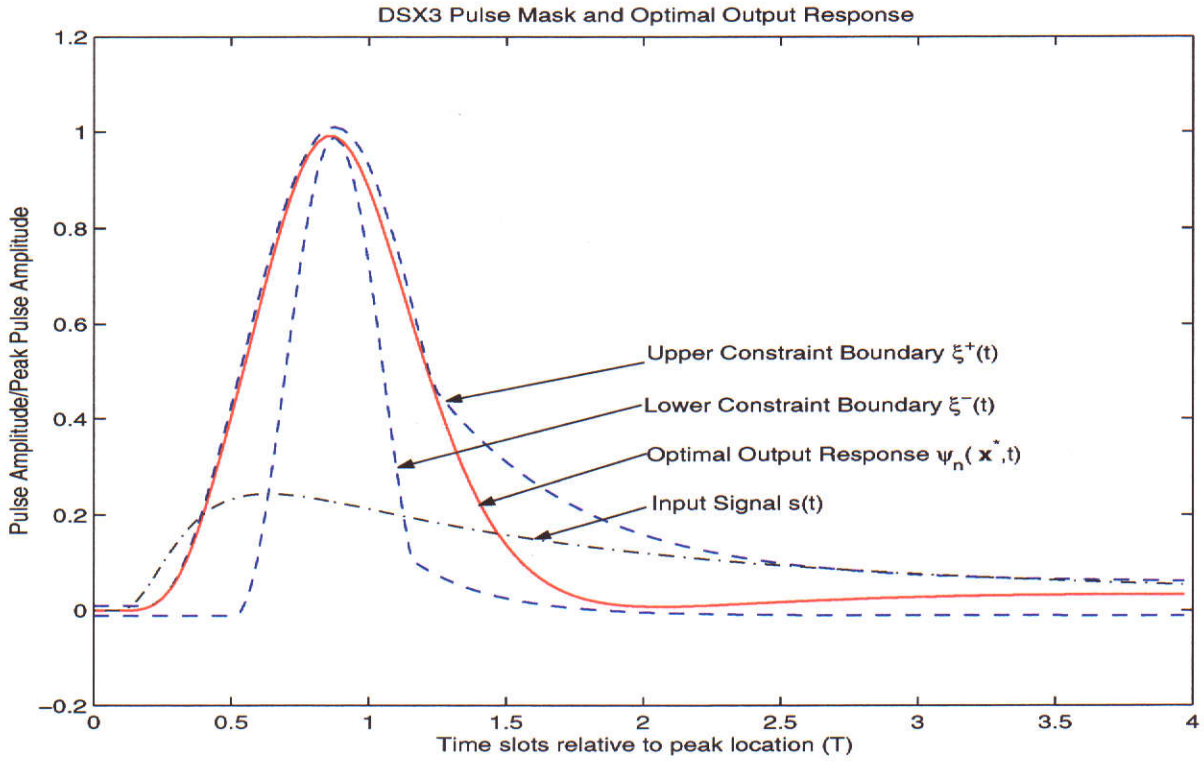

Figure 5.4: DSX3 pulse template superimposed on coaxial cable response and filter output.

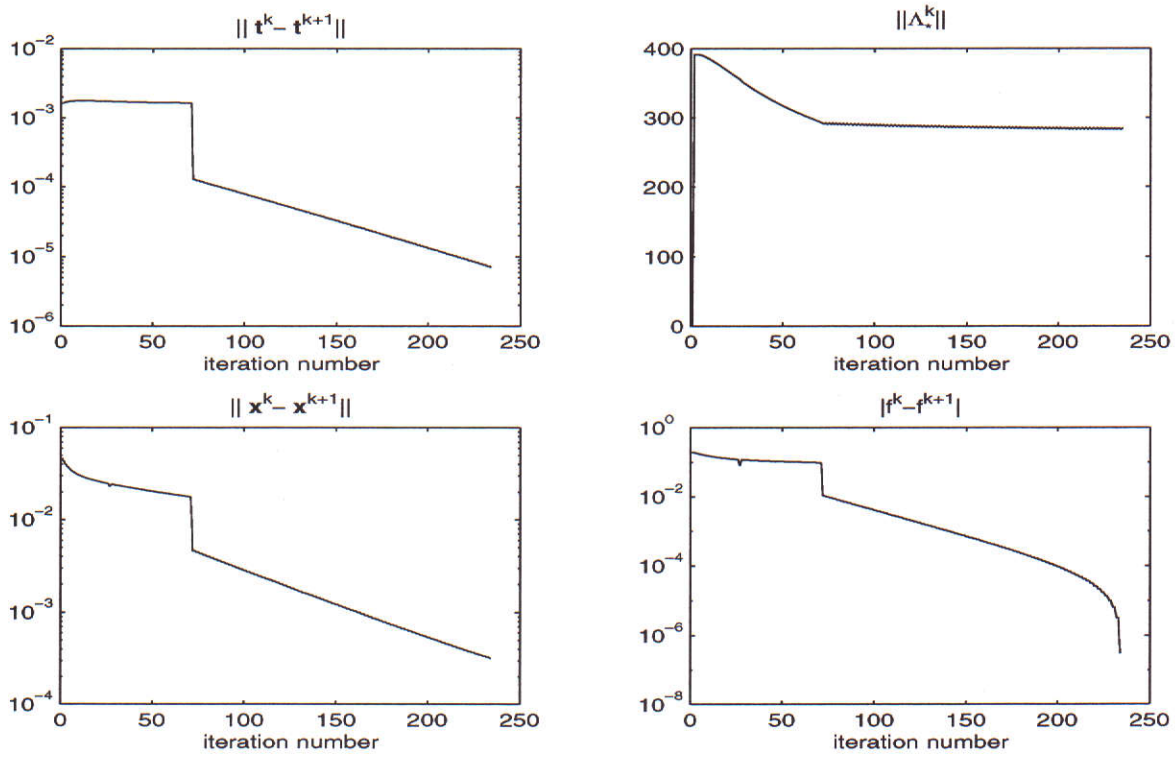

Figure 5.5: The convergence results for DSX3 pulse coaxial cable example.

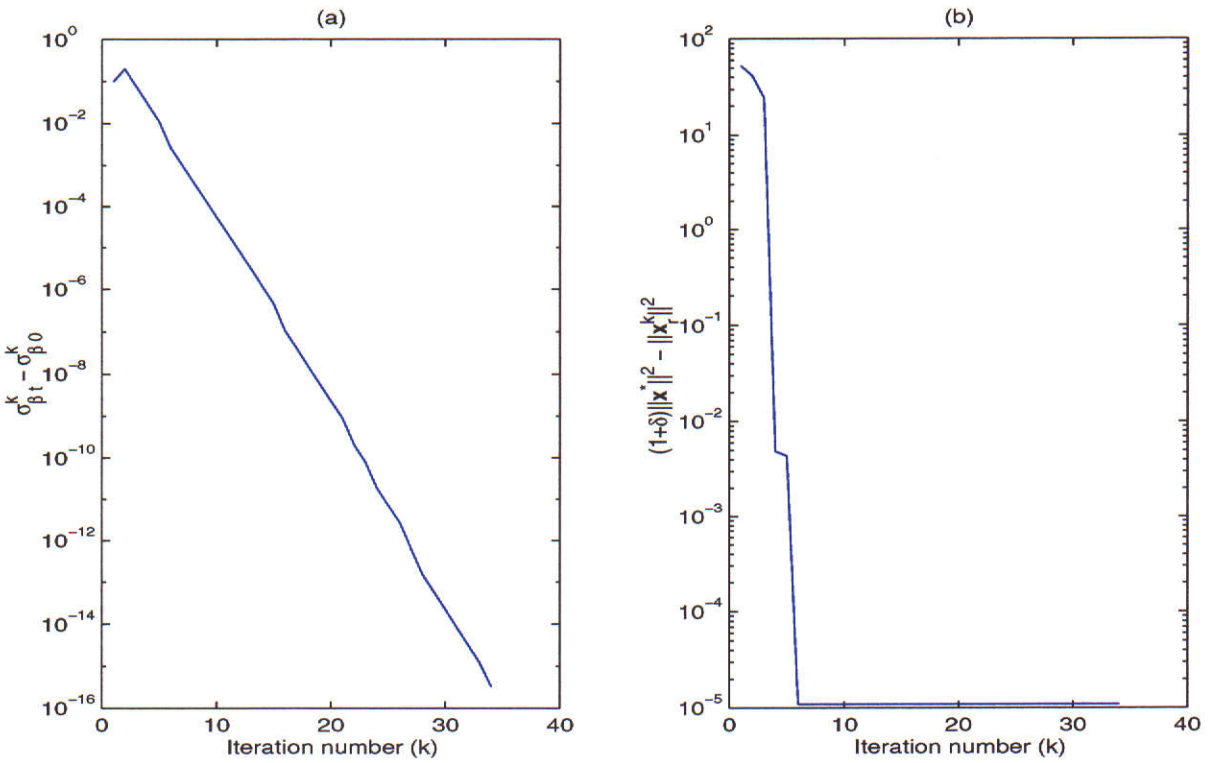

Figure 5.6: The convergence results for the robust EC filtering problem.

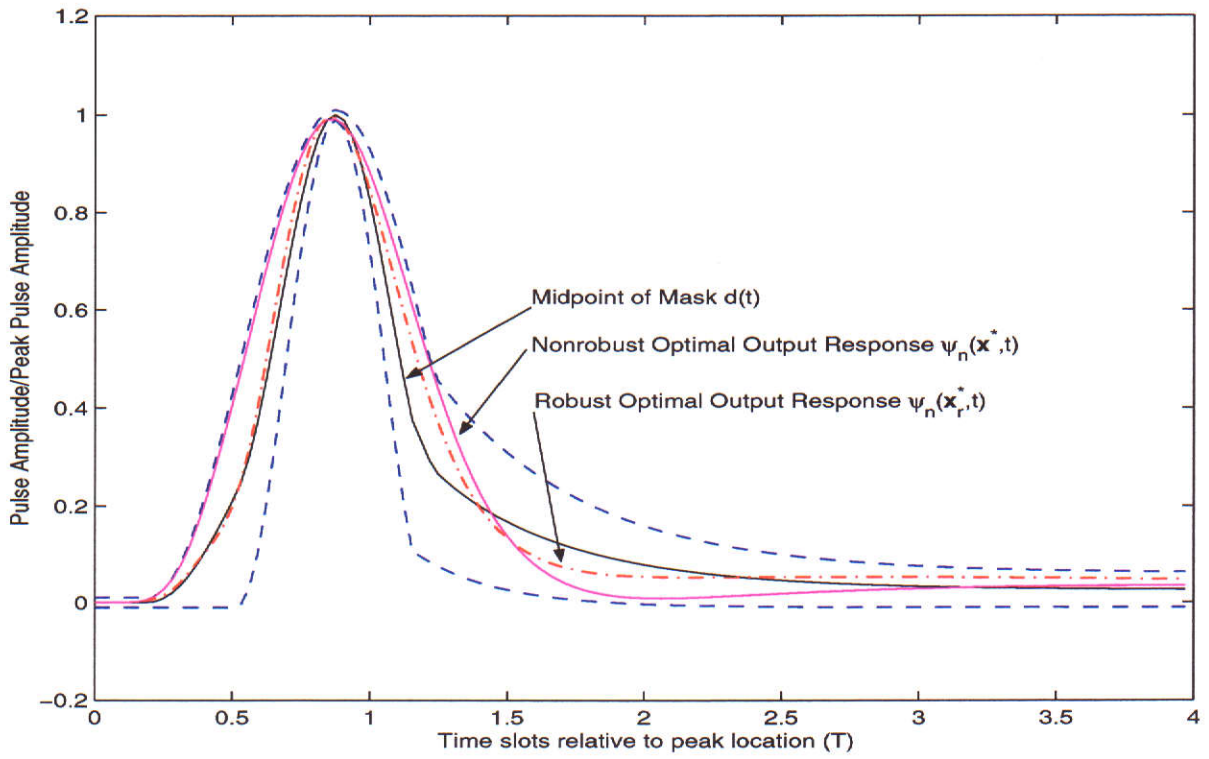

Figure 5.7: A comparison between the center of the mask, the nonrobust EC optimal output response and the robust EC optimal output response.

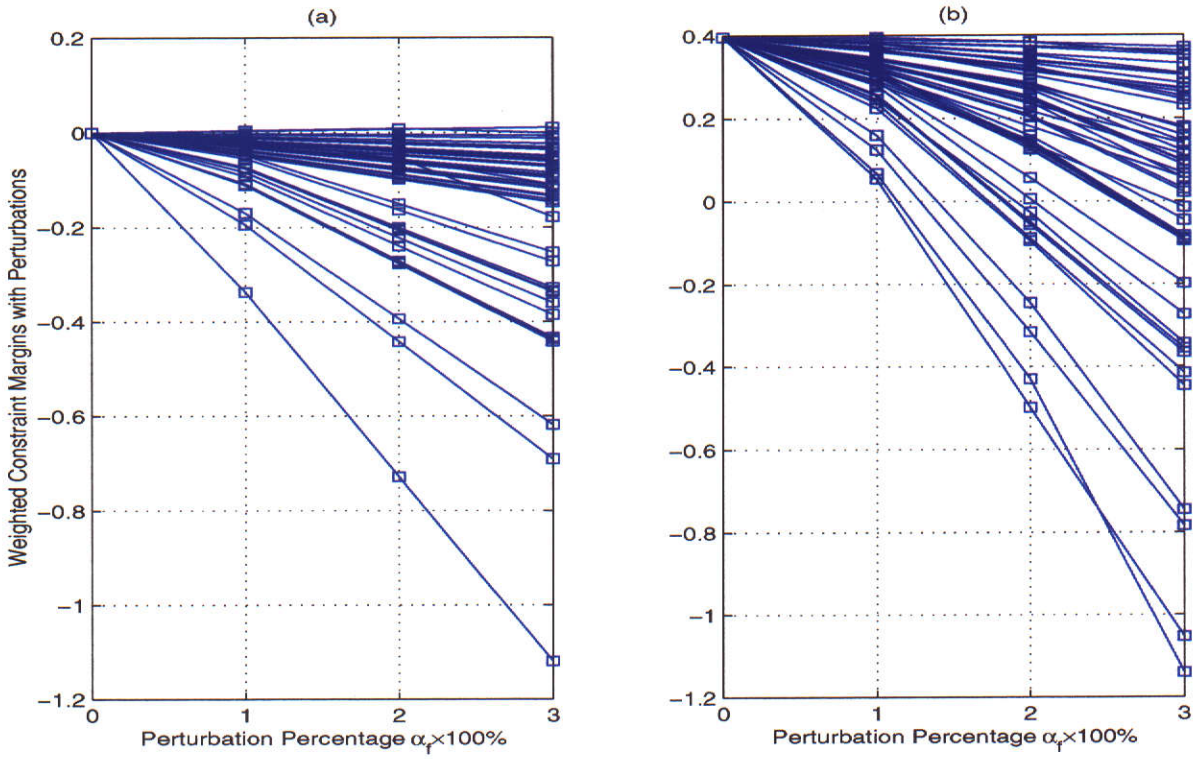

Figure 5.8: Perturbation in the optimal filter implementation. (a): Weighted constraint margin $\sigma_\beta(\tilde{\mathbf{x}}^*)$ of $\tilde{\mathbf{x}}^*$. (b): Weighted constraint margin $\sigma_\beta(\tilde{\mathbf{x}}_r^*)$ of $\tilde{\mathbf{x}}_r^*$.

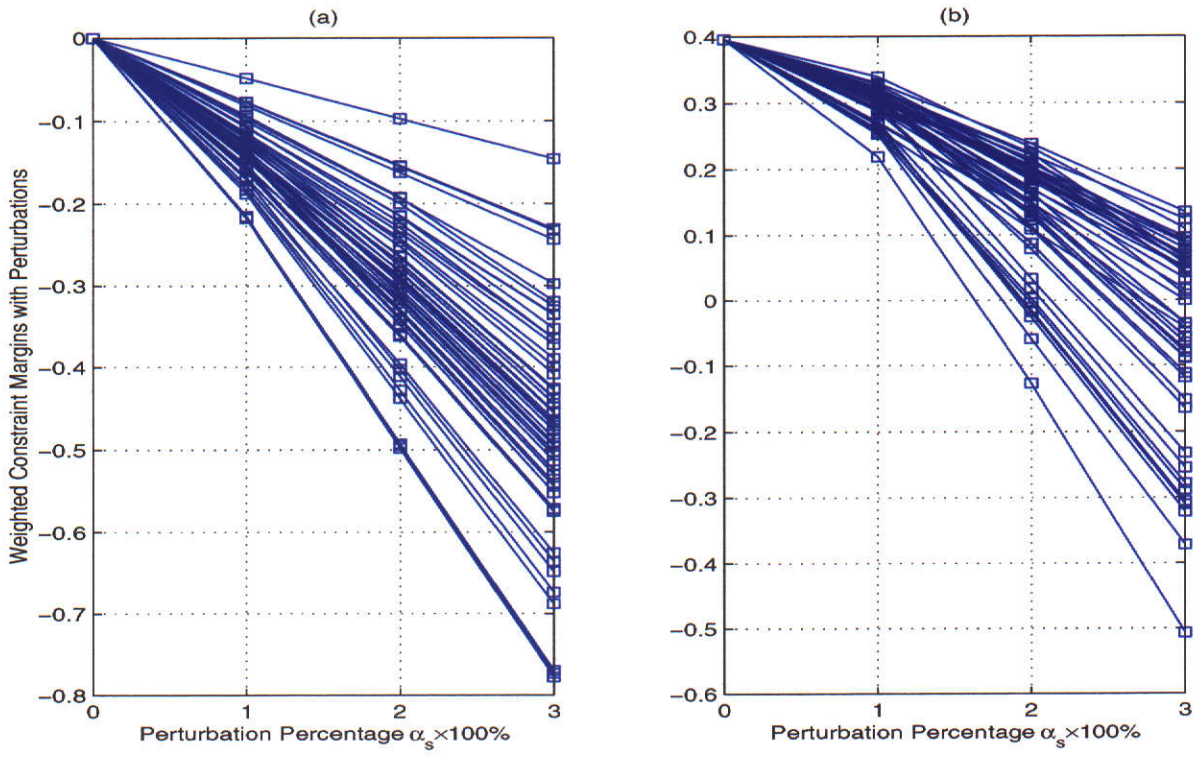

Figure 5.9: Perturbation in the input signal. (a): Weighted constraint margin $\widetilde{\sigma}_\beta(\mathbf{x}^*)$ of $\mathbf{x}^*$. (b): Weighted constraint margin $\widetilde{\sigma}_\beta(\mathbf{x}_r^*)$ of $\mathbf{x}_r^*$.

Chapter 6

Application Algorithms: Discrete-Time EC Filtering Problems

6.1 Introduction

The aim of this chapter is to apply the newly developed simple yet efficient gradient-type methods of Chapter 4 to solve the discrete-time EC filtering problems formulated in Section 2.3. The discrete-time EC filtering problems include the discrete EC optimum filter design problem with FIR model structure and the EC filtering problem with an approximate ℓ^2 orthonormal basis. Applying the Lagrangian duality theory [34] to the original EC filtering problems, we obtain the dual optimization problems. Based on the space transformation and gradient flow techniques, the barrier-gradient (BG) and barrier-Newton (BN) algorithms with a continuous barrier function are developed to solve the dual EC filtering problems. As a result of the continuous barrier function, filters generated by these algorithms with a fixed step-size globally converge to the optimal filter.

This chapter is divided into four sections. Section 6.2, two efficient iterative algorithms are developed to solve the discrete-time EC filtering problem with FIR filter. In Section 6.3, the EC filtering problem with ℓ^2 orthonormal basis is considered. We first present a characterization of the optimal filter relying on the application of the Lagrangian duality theory and properties of a complete orthonormal basis of ℓ^2 Hilbert space. Similar to Section 6.2, two efficient iterative algorithms are then constructed to solve the EC filtering problem. The convergence results obtained in Chapter 4 are directly applicable to the discrete-time EC filtering struc-

tures. Furthermore, a practical application of the discrete-time Laguerre networks is examined in Section 6.3. We note that the FIR filter is a special case of the discrete-time Laguerre filter as the pole in the Laguerre networks equals zero. Finally, some numerical results involving pulse compression and channel equalization are presented in Section 6.4 to demonstrate the effectiveness of the proposed algorithms.

The main references of this chapter are [57, 60, 61].

6.2 Tapped Delay Line FIR Filters

In this section, we consider the optimum EC filter design problem (2.3.5) using FIR model structure. Applying the BG and BN methods discussed in Chapter 4, two simple yet efficient iterative algorithms are constructed to solve the discrete-time EC filtering problem (2.3.2). Numerical results involving pulse compression Barker code signal and channel equalization of a digital transmission coaxial cable are presented.

6.2.1 Discrete Dual Parameterization

Consider the discrete-time EC filtering problem (2.3.5). Assuming that there is a $\mathbf{u}^0 \in \Re^n$ such that $\mathbf{A}\mathbf{u}^0 < \mathbf{b}$ where $\mathbf{A}$ and $\mathbf{b}$ are, respectively, defined in (2.3.4), and applying the Lagrangian duality theory introduced in Section 4.3, we obtain the filter response $\mathbf{u}$ in terms of the Lagrange multiplier vector $\lambda \in \Re^{2N}$ as follows:

$$\mathbf{u}(\lambda) \;=\; -\frac{1}{2}\mathbf{A}'\lambda. \tag{6.2.1}$$

Substituting (6.2.1) into the primal EC filtering problem (2.3.5) yields the following dual optimization problem

$$\begin{array}{ll} \min & \phi(\lambda) = \frac{1}{2}\lambda'\bar{\mathbf{A}}\lambda + \lambda'\mathbf{b} \\ \text{subject to} & \lambda \geq 0_{2N} \end{array} \tag{6.2.2}$$

where the Hessian $\bar{\mathbf{A}} \triangleq \frac{1}{2}\mathbf{A}\mathbf{A}'$ is a symmetric positive semi-definite matrix and hence the dual cost function $\phi(\lambda)$ is convex. Once the dual vector is found, the optimal solution of the primal EC filtering problem (2.3.5) can be readily obtained. To solve the dual problem (6.2.2) efficiently, two gradient-based schemes obtained in Chapter 4 are applied to this problem.

6.2.2 Iterative Algorithms

In view of the BG and BN methods developed in Section 4.4, two efficient iterative algorithms are constructed to solve the discrete-time EC filtering problem (2.3.5).

6.2.2.1 Barrier-Gradient Algorithm

Consider the quadratic component-wise space transformation function (4.4.3) with the coordinate vector $\mathbf{y} \stackrel{\Delta}{=} [y_1, \ldots, y_{2N}]' \in \Re^{2N}$. Applying the BG method discussed in Section 4.4, we obtain a simple iterative algorithm for solving the discrete-time EC filtering problem (2.3.5).

Algorithm 6.2.1 *Set $k = 0$. Choose an initial point $\lambda^0 \in \Re^m_+$, a proper step-size h_k and the stopping criterion ϵ_λ.*

1. *Let $\mathbf{F}(\lambda^k) = \mathbf{D}(\lambda^k)\nabla\phi(\lambda^k)$ be a search direction where $\nabla\phi(\lambda^k) = \bar{\mathbf{A}}\lambda^k + \mathbf{b}$.*
   Calculate the following iterative scheme

$$\lambda^{k+1} = \lambda^k - h_k\mathbf{F}(\lambda^k), \tag{6.2.3}$$

   where the step-size h_k is chosen such that

$$\nabla\phi'(\lambda^{k+1})\mathbf{F}(\lambda^k) < 0 \quad \textit{and} \quad \lambda^{k+1} \geq 0_{2N}. \tag{6.2.4}$$

2. *Use λ^{k+1} to obtain $\mathbf{u}^{k+1}$ and f^{k+1} as follows:*

$$\mathbf{u}^{k+1} = -\frac{1}{2}\mathbf{A}'\lambda^{k+1}, \quad f^{k+1} = f(\mathbf{u}^{k+1}). \tag{6.2.5}$$

   If $\mathbf{u}^{k+1}$ satisfies the constraints $\mathbf{A}\mathbf{u}^{k+1} \leq \mathbf{b}$ and the stopping criterion $\|\mathbf{F}(\lambda^k)\|_2 \leq \epsilon_\lambda$ is satisfied, then terminate; otherwise return to Step 1 with k replaced by $k+1$.

Remark 6.2.1

1) By Theorem 4.4.1, there exists a fixed step-size $h_k = h$ such that the conditions (6.2.4) are satisfied. Furthermore, there exists a constant $h^* = \frac{2}{\eta_{max}}$, where η_{max} is the largest eigenvalue of the Jacobian matrix $\nabla\mathbf{F}(\lambda^*)$ defined by (4.4.19) such that for the fixed step-size h satisfying $0 < h < h^*$, the sequences $\{\lambda^k\}_{k=0}^{\infty}$ and $\{\mathbf{u}^k\}_{k=0}^{\infty}$ generated by schemes (6.2.3) and (6.2.5) converge, respectively, to the optimum λ^* and the optimal filter $\mathbf{u}^*$, both globally at a linear rate.
2) The proposed iterative BG algorithm 6.2.1 looks similar to the primal-dual (PD) algorithm [12] and the steepest-descent (SD) algorithm [75]. However, there are significant differences.

(a) Comparison with the PD algorithm.

- *The PD algorithm converges very slowly towards the optimum compared to the BG algorithm. Although using a larger step-size can increase the speed of convergence of the PD algorithm, this will result in a larger normalized error. In contrast, the*

BG algorithm possesses a much better transient response. Due to the preservation of the feasibility at all times (see Remark 4.4.1), the normalized error is substantially reduced. Thus, a larger step-size can be chosen in the algorithm so as to increase the speed of convergence without violating the dual constraints.

- *The PD algorithm has difficulties in ensuring that the constraints are satisfied, even when it appears to have converged after a relatively large number of iterations for variable step-size. This is because the search directions in the PD algorithm are discontinuous functions. As a result, the sequence of filters generated by the PD algorithm converges (see [12]) only to within a neighborhood of the optimal filter. On the other hand, the search directions in the BG algorithm are smooth functions and equal to zero on the boundary. Therefore, as shown in Theorem 4.4.1, the sequence of filters generated by the BG algorithm converges to the optimal filter for which the constraints are satisfied.*

(b) Comparison with the SD algorithm based on the constraint transcription and smoothing techniques.

- *In view of Theorem 4.4.1, we note that the sequences generated by the BG algorithm converge globally and asymptotically to the optimal solution. However, the SD algorithm reported in [75] does not possess such a property, as the smoothing parameter is embedded in the gradients and Hessian matrices. To ensure differentiability of the augmented cost function, the smoothing parameter is not allowed to be reduced to zero. Thus, the sequence obtained from the SD algorithm converges only to within a neighborhood of the optimal solution, leading only to a suboptimal solution.*
- *The BG algorithm is extensible to an adaptive algorithm in a stochastic environment. More specifically, an adaptive algorithm based on the BG algorithm is developed in Chapter 7 for solving the EC filtering problem in a noisy environment. However, it does not appear possible to extend the SD algorithm to an adaptive algorithm for a stochastic setting.*

6.2.2.2 Barrier-Newton Algorithm

Using the same transformation function as given in section 6.2.2.1 and following the steps given in Section 4.5, we have the following BN algorithm for solving the discrete-time EC filtering problem (2.3.5).

Algorithm 6.2.2 *Set $k = 0$. Let $\mathbf{D}(\alpha) = \mathbf{D}(e) \in \Re_+^{2N \times 2N}$. Choose an initial point $\lambda^0 \in \Re_+^{2N}$, a proper step-size h_k, and the stopping criterion ϵ_λ.*

1. *Let $\mathbf{d}^k = \nabla \mathbf{F}^{-1}(\lambda^k)\mathbf{D}(\alpha)\mathbf{F}(\lambda^k)$ be a search direction where $\mathbf{F}(\lambda^k)$ and $\nabla \mathbf{F}(\lambda^k)$ are given by*

$$\mathbf{F}(\lambda^k) = \mathbf{D}(\lambda^k)\nabla\phi(\lambda^k), \quad \nabla \mathbf{F}(\lambda^k) = \mathbf{D}(\nabla\phi(\lambda^k)) + \mathbf{D}(\lambda^k)\bar{\mathbf{A}}$$

Calculate the following iterative scheme

$$\lambda^{k+1} = \lambda^k - h_k \mathbf{d}^k$$

in which the step-size h_k is chosen such that

$$\nabla\phi'(\lambda^{k+1})\mathbf{d}^{k+1} < 0 \quad \textit{and} \quad \lambda^{k+1} \geq 0_{2N}. \tag{6.2.6}$$

2. *Use λ^{k+1} to obtain $\mathbf{u}^{k+1}$ and f^{k+1} as follows:*

$$\mathbf{u}^{k+1} = -\frac{1}{2}\mathbf{A}'\lambda^{k+1}, \quad f^{k+1} = f(u^{k+1}).$$

If $\mathbf{u}^{k+1}$ satisfies the constraints $\mathbf{A}\mathbf{u}^{k+1} \leq \mathbf{b}$ and the stopping criterion $\|\mathbf{d}^{k+1}\|_2 \leq \epsilon_\lambda$ is satisfied, then terminate; otherwise return to Step 1 with k replaced by $k+1$.

Remark 6.2.2 *There exists a fixed step-size $h_k = h$ such that the conditions in (6.2.6) are satisfied for all k. Furthermore, we note from Remark 4.4.2 that for a specified $\alpha_i = \bar{\alpha}, i = 1, \ldots, 2N$, the fixed step-size h can be chosen depending on $\mathbf{H}(\lambda^*) = \bar{\alpha}\mathbf{I}_{2N}$. In addition, if the fixed step-size satisfies $0 < h < 2/\bar{\alpha}$, and the Jacobian matrix $\nabla \mathbf{F}(\lambda)$ satisfies a Lipschitz condition in a neighborhood of λ^*, Theorem 4.4.2 ensures that the generated sequence of filters $\{\mathbf{u}^k\}_{k=0}^{\infty}$ converges quadratically to the optimal filter $\mathbf{u}^*$ if $\bar{\alpha} = e \simeq 2.71828$.*

6.3 EC Filtering Problem with ℓ^2 Orthonormal Basis

In this section, the discrete-time EC filtering problem (2.3.16) with ℓ^2 orthonormal basis is studied. The characterization of the optimal filter and the development of two new and simple yet efficient iterative algorithms for solving the EC filtering problem are presented. Applications using the discrete-time Laguerre networks are also given in this section.

6.3.1 Characterization of Optimal Filter

Consider the EC filtering problem (2.3.16) with an approximate ℓ^2 orthonormal basis. The characterization of the optimal filter $u_n^* \in \ell^2$ to the EC filtering problem (2.3.16) relies on the Lagrangian duality theory and properties of a complete orthonormal basis of ℓ^2. We assume that there is an $\mathbf{x}^0 \in \Re^n$ such that $\mathbf{A}_o\mathbf{x}^0 < \mathbf{b}_o$ where $\mathbf{A}_o$ and $\mathbf{b}_o$ are, respectively, defined in (2.3.15). Then, by applying the Lagrangian duality theory to the primal EC filtering problem (2.3.16), we obtain a dual minimization problem.

$$\begin{array}{ll} \min & \phi(\Lambda) = \frac{1}{4}\|\mathbf{A}_o'\Lambda\|_2^2 + \mathbf{b}_o'\Lambda \\ \text{subject to} & \Lambda \geq 0_{2N} \end{array} \tag{6.3.7}$$

where $\Lambda = [\lambda_1, \ldots, \lambda_{2N}]' \in \Re_+^{2N}$ is the Lagrange multiplier vector and $\mathbf{x} = [x_0, \ldots, x_{n-1}]' \in \Re^n$ is the filter coefficient vector expressed in terms of Λ as:

$$\mathbf{x} = -\frac{1}{2}\mathbf{A}_o'\Lambda. \tag{6.3.8}$$

We note from Remark 2.3.1 that the convolution matrix $\mathbf{A}_o\mathbf{A}_o'$ is symmetric positive semi-definite and hence the cost function $\phi(\Lambda)$ is convex. To characterize the optimal filter u_n^* in relation to the optimal Lagrange multipliers $\lambda_i^*, i = 1, \ldots, 2N$, we begin with analyzing the filter coefficient vector $\mathbf{x}$. Substituting the signal matrix $\mathbf{A}_o$ into (6.3.8) and combining with (2.3.10), the $(j+1)$th component of the filter coefficient vector $\mathbf{x}$ is

$$\begin{aligned} x_j &= -\frac{1}{2}\sum_{k=0}^{N-1}\theta_j(k)(\lambda_{k+1} - \lambda_{N+k+1}) = -\frac{1}{2}\sum_{k=0}^{N-1}\left[\sum_{i=0}^{\infty}\varphi_j(i)s(k-i)\right](\lambda_{k+1} - \lambda_{N+k+1}) \\ &= \sum_{i=0}^{\infty}\left[-\frac{1}{2}\sum_{k=0}^{N-1}s(k-i)(\lambda_{k+1} - \lambda_{N+k+1})\right]\varphi_j(i) \\ &= \sum_{i=0}^{\infty}u_n(i)\varphi_j(i). \end{aligned}$$

The optimal filter u_n^* can, therefore, be expressed in terms of the optimal solution of the dual EC filtering problem (6.3.7) as follows:

$$u_n^*(i) = -\frac{1}{2}\sum_{k=0}^{N-1}s(k-i)(\lambda_{k+1}^* - \lambda_{N+k+1}^*), \quad i = 0, 1, \ldots. \tag{6.3.9}$$

We note from (6.3.9) that the optimal filter can be interpreted as consisting of a filter matched to the input signal followed by an equalizer determined by the Lagrange multipliers λ_{k+1}^* and λ_{N+k+1}^*, $k = 0, \ldots, N-1$.

6.3.2 Iterative Algorithms

As in the previous section, we also develop two iterative algorithms based on the BG and BN methods for solving the EC filtering problem (2.3.16).

6.3.2.1 Barrier-Gradient Algorithm

Using the same quadratic component-wise space transformation function as given in the above section, it follows from the steps used to obtain the scheme (6.2.3) and combining with (6.3.8) that we have the BG algorithm for solving the EC filtering problem (2.3.16).

Algorithm 6.3.1 *Set $k = 0$. Choose an initial point $\Lambda^0 \in \Re_+^{2N}$, a proper step-size h_k and a stopping criterion ϵ_Λ.*

1. *Let $\mathbf{F}(\Lambda^k) = \mathbf{D}(\Lambda^k)\nabla\phi(\Lambda^k)$ be a search direction where $\nabla\phi(\Lambda^k) = \frac{1}{2}\mathbf{A}_o\mathbf{A}_o'\Lambda^k + \mathrm{b}_o$. Calculate the following iterative scheme:*

$$\Lambda^{k+1} = \Lambda^k - h_k\mathbf{F}(\Lambda^k) \tag{6.3.10}$$

where the step-size h_k is chosen such that

$$\nabla\phi'(\Lambda^{k+1})\mathbf{F}(\Lambda^{k+1}) < 0 \quad \textit{and} \quad \Lambda^{k+1} \geq 0_{2N}. \tag{6.3.11}$$

2. *Use Λ^{k+1} to obtain $\mathbf{x}^{k+1}$ and f^{k+1} as follows:*

$$\mathbf{x}^{k+1} = -\frac{1}{2}\mathbf{A}_o'\Lambda^{k+1}, \quad f^{k+1} = f(\mathbf{x}^{k+1}). \tag{6.3.12}$$

If $\mathbf{x}^{k+1}$ satisfies the constraints in the primal EC filtering problem (2.3.16), and $\|\mathbf{F}(\Lambda^{k+1})\|_2 \leq \epsilon_\Lambda$ is satisfied, then stop; otherwise return to Step 1 with k replaced by $k+1$.

In view of Theorem 4.4.1, we note that there exists a constant $h^* = \frac{2}{\eta_{max}}$ such that if a fixed step-size is chosen satisfying $0 < h_k = h < h^*$ for all k, then so are the conditions (6.3.11). Furthermore, the sequences $\{\Lambda^k\}_{k=0}^{\infty}$ and $\{\mathbf{x}^k\}_{k=0}^{\infty}$ generated by the schemes (6.3.10) and (6.3.12) converge, respectively, to the optimal solutions Λ^* and $\mathbf{x}^*$, both globally at a linear rate. Here η_{max} is the largest eigenvalue of $\nabla\mathbf{F}(\Lambda^*)$ defined analogously to $\nabla\mathbf{F}(\lambda^*)$.

6.3.2.2 Barrier-Newton Algorithm

Using the BN method as given in Section 4.5 and combining with (6.3.8), the following algorithm is obtained to solve the EC filtering problem (2.3.16):

Algorithm 6.3.2 *Set $k = 0$. Let $\mathbf{D}(\alpha) = \mathbf{D}(e) \in \Re_+^{2N\times 2N}, (e \simeq 2.71828)$. Choose an initial point $\Lambda^0 \in \Re_+^{2N}$, a proper step-size h_k and a stopping criterion ϵ_Λ.*

1. *Let $\mathbf{d}^k = \nabla\mathbf{F}^{-1}(\Lambda^k)\mathbf{D}(\alpha)\mathbf{F}(\Lambda^k)$ be a search direction where $\mathbf{F}(\Lambda^k)$ and $\nabla\mathbf{F}(\Lambda^k)$ are, respectively, defined as follows:*

$$\mathbf{F}(\Lambda^k) = \mathbf{D}(\Lambda^k)\nabla\phi(\Lambda^k), \quad \nabla\mathbf{F}(\Lambda^k) = \mathbf{D}(\nabla\phi(\Lambda^k)) + \frac{1}{2}\mathbf{D}(\Lambda^k)\mathbf{A}_o\mathbf{A}_o'.$$

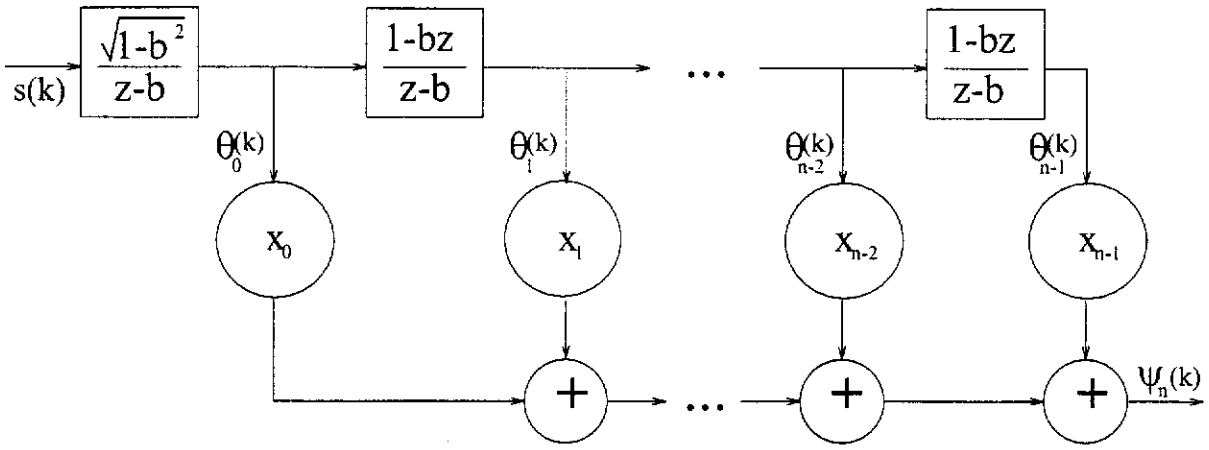

Figure 6.1: Implementation of an EC discrete-time Laguerre networks.

Calculate the following iterative scheme:

$$\Lambda^{k+1} = \Lambda^k - h_k \mathbf{d}^k$$

in which the step-size h_k is chosen such that

$$\nabla\phi'(\Lambda^{k+1})\mathbf{d}^{k+1} < 0 \quad \textit{and} \quad \Lambda^{k+1} \geq 0_{2N}. \tag{6.3.13}$$

2. *Use Λ^{k+1} to obtain $\mathbf{x}^{k+1}$ and f^{k+1} as follows:*

$$\mathbf{x}^{k+1} = -\frac{1}{2}\mathbf{A}_o'\Lambda^{k+1}, \quad f^{k+1} = f(\mathbf{x}^{k+1}).$$

If $\mathbf{x}^{k+1}$ satisfies the constraints in the EC filtering problem (2.3.16), and $\|\mathbf{d}^{k+1}\|_2 < \epsilon_\Lambda$ is satisfied, then stop; otherwise return to Step 1 with k replaced by $k+1$.

We note by Theorem 4.4.2 that the sequences $\{\Lambda^k\}_{k=0}^{\infty}$ and $\{\mathbf{x}^k\}_{k=0}^{\infty}$ generated by the above algorithm converge quadratically to the optimal solutions Λ^* and $\mathbf{x}^*$, respectively, if a fixed step-size is chosen satisfying $0 < h_k = h < 2/\bar{\alpha}$ for all k. We further note that the speed of convergence can be significantly improved by adjusting the scaling parameter $\bar{\alpha}$ and hence the fixed step-size h to meet the conditions (6.3.13).

6.3.3 Application: Discrete-Time Laguerre Networks

Consider the Laguerre orthonormal basis functions in the Hilbert space ℓ^2. Let the jth order discrete-time Laguerre function in Z-domain be given by

$$\mathcal{L}_j^b(z) = \frac{\sqrt{1-b^2}}{1-bz^{-1}}\left(\frac{z^{-1}-b}{1-bz^{-1}}\right)^j, \quad j = 0, 1, \ldots,$$

where $-1 < b < 1$ is an adjustable pole. It is well known that the discrete-time Laguerre sequence $\{\mathcal{L}_j^b(z)\}_{j=0}^{\infty}$ forms an orthonormal basis in the Hardy space [52, 67]. Since the Hardy space is isomorphic to the Hilbert space, the transfer function of the Laguerre networks is given by

$$U(z) = \sum_{j=0}^{\infty} x_j \mathcal{L}_j^b(z).$$

The corresponding present value of the noiseless output response can be written as:

$$\psi(k) = \sum_{j=0}^{\infty} \theta_j(k) x_j, \quad k = 0, 1, \ldots$$

where $\theta_j(k) = \sum_{i=0}^{\infty} \mathcal{L}_j^b(i) s(k-i)$. In the following, we consider only the nth partial sum of U_n. Then, $\|U_n\|_2^2 = \mathbf{x}'\mathbf{x}$ and the discrete-time EC filtering problem with an approximate Laguerre basis can be realized as shown in Figure 6.1, where $s(k)$ and $\psi_n(k), k = 0, \ldots$, denote, respectively, the present values of the input signal and output response. It is worth noting that the FIR filter is a special case of the Laguerre filter with $b = 0$.

6.4 Numerical Results

To demonstrate the efficiency of the proposed BG and BN algorithms, two practical examples involving pulse compression and channel equalization are solved in this section. For comparison, the quadratic programming in the MATLAB optimization toolbox [27] is applied to each of these problems. The optimal solution $\mathbf{u}_{qp}^*$ and the corresponding Lagrange multiplier λ_{qp}^* (respectively, $\mathbf{x}_{qp}^*$ and Λ_{qp}^*) are used as the benchmark in the design of the discrete-time EC optimum filter using FIR model structure (respectively, the EC filtering with discrete-time Laguerre networks).

6.4.1 Test 1: Discrete-Time EC Optimum Filter

Two practical examples involving pulse compression Barker code signal and the digital transmission channel equalization are presented. They are solved by using the BG algorithm 6.2.1 and the BN algorithm 6.2.2.

Pulse Compression

The first test example involves the rectangular pulse compression of a 13-bit Barker code signal (m=13) as shown in Figure 6.2(a) and given by

$$\mathbf{s} = [1\ 1\ 1\ 1\ 1\ -1\ -1\ 1\ 1\ -1\ 1\ -1\ 1]' \in \Re^{13}.$$

The output mask is a mainlobe peak of 0.69 ± 0.075 with sidelobe levels of ± 0.025 in conjunction with a filter with $n = 27$ samples. Correspondingly, the desired output response vector d and the tolerance band vector ϵ are given by

$$\mathbf{d} = [\underbrace{0, \ldots, 0}_{19}, 0.69, \underbrace{0, \ldots, 0}_{19}]' \quad \text{and} \quad \epsilon = [\underbrace{0.025, \ldots, 0.025}_{19}, 0.075, \underbrace{0.025 \ldots, 0.025}_{19}]'.$$

The output response is required to fit into the output mask while the noise power gain at the output response is to be minimized. The normalized error (NE) defined by $NE \triangleq \frac{\|\mathbf{u}_{qp}^* - \mathbf{u}^k\|_2}{\|\mathbf{u}_{qp}^*\|_2}$ is applied to measure the accuracy of an estimated filter $\mathbf{u}^k$.

The BG algorithm 6.2.1 was run with a fixed step-size $h = 2.8$, while the BN algorithm 6.2.2 was run with three different step-sizes in conjunction with three different $\bar{\alpha}$, i.e, $(h = 8.0 \times 10^{-2}, \bar{\alpha} = 1.0e)$, $(h = 9.0 \times 10^{-1}, \bar{\alpha} = 0.1e)$, and $(h = 1.93, \bar{\alpha} = 0.05e)$. The optimal Lagrange multiplier vector, the optimal filter (restricted to n=27 samples), and the equalized output response are shown, respectively, in Figures 6.2(b)-(d). It is clear from Figure 6.2(d) that for both methods, the output response completely fits into the mask. To illustrate the convergence results for the proposed BG and BN algorithms, we depict the results of $\|\mathbf{u}^k - \mathbf{u}_{qp}^*\|_2$, $\|\lambda^k - \lambda_{qp}^*\|_2$, $\|\psi^k - \psi_{qp}^*\|_2$, and NE with the convergence criterion $\epsilon_\lambda = 10^{-6}$, respectively, in Figure 6.3 and Figure 6.4. Clearly, the normalized errors as shown in Figures 6.3(b) and 6.4(b) have been substantially reduced to be close to zero. This means that these iterative algorithms have a high accuracy for estimating the filter. Furthermore, by adjusting the scaling parameter $\bar{\alpha}$ in combination with the Jacobian matrix $\nabla \mathbf{F}(\lambda)$, the performance of the BN Algorithm as shown in Figure 6.4 can be significantly improved compared to that of the BG algorithm as shown in Figure 6.3. However, the BG algorithm can be made adaptive which is then suitable for the stochastic noisy training case due to its simple structure. This is the subject matter of Chapter 7. On the other hand, it does not appear possible to extend the BN algorithm to an adaptive noisy training algorithm.

Channel Equalization

In this example, we concern with the equalization of a digital transmission channel consisting of a coaxial cable operating at the DSX3 rate [5]. The design objective is to find an equalizing filter which takes a sampled impulse response of a coaxial cable with a loss of $30dB$ at a normalized frequency of $1/\bar{\beta}$ as input, where $\bar{\beta}$ is the baud interval, and produces an output which lies within the envelope given by the DSX3 pulse template. Since the input signal is decayed to a negligible level at $t = 32\bar{\beta}$, it can be treated as a time limited signal over the interval $[0, 32\bar{\beta}]$. For this filter design problem, since the input signals are in a continuous-time setting and given

in Section 5.4.2, the analog input signals are discretized and sampled in a period of $\frac{\bar{\beta}}{8}$ time unit over the interval $[0, 32\bar{\beta}]$.

In this example, the fixed step-size for the BG algorithm is given by $h = 0.5$. Similar to the testing procedures in the pulse compression example, the BN algorithm was separately run with three different step-sizes in conjunction with three different scaling parameters $\bar{\alpha}$, $(h = 0.12, \bar{\alpha} = e)$, $(h = 1.3, \bar{\alpha} = 0.1e)$, and $(h = 2.85, \bar{\alpha} = 0.05e)$. It is clear from Figure 6.5 that the optimal output response completely fits into the prescribed output envelope constraints. Figure 6.6 and Figure 6.7 have shown, respectively, the convergence results obtained by using the BG and the BN algorithms with the convergence criterion $\epsilon_\lambda = 10^{-5}$. In particular, we demonstrate that without violating the dual constraints, a bigger fixed step-size h in combination with a small scaling parameter $\bar{\alpha}$ could made a significant improvement on the speed of convergence.

6.4.2 Test 2: EC Filter with Discrete-Time Laguerre Networks

In this test example, the proposed BG algorithm 6.3.1 and the BN algorithm 6.3.2 are used to design an equalization filter using Laguerre networks for a digital transmission channel consisting of a coaxial cable on which data is transmitted. The accuracy of the estimated filter coefficient vector $\mathbf{x}$ is measured by NE defined by $NE = \frac{\|\mathbf{x}^*_{qp} - \mathbf{x}^k\|_2}{\|\mathbf{x}^*_{qp}\|_2}$.

The number of taps in our simulation studies is $n = 16$ Laguerre coefficients in combination with a fixed pole $b = 0.4$ and the discretized input signal which is sampled every $\frac{\bar{\beta}}{8}$ time unit on the interval $[0, 32\bar{\beta}]$. We choose a fixed step-size $h = 0.5$ for the BG algorithm 6.3.1. For the BN algorithm 6.3.2, we use, as in the previous example, three different fixed step-sizes in conjunction with three different scaling parameters $\bar{\alpha}$, i.e, $(h = 0.12, \bar{\alpha} = e)$, $(h = 1.3, \bar{\alpha} = 0.1e)$ and $(h = 2.9, \bar{\alpha} = 0.05e)$. The noiseless optimal output response obtained by either the BG algorithm or the BN algorithm completely fits into the output envelope in a finite number of iterations and is shown in Figure 6.8. The convergence results depicted in Figure 6.9 and Figure 6.10 are obtained with the convergence criterion $\epsilon_\Lambda \leq 10^{-5}$.

We note that Test 1 and Test 2 presented in this section have clearly demonstrated that the proposed BG and BN algorithms are efficient for solving the discrete-time EC filtering problems.

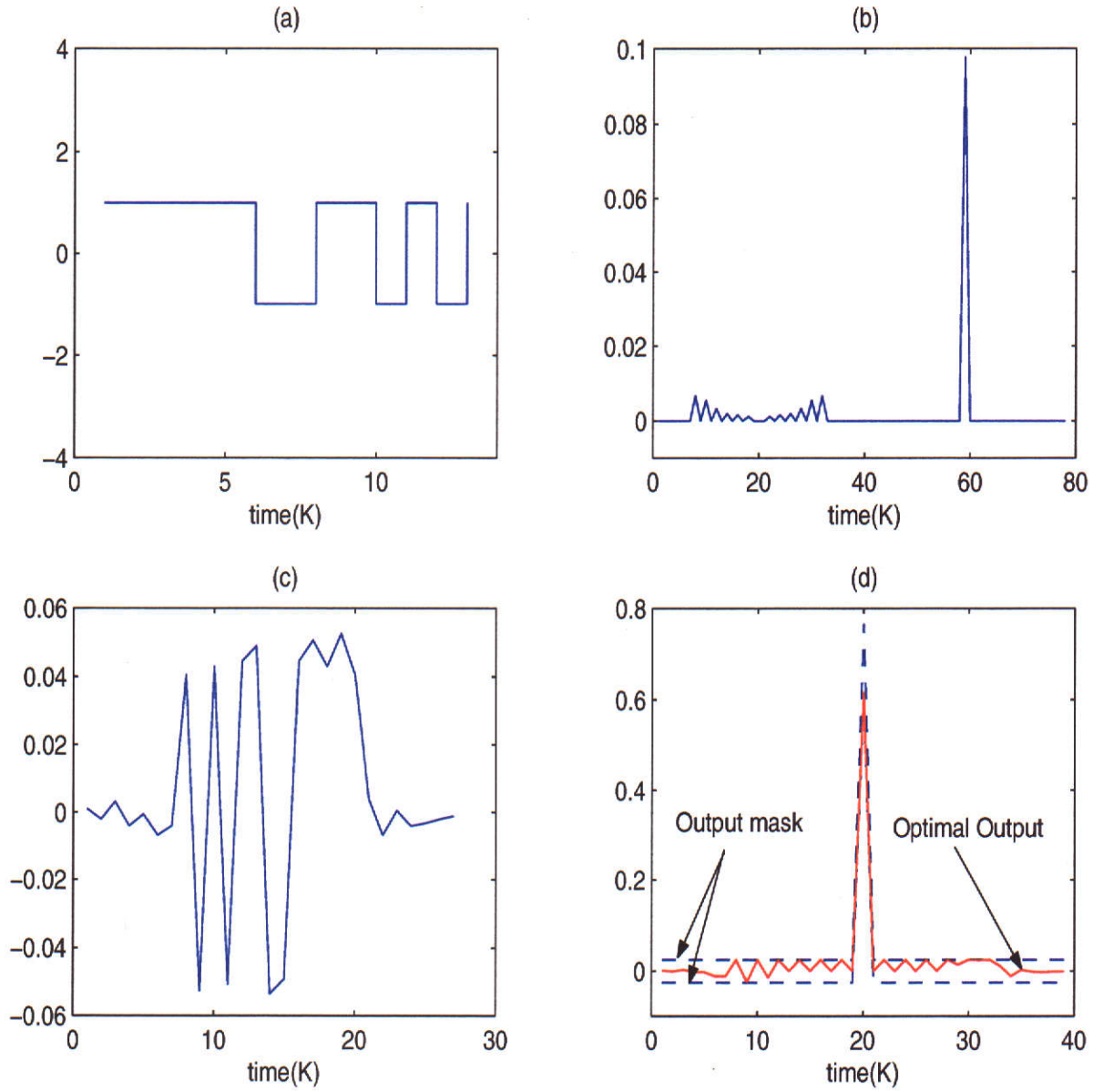

Figure 6.2: Sidelobe reduction problem for 13-bit barker-code signal (a): Original 13-bit barker-code signal **s**. (b): Optimal Lagrange multiplier vector λ^*. (c): Optimal filter $\mathbf{u}^*$. (d): Optimal output response ψ^* and output mask (dash line).

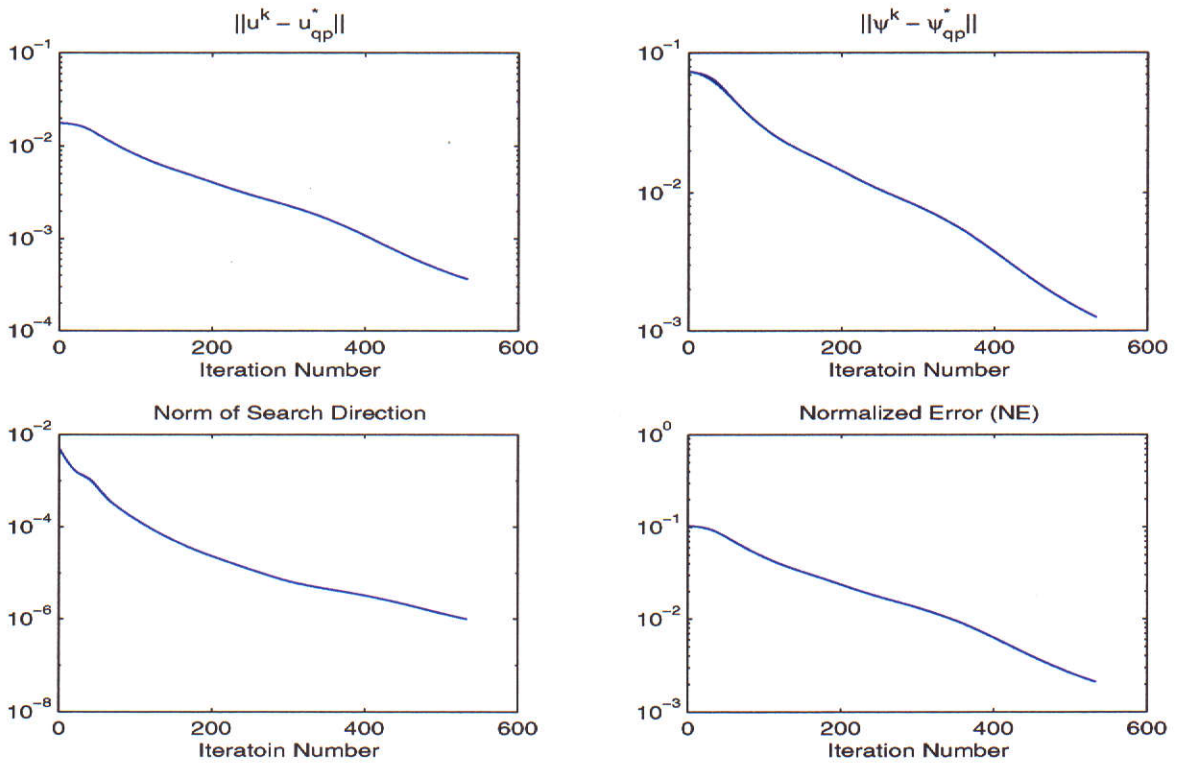

Figure 6.3: The convergence results for the iterative barrier-gradient algorithm.

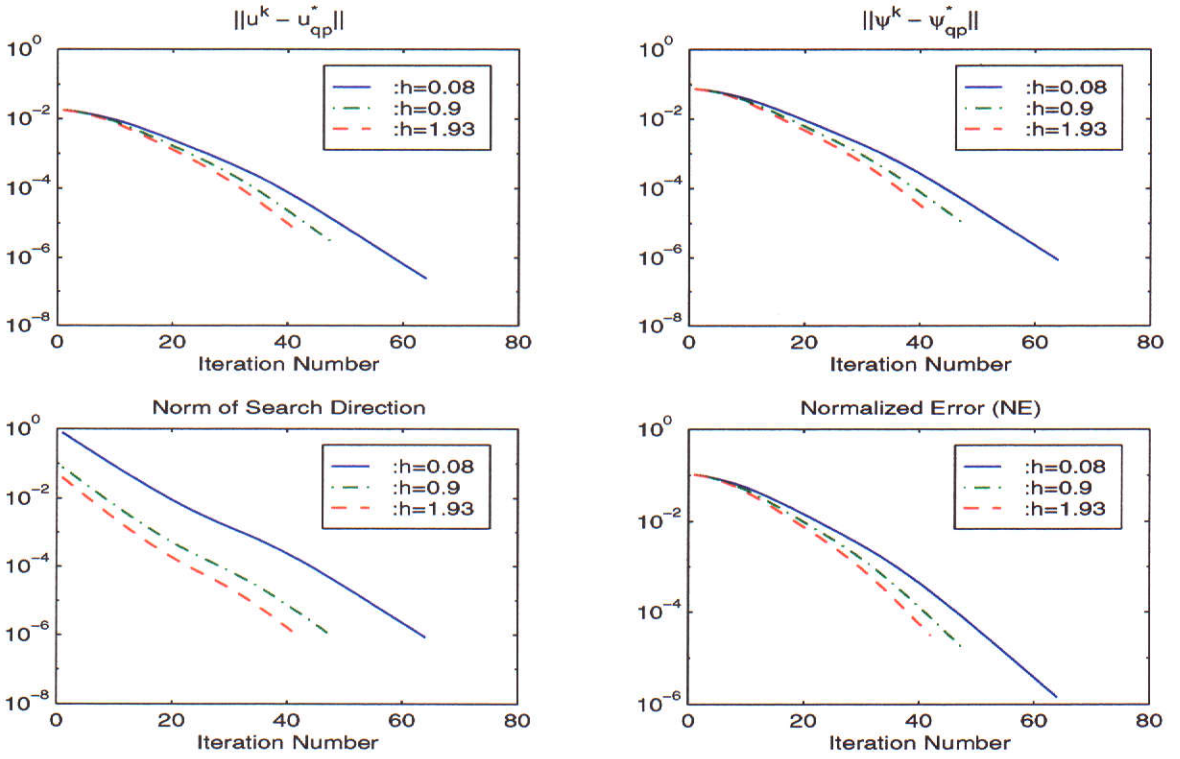

Figure 6.4: The convergence results for the iterative barrier-Newton algorithm.

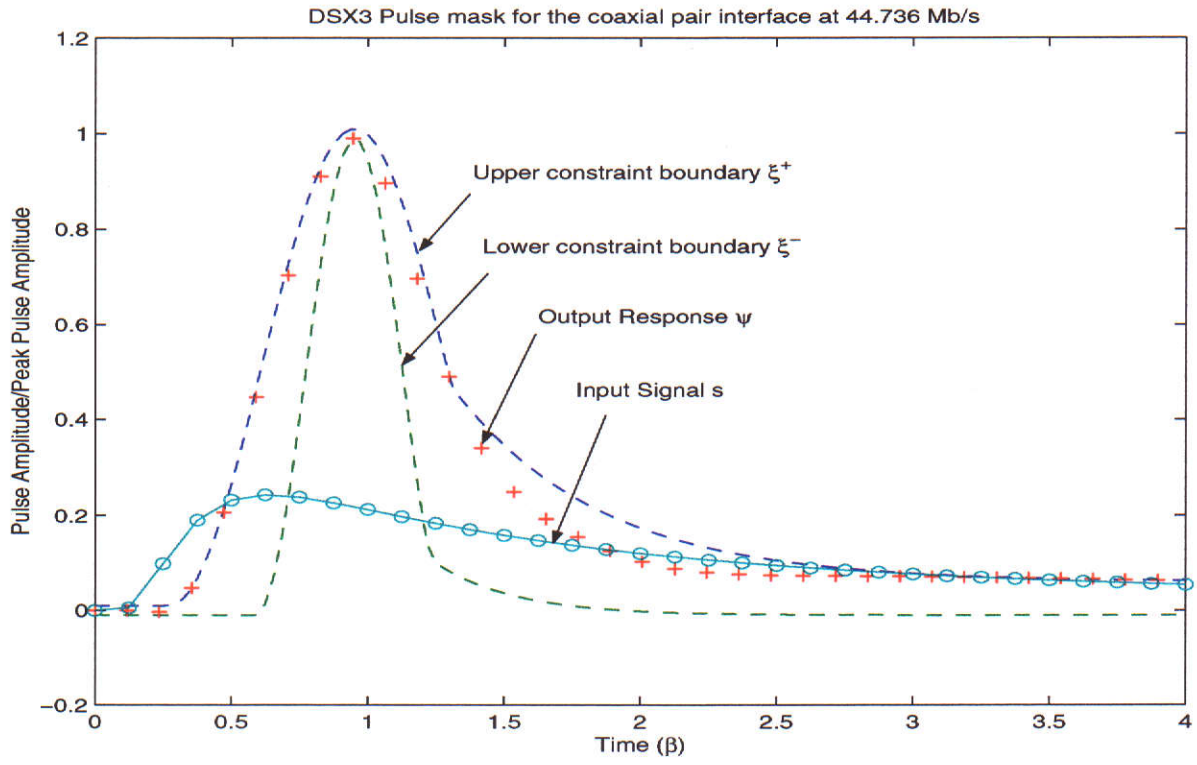

Figure 6.5: Input signal and output response with sampling period $\frac{\bar{\beta}}{8}$ for the optimal FIR EC filter.

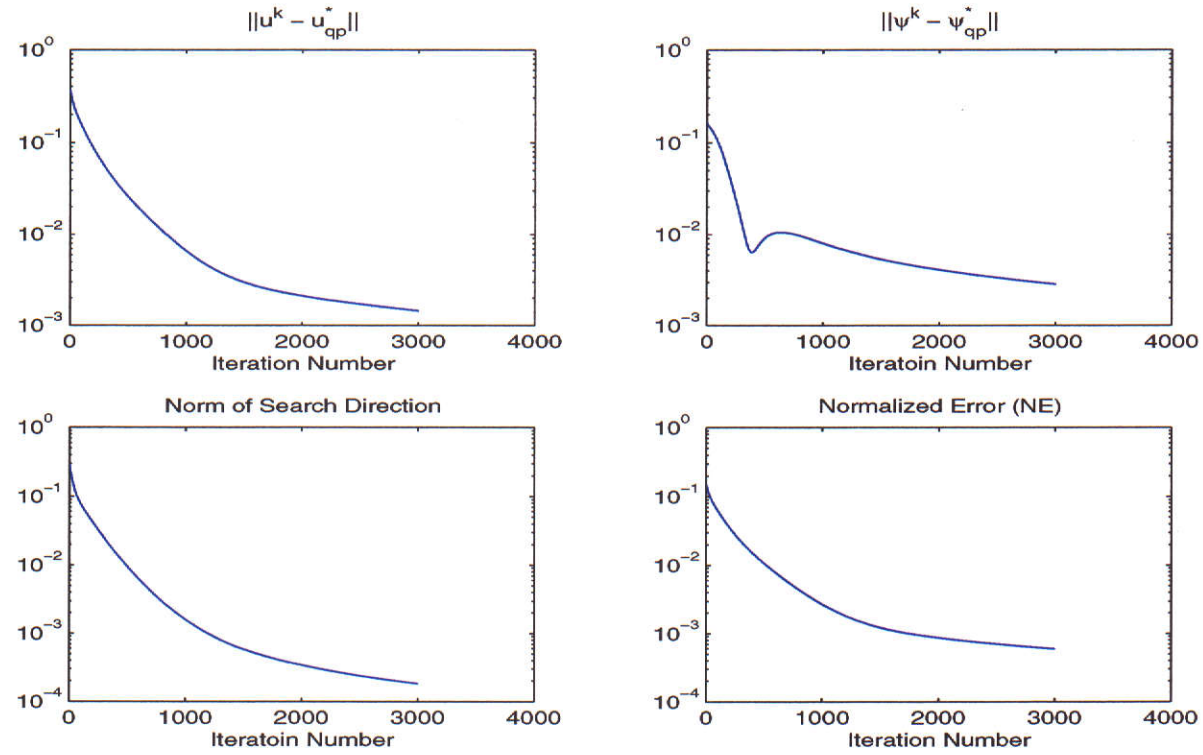

Figure 6.6: The convergence results for the barrier-gradient algorithm using FIR EC filter.

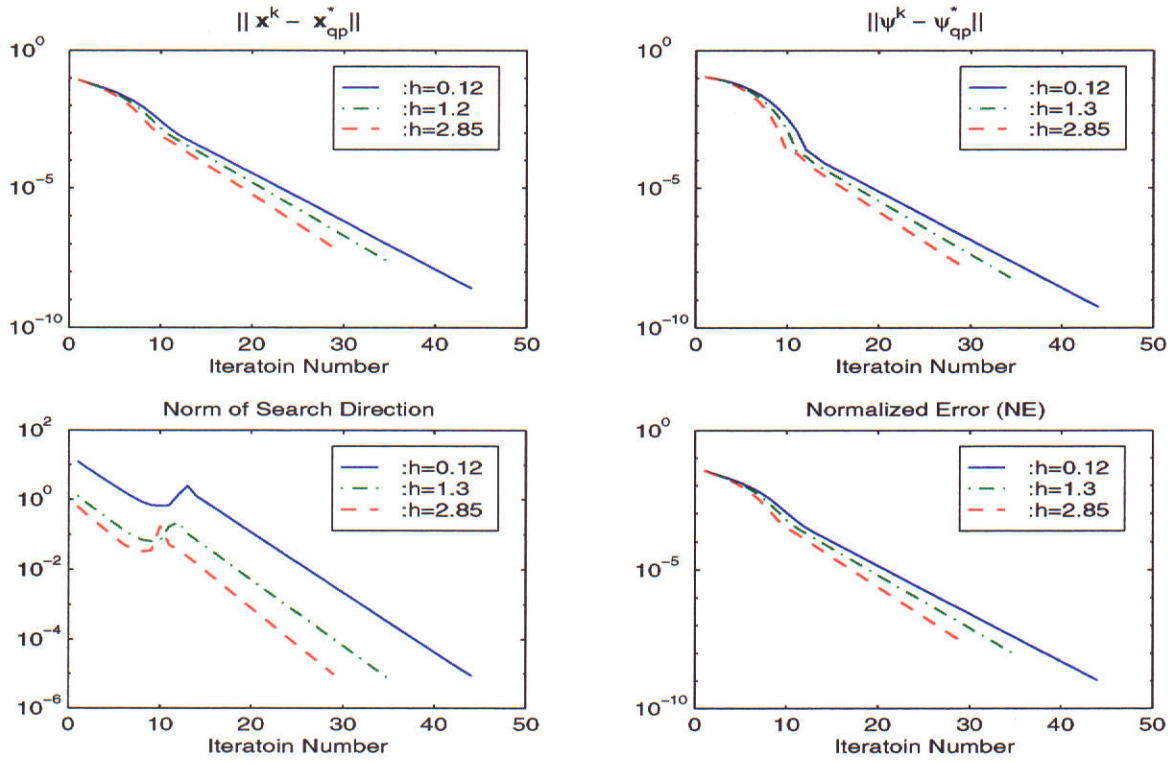

Figure 6.7: The convergence results for the barrier-Newton algorithm using FIR EC filter.

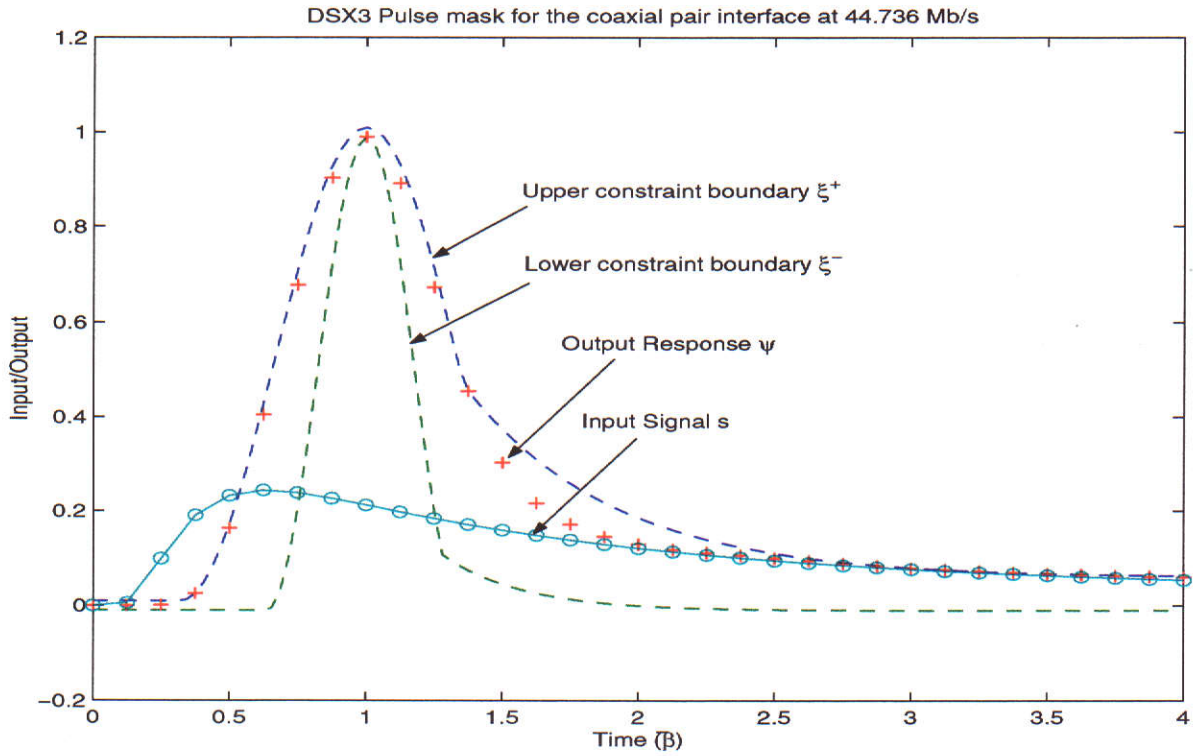

Figure 6.8: Input signal and output response with sampling period $\frac{\bar{\beta}}{8}$ for the optimal Laguerre EC filters

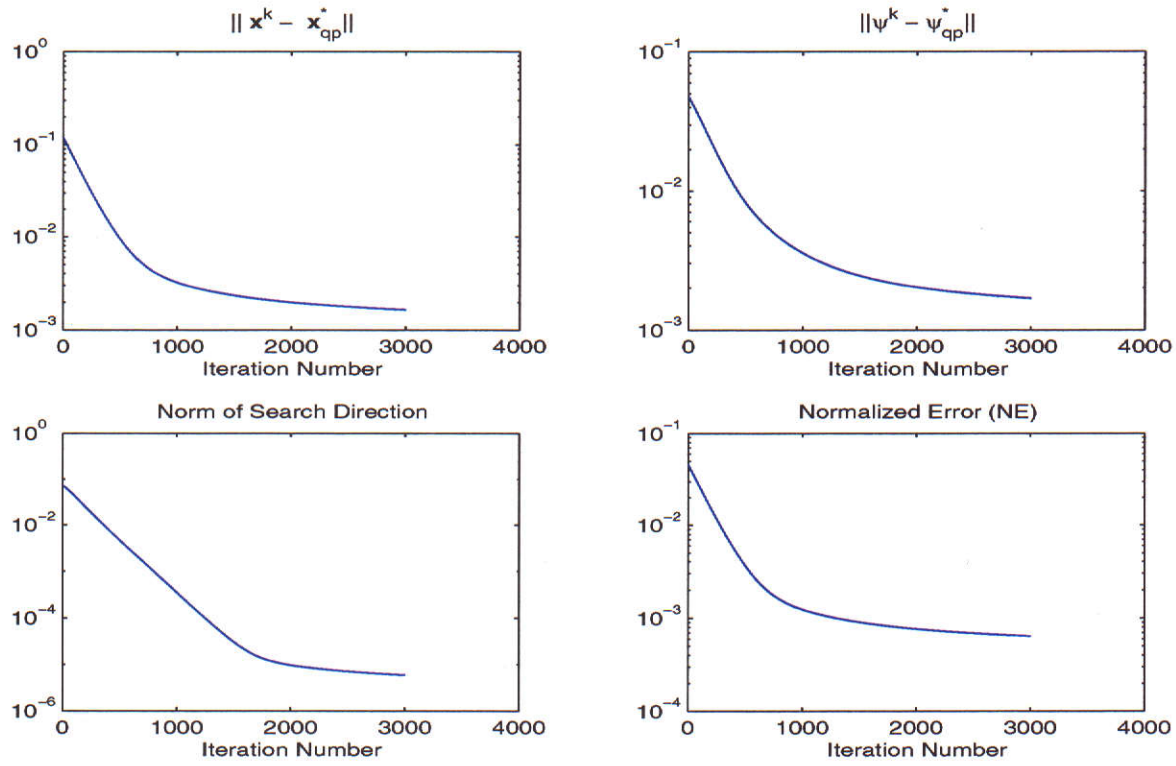

Figure 6.9: The convergence results for the barrier-gradient algorithm using Laguerre EC filter.

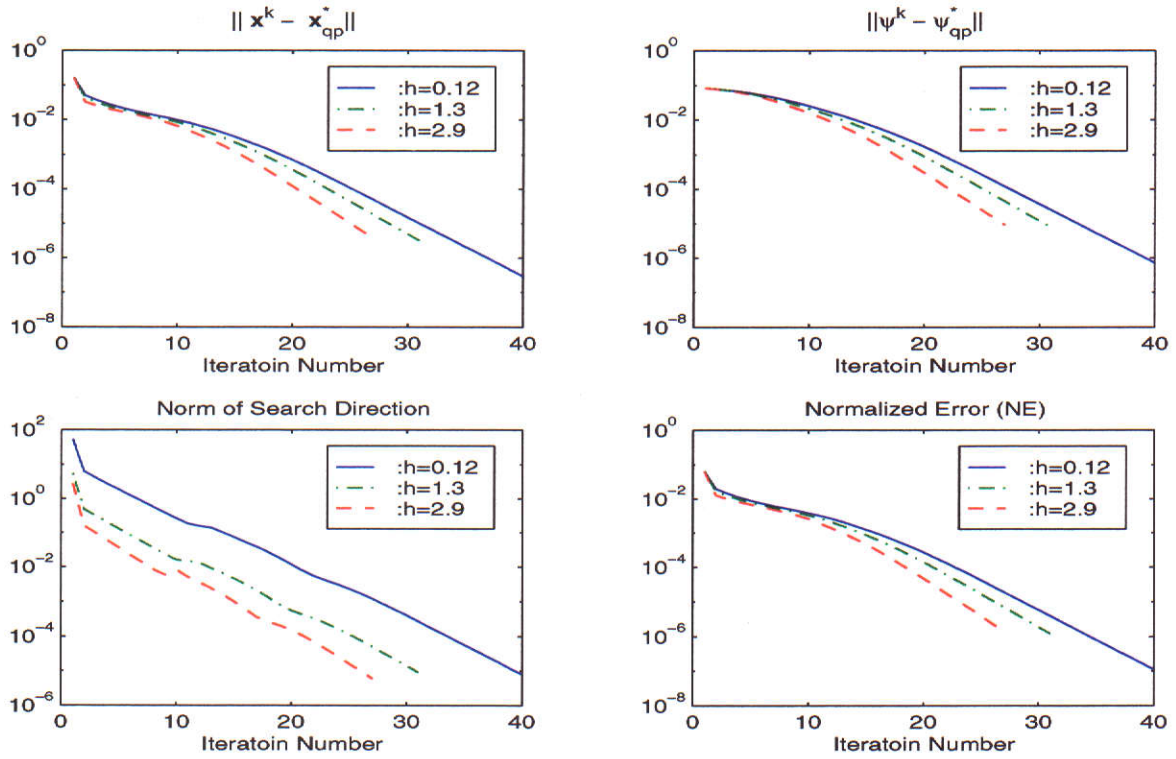

Figure 6.10: The convergence results for the barrier-Newton algorithm using Laguerre EC filter.

Chapter 7

Adaptive Implementation for Discrete-Time EC Filtering Problem

7.1 Introduction

For an adaptive (on-line) version of the EC filtering problem, the signal $\mathbf{s}$ is the input to the adaptive filter $\mathbf{u}$. Typically, $\mathbf{s}$ results from passing periodically a known test or training signal s_T at a predetermined time through a channel that may be time-varying or unknown. The output response ψ is checked against the required mask as shown in Figure 7.1.

The adjustable filter $\mathbf{u}$ in Figure 7.1 is an equalizing filter to combat the distortion introduced by the unknown channel. The result of the comparison between the output response ψ and the constraint boundaries ϵ^+ and ϵ^- is then processed in some way and fed back to adjust the filter $\mathbf{u}$. This process is repeated until the filter is sufficiently well trained and hence is ready to process data. Additional test pulses are then inserted in the data stream at regular intervals so that the filter can continue to adjust itself and track any change in the channel through which it passes. Ideally, the equalization filter would be obtained adaptively.

The motivation for considering this type of adaptive structure is very strong as discussed by Widrow, Haykin, and others [26, 29, 69]. It is important to note that, although the structures are similar, the adaptive EC filter differs in a fundamental way from all other adaptive filters. The distinctive feature is the set of inequality constraints on the output waveform: rather than attempt to match a specific desired pulse shape, we deal with a whole set of allowable outputs and seek an optimal point of that set.

The EC filters posted in the 1970's [12, 13] soon led to attempt to analyze its convergence behavior in noisy and noise-free environments. Combining the primal-dual (PD) algorithm [22]

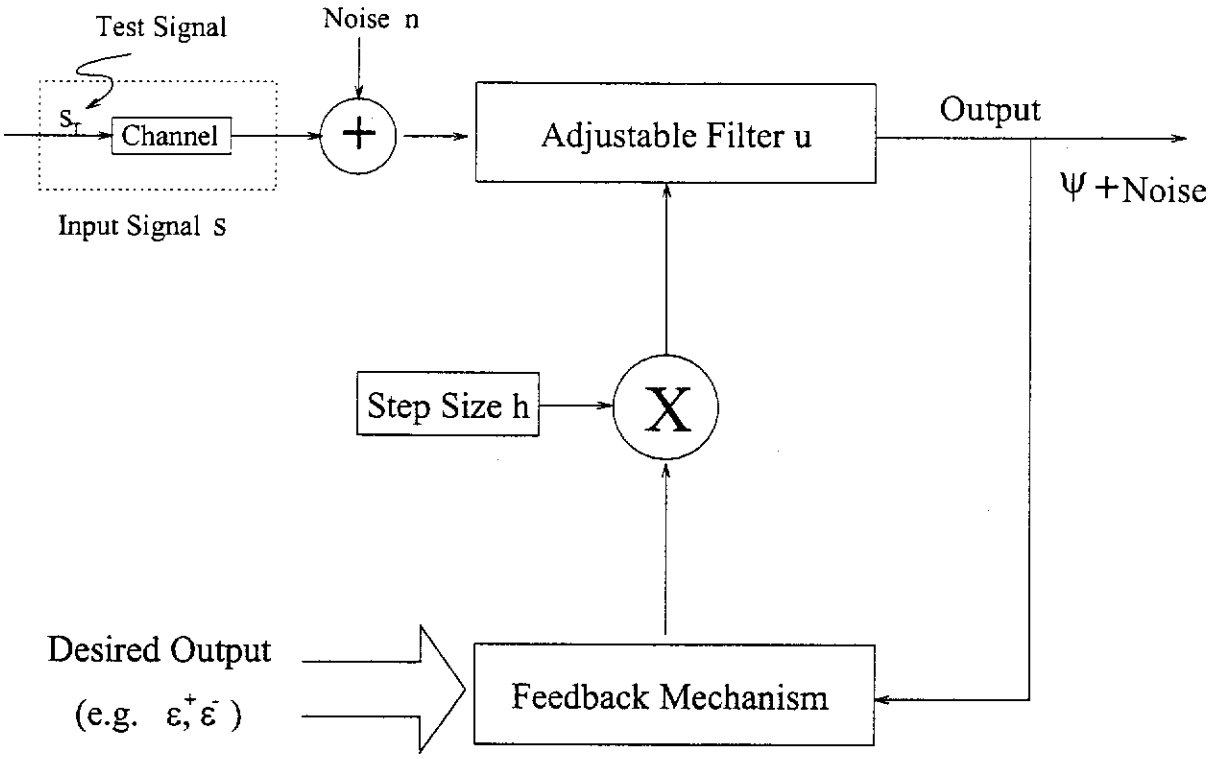

Figure 7.1: Feedback adaptive structure.

with the Goldstein-Levitin-Poljak gradient projection method [23], a number of results have been obtained in both the deterministic and the stochastic settings. However, the convergence properties of the iterative PD algorithm are rather slow and poor. For the case of a fixed step-size, since the search directions in the PD algorithm are discontinuous, the sequence of filters generated by the iterative noise-free algorithm (respectively, the adaptive algorithm) converges only to within a neighborhood of the noiseless optimal filter.

In [75], the constraint transcription and smoothing techniques [28] are used to convert the EC filtering problem into an unconstrained optimization problem involving a penalty parameter and a smoothing parameter. The summation of all the obtained approximate constraints is appended to the cost function as a penalty function. Recursive procedures are thus developed to solve the EC filtering problem leading to iterative design algorithms suitable for applications with large signal-to-noise ratios. However, The extension to an adaptive algorithm for a stochastic environment does not appear possible.

In this chapter, we develop an adaptive training algorithm based on the iterative BG algorithm proposed in Section 6.2 for dealing with the EC filtering problem in a stochastic environment. The convergence properties of the adaptive algorithm are established in the mean sense, and in the mean square sense for a fixed step-size. Moreover, the adaptive algorithm

converges in mean square sense and with probability one when a sequence of decreasing step-sizes is used. The results in this chapter are analogous to those obtained by using the adaptive PD algorithm [12, 13] for solving the EC filtering problem in stochastic setting. Furthermore, these results are analogous to Widrow's work on adaptive least mean square (LMS) filters, but in the context of a constrained pulse shaping.

This chapter is organized as follows: Consider the case in which the input signal is corrupted by additive random noise. Then, by the iterative BG algorithm developed in Section 6.2, an adaptive algorithm is developed in Section 7.2 for solving the discrete-time EC filtering problem (2.3.5) in a stochastic setting. The convergence properties in mean sense and in mean square sense are established in Section 7.3 for the adaptive algorithm with a fixed step-size in Theorem 7.3.1 and Theorem 7.3.2, respectively. For a sequence of decreasing step-sizes, the convergence properties in mean square sense and with probability one (w.p.1) are obtained in Theorem 7.3.3.

In Section 7.4, the structure and convergence properties of the adaptive BG filter are compared with those of the adaptive PD filter given in [12, 13], and with those of the adaptive LMS filter given in [9, 68, 69]. In Section 7.5, some numerical results involving pulse compression and channel equalization are given to illustrate the convergence in mean sense and in mean square sense through solving the EC filtering problem (2.3.5) in a noisy environment. In particular, the approximate mean of the adaptive EC filter and the corresponding approximate mean filter output are compared with those obtained by the off-line optimal EC filter and the corresponding optimal output response. For testing the convergence properties in mean square sense, many simulations have been carried out using different fixed step-sizes. We observed that when the adaptive algorithm approaches steady state, a smaller fixed step-size gives rise to a smaller magnitude of mean square error.

The main references of this chapter are [60, 63, 64].

7.2 Adaptive Structures

Consider the iterative BG algorithm 6.2.1. There are basically three approaches [12] of interest when noise is present:

1) The input signal-to-noise ratio (SNR) is high enough so that the effects of the noise can be ignored;

2) Before processing adaptive iterations, many noise test pulses are averaged, stored and used repeatedly in the iteration process;

3) The noisy inputs are used directly in the adaptive algorithm.

Approach 1 can be considered as a noise-free case (i.e., the input signal s used for updating the filter is not corrupted by noise). Thus, the iterative BG scheme obtained in Chapter 6 is directly applicable.

For the noisy case, the input signal $\mathbf{s}$ is contaminated by additive input noise $\mathbf{n}$. This noise has the effect of distorting the input signal so that the signal matrix $\mathbf{S}$ defined by (2.3.1) and the filter output response $\psi = \mathbf{Su}$ are noisy. As a result, the search direction $\mathbf{F}(\lambda)$ determined in the iterative Algorithm 6.2.1 is corrupted. This leads to the use of an adaptive processor stated in Approach 2 and Approach 3. More specifically, Approach 2 is to average enough noisy input signals so that a good estimate of input signal $\mathbf{s}$ is obtained. The averaged signal is then stored and used repeatedly in the training process. Since the input signal has become deterministic, the training process can be analyzed as in Section 4.4 with the same convergence properties given in Theorem 4.4.1.

A possible hardware structure for implementing Approach 2 using the adaptive BG algorithm is indicated schematically as shown in Figure 7.2. The hardware requirements for the adaptive EC filter are relatively modest. A tapped delay line realizes the filter itself, and three other delay lines store the Lagrange multipliers and the constraint boundaries. The calculation of the new filter $\mathbf{u}^{k+1}$ requires n multipliers and n accumulators.

The operation of the hardware structure is synchronous, starting when the first component $\mathbf{s}_1$ of the input sequence enters the tapped delay line. For each component $\mathbf{s}_i, i = 1, \ldots, m$, enters ψ_i^k, $\mathbf{d}_i$, and ϵ_i are all added together to determine the descent search direction $-\mathbf{F}(\lambda^k)$ following by feeding back the λ_i^k. The input is also correlated with $-\frac{1}{2}\lambda_i^k$. After the entire signal has traversed the tapped delay line, the correlator contains the new filter $\mathbf{u}^{k+1} = -\frac{1}{2}\mathbf{A}'\lambda^{k+1}$ to form the new output response $\psi^{k+1} = \mathbf{Su}^{k+1}$ and then fed back the error between the output, and the upper and lower boundaries where the feed back output is formed by

$$\begin{bmatrix} \psi^{k+1} \\ -\psi^{k+1} \end{bmatrix} = -\frac{1}{2}\mathbf{A}\mathbf{A}'\lambda^{k+1} \quad \text{and} \quad \mathbf{A} \triangleq \begin{bmatrix} \mathbf{S} \\ -\mathbf{S} \end{bmatrix}.$$

In Approach 3, each iterate uses the noisy search direction $\mathbf{F}(\tilde{\lambda})$. Thus, the adaptive filters are determined in accordance with the changing statistics of the input signals to be filtered. It is, therefore, more practical than Approach 2. This is the main subject matter of this chapter.

We assume that the noisy input signal at the kth iteration is

$$\tilde{\mathbf{s}}^k = \mathbf{s} + \mathbf{n}^k = [s_1, \ldots, s_m]' + [n_1^k, \ldots, n_m^k]'$$

where $\mathbf{n}^k$ is a vector of zero-mean and white noise samples with variance σ^2. Then, the noisy

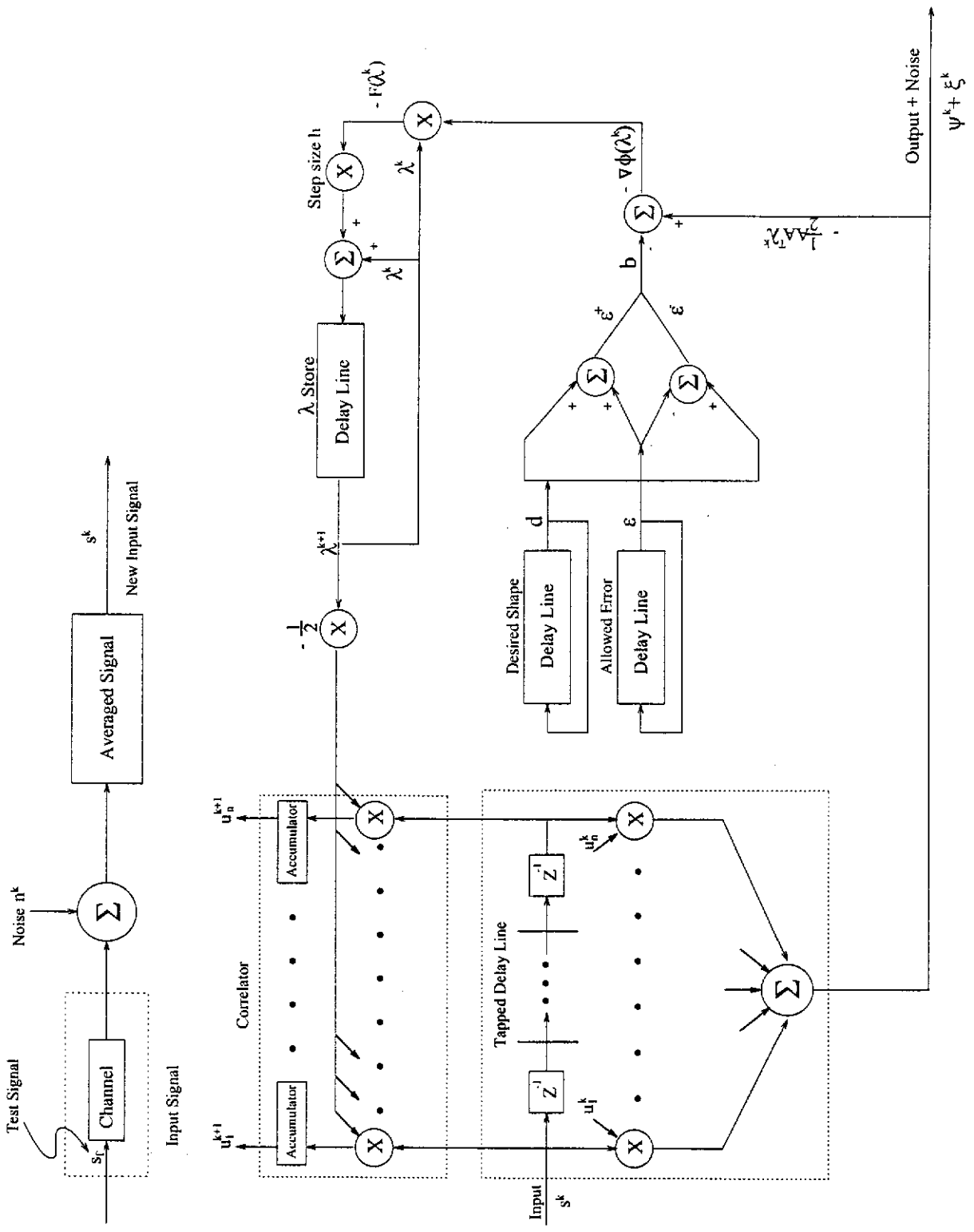

Figure 7.2: Adaptive barrier-gradient filter.

output signal at the kth iteration is

$$\tilde{\psi}^k \triangleq (\mathbf{S} + \mathbf{N}^k)\tilde{\mathbf{u}}^k = \psi^k + \xi^k$$

where $\mathbf{N}^k$ is a $N \times n$ matrix of noise sample defined by

$$\mathbf{N}^k = \begin{bmatrix} n_{j+1}^k & 0 & \cdots & 0 \\ \vdots & n_{j+1}^k & \ddots & \vdots \\ n_{j+m}^k & \vdots & \ddots & 0 \\ 0 & n_{j+m}^k & & n_{j+1}^k \\ \vdots & \ddots & \ddots & \vdots \\ 0 & \cdots & 0 & n_{j+m}^k \end{bmatrix},$$

while $(n_{j+1}^k, \ldots, n_{j+m}^k)$ are the last m noise samples. The adaptive training version is thus given by

$$\begin{cases} \mathbf{F}(\tilde{\lambda}^k) &= \mathbf{D}(\tilde{\lambda}^k)[\frac{1}{2}(\mathbf{A} + \tilde{\mathbf{N}}^k)(\mathbf{A} + \tilde{\mathbf{N}}^k)'\tilde{\lambda}^k + \mathbf{b}] \\ \tilde{\lambda}^{k+1} &= \tilde{\lambda}^k - h\mathbf{F}(\tilde{\lambda}^k) \\ \tilde{\mathbf{u}}^{k+1} &= -\frac{1}{2}(\mathbf{A} + \tilde{\mathbf{N}}^k)'\tilde{\lambda}^{k+1}, \quad k = 0, 1, \ldots \end{cases} \tag{7.2.4}$$

where $\tilde{\mathbf{N}}^{k'} = [\mathbf{N}^{k'}, -\mathbf{N}^{k'}] \in \Re^{n \times 2N}$. Since both $\tilde{\mathbf{u}}^{k+1}$ and $\tilde{\lambda}^{k+1}$ depend on $(\mathbf{A} + \tilde{\mathbf{N}}^k)$, a bias is introduced in the filter update equation (7.2.4). This difficulty is well-known in adaptive least mean square filter design [24, 46]. To eliminate the bias, one method known as the dual test pulse method was introduced in [12, 13]. It was achieved by using two noisy input signals per iteration. The first noisy input signal is used to update the noisy Lagrange multiplier vector $\tilde{\lambda}^{k+1}$, while the second one is cross correlated with this updated $\tilde{\lambda}^{k+1}$ to simultaneously update the noisy filter $\tilde{\mathbf{u}}^{k+1}$. The corresponding adaptive training scheme is as follows:

$$\begin{cases} \mathbf{F}(\tilde{\lambda}^k) &= \mathbf{D}(\tilde{\lambda}^k)\nabla\phi(\tilde{\lambda}^k) \\ \tilde{\lambda}^{k+1} &= \tilde{\lambda}^k - h_k\mathbf{F}(\tilde{\lambda}^k) \\ \tilde{\mathbf{u}}^{k+1} &= -\frac{1}{2}(\mathbf{A} + \tilde{\mathbf{N}}_2^k)'\tilde{\lambda}^{k+1}, \quad k = 0, 1, \ldots \end{cases} \tag{7.2.5}$$

where $\nabla\phi(\tilde{\lambda}^k) = \frac{1}{2}(\mathbf{A} + \tilde{\mathbf{N}}_1^k)(\mathbf{A} + \tilde{\mathbf{N}}_2^k)'\tilde{\lambda}^k + \mathbf{b}$, while $(\mathbf{A} + \tilde{\mathbf{N}}_1^k)$ is the signal convolution matrix obtained from the first noisy input signal and $(\mathbf{A} + \tilde{\mathbf{N}}_2^k)$ is from the second noisy input signal. Provided $\tilde{\mathbf{N}}_1^k$ is uncorrelated with $\tilde{\mathbf{N}}_2^k$, no bias is introduced.

Algorithm 7.2.1 *Set $k = 0$. Choose an initial point $\lambda^0 \in \Re_+^{2N}$, two stopping criteria ε_λ and ε_κ, and a proper step-size h_k.*

1. *Let* $\mathbf{F}(\tilde{\lambda}^k) \triangleq \mathbf{D}(\tilde{\lambda}^k)\nabla\phi(\tilde{\lambda}^k)$ *be a search direction where*

$$\nabla\phi(\tilde{\lambda}^k) \triangleq \frac{1}{2}(\mathbf{A}+\tilde{\mathbf{N}}_1^k)(\mathbf{A}+\tilde{\mathbf{N}}_2^k)'\lambda^k + \mathbf{b}.$$

Calculate the following scheme

$$\tilde{\lambda}^{k+1} = \tilde{\lambda}^k - h_k\mathbf{F}(\tilde{\lambda}^k) \tag{7.2.6}$$

in which the step-size h_k *is chosen such that*

$$\nabla\phi'(\tilde{\lambda}^{k+1})\mathbf{F}(\tilde{\lambda}^{k+1}) < 0 \quad \textit{and} \quad \tilde{\lambda}^{k+1} \geq 0_{2N}.$$

2. *Use* $\tilde{\lambda}^{k+1}$ *to obtain* $\tilde{\mathbf{u}}^{k+1}$ *as follows:*

$$\tilde{\mathbf{u}}^{k+1} = -\frac{1}{2}(\mathbf{A}+\tilde{\mathbf{N}}_2^k)'\tilde{\lambda}^{k+1}. \tag{7.2.7}$$

If either $\|\mathbf{F}(\tilde{\lambda}^{k+1})\|_2 < \varepsilon_\lambda$ *or* $k > \varepsilon_\kappa$, *then terminate; otherwise return to Step 1 with* k *replaced by* $k+1$.

7.3 Convergence Results

In this section, the convergence of the adaptive EC filter using the adaptive BG scheme (7.2.5) are established in mean sense and in mean square sense to the noiseless optimum filter $\mathbf{u}^*$ when the step-size is fixed. For a sequence of decreasing step-sizes $\{h_k\}_{k=0}^{\infty}$, the adaptive scheme converges in mean square sense and with probability one to the noiseless optimum filter. To analyze the adaptive BG scheme (7.2.5), the following assumptions are made on the sequence of input noises.

Assumption 7.3.1

1) For each $k = 0, 1, \ldots$, *the components* n_i^k *of the noise vector* $\mathbf{n}^k$ *satisfy*

$$E[n_i^k] = 0 \quad \textit{and} \quad var(n_i^k) = \sigma^2, \quad \forall i,$$

where $E[\cdot]$ *denotes the mathematical expectation.*

2) For each $k = 0, 1, \ldots$, *the noise matrices* $\tilde{\mathbf{N}}_1^k$ *and* $\tilde{\mathbf{N}}_2^k$ *are of mean zero and uncorrelated with one another. This is clearly the case for white noise and in practice is true if the noise samples are sufficiently spaced in time.*

3) The sample noise matrix $\tilde{\mathbf{N}}_1^k$ *(respectively,* $\tilde{\mathbf{N}}_2^k$*) is statistically independent of all previous sample matrices* $\{\tilde{\mathbf{N}}_1^j, j = 0, 1, \ldots, k-1\}$ *(respectively,* $\{\tilde{\mathbf{N}}_2^j, j = 0, 1, \ldots, k-1\}$*).*

Theorem 7.3.1 *Consider a sequence $\{\tilde{\lambda}^k\}_{k=0}^{\infty}$ generated by the adaptive training scheme (7.2.6). Let $\mathbf{e}^k \triangleq \tilde{\lambda}^k - \lambda^*$ where λ^* denotes the noiseless optimal solution of the dual problem (6.2.2). If $\mathbf{e}^0$ is such that $E[\|\mathbf{e}^0\|_2^2]$ is in an appropriate neighborhood of the origin and the step-size h_k is chosen such that $0 < h = h_k < \frac{2}{\eta_{max}}$ for all k where η_{max} is the largest eigenvalues of the positive definite Jacobian matrix $\nabla\mathbf{F}(\lambda^*)$ defined by (4.4.19), then the sequence $\{\tilde{\lambda}^k\}_{k=0}^{\infty}$ and the corresponding sequence $\{\tilde{\mathbf{u}}^k\}_{k=0}^{\infty}$ generated by schemes (7.2.6) and (7.2.7) converge, respectively, to the optimal solution λ^* and the optimal filter $\mathbf{u}^*$, in the sense that*

$$\begin{aligned} \lim_{k\to\infty} \|E[\mathbf{e}^k]\|_2^2 &= 0 \\ \lim_{k\to\infty} \|E[\tilde{\mathbf{u}}^k] - \mathbf{u}^*\|_2^2 &= 0. \end{aligned}$$

Proof: See Appendix D.1. ∎

Remark 7.3.1 *In the numerical study, it is important to ensure that the adaptive Lagrange multiplier vector $\tilde{\lambda}^k$, after processing k iterations, is in a small neighborhood of the optimum Lagrange multiplier vector λ^*. We then start to collect and average certain samples of filters as an approximate mean filter.*

Theorem 7.3.2 *Let conditions in Theorem 7.3.1 be satisfied and let $\{\tilde{\lambda}^k\}_{k=0}^{\infty}$ be a sequence generated by the adaptive training scheme (7.2.6). Assume that there exists a constant ℓ such that $E[\|\mathbf{e}^k\|_2^4] \leq \ell(E[\|\mathbf{e}^k\|_2^2)^2$. If the step-size h_k is fixed at $0 < h_k = h < \frac{2}{\eta_{max}}$ for all k, then the resulting sequences $\{\tilde{\lambda}^k\}_{k=0}^{\infty}$ and $\{\tilde{\mathbf{u}}^k\}_{k=0}^{\infty}$ enter and remain, respectively, in a neighborhood of the optimum λ^* and the optimal filter $\mathbf{u}^*$, in the sense that*

$$\begin{aligned} \overline{\lim_{k\to\infty}} E[\|\mathbf{e}^k\|_2^2] &\leq V(h) \\ \overline{\lim_{k\to\infty}} E[\|E[\tilde{\mathbf{u}}^k|\tilde{\lambda}^k] - \mathbf{u}^*\|_2^2] &\leq \frac{1}{4}\|\mathbf{A}\|_2^2 V(h) \end{aligned}$$

where $\overline{\lim}$ denotes the limit superior, $E[\tilde{\mathbf{u}}^k|\tilde{\lambda}^k]$ indicates the conditional expectation of $\tilde{u}^k$ given $\tilde{\lambda}^k$, and the h-neighborhood $V(h)$ satisfies $V(h) \to 0$ as $h \to 0$.

Proof: See Appendix D.2. ∎

Remark 7.3.2

1) In Theorem 7.3.2, we assume the fourth moments to simplify the results, i.e,

$$E[\|\mathbf{e}^k\|_2^4] \leq \ell(E[\|\mathbf{e}^k\|_2^2)^2.$$

In the white noise case, the fourth moments naturally emerge since the calculation is based on variance. Therefore, in that sense, it seems unlikely that a much better result can be obtained.

2) The proof of Theorem 7.3.2 also shows that $V(h) \xrightarrow{\sigma \to 0} 0$, *for* $0 < h_k = h < \frac{2}{\eta_{max}}$ *where* $\sigma = \sqrt{var(n_i)}$.

The next theorem is concerned with using a sequence of decreasing step-sizes in the adaptive noisy training algorithm 7.2.1.

Theorem 7.3.3 *Let conditions in Theorem 7.3.1 be satisfied and let* $\{\tilde{\lambda}^k\}_{k=0}^{\infty}$ *be a sequence generated by the adaptive training scheme (7.2.6). Suppose that the sequence of step-sizes* $\{h_k\}_{k=0}^{\infty}$ *satisfies*

$$h_k > 0, \quad k = 0, 1, \ldots, \tag{7.3.8}$$

$$\sum_{k=0}^{\infty} h_k = \infty, \quad \sum_{k=0}^{\infty} h_k^2 < \infty. \tag{7.3.9}$$

Then, the resulting sequence $\{\tilde{\lambda}^k\}_{k=0}^{\infty}$ *and the corresponding sequence* $\{\tilde{\mathbf{u}}^k\}_{k=0}^{\infty}$ *converge, respectively, to the optimum Lagrange multiplier vector* λ^* *and the optimal filter* $\mathbf{u}^*$, *both in the mean square sense and with probability one, i.e,*

$$\lim_{k\to\infty} E[\|\tilde{\lambda}^k - \lambda^*\|_2^2] = 0, \quad \lim_{k\to\infty} E[\|E[\tilde{\mathbf{u}}^k|\tilde{\lambda}^k] - \mathbf{u}^*\|_2^2] = 0, \quad \textit{(ms)}$$

$$Prob\left\{\lim_{k\to\infty} \|\tilde{\lambda}^k - \lambda^*\|_2 = 0\right\} = 1, \quad Prob\left\{\lim_{k\to\infty} \|E[\tilde{\mathbf{u}}^k|\tilde{\lambda}^k] - \mathbf{u}^*\|_2 = 0\right\} = 1, \quad \textit{(w.p.1)}$$

Proof: *See Appendix D.3.* ∎

Remark 7.3.3

1) The sequence of step-sizes $\{h_k\}_{k=0}^{\infty}$ *satisfying conditions (7.3.8)-(7.3.9) ensures that* $\{h_k\}_{k=0}^{\infty}$ *is a sequence of decreasing step-sizes, i.e,* $h_k \xrightarrow{k\to\infty} 0$.

2) In view of Theorem 7.3.3, the adaptive training algorithm using a sequence of decreasing step-sizes converges to the noiseless optimum filter on a fixed mean-square-error (MSE) surface. We note that the MSE is a quadratic function of the tap-weights forming a hyperparaboloid surface with a uniquely defined bottom or minimum point. However, it is not practical to apply variable step-sizes in the adaptive training algorithm because the MSE surface changes constantly with time. Furthermore, as the step-size approaches zero, the adaptive algorithm tends to cease to move. Thus, as a result of the changing MSE surface, the learning procedure of the adaptive algorithm is force to stop. Therefore, we never get close to the noiseless optimum filter (i.e, the minimum point of the MSE surface).

7.4 Comparison with Adaptive LMS and PD Algorithms

It is important to compare the structure and convergence properties of the adaptive BG filter presented here with those of the adaptive PD filter given in [12, 13], and with those of the

adaptive LMS filter presented in [9, 68, 69]. In what follows, we briefly address the key results associated with the PD and the LMS structures.

7.4.1 PD Algorithm

The iterative PD algorithm is used to find the optimum EC filter $\mathbf{u}^*$ by solving the discrete-time EC filtering problem (2.3.2). This algorithm consists of the following procedures:

1) Converting the primal problem into an unconstrained dual problem;

2) Solving the unconstrained dual problem using the directional differential of the cost function leading to a non-differentiable search direction $\mathbf{I}(\lambda)$.

An iterative algorithm was thus developed as follows:

$$\lambda^{k+1} = \lambda^k + h_k \mathbf{I}(\lambda^k) \tag{7.4.10}$$

$$\mathbf{u}^{k+1} = -\frac{1}{2}\mathbf{S}'\lambda^{k+1} \tag{7.4.11}$$

where h_k is the step-size and $\mathbf{I}(\lambda^k) = \psi^k - \mathbf{d} + \mathbf{f}(\epsilon, \psi^k, \lambda^k)$ is a generalized direction of the steepest ascent based on the directional differential, while the ith component of $\mathbf{f}(\epsilon, \psi^k, \lambda^k)$ is

$$f_i(\epsilon, \psi^k, \lambda^k) = \begin{cases} -\epsilon_i, & \text{if } \lambda_i > 0, \text{ or if } \lambda_i = 0 \text{ and } \psi_i > \epsilon_i^+ \\ \epsilon_i, & \text{if } \lambda_i < 0, \text{ or if } \lambda_i = 0 \text{ and } \psi_i < \epsilon_i^- \\ 0, & \text{if } \lambda_i = 0 \text{ and } \epsilon_i^- \leq \psi_i \leq \epsilon_i^+. \end{cases}$$

Let $\mathbf{e}^k = \lambda^k - \lambda^*$ denote the error vector where λ^* is the optimal solution of the dual problem. From (7.4.10)-(7.4.11), it follows that for variable decreasing step-sizes, we have

$$\|\mathbf{e}^{k+1}\|_2^2 = \|\mathbf{e}^k\|_2^2 + 2h_k \left\langle \mathbf{I}^k, \mathbf{e}^k \right\rangle + h_k^2 \|\mathbf{I}^k\|_2^2.$$

Thus, the noise-free training algorithm converges to the optimal filter $\mathbf{u}^*$ if the sequence of step-sizes $\{h_k\}_{k=0}^{\infty}$ satisfies conditions (7.3.9)-(7.3.8). Furthermore, if the step-size is fixed at $0 < h_k = h < \frac{2}{\|\mathbf{S}\|_2^2}$ for all k, where $\|\mathbf{S}\|_2$ is the spectral norm of the matrix $\mathbf{S}$, then the noise-free training algorithm converges to a neighborhood of the optimal filter. A possible structure of the PD algorithm is depicted in Figure 7.3. We note that the functions of tapped delay line for generating the output response, correlator for generating a new tap weight, and three other delay lines for storing the Lagrange multipliers, and the constraint boundaries are the same as those given in Figure 7.2.

If the input signal $\mathbf{s} \in \Re^m$ is corrupted by an additive white noise samples with mean zero

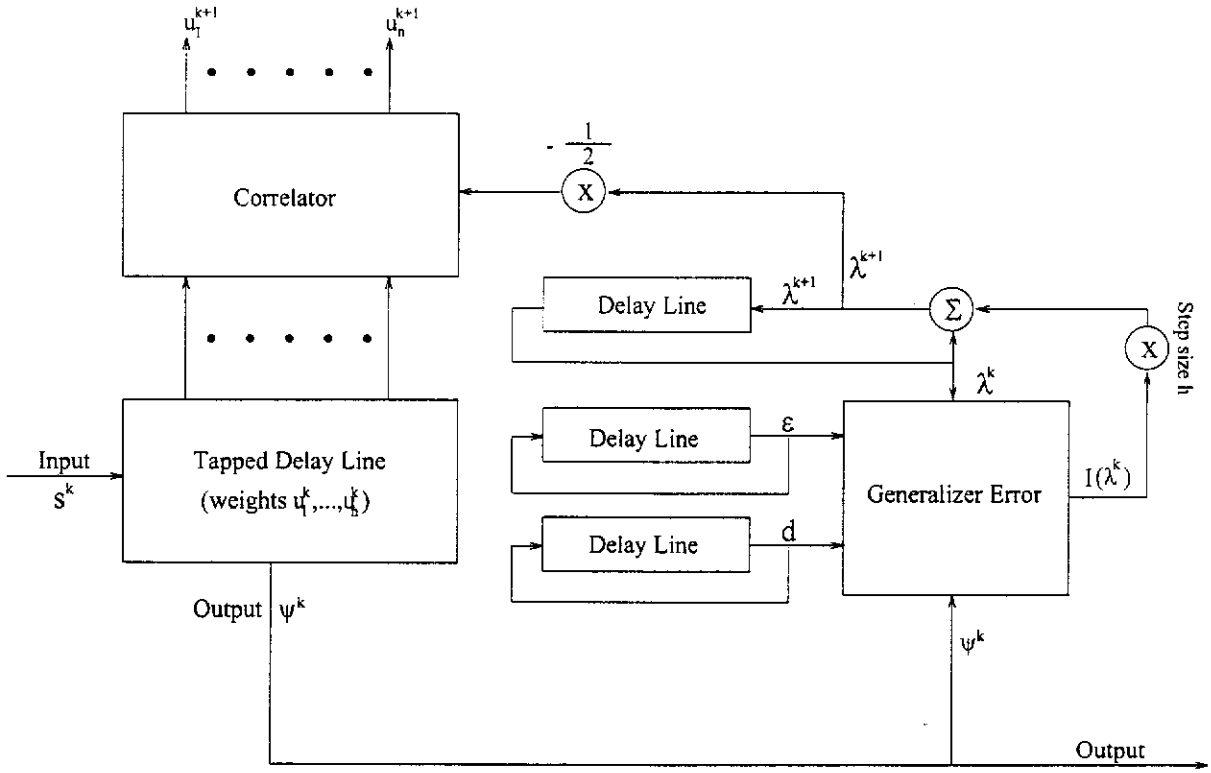

Figure 7.3: Adaptive primal-dual filter.

and variance σ^2, then the adaptive algorithm with noisy training pulses is given by

$$\begin{cases} \mathbf{I}(\tilde{\lambda}^k) &= (\mathbf{S}+\mathbf{N}^k)\tilde{\mathbf{u}}^k - \mathbf{d} + \mathbf{f}(\epsilon, \tilde{\psi}^k, \tilde{\lambda}^k) \\ \tilde{\lambda}^{k+1} &= \tilde{\lambda}^k + h_k \mathbf{I}(\tilde{\lambda}^k) \\ \tilde{\mathbf{u}}^{k+1} &= -\tfrac{1}{2}(\mathbf{S}+\mathbf{M}^k)'\tilde{\lambda}^{k+1} \end{cases} \tag{7.4.12}$$

where $\mathbf{N}^k$ and $\mathbf{M}^k$ are two uncorrelated matrices of noise sample. For a fixed step-size $0 < h_k = h < \frac{2}{\|\mathbf{S}\|_2^2}$, it can be shown [12, 13] that

$$\begin{aligned} \overline{\lim_{k\to 0}} \|E[\tilde{\mathbf{u}}^k - \mathbf{u}^*]\|_2^2 &\leq V_1(h) \\ \overline{\lim_{k\to 0}} E[\|E[\tilde{\mathbf{u}}^k|\lambda^k] - \mathbf{u}^*\|_2^2] &\leq V_2(h) \end{aligned}$$

where $\lim_{h\to 0} V_i(h) = 0$, for $i = 1, 2$. Furthermore, if the sequence of step-sizes $\{h_k\}_{k=0}^{\infty}$ satisfies conditions (7.3.8)-(7.3.9), then the adaptive PD algorithm (7.4.12) converges in the mean square sense and with probability one (w.p.1) to λ^*, i.e,

$$\begin{aligned} \lim_{k\to\infty} E[\|\tilde{\lambda}^k - \lambda^*\|_2^2] &= 0, \quad \text{(ms)} \\ Prob\left\{\lim_{k\to\infty} \|\tilde{\lambda}^k - \lambda^*\|_2 = 0\right\} &= 1, \quad \text{(w.p.1)}. \end{aligned}$$

7.4.2 LMS Algorithm

The iterative LMS algorithm is used to find a filter $\mathbf{u} \in \Re^n$ whose output approximates a desired output $\mathbf{d} \in \Re^N$ by solving the following unconstrained minimization problem in a least square error sense:

$$\min_{\mathbf{u}} \quad \|\mathbf{S}\mathbf{u} - \mathbf{d}\|_2^2, \quad \mathbf{u} \in \Re^n. \tag{7.4.13}$$

The optimal (Wiener) solution is given by

$$\mathbf{u}^* \;=\; (\mathbf{S}'\mathbf{S})^{-1}\mathbf{S}'\mathbf{d}. \tag{7.4.14}$$

For the fixed step-size h, a steepest-descent-based algorithm can be used to search for the Wiener solution (7.4.14) as follows:

$$\begin{aligned} \mathbf{u}^{k+1} &= \mathbf{u}^k - h\mathbf{g}_{\mathbf{u}}^k = \mathbf{u}^k - 2h\mathbf{S}'(\psi^k - \mathbf{d}) \\ &= (\mathbf{I} - 2h\mathbf{S}'\mathbf{S})\mathbf{u}^k + 2h\mathbf{S}'\mathbf{d} \end{aligned} \tag{7.4.15}$$

where $\mathbf{g}_{\mathbf{u}}^k = 2\mathbf{S}'(\psi^k - \mathbf{d})$ represents a gradient vector of the cost function with respect to the filter $\mathbf{u}$. Clearly, the procedure of the adaptive algorithm for solving the least square problem (7.4.13) simply consists of the difference between the output response and the desired shape $\mathbf{d}$. Therefore, the LMS algorithm can be implemented adaptively by employing the structure as shown in Figure 7.4.

Combining the optimal solution (7.4.14) with (7.4.15), we obtain

$$\mathbf{u}^{k+1} - \mathbf{u}^* \;=\; (\mathbf{I} - h\mathbf{S}'\mathbf{S})(\mathbf{u}^k - \mathbf{u}^*).$$

Thus, for a fixed step-size satisfying $0 < h < \frac{2}{\eta_{max}}$ where η_{max} is the largest eigenvalues of matrix $S'S$, the noise-free training scheme (7.4.15) converges to the noiseless optimal LMS filter $\mathbf{u}^*$.

For the noisy case whose input signal is contaminated by additive mean zero stationary white noise with variance σ^2, the adaptive training scheme, which is obtained by extending the noise-free training scheme (7.4.15) for solving the LMS problem to a stochastic environment, is given by

$$\tilde{\mathbf{u}}^{k+1} \;=\; [\mathbf{I} - 2h(\mathbf{S} + \mathbf{N}^k)'(\mathbf{S} + \mathbf{N}^k)]\tilde{\mathbf{u}}^k + 2h(\mathbf{S} + \mathbf{N}^k)'\mathbf{d} \tag{7.4.16}$$

where $\mathbf{N}^k$ is a matrix of noise samples consisting of m input noise sample shifted N times.

For the convergence in mean sense, similar to the noiseless lease square problem (7.4.13), we minimize the expected value of square norm error between the noisy output and the desired

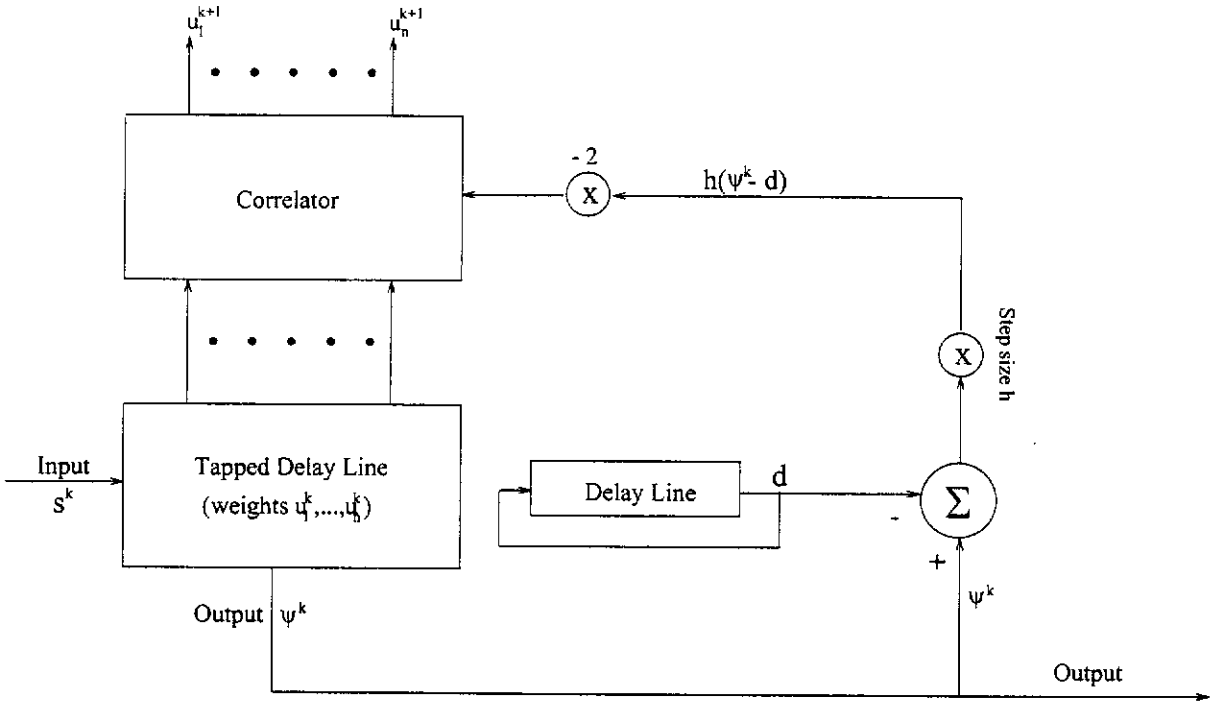

Figure 7.4: Adaptive least-squares filter.

output as follows:

$$\min_{\tilde{\mathbf{u}}} \quad E[\|(\mathbf{S}+\mathbf{N})\tilde{\mathbf{u}}-\mathbf{d}\|_2^2], \quad \tilde{\mathbf{u}} \in \Re^n. \tag{7.4.17}$$

Clearly, the solution of the above unconstrained minimization is given by

$$\hat{\mathbf{u}}^* \;=\; (\sigma^2\mathbf{I}+\mathbf{S}'\mathbf{S})^{-1}\mathbf{S}'\mathbf{d}. \tag{7.4.18}$$

Associated (7.4.16) with the optimum solution (7.4.18) of the least mean square problem (7.4.17), we have

$$\|E[\tilde{\mathbf{u}}^k-\hat{\mathbf{u}}^*]\|_2 \;\leq\; \|\mathbf{I}-h(\sigma^2\mathbf{I}+\mathbf{S}'\mathbf{S})\|_2\|E[\tilde{\mathbf{u}}^k-\hat{\mathbf{u}}^*]\|_2.$$

Thus, for a fixed step-size satisfying $0 < h < \frac{2}{\hat{\eta}_{max}}$ where $\hat{\eta}_{max}$ is the largest eigenvalue of the matrix $(\sigma^2\mathbf{I}+\mathbf{S}'\mathbf{S})$, $E[\tilde{\mathbf{u}}^k]$ converges to the noiseless sub-optimal LMS filter $\hat{\mathbf{u}}^*$. We note that as compared with the Wiener solution (noiseless optimum filter) given by (7.4.14), $\hat{\mathbf{u}}^*$ is a sub-optimum LMS filter. Moreover, it was shown in [24] that the variance about this noiseless sub-optimal filter is bounded, i.e,

$$\overline{\lim_{k\to\infty}} E[\|\tilde{\mathbf{u}}^k-\hat{\mathbf{u}}^*\|_2^2] \;\leq\; V(h),$$

where $V(h) \to 0$ as $h \to 0$.

Finally, if the sequence of decreasing step-sizes $\{h_k\}_{k=0}^{\infty}$ satisfies conditions (7.3.8)-(7.3.9), then the adaptive LMS algorithm converges in mean square sense and with probability one to the noiseless sub-optimum filter $\hat{\mathbf{u}}^*$.

A comparison among the adaptive barrier-gradient (BG) filter, the adaptive primal-dual (PD) filter, and the adaptive least mean square (LMS) filter is summarized as follows:

Structure

LMS: Feed back the error between the output and the desired output.

PD: Feed back the error between the output and the upper boundary when $\lambda_i^k > 0$, the output and the lower boundary when $\lambda_i^k < 0$, and the constraint violation, either upper or lower boundary when $\lambda_i^k = 0$.

BG: Feed back the error between the output and the constraint boundaries.

Convergence without Noise

LMS: Converges linearly to the optimal filter for a small fixed step-size.

PD: Converges linearly to within a neighborhood of the optimal filter for a small fixed step-size and converges to the optimal filter exactly for variable step-sizes satisfying conditions (7.3.9)-(7.3.8).

BG: Converges linearly to the optimal filter for a fixed step-size.

Convergence with Noise

LMS: Mean converges linearly to a noiseless sub-optimum filter for a small fixed step-size. The mean square error about this sub-optimal filter is bounded and step-size-dependent. For variable decreasing step-sizes, the adaptive algorithm converges in mean square sense and with probability one to the suboptimal filter.

PD: For a small fixed step-size, the mean converges linearly to within a neighborhood of the noiseless optimum filter. The mean square error is bounded and step-size-dependent. For variable decreasing step-sizes, the adaptive algorithm converges in mean square sense and with probability one to the optimal filter.

BG: Mean converges linearly to the noiseless optimal filter with a small fixed step-size. The mean square error about the optimal filter is bounded and step-size-dependent. For vari-

able decreasing step-sizes, the adaptive algorithm converges in mean square sense and with probability one to the optimal filter.

7.5 Numerical Results

In this section, two practical examples involving pulse compression 13-bit Barker code input signal and digital transmission channel equalization operating at the DSX3 rate are solved by the adaptive EC filtering problem in a noisy environment. It is assumed that a test signal is sent periodically by the transmitter and the response is obtained as shown in Figure 7.1. There are guard samples between the test signal and the normal signal so that the responses of the filter to the test signal are the only samples. When the distorted test signal (filter input, Figure 7.1) is received, the coefficient update algorithm is executed for the noise-free case discussed in Chapter 6. For the noisy case, however, the channel output (filter input, Figure 7.1) is corrupted by a stationary zero-mean and unity variance white Gaussian noise with input signal-to-noise ratio (SNR) defined by

$$SNR \triangleq 10\log_{10}\left[\frac{(\text{peak signal})^2}{\text{noise variance}}\right].$$

Adaptive training algorithm is then applied to examine the noisy case.

7.5.1 Pulse Compression

For the rectangular pulse compression example, the adaptive noisy training BG algorithm 7.2.1 is applied to solve the discrete-time EC filtering problem with an approximate $12dB$ input signal-to-noise ratio. The noiseless input signal is a 13-bit Barker code signal and the output mask is a mainlobe peak of 0.69 ± 0.075 with sidelobe levels of ± 0.025 and the order of the filter is fixed at $n = 27$. In the following two tests, we wish to verify the convergence results presented in Theorem 7.3.1 and Theorem 7.3.2 for the adaptive BG algorithm 7.2.1 in mean sense and in mean square sense. The noiseless optimal solution $\mathbf{u}_{qp}^*$ and the corresponding Lagrange multiplier vector λ_{qp}^* are obtained by the quadratic programming in the Matlab optimization toolbox and are used as the benchmark for both tests.

7.5.1.1 Test 1: Convergence in Mean

For the first test, the adaptive training algorithm 7.2.1 is implemented to verify the convergence in mean sense. To compare the performance, the iterative BG algorithm 6.2.1 is applied to the same off-line problem depicted in Figure 7.5(a) as the scheme (a). We first implement the

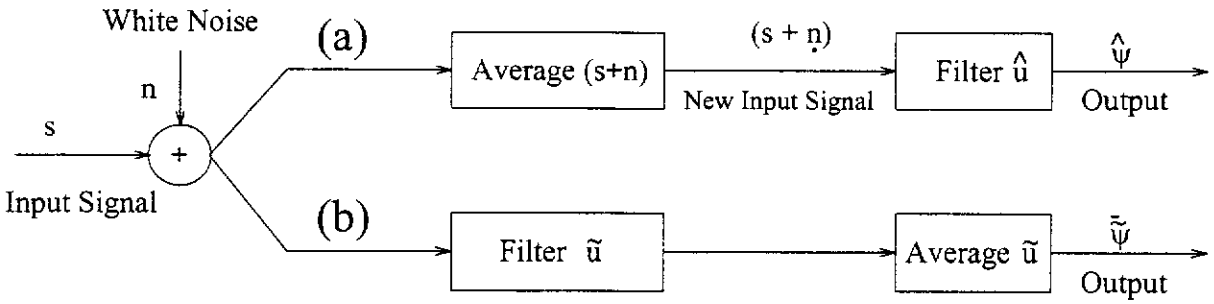

Figure 7.5: An EC filter diagram for implementing the noise case.

adaptive algorithm depicted in Figure 7.5(b) as the scheme (b). The adaptive scheme (b) was run with a fixed step-size $h = 0.085$. After 2488 iterations, we start to collect and average extra samples of filters as the successive approximate mean filters $\bar{\tilde{\mathbf{u}}}^k$ for $k = 2^3, 2^5, 2^7$, and 2^9. These results are depicted in Figures 7.6(a)-(d). These approximate mean filters are compared with the noiseless optimal filter $\mathbf{u}^*_{qp}$. We also show the corresponding approximate mean filter outputs $\bar{\tilde{\psi}}^k$ for $k = 2^3, 2^5, 2^7$, and 2^9 in Figure 7.7(a)-(d). Clearly, the approximate mean filters and their corresponding approximate mean filter outputs are getting closer to the noiseless optimal filter and its output response, respectively. These numerical results are given in Table 7.1. They are consistent with Theorem 7.3.1.

Mean Convergence for Pulse Compression Example, $n = 27$						
Noise Sample No. k		8	32	128	512	1024
Scheme(a)	$\|\mathbf{u}^k - \mathbf{u}^*_{qp}\|_2^2$	3.55×10^{-3}	1.41×10^{-3}	1.78×10^{-4}	6.99×10^{-5}	2.61×10^{-5}
h=2.0	$\|\psi^k - \psi^*_{qp}\|_2$	2.04×10^{-1}	1.32×10^{-1}	4.61×10^{-2}	2.91×10^{-2}	1.82×10^{-2}
Scheme(b)	$\|\bar{\tilde{\mathbf{u}}}^k - u^*_{qp}\|_2^2$	7.77×10^{-3}	1.85×10^{-3}	3.62×10^{-4}	1.50×10^{-4}	6.57×10^{-5}
h=8.5×10^{-2}	$\|\bar{\tilde{\psi}}^k - \psi^*_{qp}\|_2$	3.01×10^{-1}	1.49×10^{-1}	6.85×10^{-2}	4.24×10^{-2}	2.91×10^{-2}
Scheme(a)	$\|\mathbf{u}^k - \mathbf{u}^*_{qp}\|_2^2$	4.83×10^{-3}	1.83×10^{-3}	3.62×10^{-4}	3.10×10^{-4}	2.76×10^{-4}
h=8.13×10^{-3}	$\|\psi^k - \psi^*_{qp}\|_2$	2.40×10^{-1}	1.49×10^{-1}	7.73×10^{-2}	7.10×10^{-2}	6.84×10^{-2}

Table 7.1: Filter and Filter Output for Scheme (a) and Scheme (b).

For comparison, the off-line scheme (a) was simulated with a fixed step-size $h = 2.0$ where the same numbers of noisy input signal samples used for generating the approximate mean filters and their corresponding approximate mean output responses are collected and averaged. With these averaged noisy signal samples, the iterative BG algorithm 6.2.1 is used to obtain the optimal filter, denoted by $\mathbf{u}^k$, and the corresponding output response, denoted by ψ^k. They

are then compared with the noiseless optimum filter and the corresponding output response. These results are also given in Table 7.1.

Remark 7.5.1 *From Table 7.1, we observe that*

1) The performance of the scheme (a) is similar to that of the scheme (b). However, the adaptive noisy training scheme (b) is more practical than the noise-free training scheme (a), as the filters are determined in accordance with the changing statistics of the signals to be filtered.

2) If the step-size is reduced to $h = 8.13 \times 10^{-3}$ *in the scheme (a), we obtain the results similar to those obtained by the scheme (b) for cases where the number of input noise samples is* $k = 32$ *and* $k = 128$.

7.5.1.2 Test 2: Convergence in Mean Square

The adaptive EC filter with a fixed step-size is applied to this test for verifying the convergence in mean square sense about λ^* to within an upper bound.

To compare the results obtained with different fixed step-sizes, the adaptive training BG algorithm 7.2.1 was run separately with three different fixed step-sizes $h = 0.1, h = 0.06$, and $h = 0.02$. After 500 iterations, we start to collect samples of square error, $\|\mathbf{e}^k\|_2^2, k = 0, 1, \ldots$, for each specified fixed step-size mentioned above. These samples are stored as a sequence of square errors until the filter is sufficiently well trained, i.e, at the steady state. For a specified fixed step-size, many sequences of square errors are collected and averaged to achieve the sequence of approximate mean square errors, i.e, $\left\{\overline{\|\mathbf{e}^k\|_2^2}\right\}$. This process is repeated for the three different fixed step-sizes and their corresponding sequences of approximate mean square errors are depicted in Figure 7.8 and Table 7.2. In view of Figure 7.8, we see that the approximate MSE curve (i.e, the sequence of approximate mean square errors) with the smallest fixed step-size approaches steady state more slowly compared with the other two approximate MSE curves with two larger fixed step-sizes. However, as shown in Figure 7.8 and in Table 7.2, the approximate MSE magnitude for the smallest step-size at the steady state is the smallest. Furthermore, a smaller step-size corresponds to a smoother convergence path.

These results shown in Figure 7.8 and Table 7.2 are consistent with Theorem 7.3.2. Note that the MSE value approaches to zero as the fixed step-size tends to zero.

7.5.2 Channel Equalization

In this test example, the proposed adaptive BG algorithm is applied to design equalization of a digital transmission channel consisting of a coaxial cable on which data is operating at

MSE Pulse Compression, $n = 27$, Iteration No. $k = 3.0 \times 10^4$			
Step Size	$h = 1.0 \times 10^{-1}$	$h = 6.0 \times 10^{-2}$	$h = 2.0 \times 10^{-2}$
$\overline{\|\mathbf{e}^k\|_2^2}$	6.94×10^{-5}	5.50×10^{-5}	3.22×10^{-5}

Table 7.2: Approximate Mean Square Errors for Pulse Compression Example at the Steady State.

the DSX3 rate. The discrete-time EC filtering problem is solved with an approximate $26dB$ input SNR. For this filter design problem, the order of the filter is fixed at $n = 16$, and the input signal is sampled every $\frac{\bar{\beta}}{8}$ time unit over the interval $[0, 32\bar{\beta}]$ where $\bar{\beta}$ is the baud interval $(22.35 \times 10^{-9}s)$.

7.5.2.1 Test 1: Convergence in Mean

The test of convergence in mean sense is concerned with the same testing procedure as in the pulse compression example. The adaptive scheme (b) in Figure 7.5 is compared with the same problem as in the off-line scheme (a).

The adaptive scheme (b) was run with a fixed step-size $h = 1.2 \times 10^{-3}$ while the off-line scheme (a) was run with a fixed step-size $h = 3.0 \times 10^{-2}$. Following the process of the scheme (b), after 4488 runs of the adaptive noisy training algorithm we start to collect and average samples of filters as the successive approximate mean filter $\overline{\mathbf{u}}^k$ for $k = 2^3, 2^5, 2^7$, and 2^9. The corresponding approximate mean output responses $\overline{\psi}^k$ are also obtained for $k = 2^3, 2^5, 2^7$, and 2^9 samples. These approximate mean filters and mean output responses are depicted in Figure 7.9 and Figure 7.10. Table 7.3(b) shows the obtained results of the square norm difference between the noiseless optimum filter $\mathbf{u}_{qp}^*$ and each approximate mean filter (respectively, the norm difference between the noiseless filter output ψ_{qp}^* and each approximate mean filter output).

Regarding the process in the off-line scheme (a), the same number of noisy input signal samples as those used for generating the approximate mean filters and their corresponding mean output responses are stored and averaged so that a good estimated input signal is obtained for individual number of noisy input signal samples. The noise-free training algorithm 6.2.1 is then applied to generate the filters and its corresponding output responses. The obtained filters and their corresponding output responses are compared with the noiseless optimum filter and the corresponding filter output. (See Table 7.3(a) for details).

Mean Convergence for Channel Equalization Example, $n = 16$						
Noise Sample No. k		8	32	128	512	1024
Scheme(a)	$\|\mathbf{u}^k - \mathbf{u}_{qp}^*\|_2^2$	7.7688	7.40×10^{-1}	1.93×10^{-2}	9.52×10^{-3}	2.46×10^{-3}
h=3.0×10^{-2}	$\|\psi^k - \psi_{qp}^*\|_2$	1.0537	4.36×10^{-1}	1.15×10^{-1}	3.46×10^{-2}	2.55×10^{-2}
Scheme(b)	$\|\overline{\mathbf{u}}^k - \mathbf{u}_{qp}^*\|_2^2$	10.3580	9.12×10^{-1}	5.02×10^{-2}	1.85×10^{-2}	7.79×10^{-3}
h=1.2×10^{-3}	$\|\overline{\psi}^k - \psi_{qp}^*\|_2$	3.0188	8.49×10^{-1}	6.85×10^{-1}	7.24×10^{-2}	5.91×10^{-2}

Table 7.3: Filter and Filter Output for Scheme (a) and Scheme (b).

Test 2: Convergence in Mean Square

To test the convergence in mean square sense, the adaptive BG algorithm was separately run with three different fixed step-sizes $h = 1.0 \times 10^{-3}$, $h = 5.0 \times 10^{-4}$, and $h = 1.0 \times 10^{-4}$.

Following the same procedure for obtaining the value of approximate mean square error in the pulse compression example, we obtained three approximate MSE curves corresponding to the three different fixed step-sizes. Each curve represents a sequence of values of approximate mean square errors, i.e, $\left\{\overline{\|\mathbf{e}^k\|_2^2}\right\}$. These results are depicted in Figure 7.11 and Table 7.4. From Figure 7.11, it clearly shows that although the sequence of approximate MSE values with the smallest step-size approaches steady state slower than the other two with larger step-sizes, the magnitude of the approximate MSE at the steady state is smaller than the other two. This is also verified by the results shown in Table 7.4. Furthermore, a smaller step-size also ensures a smoother convergence path.

MSE Channel Equalization, $n = 16$, Iteration No. $k = 5.0 \times 10^4$			
Step Size	$h = 1.0 \times 10^{-3}$	$h = 5.0 \times 10^{-4}$	$h = 1.0 \times 10^{-4}$
$\overline{\|\mathbf{e}^k\|_2^2}$	8.03×10^{-3}	3.61×10^{-3}	2.23×10^{-3}

Table 7.4: Approximate Mean Square Errors for Channel Equalization Example at the Steady State.

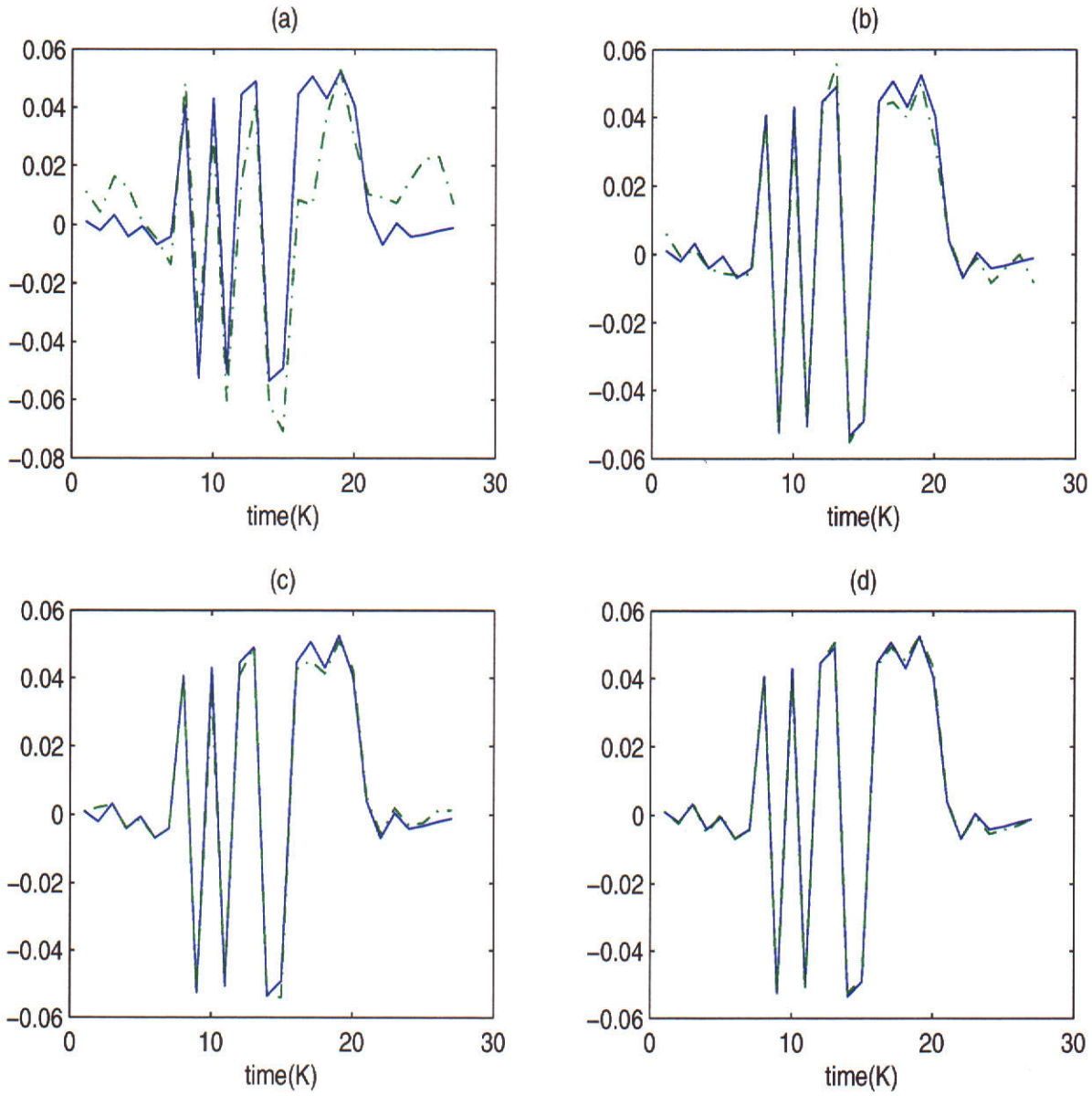

Figure 7.6: Pulse compression example. Solid line: optimal filter $\mathbf{u}_{qp}^{*}$. Dash-dot line: approximate mean filters $\bar{\tilde{\mathbf{u}}}^{k}$ about (a): $k = 2^3$ samples. (b): $k = 2^5$ samples. (c): $k = 2^7$ samples. (d): $k = 2^9$ samples.

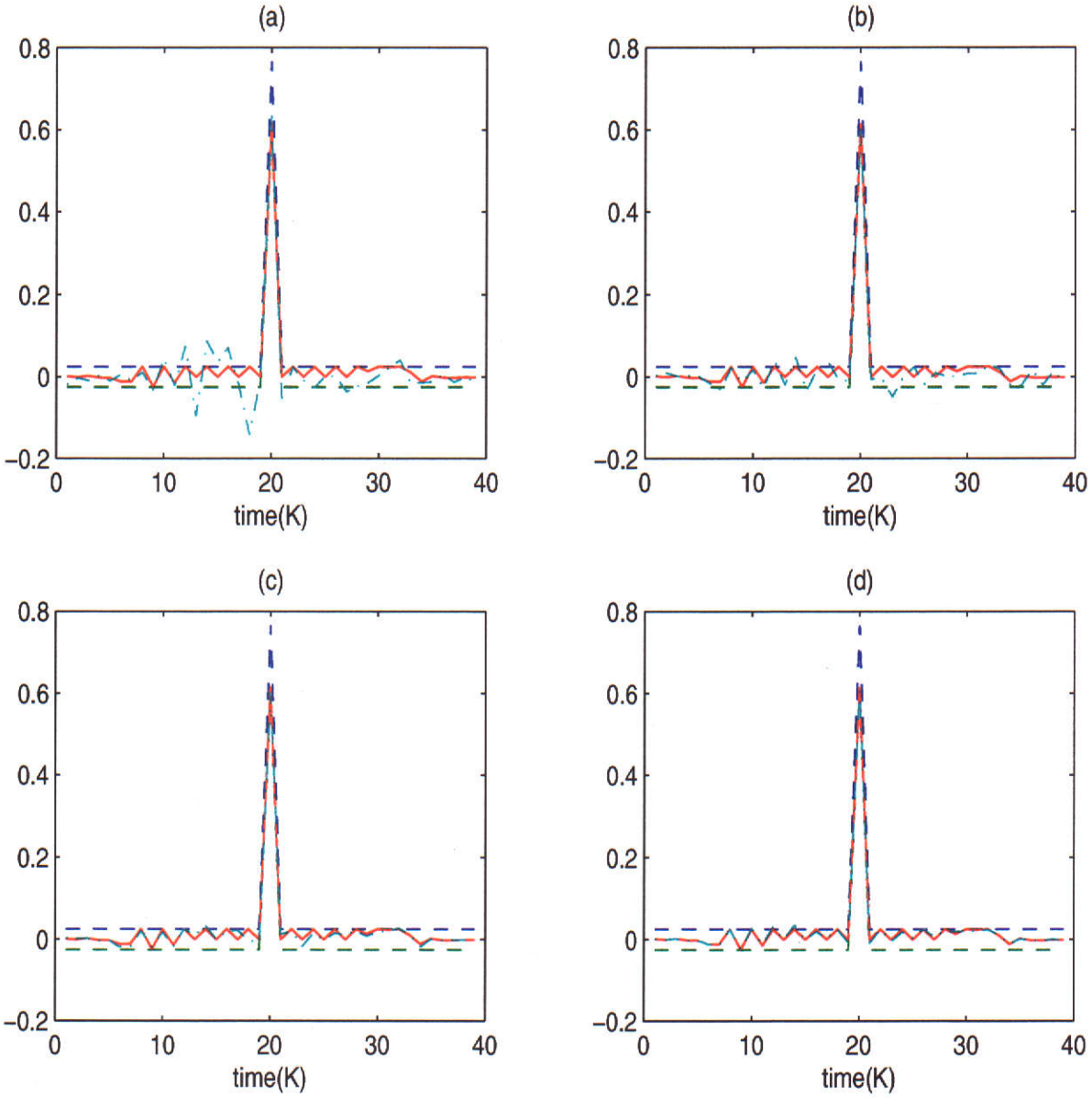

Figure 7.7: Pulse compression example. Solid line: optimal output response ψ^*_{qp}. Dash-dot line: approximate mean output responses $\overline{\widetilde{\psi}^k}$ about (a): $k = 2^3$ samples. (b): $k = 2^5$ samples. (c): $k = 2^7$ samples. (d): $k = 2^9$ samples.

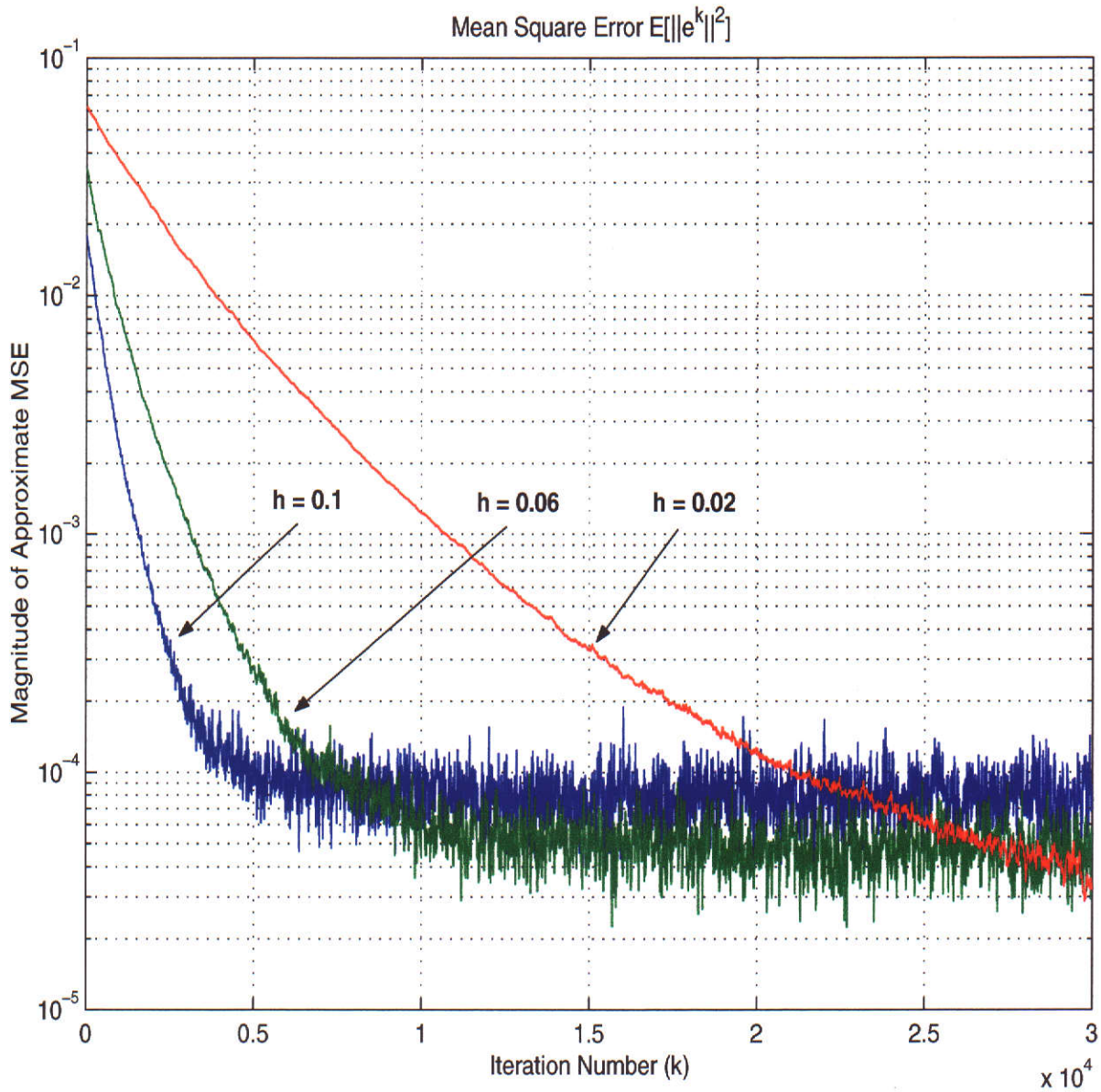

Figure 7.8: Mean square convergence results for pulse compression example using three different fixed step-sizes.

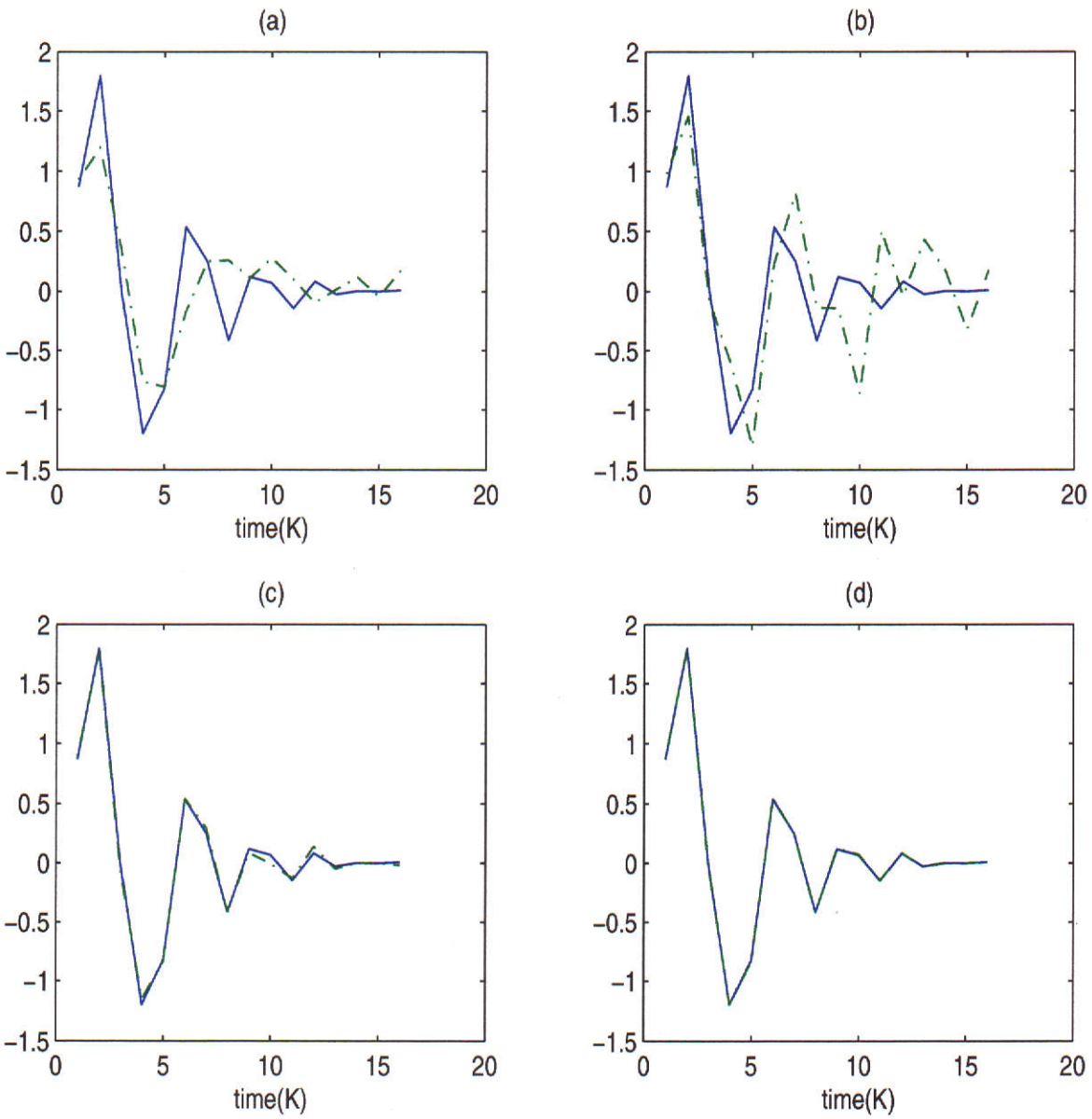

Figure 7.9: Channel equalization example. Solid Line: optimal filter $\mathbf{u}_{qp}^*$. Dash-dot Line: approximate mean filters $\bar{\tilde{\mathbf{u}}}^k$ about (a): $k = 2^3$ samples. (b): $k = 2^5$ samples. (c): $k = 2^7$ samples. (d): $k = 2^9$ samples.

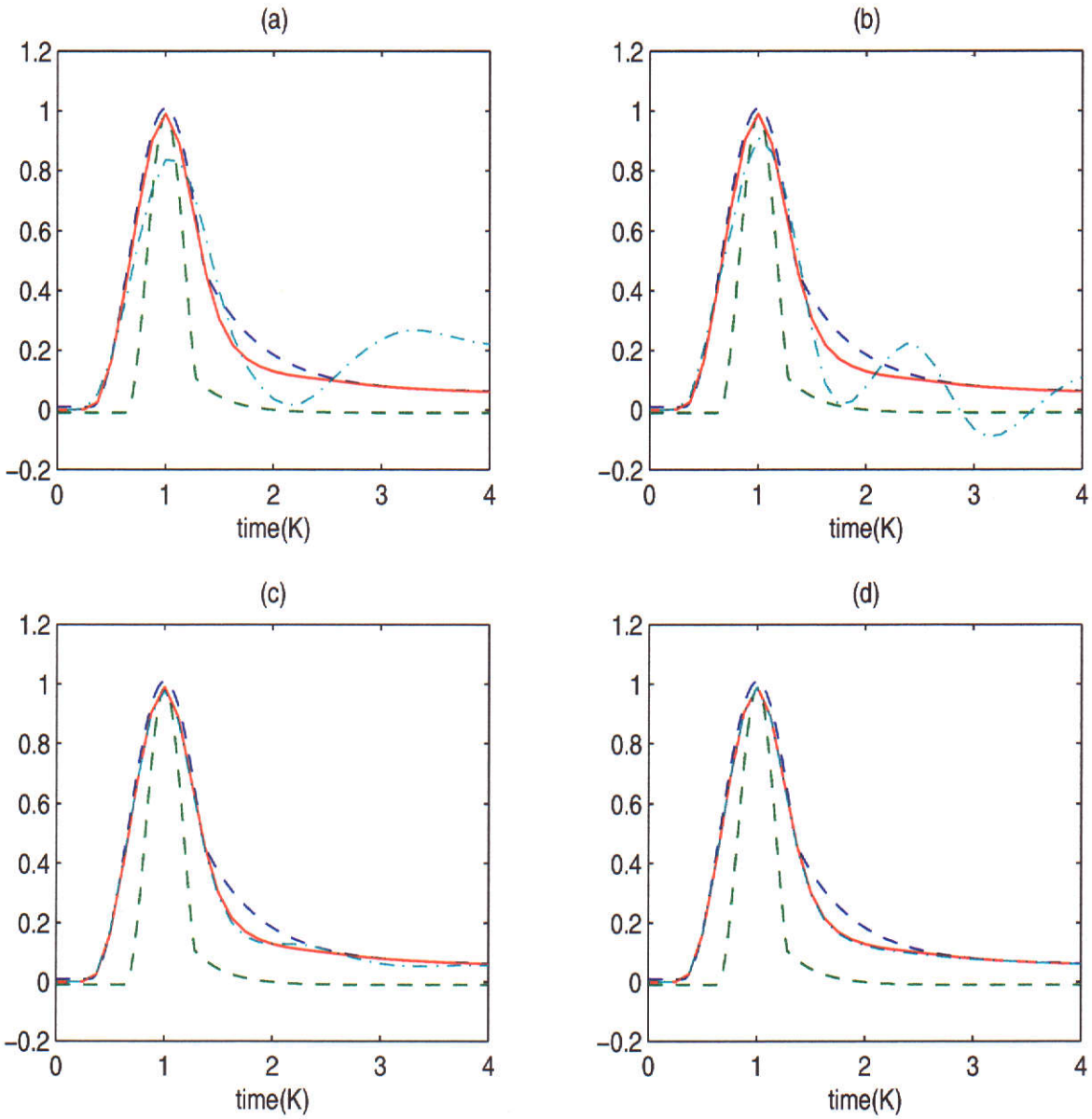

Figure 7.10: Channel equalization example. Solid line: optimal output response ψ^*_{qp}. Dash-dot line: approximate mean output responses $\bar{\tilde{\psi}}^k$ about (a): $k = 2^3$ samples. (b): $k = 2^5$ samples. (c): $k = 2^7$ samples. (d): $k = 2^9$ samples.

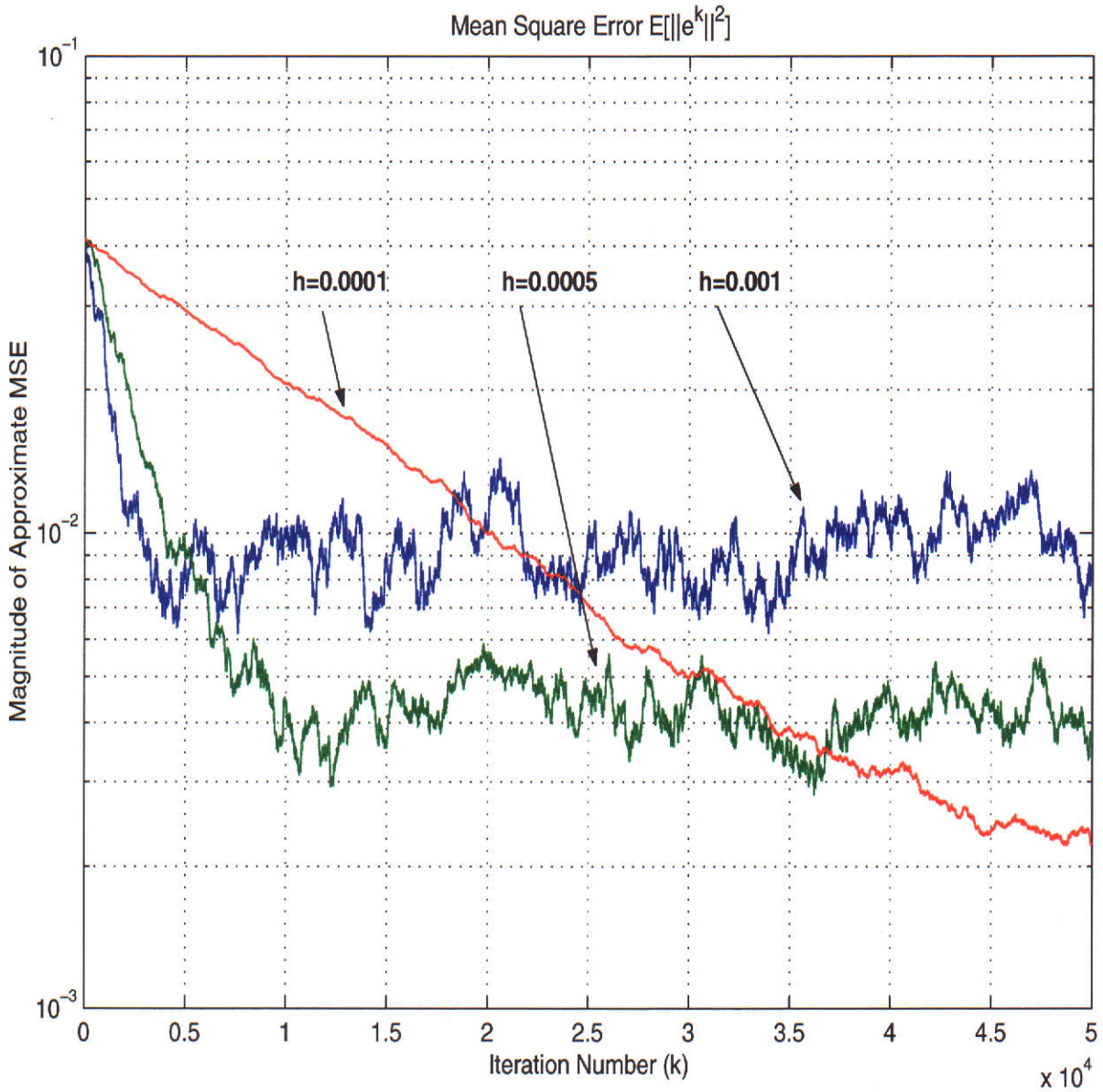

Figure 7.11: Mean square convergence results for channel equalization example using three different fixed step-sizes.

Chapter 8

Conclusion and Extensions

8.1 Summary and Conclusion

1. In this thesis, we studied a variety of EC filtering problems including continuous and discrete problems. The EC filtering problems with orthonormal bases in Hilbert spaces L^2 and ℓ^2 were also considered. These problems were formulated as quadratic programming (QP) problems with linear inequality constraints.

2. For discrete-time EC filtering problem:

   - We have developed two efficient iterative algorithms, barrier-gradient (BG) and barrier-Newton (BN) algorithms, for solving a class of deterministic EC filtering problems. Using Lagrangian duality theory followed by a space transformation leads to ordinary differential equations (ODE). Then, by appropriate discretization of the ODE's, the BG and BN algorithms are obtained.
   - We have shown that the sequences of filters generated by these two iterative algorithms with a fixed step-size globally converge to the optimal filter with linear and quadratic rates of convergence. This has substantially improved the results obtained by either the gradient-projection based primal-dual (PD) algorithm or the constraint transcription based steepest-descent (SD) and Newton-Raphon (NR) algorithms. More specifically, the sequence of filters generated by the PD algorithm with a fixed step-size converges only to within a neighborhood of the optimal filter due to a non-differentiable cost function. For the SD and NR algorithms, the obtained sequence of filters converges only to a suboptimal filter in a neighborhood of the optimal filter since the smoothing parameter embedded in the gradients and Hessian matrices is not allowed to reduced to zero.

3. For continuous-time (semi-infinite) EC filtering problem:

   - We have shown that the parameterization method for the dual semi-infinite programming problem in combination with the barrier-Newton method can be used to solve the continuous-time EC filtering problem.
   - A significant advantage of this approach is that the original semi-infinite dimensional constrained problem can be solved as an equivalent finite dimensional minimization problem. In particular, we have demonstrated that a small number of active supporting points can provide enough information to define the optimal solution such that the solution fits into the output mask. In comparison, discrete approximation methods cannot guarantee that the optimal solution obtained satisfies the continuous constraints of the original problem.

4. For adaptive EC filtering problem:

   - Based on the iterative barrier-gradient algorithm, we have developed an adaptive training algorithm for solving the stochastic EC filtering problem in which the input signal is contaminated by additive zero mean, stationary white noise.
   - We have shown that the sequences of filters generated by our adaptive training algorithm using a fixed step-size converge to the noiseless optimum filter in mean sense and in mean square sense. If a sequence of decreasing step-sizes is used, the convergence of the adaptive BG algorithm is also established in mean square sense as well as with probability one to the noiseless optimum filter.

5. For the robustness of EC filtering problem:

   - The tolerance of the continuous-time EC filtering problem to input signal perturbations and implementations errors has been examined and a robust optimal filter formulation was introduced. An efficient algorithm was proposed to solve the robust optimal filter problem.
   - The key idea to the development of the proposed algorithm is to seek a feasible point to the constraint set $\mathcal{F}_{\sigma_\beta}(\mathbf{x})$ where $0 \leq \sigma_\beta(\mathbf{x}) \leq \sigma_\beta(\mathbf{x}_r^*)$. A smoothing technique is then applied to solve this problem. This converts the semi-infinite constrained minimization problem into a finite constrained minimization problem with integral cost and strictly convex constraint. The numerical examples presented show that the algorithm is effective and that the robust optimal filter is tolerant to input signal perturbations and implementation errors.

8.2 Extensions

There are two interesting aspects of the envelope-constrained approach that require further study.

- The possibility of applying the time-domain constrained robustness formulation problem into the frequency-domain problem. Although the present constrained robustness formulation problem is based on the continuous time-domain, many results presented here do have an analogue in the frequency-domain. Accordingly, the formulation of the CRF problem in frequency-domain is of interest and is mathematical challenging.

- Relaxation of the conditions for convergence of the proposed adaptive noisy training algorithm. Convergence has been established when the given initial point of the adaptive algorithm is in a small neighborhood of the optimal filter. It thus represents a challenge to relax the small neighborhood condition.

Appendix A

Proofs of Results in Chapter 3

A.1 Proof of Lemma 3.4.2

Let $(\mathbf{x}^*, \lambda^*(t))$ be the solution of the unconstrained minimization problem (3.3.1). Clearly, it satisfies the stationary condition in (3.4.1). We shall show that λ^* in the unconstrained minimization problem (3.3.1) solves the dual problem (3.3.3). Since f and $\mathbf{g}(\cdot, t)$ are convex and differentiable at $\mathbf{x}$, for all $\mathbf{x} \in \Re^n$, we have

$$\begin{aligned} f(\mathbf{x}) &\geq f(\mathbf{x}^*) + \langle \nabla f(\mathbf{x}^*), (\mathbf{x} - \mathbf{x}^*) \rangle \\ \mathbf{g}(\mathbf{x}, t) &\geq \mathbf{g}(\mathbf{x}^*, t) + \langle \nabla \mathbf{g}(\mathbf{x}^*, t), (\mathbf{x} - \mathbf{x}^*) \rangle . \end{aligned}$$

Combining with $\lambda^* \geq 0_m$ and $\nabla_{\mathbf{x}} \mathcal{L}(\mathbf{x}^*, \lambda^*) = 0$, for all $\mathbf{x} \in \Re^n$, the Lagrange function at λ^* is

$$\begin{aligned} \mathcal{L}(\mathbf{x}, \lambda^*) &= f(\mathbf{x}) + \langle \mathbf{g}(\mathbf{x}, t), \lambda^*(t) \rangle \\ &\geq f(\mathbf{x}^*) + \langle \mathbf{g}(\mathbf{x}^*, t), \lambda^*(t) \rangle + \langle \nabla f(\mathbf{x}^*) + \langle \nabla \mathbf{g}'(\mathbf{x}^*, t), \lambda^*(t) \rangle , (\mathbf{x} - \mathbf{x}^*) \rangle \\ &= f(\mathbf{x}^*) + \langle \mathbf{g}(\mathbf{x}^*, t), \lambda^*(t) \rangle + \langle \nabla_{\mathbf{x}} \mathcal{L}(\mathbf{x}^*, \lambda^*), (\mathbf{x} - \mathbf{x}^*) \rangle \\ &= \mathcal{L}(\mathbf{x}^*, \lambda^*). \end{aligned} \tag{A.1.1}$$

Since $\mathbf{g}(\mathbf{x}^*, t) \leq 0_m$ and $\langle \mathbf{g}(\mathbf{x}^*, t), \lambda^*(t) \rangle = 0$, the Lagrange function at $\mathbf{x}^*$ is reduced to

$$\begin{aligned} \mathcal{L}(\mathbf{x}^*, \lambda) &= f(\mathbf{x}^*) + \langle \mathbf{g}(\mathbf{x}^*, t), \lambda(t) \rangle \leq f(\mathbf{x}^*) \\ &= f(\mathbf{x}^*) + \langle \mathbf{g}(\mathbf{x}^*, t), \lambda^*(t) \rangle = \mathcal{L}(\mathbf{x}^*, \lambda^*), \end{aligned} \tag{A.1.2}$$

for all $\lambda \geq 0_m$. Combining (A.1.2) with (A.1.1), it is clear that $(\mathbf{x}^*, \lambda^*(t))$ satisfies the saddle point condition for all $\mathbf{x} \in \Re^n$ and $\lambda(t) \geq 0_m, t \in \Omega$:

$$\mathcal{L}(\mathbf{x}, \lambda^*) \geq \mathcal{L}(\mathbf{x}^*, \lambda^*) \geq \mathcal{L}(\mathbf{x}^*, \lambda).$$

Thus, it follows that

$$\min_{\mathbf{x}} \mathcal{L}(\mathbf{x}, \lambda^*) = \mathcal{L}(\mathbf{x}^*, \lambda^*) \geq \mathcal{L}(\mathbf{x}^*, \lambda) = \min_{\mathbf{x}} \mathcal{L}(\mathbf{x}, \lambda) \quad \text{for all } \lambda(t) \geq 0_m, \forall t \in \Omega.$$

The above equation implies that

$$\lambda^* \;=\; arg \max_{\lambda \in \Lambda} \min_{\mathbf{x}} \mathcal{L}(\mathbf{x}, \lambda)$$

where $\Lambda = \{\lambda(t) : \lambda(t) \geq 0_m, t \in \Omega\}$. Hence, λ^* solves the dual problem (3.3.3). ∎

A.2 Proof of Lemma 3.4.3

For each $i = 1, \ldots, m$, $\mathbf{X}_{1,i}$ is a convex cone and $\mathbf{X}_{1,i} \supset \mathbf{X}_{2,i}$. This, in turn, implies that $\mathbf{X}_{1,i} \supset co\mathbf{X}_{2,i}$, where $co\mathbf{X}_{2,i}$ denotes the convex hull of $\mathbf{X}_{2,i}$ which is the collection of all convex combination of elements of the set $\mathbf{X}_{2,i}$.

Let $0 \neq \mathbf{x} \in \mathbf{X}_{1,i}$. Then, there exists a $0 \leq \lambda_i \in M(\bar{\Omega}, \Re)$ such that $\int_{\bar{\Omega}(\mathbf{x}^*)} d\lambda_i(t) \neq 0$ and

$$\mathbf{x} \;=\; \int_{\bar{\Omega}(\mathbf{x}^*)} \nabla_{\mathbf{x}} \mathbf{g}_i(\mathbf{x}^*, t) d\lambda_i(t)$$

By the continuity of $\mathbf{g}_i(\mathbf{x}^*, \cdot)$, we see that the set $\bar{\Omega}(\mathbf{x}^*)$ is closed, and hence compact in Ω. Again, by the continuity of $\nabla_{\mathbf{x}} \mathbf{g}_i$, the set $\mathbf{X}_{2,i}$ is compact in $\Re^n$. Thus, the set $co\mathbf{X}_{2,i}$ is compact and closed. Assume that $\mathbf{x}_0 \notin co\mathbf{X}_{2,i}$, i.e,

$$\mathbf{x}_0 \;\triangleq\; \mathbf{x} \Big/ \int_{\bar{\Omega}(\mathbf{x}^*)} d\lambda_i(t) \notin co\mathbf{X}_{2,i} \; .$$

Since $\mathbf{x} \in \mathbf{X}_{1,i}$ and the set $\mathbf{X}_{1,i}$ is a convex cone, it is clear that $\mathbf{x}_0 \in \mathbf{X}_{1,i}$. Then, by the strict separation theorem [51] of convex sets, there exist an $\mathbf{a} \in \Re^n$ and an $\alpha \in \Re$ such that

$$\mathbf{a}'\mathbf{x}_0 > \alpha \tag{A.2.1}$$

$$\mathbf{a}'\mathbf{y} < \alpha \quad \text{for all } \mathbf{y} \in co\mathbf{X}_{2,i}. \tag{A.2.2}$$

Clearly, from (A.2.2), we have

$$\mathbf{a}'\nabla_{\mathbf{x}} \mathbf{g}_i(\mathbf{x}^*, t) < \alpha, \quad \text{for all } t \in \bar{\Omega}(\mathbf{x}^*),$$

and hence

$$\mathbf{a}'\mathbf{x}_0 = \int_{\bar{\Omega}(\mathbf{x}^*)} \mathbf{a}'\nabla_{\mathbf{x}} \mathbf{g}_i(\mathbf{x}^*, t) d\lambda_i(t) \Big/ \int_{\bar{\Omega}(\mathbf{x}^*)} d\lambda_i(t) < \alpha.$$

This contradicts (A.2.1). Thus, $\mathbf{x}_0 \in co\mathbf{X}_{2,i}$ and hence $\mathbf{X}_{1,i} = co\mathbf{X}_{2,i}$. Therefore, $\mathbf{X}_1 = \mathbf{X}_2$. ∎

A.3 Proof of Theorem 3.4.2

The set $\bar{\Omega}(x^*)$ is defined in Lemma 3.4.3. Then, its complement set is:

$$\Omega\backslash\bar{\Omega}(\mathbf{x}^*) \;=\; \{t \in \Omega | \mathbf{g}(\mathbf{x}^*, t) < 0\}$$

Clearly, the complement set $\Omega\backslash\bar{\Omega}(\mathbf{x}^*)$is open since $\bar{\Omega}(\mathbf{x}^*)$ is closed. Thus, the complementary condition (i.e, the second condition in (3.4.1)) ensures that $\lambda^*(t) = 0_m$ on $t \in \Omega\backslash\bar{\Omega}(\mathbf{x}^*)$. Thus, the stationary condition in (3.4.1) is reduced to

$$\nabla f(\mathbf{x}^*) + \int_{\bar{\Omega}(\mathbf{x}^*)} \nabla_{\mathbf{x}} \mathbf{g}'(\mathbf{x}^*, t) d\lambda^*(t) = 0.$$

Therefore, it follows from Lemma 3.4.3 that $-\nabla f(\mathbf{x}^*) \in \mathbf{X}_2$, where

$$\mathbf{X}_2 = \sum_{i=1}^{m} co\mathbf{X}_{2,i} \quad \text{and } \mathbf{X}_{2,i} = \left\{\nabla_{\mathbf{x}} \mathbf{g}_i(\mathbf{x}^*, t) | t \in \bar{\Omega}(\mathbf{x}^*)\right\}, i = 1, \ldots, m.$$

By Carathéodory's dimensionality theorem [51], there exists, for each $i = 1, \ldots, k_j, j = 1, \ldots, m$, a positive $\lambda^*_{i,j}$ such that

$$-\nabla f(\mathbf{x}^*) \;=\; \sum_{j=1}^{m} \sum_{i=1}^{k_j} \nabla_{\mathbf{x}} \mathbf{g}_j(\mathbf{x}^*, t_{j,i}) \lambda^*_{i,j}, \text{for some } t_{j,i} \in \bar{\Omega}(\mathbf{x}^*) \tag{A.3.1}$$

where, for $i = 1, \ldots, k_j$, $\lambda^*_{i,j}$ is the jth component of $\lambda^*_i \triangleq [\lambda^*_{i,1}, \ldots, \lambda^*_{i,m}]'$ and $k_j \leq n$.

It is clear from (A.3.1) that $\Lambda^* \triangleq [\lambda^{*'}_1, \ldots, \lambda^{*'}_{k_m}]' \in \Re_+^{mk_m}$ satisfies the stationary condition in (3.4.1). The corresponding time supporting points are, thus, given by

$$\Gamma = \left\{ (t_{1,1}, \ldots, t_{1,k_1}), (t_{2,1}, \ldots, t_{2,k_2}), \ldots, (t_{m,1}, \ldots, t_{m,k_m}) \right\} \tag{A.3.2}$$

Accordingly, it is a measure with finite support at these points. We now rearrange (A.3.2) as $(t_1, t_2, \ldots, t_k)$, where $k = k_1 + k_2 + \ldots + k_m \leq mn$. Then, we consider the same k points for the following m constraints,

$$\mathbf{g}_j(\mathbf{x}^*, t_i) \;\leq\; 0, \quad j = 1, \ldots, m; i = 1, \ldots, k.$$

More specifically, for each $j = 1, \ldots, m$, we add in $\sum_{\substack{i=1 \\ i \neq j}}^{m} k_i$ extra points for the constraint $\mathbf{g}_j(\mathbf{x}^*, t) \leq 0$. Clearly, for each $j = 1, \ldots, m$, these additional points give rise to inactive constraints. Thus, the associated Lagrange multipliers are zero. On this basis, (A.3.1) can be written as:

$$-\nabla f(\mathbf{x}^*) \;=\; \sum_{i=1}^{k} \sum_{j=1}^{m} \nabla_{\mathbf{x}} \mathbf{g}_j(\mathbf{x}^*, t_i) \lambda^*_{i,j}, \quad \text{for some } t_i \in \bar{\Omega}(\mathbf{x}^*)$$

∎

Appendix B

Proofs of Results in Chapter 4

B.1 Proof of Lemma 4.4.1

We rearrange the optimal Lagrangian multiplier vector λ^* as:

$$\lambda^* = \begin{bmatrix} \lambda^B \\ \lambda^N \end{bmatrix} \tag{B.1.1}$$

where the vectors $\lambda^B \in \Re^{n_1}$, $\lambda^N \in \Re^{n_2}$ and $n_1 + n_2 = m$. Here λ^B and λ^N are, respectively, given by

$$\lambda^B = \begin{bmatrix} \lambda_1^B \\ \vdots \\ \lambda_{n_1}^B \end{bmatrix} \quad \text{and} \quad \lambda^N = \begin{bmatrix} \lambda_1^N \\ \vdots \\ \lambda_{n_2}^N \end{bmatrix}$$

with $\lambda_i^B > 0, i = 1, \ldots, n_1$ and $\lambda_j^N = 0, j = 1, \ldots, n_2$. Accordingly, we rearrange the following matrices

$$\mathbf{D}(\lambda^*) = \begin{bmatrix} \mathbf{D}(\lambda^B) & 0 \\ 0 & \mathbf{D}(\lambda^N) \end{bmatrix}, \nabla\phi(\lambda^*) = \begin{bmatrix} \nabla\phi^B(\lambda^*) \\ \nabla\phi^N(\lambda^*) \end{bmatrix}, \mathbf{P} = \begin{bmatrix} \mathbf{P}^B & \mathbf{P}^{BN} \\ \mathbf{P}^{NB} & \mathbf{P}^N \end{bmatrix}$$

where the matrix $\mathbf{P}^B > 0$, and the matrices $\mathbf{P}^{BN}$, $\mathbf{P}^{NB}$ and $\mathbf{P}^N$ are all null matrices. The Jacobian matrix $\nabla\mathbf{F}(\lambda^*)$ can be decomposed into blocks as follows:

$$\begin{aligned} \nabla\mathbf{F}(\lambda^*) &= \mathbf{D}(\nabla\phi(\lambda^*)) + \mathbf{D}(\lambda^*)\mathbf{P} \\ &= \begin{bmatrix} \mathbf{D}(\nabla\phi^B(\lambda^*)) & 0 \\ 0 & \mathbf{D}(\nabla\phi^N(\lambda^*)) \end{bmatrix} + \begin{bmatrix} \mathbf{D}(\lambda^B) & 0 \\ 0 & \mathbf{D}(\lambda^N) \end{bmatrix} \begin{bmatrix} \mathbf{P}^B & 0 \\ 0 & 0 \end{bmatrix} \end{aligned} \tag{B.1.2}$$

From the strict complementary condition (SCC), it follows that

$$\lambda^{*\prime}\nabla\phi(\lambda^*) = \lambda^{B\prime}\nabla\phi^B(\lambda^*) + \lambda^{N\prime}\nabla\phi^N(\lambda^*) = 0$$

and

$$\begin{aligned} \nabla\phi^B(\lambda^*) &= 0_{n_1} \\ \nabla\phi^N(\lambda^*) &> 0_{n_2}. \end{aligned} \tag{B.1.3}$$

Therefore, (B.1.2) is reduced to blocks as follows:

$$\nabla\mathbf{F}(\lambda^*) = \begin{bmatrix} \mathbf{D}(\lambda^B)\mathbf{P}^B & 0 \\ 0 & \mathbf{D}(\nabla\phi^N(\lambda^*)) \end{bmatrix} \triangleq \begin{bmatrix} \nabla\mathbf{F}^1 & 0 \\ 0 & \nabla\mathbf{F}^2 \end{bmatrix}$$

where the matrix $\nabla\mathbf{F}^1 \triangleq \mathbf{D}(\lambda^B)\mathbf{P}^B$ and the matrix $\nabla\mathbf{F}^2 \triangleq \mathbf{D}(\nabla\phi^N(\lambda^*))$.

To find out the eigenvalues of the Jacobian matrix $\nabla\mathbf{F}(\lambda^*)$, we consider the characteristic equation:

$$|\nabla\mathbf{F}(\lambda^*) - \eta\mathbf{I}_m| = \left| \begin{bmatrix} \nabla\mathbf{F}^1 - \eta\mathbf{I}_{n_1} & 0 \\ 0 & \nabla\mathbf{F}^2 - \eta\mathbf{I}_{n_2} \end{bmatrix} \right| = 0, \tag{B.1.4}$$

where the roots η of the characteristic equation are the eigenvalues of the Jacobian matrix $\nabla\mathbf{F}(\lambda^*)$. It suffices to consider the following two characteristic equations:

$$\left|\nabla\mathbf{F}^1 - \eta\mathbf{I}_{n_1}\right| = 0, \tag{B.1.5}$$

$$\left|\nabla\mathbf{F}^2 - \eta\mathbf{I}_{n_2}\right| = 0. \tag{B.1.6}$$

Let us first consider the characteristic equation (B.1.5). Let (z_i, η_i), $z_i \neq 0$, $1 \leq i \leq n_1$, be an eigenvector-eigenvalue pair of the matrix $\nabla\mathbf{F}^1$. Then, the eigenvalues of the matrix $\nabla\mathbf{F}^1$ are

$$\eta_i = \frac{z_i'\mathbf{D}(\lambda^B)\mathbf{P}^B z_i}{\|z_i\|^2} > 0, \quad \forall i = 1, \ldots, n_1 \tag{B.1.7}$$

For the second characteristic equation (B.1.6), it follows from (B.1.3) that

$$\begin{aligned} &\left|\mathbf{D}(\nabla\phi^N(\lambda^*)) - \eta\mathbf{I}_{n_2}\right| = 0 \\ \Longleftrightarrow\quad &\eta_j = \nabla\phi_j^N(\lambda^*) > 0, \quad \forall j = n_1 + 1, \ldots, m. \end{aligned} \tag{B.1.8}$$

From (B.1.7)- (B.1.8), we conclude that all the roots of the characteristic equation for the Jacobian matrix $\nabla\mathbf{F}(\lambda^*)$ are real and the smallest root η_{min} is positive. This completes the proof. ∎

B.2 Proof of Theorem 4.4.1

Clearly, $\mathbf{F}(\lambda) = \mathbf{D}(\lambda)\nabla\phi(\lambda)$ is a differentiable function of λ with $\mathbf{F}(\lambda^*) = 0$. Applying the Taylor series expansion of the function $\mathbf{F}(\lambda)$ about the point λ^* yields

$$\mathbf{F}(\lambda) = \mathbf{F}(\lambda^*) + \nabla\mathbf{F}'(\lambda^*)\Delta\lambda + O(\|\Delta\lambda\|_2^2) \tag{B.2.1}$$

where $\nabla \mathbf{F}'(\lambda) = \nabla \mathbf{F}(\lambda)$ is the Jacobian matrix of $\mathbf{F}(\lambda)$ defined by (4.4.19), and is symmetric, $\Delta\lambda(t) = \lambda(\lambda^0, t) - \lambda^*$ and

$$\lim_{\lambda \to \lambda^*} \frac{O(\|\Delta\lambda\|_2^2)}{\|\Delta\lambda\|_2} = 0.$$

Linearize the system (4.4.15) in a neighborhood of the equilibrium point λ^*. Then by (B.2.1), we obtain the system of the first order approximation:

$$\Delta\dot{\lambda}(t) = -\nabla \mathbf{F}(\lambda^*)\Delta\lambda(t), \quad \lambda(0) = \lambda^0. \tag{B.2.2}$$

We first establish the stability of the system (B.2.2) by considering the characteristic equation

$$|\nabla \mathbf{F}(\lambda^*) - \eta \mathbf{I}_m| = 0 \tag{B.2.3}$$

where the roots η of the characteristic equation are the eigenvalues of the Jacobian matrix $\nabla \mathbf{F}(\lambda^*)$. In Lemma 4.4.1, we have shown that all eigenvalues of $\nabla \mathbf{F}(\lambda^*)$ are real and positive. Thus, by the Lyapunov's linearization principle [14], the system (4.4.15) is asymptotically stable at the equilibrium point λ^*. In particular, condition (i) of Definition 4.4.3 is satisfied with $\sigma = \eta_{min}$, where η_{min} denotes the smallest eigenvalue of the Jacobian matrix $\nabla \mathbf{F}(\lambda^*)$.

To establish the convergence of the scheme (4.4.18), we consider the scheme (4.4.17) defined by

$$\mathbf{T}(\lambda^k) = \lambda^k - h_k \mathbf{F}(\lambda^k).$$

Since both $\mathbf{T}(\lambda)$ and $\mathbf{F}(\lambda)$ are differentiable at $\lambda = \lambda^*$, we obtain

$$\nabla \mathbf{T}(\lambda^*) = \mathbf{I} - h_k \nabla \mathbf{F}(\lambda^*).$$

Since the Jacobian matrix $\nabla \mathbf{F}(\lambda^*)$ is positive definite, there exists a constant h^* such that if $h_k = h$ is a fixed step size for all k and satisfies $0 < h < h^*$, the norm of the matrix $\nabla \mathbf{T}(\lambda^*) = \mathbf{I} - h\nabla \mathbf{F}(\lambda^*)$ is less than unity. Consequently, all eigenvalues of the matrix $\nabla \mathbf{T}(\lambda^*)$ are less than unity. Thus, the spectral radius $\rho(\nabla \mathbf{T}(\lambda^*)) < 1$. By Theorem 2.3.4 of [14] and the convexity property established in Theorem 9.4.1 of [22], the sequence $\{\lambda^k\}_{k=0}^{\infty}$ and the corresponding sequence $\{\mathbf{x}^k\}_{k=0}^{\infty}$ generated by the scheme (4.4.18) converge globally to the optimal solutions λ^* and $\mathbf{x}^*$, respectively, both at a linear rate. Thus, the scheme 4.4.18 is convergent if the fixed step size h is chosen such that $0 < h < h^*$.

To find out h^*, we consider the characteristic equation of matrix $\nabla T(\lambda)$ at λ^*

$$|\nabla \mathbf{T}(\lambda^*) - \gamma \mathbf{I}_m| = |\mathbf{I}_{2N} - h_k \nabla \mathbf{F}(\lambda^*) - \gamma \mathbf{I}_m| = 0.$$

The above equation can be written as:

$$\left|\nabla \mathbf{F}(\lambda^*) - \frac{1-\gamma}{h_k}\mathbf{I}_m\right| \;=\; 0.$$

Comparing with (B.2.3), it is clear that the roots of these two equations are related in a simple way: $\eta = \frac{1-\gamma}{h_k}$, i.e.,

$$\gamma = 1 - h_k\eta \implies \gamma^2 = 1 - (2 - h_k\eta)h_k\eta.$$

The conditions $0 < \gamma < 1$, since $\rho(\nabla \mathbf{T}(\lambda^*)) < 1$, and $h_k > 0$ yield

$$2 - h_k\eta \;>\; 0.$$

Thus, for any $h_k = h > 0$, it follows that

$$h^* = 2 \min_{i\in[1:m]} \left[\frac{1}{\eta_i}\right] = \frac{2}{\eta_{max}}$$

where η_{max} denotes the largest eigenvalue of the Jacobian matrix $\nabla \mathbf{F}(\lambda^*)$. This completes the proof. ∎

B.3 Proof of Theorem 4.4.2

The linearized system (4.4.22) about the point λ^* is:

$$\Delta\dot{\lambda}(t) \;=\; -\mathbf{H}(\lambda^*)\Delta\lambda(t) \tag{B.3.1}$$

where the matrix $\mathbf{H}(\lambda^*)$ is given by

$$\mathbf{H}(\lambda^*) \;=\; \nabla \mathbf{F}^{-1}(\lambda^*)\mathbf{D}(\alpha)\nabla \mathbf{F}(\lambda^*). \tag{B.3.2}$$

It is clear from (B.3.2) that the matrix $\mathbf{H}(\lambda^*)$ is a similarity transform of the diagonal matrix $\mathbf{D}(\alpha)$ consisting of the scaling vector $\alpha = [\alpha_1, \ldots, \alpha_m]'$.

To establish the asymptotic stability of the system (B.3.1), we consider the characteristic equation:

$$|\mathbf{H}(\lambda^*) - \eta\mathbf{I}_m| \;=\; 0$$

where the roots η of the characteristic equation are the eigenvalues of the matrix $\mathbf{H}(\lambda^*)$.

Since the matrix $\mathbf{H}(\lambda^*)$ is similar to the diagonal matrix $\mathbf{D}(\alpha)$, they have the same eigenvalues $\eta_i = \alpha_i > 0$, $i = 1, \ldots, m$. Thus, it follows from the Lyapunov's linearization principle [71] that the system (4.4.22) is asymptotically stable at the equilibrium point λ^*.

To establish the convergence of the scheme (4.4.21), we first show that for each k the mapping $\mathbf{T}(\lambda^k)$ defined by

$$\mathbf{T}(\lambda^k) \triangleq \lambda^k - h_k \nabla \mathbf{F}^{-1}(\lambda^k)\mathbf{D}(\alpha)\mathbf{F}(\lambda^k)$$

is differentiable at λ^*. This is equivalent to showing for each k

$$\lim_{\lambda^k \to \lambda^*} \frac{\|\mathbf{T}(\lambda^k) - \mathbf{T}(\lambda^*)\|_2}{\|\lambda^k - \lambda^*\|_2} = \|\nabla \mathbf{T}(\lambda^*)\|_2. \tag{B.3.3}$$

By $\mathbf{F}(\lambda^*) = 0$, we obtain

$$\begin{aligned}
& \|\mathbf{T}(\lambda^k) - \mathbf{T}(\lambda^*)\|_2 = \|\lambda^k - \lambda^* - h_k \nabla \mathbf{F}^{-1}(\lambda^k)\mathbf{D}(\alpha)\mathbf{F}(\lambda^k)\|_2 \\
= \; & \|\nabla \mathbf{F}^{-1}(\lambda^k)\mathbf{D}(\alpha)[\mathbf{D}^{-1}(\alpha)\nabla \mathbf{F}(\lambda^k)(\lambda^k - \lambda^*) - h_k \mathbf{F}(\lambda^k)]\|_2 \\
= \; & \|\nabla \mathbf{F}^{-1}(\lambda^k)\mathbf{D}(\alpha)\{-h_k[\mathbf{F}(\lambda^k) - \mathbf{F}(\lambda^*) - \nabla \mathbf{F}(\lambda^k)(\lambda^k - \lambda^*)] - h_k \nabla \mathbf{F}(\lambda^k)(\lambda^k - \lambda^*) \\
& + \mathbf{D}^{-1}(\alpha)\nabla \mathbf{F}(\lambda^k)(\lambda^k - \lambda^*)\}\|_2 \\
\leq \; & h_k \|\nabla \mathbf{F}^{-1}(\lambda^k)\mathbf{D}(\alpha)\|_2 \|\mathbf{F}(\lambda^k) - \mathbf{F}(\lambda^*) - \nabla \mathbf{F}(\lambda^k)(\lambda^k - \lambda^*)\|_2 \\
& + \|\mathbf{I} - h_k \mathbf{H}(\lambda^k)\|_2 \|\lambda^k - \lambda^*\|_2,
\end{aligned} \tag{B.3.4}$$

where $\mathbf{H}(\cdot)$ is defined by (B.3.2) in terms of λ^k. From the continuity of the derivative $\nabla \mathbf{F}(\lambda^k)$ for each k at the point λ^* yields

$$\lim_{\lambda^k \to \lambda^*} \frac{\|\mathbf{F}(\lambda^k) - \mathbf{F}(\lambda^*) - \nabla \mathbf{F}(\lambda^k)(\lambda^k - \lambda^*)\|_2}{\|\lambda^k - \lambda^*\|_2} = 0. \tag{B.3.5}$$

Combining (B.3.5) with (B.3.4), we obtain (B.3.3) that is given by

$$\|\nabla \mathbf{T}(\lambda^*)\|_2 \leq \|\mathbf{I} - h_k \mathbf{H}(\lambda^*)\|_2.$$

Since the matrix $\mathbf{H}(\lambda^*)$ is positive definite, there exists a constant h^* such that if $h_k = h$ is a fixed step-size for all k and satisfies $0 < h < h^*$, the matrix norm $\|\mathbf{I} - h_k \mathbf{H}(\lambda^*)\|_2$ is less than unity. As a result, all eigenvalues of the matrix $\nabla \mathbf{T}(\lambda^*)$ are less than unity and hence, the spectral radius $\rho(\mathbf{T}(\lambda^*)) < 1$. We note that for a specified $\alpha_i = \bar{\alpha}$ for every $i = 1, \ldots, m$, the matrix $\mathbf{H}(\lambda^*) = \bar{\alpha}\mathbf{I}$. Accordingly, $\|\nabla \mathbf{T}(\lambda^*)\|_2 \leq 1 - h\bar{\alpha}$. Thus, the spectral radius $\rho(\mathbf{T}(\lambda^*)) = 0$ can be achieved depending on the choices of h and $\bar{\alpha}$. By Theorem 2.3.4 of [14] and the convexity property established in Theorem 9.4.1 of [22], the sequence $\{\lambda^k\}_{k=0}^{\infty}$ and the corresponding sequence $\{\mathbf{x}^k\}_{k=0}^{\infty}$ generated by the scheme (4.4.21) converge globally to the optimal solutions λ^* and $\mathbf{x}^*$, respectively, both at least a linear rate. The remaining part for finding h^* is similar to that given for the corresponding part of Theorem 4.4.1. Thus, we obtain $h^* = \frac{2}{\alpha^*}$ where $\alpha^* = \max_i[\alpha_i]$.

Let $\alpha_i = e$, $\forall i$ and choose the step-size $h_k = \frac{1}{e}$ for each k. If there exists a constant $\ell > 0$ such that for each k the Jacobian matrix $\nabla \mathbf{F}(\lambda^k)$ defined by (4.4.19) satisfies a Lipschitz condition in the neighborhood of the point λ^*, we have

$$\begin{aligned}
&\|\mathbf{T}(\lambda^k) - \mathbf{T}(\lambda^*)\|_2 = \|\lambda^k - \lambda^* - \nabla \mathbf{F}^{-1}(\lambda^k)\mathbf{F}(\lambda^k)\|_2 \\
\leq\ & \|\nabla \mathbf{F}^{-1}(\lambda^k)\|_2[\|\nabla \mathbf{F}(\lambda^k) - \nabla \mathbf{F}(\lambda^*)\|_2\|\lambda^k - \lambda^*\|_2 + \|\mathbf{F}(\lambda^k) - \mathbf{F}(\lambda^*) - \nabla \mathbf{F}(\lambda^*)(\lambda^k - \lambda^*)\|_2] \\
\leq\ & \|\nabla \mathbf{F}^{-1}(\lambda^k)\|_2[\ell\|\lambda^k - \lambda^*\|_2^2 + \|\lambda^k - \lambda^*\|_2^2\|\Phi(\lambda^*)\|_2] \\
\leq\ & (\ell + c)\|\nabla \mathbf{F}^{-1}(\lambda^k)\|_2\|\lambda^k - \lambda^*\|_2^2,
\end{aligned}$$

where $\mathbf{F}(\lambda^k)$ is Fréchet differentiable at the point λ^* for each k and the vector function $\Phi(\lambda^*)$ is bounded at a constant c , i.e., $\|\Phi(\lambda^*)\|_2 \leq c$. Clearly,

$$\lim_{\lambda^k \to \lambda^*} \frac{\|\mathbf{T}(\lambda^k) - \mathbf{T}(\lambda^*)\|_2}{\|\lambda^k - \lambda^*\|_2^2} \leq (\ell + c)\|\nabla \mathbf{F}^{-1}(\lambda^*)\|_2 < \infty,$$

where $\|\nabla \mathbf{F}^{-1}(\lambda^*)\|_2$ is bounded since $\nabla \mathbf{F}(\lambda^*)$ is nonsingular. Following from Theorem 2.5.3 of [14] and the convexity property established in Theorem 9.4.1 of [22] , the sequence $\{\lambda^k\}_{k=0}^{\infty}$ and the corresponding sequence $\{\mathbf{x}^k\}_{k=0}^{\infty}$ globally converge to the optimum λ^* and $\mathbf{x}^*$, respectively, at a quadratic rate. This completes the proof. ∎

Appendix C

Proofs of Results in Chapter 5

C.1 Gradients of the dual cost function $\phi(\mathbf{t}, \Lambda)$ about t and Λ

The gradients of the dual cost function $\phi(\mathbf{t}, \Lambda)$ about t and Λ are as follows:

$$\begin{aligned}
\nabla_t \phi(\mathbf{t}, \Lambda) &= \frac{1}{2}\left[\mathbf{D}(\Lambda)\nabla_t \mathbf{A}(\mathbf{t})\mathbf{A}'(\mathbf{t})\Lambda\right] + \nabla_t \mathbf{b}'(\mathbf{t})\Lambda \in \Re^k \\
&= \frac{1}{2}\begin{bmatrix} \lambda_1^T \frac{\partial \mathbf{A}(t_1)}{\partial t_1}\mathbf{A}'(t_1)\lambda_1 + \ldots + \lambda_1^T \frac{\partial \mathbf{A}(t_1)}{\partial t_1}\mathbf{A}'(t_k)\lambda_k \\ \vdots \\ \lambda_k^T \frac{\partial \mathbf{A}(t_k)}{\partial t_m}\mathbf{A}'(t_1)\lambda_1 + \ldots + \lambda_k^T \frac{\partial \mathbf{A}(t_k)}{\partial t_m}\mathbf{A}'(t_k)\lambda_k \end{bmatrix} + \begin{bmatrix} \lambda_1' \frac{\partial \mathbf{b}(t_1)}{\partial t_1} \\ \vdots \\ \lambda_m' \frac{\partial \mathbf{b}(t_k)}{\partial t_k} \end{bmatrix} \\
&= \frac{1}{2}\begin{bmatrix} \lambda_1' \frac{\partial \mathbf{A}(t_1)}{\partial t_1}\mathbf{A}'(\mathbf{t})\Lambda \\ \vdots \\ \lambda_m' \frac{\partial \mathbf{A}(t_k)}{\partial t_m}\mathbf{A}'(\mathbf{t})\Lambda \end{bmatrix} + \begin{bmatrix} \lambda_1' \frac{\partial \mathbf{b}(t_1)}{\partial t_1} \\ \vdots \\ \lambda_k' \frac{\partial \mathbf{b}(t_k)}{\partial t_k} \end{bmatrix},
\end{aligned}$$

and

$$\begin{aligned}
\nabla_\Lambda \phi(\mathbf{t}, \Lambda) &= \frac{1}{2}\mathbf{A}(\mathbf{t})\mathbf{A}'(\mathbf{t})\Lambda + \mathbf{b}(\mathbf{t}) \in \Re^{2k} \\
&= \frac{1}{2}\begin{bmatrix} \mathbf{A}(t_1)\mathbf{A}'(t_1)\lambda_1 + \ldots + \mathbf{A}(t_1)\mathbf{A}'(t_k)\lambda_k \\ \vdots \\ \mathbf{A}(t_k)\mathbf{A}'(t_1)\lambda_1 + \ldots + \mathbf{A}(t_k)\mathbf{A}'(t_k)\lambda_k \end{bmatrix} + \begin{bmatrix} \mathbf{b}(t_1) \\ \vdots \\ \mathbf{b}(t_k) \end{bmatrix} \\
&= \frac{1}{2}\begin{bmatrix} \mathbf{A}(t_1)\mathbf{A}'(\mathbf{t})\Lambda \\ \vdots \\ \mathbf{A}(t_k)\mathbf{A}'(\mathbf{t})\Lambda \end{bmatrix} + \begin{bmatrix} \mathbf{b}(t_1) \\ \vdots \\ \mathbf{b}(t_k) \end{bmatrix}
\end{aligned}$$

where

$$\frac{\partial \mathbf{b}(t_i)}{\partial t_i} = \begin{bmatrix} \frac{\partial \varepsilon^+(t_i)}{\partial t_i} \\ -\frac{\partial \varepsilon^-(t_i)}{\partial t_i} \end{bmatrix}, \quad \frac{\partial \mathbf{A}(t_i)}{\partial t_i} = \begin{bmatrix} \frac{\partial \Theta'(t_i)}{\partial t_i} \\ -\frac{\partial \Theta'(t_i)}{\partial t_i} \end{bmatrix},$$

$$
\begin{aligned}
\frac{\partial \Theta'(t_i)}{\partial t_i} &= \left[\frac{\partial \theta_0(t_i)}{\partial t_i}, \ldots, \frac{\partial \theta_{n-1}(t_i)}{\partial t_i} \right] \\
\frac{\partial \theta_j(t_i)}{\partial t_i} &= \int_0^\infty L_j^p(\tau)\tilde{s}(t_i - \tau)d\tau, i = 1, \ldots, k, j = 0, 1, \ldots, n-1, \\
\varepsilon^+(t) &= \begin{cases} 0 & t \le -0.68 \\ 0.5[1 + \sin(\frac{\pi}{2}(1 + \frac{t}{0.34}))] & -0.68 \le t \le 0.36 \\ 0.05 + 0.407e^{-1.84(t-0.36)} & 0.36 \le t \end{cases} \\
\varepsilon^-(t) &= \begin{cases} 0 & t \le -0.36 \\ 0.5[1 + \sin(\frac{\pi}{2}(1 + \frac{t}{0.18}))] & -0.36 \le t \le 0.28 \\ 0.11e^{-3.42(t-0.3)} & 0.28 \le t. \end{cases}
\end{aligned}
$$

C.2 Hessians of the dual cost function $\phi(\mathbf{t}, \Lambda)$ about $\mathbf{t}$ and Λ

The Hessians of the dual cost function $\phi(\mathbf{t}, \Lambda)$ about $\mathbf{t}$ and Λ are as follows:

$$
\nabla_{\mathbf{t}}^2\phi(\mathbf{t},\Lambda) = \begin{bmatrix} \frac{\partial^2\phi(\mathbf{t},\Lambda)}{\partial t_1^2} & \cdots & \frac{\partial^2\phi(\mathbf{t},\Lambda)}{\partial t_1 \partial t_k} \\ \vdots & \ddots & \vdots \\ \frac{\partial^2\phi(\mathbf{t},\Lambda)}{\partial t_k \partial t_1} & \cdots & \frac{\partial^2\phi(\mathbf{t},\Lambda)}{\partial t_k^2} \end{bmatrix}_{k\times k}, \nabla_{(\mathbf{t},\Lambda)}^2\phi(\mathbf{t},\Lambda) = \begin{bmatrix} \frac{\partial^2\phi(\mathbf{t},\Lambda)}{\partial t_1 \partial \lambda_1} & \cdots & \frac{\partial^2\phi(\mathbf{t},\Lambda)}{\partial t_1 \partial \lambda_k} \\ \vdots & \ddots & \vdots \\ \frac{\partial^2\phi(\mathbf{t},\Lambda)}{\partial t_k \partial \lambda_1} & \cdots & \frac{\partial^2\phi(\mathbf{t},\Lambda)}{\partial t_k \partial \lambda_k} \end{bmatrix}_{k\times 2k}
$$

$$
\nabla_{\Lambda}^2\phi(\mathbf{t},\Lambda) = \frac{1}{2}\begin{bmatrix} \mathbf{A}(t_1)\mathbf{A}'(t_1) & \cdots & \mathbf{A}(t_1)\mathbf{A}'(t_k) \\ \vdots & \ddots & \vdots \\ \mathbf{A}(t_k)\mathbf{A}'(t_1) & \cdots & \mathbf{A}(t_m)\mathbf{A}'(t_k) \end{bmatrix}_{2k\times 2k}
$$

$$
\nabla_{(\Lambda,\mathbf{t})}^2\phi(\mathbf{t},\Lambda) = \begin{bmatrix} \frac{\partial^2\phi(\mathbf{t},\Lambda)}{\partial \lambda_1 \partial t_1} & \cdots & \frac{\partial^2\phi(\mathbf{t},\Lambda)}{\partial \lambda_1 \partial t_k} \\ \vdots & \ddots & \vdots \\ \frac{\partial^2\phi(\mathbf{t},\Lambda)}{\partial \lambda_k \partial t_1} & \cdots & \frac{\partial^2\phi(\mathbf{t},\Lambda)}{\partial \lambda_k \partial t_k} \end{bmatrix}_{2k\times k},
$$

where

$$
\begin{aligned}
\frac{\partial^2\phi(\eta)}{\partial t_i \partial t_j} &= \begin{cases} \frac{1}{2}\lambda_i' \frac{\partial \mathbf{A}(t_i)}{\partial t_i}\frac{\partial \mathbf{A}'(t_j)}{\partial t_j}\lambda_j, & (i \ne j) \\ \frac{1}{2}\left(\lambda_i' \frac{\partial^2 \mathbf{A}(t_i)}{\partial t_i^2}\mathbf{A}'(\mathbf{t})\Lambda + \lambda_i' \frac{\partial \mathbf{A}(t_i)}{\partial t_i}\frac{\partial \mathbf{A}'(t_i)}{\partial t_i}\lambda_i\right) + \lambda_i' \frac{\partial^2 \mathbf{b}(t_i)}{\partial t_i^2} & (i = j) \end{cases} \\
\Re^{1\times 2} \ni \frac{\partial^2\phi(\eta)}{\partial t_i \partial \lambda_j} &= \begin{cases} \frac{1}{2}\lambda_i' \mathbf{A}(t_j)\frac{\partial \mathbf{A}'(t_i)}{\partial t_i} & (i \ne j) \\ \frac{1}{2}\left(\Lambda' \mathbf{A}(\mathbf{t})\frac{\partial \mathbf{A}'(t_i)}{\partial t_i} + \lambda_i' \mathbf{A}(t_i)\frac{\partial \mathbf{A}'(t_i)}{\partial t_i}\right) + \frac{\partial \mathbf{b}(t_i)}{\partial t_i} & (i = j) \end{cases} \\
\Re^{2\times 1} \ni \frac{\partial^2\phi(\eta)}{\partial \lambda_i \partial t_j} &= \begin{cases} \frac{1}{2}\frac{\partial \mathbf{A}(t_j)}{\partial t_j}\mathbf{A}'(t_i)\lambda_j & (i \ne j) \\ \frac{1}{2}\left(\frac{\partial \mathbf{A}(t_i)}{\partial t_i}\mathbf{A}'(\mathbf{t})\Lambda + \frac{\partial \mathbf{A}(t_i)}{\partial t_i}\mathbf{A}'(t_i)\lambda_i\right) + \frac{\partial \mathbf{b}(t_i)}{\partial t_i} & (i = j) \end{cases} \\
\frac{\partial \mathbf{A}(t_i)}{\partial t_i}\frac{\partial \mathbf{A}'(t_j)}{\partial t_j} &= \sum_{l=0}^{N-1} \frac{\partial \theta_l(t_i)}{\partial t_i}\frac{\partial \theta_l(t_j)}{\partial t_j}\begin{bmatrix} 1 & -1 \\ -1 & 1 \end{bmatrix},
\end{aligned}
$$

$$\frac{\partial^2 \mathbf{A}(t_i)}{\partial t_i^2}\mathbf{A}'(t_j) = \sum_{l=0}^{N-1} \frac{\partial^2 \theta_l(t_i)}{\partial t_i^2}\theta_l(t_j)\begin{bmatrix} 1 & -1 \\ -1 & 1 \end{bmatrix},$$

$$\frac{\partial^2 \mathbf{b}(t_i)}{\partial t_i^2} = \begin{bmatrix} \frac{\partial^2 \varepsilon^+(t_i)}{\partial t_i^2} \\ -\frac{\partial^2 \varepsilon^-(t_i)}{\partial t_i^2} \end{bmatrix},$$

while

$$\frac{\partial^2 \theta_j(t)}{\partial t^2} = \int_0^\infty L_j^p(\tau)\frac{d\tilde{s}(t-\tau)}{dt}d\tau, \quad \forall j = 0, 1, \ldots, n-1$$

$$\frac{\partial \varepsilon^+(t)}{\partial t} = \begin{cases} 0 & t \le -0.68 \\ \frac{5\pi}{6.8}\cos[\frac{\pi}{2}(1+\frac{t}{0.34})] & -0.68 \le t \le 0.36 \\ -0.7489e^{-1.84(t-0.36)} & 0.36 \le t \le T \\ 0 & t > T \end{cases}$$

$$\frac{\partial \varepsilon^-(t)}{\partial t} = \begin{cases} 0 & t \le -0.36 \\ \frac{5\pi}{3.6}\cos[\frac{\pi}{2}(1+\frac{t}{0.18})] & -0.36 \le t \le 0.28 \\ -0.3762e^{-3.42(t-0.3)} & 0.28 \le t \le T \\ 0 & t > T \end{cases}$$

$$\frac{\partial^2 \varepsilon^+(t)}{\partial t^2} = \begin{cases} 0 & t \le -0.68 \\ \frac{-50\pi}{6.8^2}\sin[\frac{\pi}{2}(1+\frac{t}{0.34})] & -0.68 \le t \le 0.36 \\ 1.378e^{-1.84(t-0.36)} & 0.36 \le t \le T \\ 0 & t > T \end{cases}$$

$$\frac{\partial^2 \varepsilon^-(t)}{\partial t^2} = \begin{cases} 0 & t \le -0.36 \\ \frac{-50\pi}{3.6^2}\sin[\frac{\pi}{2}(1+\frac{t}{0.18})] & -0.36 \le t \le 0.28 \\ 1.2866e^{-3.42(t-0.3)} & 0.28 \le t \le T \\ 0 & t > T \end{cases}$$

and

$$s(t) = \begin{cases} 0 & t \le 0 \\ \frac{A_s e^{-\frac{A_s^2}{4t}}}{2\sqrt{\pi t^3}} & 0 < t \le T, \\ 0 & t > T \end{cases}$$

$$A_s = \frac{A_{s0}}{20\log_{10}(e)\sqrt{\pi f_0}}, \quad A_{s0} = 30 \text{ and } f_0 = 1$$

$$\tilde{s}(t) = \frac{ds(t)}{dt} = \begin{cases} 0 & t \le 0 \\ \frac{A_s e^{-\frac{A_s^2}{4t}}}{4\sqrt{\pi t^5}}\left[\frac{A_s^2}{2t} - 3\right] & t > 0 \end{cases},$$

$$\frac{d\tilde{s}(t)}{dt} = \begin{cases} 0 & t \le 0 \\ \frac{A_s e^{-\frac{A_s^2}{4t}}}{8t^3\sqrt{\pi t}}\left[(\frac{A_s^2}{2t} - 8)(\frac{A_s^2}{2t} - 2) - 1\right] & t > 0. \end{cases}$$

C.3 Proof of Theorem 5.3.1

There are three possibilities for the optimal σ_β of the CRF problem (2.2.12): (i) $\sigma_\beta = 0$; (ii) $\sigma_\beta = \infty$; and (iii) $0 < \sigma_\beta < \infty$. We note that $\sigma_\beta = 0$ is the solution obtained by solving the nonrobust continuous-time EC filtering problem (2.2.8). Case (ii) implies that there exists no output mask. Thus, it suffices to consider case (iii), i.e, σ_β is a bounded positive constant.

From (5.3.1), it follows that for, $0 < \sigma_\beta^1 \leq \sigma_\beta^2$,

$$\mathcal{F}_{\sigma_\beta^2}(\mathbf{x}) \neq \emptyset \Rightarrow \mathcal{F}_{\sigma_\beta^1}(\mathbf{x}) \neq \emptyset \quad \text{or} \quad \mathcal{F}_{\sigma_\beta^1}(\mathbf{x}) = \emptyset \Rightarrow \mathcal{F}_{\sigma_\beta^2}(\mathbf{x}) = \emptyset. \tag{C.3.1}$$

Thus, by using Steps 2 and 3 of Algorithm 5.3.2, we can find $\sigma_{\beta 0}$ and $\sigma_{\beta t}$ such that $\sigma_\beta^* \in [\sigma_{\beta 0}, \sigma_{\beta t}]$ in a finite number of steps.

By (C.3.1), it follows from Steps 4 – 6 of Algorithm 5.3.2 that, after k iterations, the interval of uncertainty is reduced to

$$\bar{\sigma}_{\beta t} - \bar{\sigma}_{\beta 0} \quad \leq \quad \lambda^k(\sigma_{\beta t} - \sigma_{\beta 0}) \tag{C.3.2}$$

where $\lambda \simeq 0.618$. If k is such that

$$\lambda^k(\sigma_{\beta t} - \sigma_{\beta 0}) \quad \leq \quad \gamma_1 \tag{C.3.3}$$

where γ_1 is a pre-assigned accuracy, then it follows from (C.3.2) and (C.3.3) that $\bar{\sigma}_{\beta t} - \bar{\sigma}_{\beta 0} \leq \gamma_1$. Since a finite positive integer k can be determined from (C.3.3), the golden section method can locate σ_β^* to the required interval $[\bar{\sigma}_{\beta 0}, \bar{\sigma}_{\beta t}]$ in a finite number of iterations. This completes the proof. ∎

C.4 Proof of Theorem 5.3.2

Since $\tilde{\mathbf{x}}_r^* = \mathbf{x}_r^* + \alpha_f \Delta\mathbf{x} \|\mathbf{x}_r^*\|_2$, the output response of the perturbed robust optimal filter coefficient vector $\tilde{\mathbf{x}}_r^*$ can be obtained from (5.3.6) as:

$$\begin{aligned} \psi_n(\tilde{\mathbf{x}}_r^*, t) &= \Theta'(t)\tilde{\mathbf{x}}_r^* = \Theta'(t)\left(\mathbf{x}_r^* + \alpha_f \Delta\mathbf{x}\|\mathbf{x}_r^*\|_2\right) \\ &= \psi_n(\mathbf{x}_r^*, t) + \alpha_f \psi_n(\Delta\mathbf{x}, t)\|\mathbf{x}_r^*\|_2, \quad t \in [0, \infty) \end{aligned} \tag{C.4.1}$$

where $\psi_n(\Delta\mathbf{x}, t) = \Theta'(t)\Delta\mathbf{x}$ is the output rresponse of the error vector due to error in the implementation of the optimal filter.

By the assumptions: $\|\Theta(t)\|_2 \leq C, t \in [0, \infty)$ and $\|\Delta\mathbf{x}\|_2 \leq \bar{\eta}$, and noting that $\mathbf{x}_r^*$ satisfies the constraints in the CRF problem (2.2.12), we obtain a bound for the perturbation term $\psi_n(\Delta\mathbf{x}, t)\|\mathbf{x}_r^*\|$ in (C.4.1) as:

$$|\psi_n(\Delta\mathbf{x}, t)|\|\mathbf{x}_r^*\|_2 \leq \|\Theta(t)\|_2 \|\Delta\mathbf{x}\|_2 \|\mathbf{x}_r^*\|_2 \leq M_{\mathbf{x}} \tag{C.4.2}$$

where $M_{\mathbf{x}} = \sqrt{(1+\delta)}C\bar{\eta}\|\mathbf{x}^*\|_2$ is a constant.

Combining with (C.4.2) and the weighted constraints in the CRF problem (2.2.12) at $\mathbf{x}_r^*$ and $\sigma_\beta(\mathbf{x}_r^*)$, we obtain the upper and lower bounds of the perturbed robust optimal output response

$$\varepsilon^-(t) + (\beta(t)\sigma_\beta(\mathbf{x}_r^*) - \alpha_f M_{\mathbf{x}}) \leq \psi_n(\tilde{\mathbf{x}}_r^*, t) \leq \varepsilon^+(t) - (\beta(t)\sigma_\beta(\mathbf{x}_r^*) - \alpha_f M_{\mathbf{x}}).$$

Choosing the scaling parameter $\alpha_f > 0$ sufficiently small such that

$$\beta(t)\sigma_\beta(\mathbf{x}_r^*) - \alpha_f M_{\mathbf{x}} \geq 0 \iff \alpha_f \leq \alpha_f^* = \frac{\beta^*\sigma_\beta(\mathbf{x}_r^*)}{M_{\mathbf{x}}}$$

where $\beta^* = \max_t[\beta(t)]$. Then, for any $0 < \alpha_f \leq \alpha_f^*$, we have

$$\begin{aligned} & \varepsilon^-(t) + (\beta(t)\sigma_\beta(\mathbf{x}_r^*) - \alpha_f M_{\mathbf{x}}) \leq \psi_n(\tilde{\mathbf{x}}_r^*, t) \leq \varepsilon^+(t) - (\beta(t)\sigma_\beta(\mathbf{x}_r^*) - \alpha_f M_{\mathbf{x}}) \\ \Longrightarrow \quad & \varepsilon^-(t) \leq \psi_n(\tilde{\mathbf{x}}_r^*, t) \leq \varepsilon^+(t). \end{aligned}$$

Thus, by the definition of the weighted constraint margin given by (5.3.8) with respect to the perturbed robust optimal filter coefficient vector, we obtain $\sigma_\beta(\mathbf{x}_r^*) \geq 0$. This means that the output response $\psi_n(\tilde{\mathbf{x}}_r^*, t)$ of the perturbed optimal filter remains in the original envelope constraints for any $t \in [0, \infty)$.

Next, we will show that the weighted constraint margin with respect to the perturbed nonrobust optimal filter coefficient vector is negative if the perturbation results due to error in the implementation of the nonrobust EC optimal filter u_n^*, i.e, $\sigma_\beta(\tilde{\mathbf{x}}^*) < 0$.

Similar to (C.4.1), if the perturbed nonrobust EC optimal filter coefficient vector $\tilde{\mathbf{x}}^*$, that results from the implementation error, is given by $\tilde{\mathbf{x}}^* = \mathbf{x}^* + \alpha_f \Delta\mathbf{x}\|\mathbf{x}^*\|_2$, then the corresponding output response is

$$\psi_n(\tilde{\mathbf{x}}^*, t) \quad = \quad \psi_n(\mathbf{x}^*, t) + \alpha_f \psi_n(\Delta\mathbf{x}, t)\|\mathbf{x}^*\|_2, \forall t \in [0, \infty). \tag{C.4.3}$$

Since $\|\Theta(t)\|_2 \leq C$ and $\|\Delta\mathbf{x}\|_2 \leq \bar{\eta}$, the perturbation term is bounded by

$$|\psi_n(\Delta\mathbf{x}, t)|\|\mathbf{x}^*\|_2 \leq \|\Theta(t)\|_2\|\Delta\mathbf{x}\|_2\|\mathbf{x}^*\|_2 \leq M_{\mathbf{x}} \tag{C.4.4}$$

Making use of (C.4.4) and the output constraints at the optimal solution $\mathbf{x}^*$ of the nonrobust EC filtering problem (2.2.8), the perturbed nonrobust optimal output response is bounded by

$$\varepsilon^-(t) - \alpha_f M_{\mathbf{x}} \leq \psi_n(\tilde{\mathbf{x}}^*, t) \leq \varepsilon^+(t) + \alpha_f M_{\mathbf{x}}. \tag{C.4.5}$$

Following the definition of the weighted constraint robustness margin given by (2.2.11), we have

$$\sigma_\beta(\tilde{\mathbf{x}}^*) = -\frac{\alpha_f M_{\mathbf{x}}}{\beta^*} < 0$$

i.e, the output response $\psi_n(\tilde{\mathbf{x}}^*, t)$ of $\tilde{\mathbf{x}}^*$ is outside the envelope constraints. ∎

C.5 Proof of Theorem 5.3.3

Combining the input signal $\tilde{s}(t) = s(t) + \alpha_s \Delta s(t) s^*, t \in [0, \infty)$ contaminated by perturbation with (5.3.10), we obtain

$$\begin{aligned}
\tilde{\theta}_j(t) &= \int_0^\infty \varphi_j(\tau)\tilde{s}(t-\tau)d\tau \\
&= \int_0^\infty \varphi_j(\tau)(s(t-\tau) + \alpha_s \Delta s(t-\tau)s^*)d\tau \\
&= \theta_j(t) + \alpha_s \Delta\theta_j(t)s^*, \quad t \in [0, \infty)
\end{aligned}$$

where $\Delta\theta_j(t)$ is given by

$$\Delta\theta_j(t) = \int_0^\infty \varphi_j(\tau)\Delta s(t-\tau)d\tau. \tag{C.5.1}$$

The output response (5.3.12) of the robust optimal filter coefficient vector to the perturbed input signal thus yields

$$\begin{aligned}
\tilde{\psi}_n(\mathbf{x}_\tau^*, t) &= (\Theta'(t) + \alpha_s \Delta\Theta'(t)s^*)\mathbf{x}_\tau^* \\
&= \psi_n(\mathbf{x}_\tau^*, t) + \alpha_s s^* \Delta\psi_n(\mathbf{x}_\tau^*, t)
\end{aligned}$$

where $\Delta\psi_n(\mathbf{x}_\tau^*, t) = \Delta\Theta'(t)\mathbf{x}_\tau^*$ is the perturbation term appeared in the output, while $\Delta\Theta'(t) = [\Delta\theta_0(t), \ldots, \Delta\theta_{n-1}(t)]$ is a vector of perturbation. Since the perturbation attached to the input signal is bounded, i.e, $|\Delta s(t)| \le \bar{\gamma}, t \in [0, \infty)$, it follows from (C.5.1) that

$$\begin{aligned}
|\Delta\theta_j(t)|^2 &= \left|\int_0^\infty \varphi_j(\tau)\Delta s(t-\tau)d\tau\right|^2 \le \int_0^\infty |\varphi_j(\tau)\Delta s(t-\tau)|^2 d\tau \\
&\le \int_0^\infty |\varphi_j(\tau)|^2 |\Delta s(t-\tau)|^2 d\tau \le \int_0^\infty |\varphi_j(\tau)|^2 \bar{\gamma}^2 d\tau \\
&= <\varphi_j, \varphi_j> \bar{\gamma}^2 = \bar{\gamma}^2.
\end{aligned} \tag{C.5.2}$$

By (C.5.2) and making use of the Cauchy-Schwarz inequality, we obtain the perturbation term appeared in the output response as follows

$$\begin{aligned}
|\Delta\psi_n(\mathbf{x}_\tau^*, t)| &= |\Delta\Theta'(t)\mathbf{x}_\tau^*| \le \|\Delta\Theta(t)\|_2 \|\mathbf{x}_\tau^*\|_2 \\
&= \sqrt{\sum_{j=0}^{n-1} |\Delta\theta_j(t)|^2} \|\mathbf{x}_\tau^*\|_2 \le M_s
\end{aligned} \tag{C.5.3}$$

where $M_s = \sqrt{n(1+\delta)}\bar{\gamma}\|\mathbf{x}^*\|_2$ is a constant.

Note that the output response $\psi_n(\mathbf{x}_\tau^*, t)$ of the robust EC optimal filter satisfies the weighted constraints in the CRF problem (2.2.12). Thus, it follows from (C.5.3) that

$$\begin{aligned}
&\varepsilon^-(t) + (\beta(t)\sigma_\beta(\mathbf{x}_\tau^*) - \alpha_s s^* M_s) \le \tilde{\psi}(\mathbf{x}_\tau^*, t) \le \varepsilon^+(t) - (\beta(t)\sigma_\beta(\mathbf{x}_\tau^*) - \alpha_s s^* M_s) \\
\Longrightarrow\ &\varepsilon^-(t) \le \tilde{\psi}(\mathbf{x}_\tau^*, t) \le \varepsilon^+(t).
\end{aligned}$$

The proofs of $\tilde{\sigma}_\beta(\mathbf{x}_\tau^*) \ge 0$ and $\tilde{\sigma}_\beta(\mathbf{x}^*) < 0$ are identical to those given for Theorem 5.3.2. ∎

Appendix D

Proofs of Results in Chapter 7

D.1 Proof of Theorem 7.3.1

Consider the following adaptive pulse scheme:

$$\begin{aligned}\tilde{\lambda}^{k+1} &= \tilde{\lambda}^k - \frac{h}{2}\mathbf{D}(\tilde{\lambda}^k)(\mathbf{A}+\tilde{\mathbf{N}}_1^k)(\mathbf{A}+\tilde{\mathbf{N}}_2^k)'\tilde{\lambda}^k + h\mathbf{D}(\tilde{\lambda}^k)\mathbf{b} \\ &= \tilde{\lambda}^k - h\mathbf{F}(\tilde{\lambda}^k) \qquad \text{(D.1.1)}\end{aligned}$$

where $\mathbf{F}(\tilde{\lambda}^k) = \mathbf{D}(\tilde{\lambda}^k)[\tilde{\mathbf{H}}^k\tilde{\lambda}^k + \mathbf{b}]$, while $\tilde{\mathbf{H}}^k = \frac{1}{2}(\mathbf{A}+\tilde{\mathbf{N}}_1^k)(\mathbf{A}+\tilde{\mathbf{N}}_2^k)'$, and $\tilde{\lambda}^k$ is independent of $\tilde{\mathbf{N}}_1^k$ and $\tilde{\mathbf{N}}_2^k$. Let $\mathbf{T}(\tilde{\lambda}) \triangleq [\mathbf{T}_1(\tilde{\lambda}),\ldots,\mathbf{T}_{2N}(\tilde{\lambda})]' \in \Re^{2N}$ be given by

$$\mathbf{T}(\tilde{\lambda}) \triangleq \tilde{\lambda} - h\mathbf{D}(\tilde{\lambda})[\tilde{\mathbf{H}}\tilde{\lambda} + \mathbf{b}].$$

We consider the *ith* component of the function $\mathbf{T}(\tilde{\lambda})$ as:

$$\mathbf{T}_i(\tilde{\lambda}) = \tilde{\lambda}_i - h\tilde{\lambda}_i(\tilde{\mathbf{H}}_{i,1}\tilde{\lambda}_1 + \ldots + \tilde{\mathbf{H}}_{i,2N}\tilde{\lambda}_{2N} + \mathbf{b}_i), \quad 1 \le i \le 2N.$$

where $\tilde{\mathbf{H}}_{i,j}$ represents the ijth element of the matrix $\tilde{\mathbf{H}}$.

Clearly, $\mathbf{T}_i(\tilde{\lambda})$ is a quadratic differentiable function of $\tilde{\lambda}$. Using the differentiability of $\mathbf{T}_i(\tilde{\lambda})$, we obtain

$$\begin{aligned}&\mathbf{T}_i(\tilde{\lambda}) = \tilde{\mathbf{T}}_i(\lambda^*) + \nabla\tilde{\mathbf{T}}_i'(\lambda^*)(\tilde{\lambda}-\lambda^*) - \frac{h}{2}\wp_i'(\lambda^*,\tilde{\lambda})(\tilde{\lambda}-\lambda^*) \\ \Rightarrow\ &\mathbf{T}_i(\tilde{\lambda}) = \lambda_i^* + \nabla\tilde{\mathbf{T}}_i'(\lambda^*)(\tilde{\lambda}-\lambda^*) - \frac{h}{2}\wp_i'(\lambda^*,\tilde{\lambda})(\tilde{\lambda}-\lambda^*) - h\lambda_i^*\left(\sum_{j=1}^{2N}\tilde{\mathbf{H}}_{i,j}^*\lambda_j^* + \mathbf{b}_i\right) \\ \Rightarrow\ &\mathbf{T}(\tilde{\lambda}) - \lambda^* = \nabla\tilde{\mathbf{T}}'(\lambda^*)(\tilde{\lambda}-\lambda^*) - \frac{h}{2}\wp'(\lambda^*,\tilde{\lambda})(\tilde{\lambda}-\lambda^*) - h\tilde{\mathbf{F}}(\lambda^*) \qquad \text{(D.1.2)}\end{aligned}$$

where

$$\tilde{\mathbf{T}}(\lambda^*) \triangleq [\tilde{\mathbf{T}}_1(\lambda^*),\ldots,\tilde{\mathbf{T}}_{2N}(\lambda^*)]' \in \Re^{2N}$$

$$
\begin{aligned}
\nabla\tilde{\mathbf{T}}(\lambda^*) &\triangleq [\nabla\tilde{\mathbf{T}}_1(\lambda^*),\ldots,\nabla\tilde{\mathbf{T}}_{2N}(\lambda^*)] \in \Re^{2N\times 2N} \\
\nabla\tilde{\mathbf{T}}_i(\lambda^*) &\triangleq [\nabla\tilde{\mathbf{T}}_{i1}(\Lambda^*),\ldots,\nabla\tilde{\mathbf{T}}_{i,2N}(\Lambda^*)]', \quad \forall i=1,\ldots,2N \\
\tilde{\mathbf{F}}(\lambda^*) &= \frac{1}{2}\mathbf{D}(\lambda^*)(\mathbf{A}+\tilde{\mathbf{N}}_1^*)(\mathbf{A}+\tilde{\mathbf{N}}_2^*)'\lambda^* + \mathbf{D}(\lambda^*)\mathbf{b} \\
\tilde{\wp} &\triangleq [\tilde{\wp}_1,\ldots,\tilde{\wp}_{2N}] \in \Re^{2N\times 2N},
\end{aligned}
$$

while $\tilde{\wp}_i \triangleq \tilde{\mathbf{P}}_i'(\tilde{\lambda}-\lambda^*) \in \Re^{2N\times 1}$ ($\tilde{\wp}$ and $\tilde{\wp}_i$ are used to denote $\wp(\lambda^*,\tilde{\lambda})$ and $\wp_i(\lambda^*,\tilde{\lambda})$, respectively). Here $\tilde{\mathbf{T}}_i(\lambda^*)$, $\nabla\tilde{\mathbf{T}}_{ij}(\Lambda^*), \forall j=1,\ldots,2N$, and $\tilde{\mathbf{P}}_i, \forall i=1,\ldots 2N$, are given, respectively, by

$$
\begin{aligned}
\tilde{\mathbf{T}}_i(\lambda^*) &= \lambda_i^* - h\lambda_i^*\left(\sum_{j=1}^{2N}\tilde{\mathbf{H}}_{i,j}^*\lambda_j^* + \mathbf{b}_i\right) \\
\nabla\tilde{\mathbf{T}}_{ij}(\lambda^*) &= \begin{cases} -h\tilde{\mathbf{H}}_{i,1}\lambda_i^*, & \text{if } i\neq j \\ 1-h\left(\sum_{j=1}^{2m}\tilde{\mathbf{H}}_{i,j}\lambda_j^* + \tilde{\mathbf{H}}_{i,i}\lambda_i^* + \mathbf{b}_i\right), & \text{if } i=j \end{cases}
\end{aligned} \tag{D.1.3}
$$

$$
\tilde{\mathbf{P}}_i = \begin{bmatrix}
0 & \ldots & 0 & \tilde{\mathbf{H}}_{i,1} & 0 & \ldots & 0 \\
\vdots & & \vdots & \vdots & \vdots & & \vdots \\
0 & \ldots & 0 & \tilde{\mathbf{H}}_{i,i-1} & 0 & \ldots & 0 \\
\tilde{\mathbf{H}}_{i,1} & \ldots & \tilde{\mathbf{H}}_{i,i-1} & 2\tilde{\mathbf{H}}_{i,i} & \tilde{\mathbf{H}}_{i,i+1} & \ldots & \tilde{\mathbf{H}}_{i,2N} \\
0 & \ldots & 0 & \tilde{\mathbf{H}}_{i,i+1} & 0 & \ldots & 0 \\
\vdots & & \vdots & \vdots & \vdots & & \vdots \\
0 & \ldots & 0 & \tilde{\mathbf{H}}_{i,2N} & 0 & \ldots & 0
\end{bmatrix} \tag{D.1.4}
$$

Let $\mathbf{e}^k \triangleq \tilde{\lambda}^k - \lambda^*$ be the kth error vector about λ^*. Since λ^* is deterministic, we have

$$
\begin{aligned}
E[\tilde{\mathbf{F}}(\lambda^*)] &= E[\mathbf{D}(\lambda^*)(\tilde{\mathbf{H}}^*\lambda^* + \mathbf{b})] = \mathbf{D}(\lambda^*)[E[\tilde{\mathbf{H}}^*]\lambda^* + \mathbf{b}] \\
&= \mathbf{F}(\lambda^*) = 0_{2N}.
\end{aligned} \tag{D.1.5}
$$

We now take the expectations of (D.1.2) with $\tilde{\lambda} = \tilde{\lambda}^k$, where the sequence $\{\tilde{\lambda}^k\}$ is generated by the adaptive training scheme (D.1.1) with $\mathbf{e}^0 = \lambda^0 - \lambda^* \in N_\delta = \left\{\mathbf{e}^0 \in \Re^{2N} : \|\mathbf{e}^0\| \leq \delta\right\}$, while δ is an appropriate positive constant.

By the fact that $\mathbf{e}^k$ is independent of the matrix $\nabla\tilde{\mathbf{T}}(\lambda^*)$, we obtain

$$
\begin{aligned}
\|E[\tilde{\mathbf{T}}(\tilde{\lambda}^k) - \lambda^*]\|_2 &= \|E[\nabla\tilde{\mathbf{T}}'(\lambda^*)]E[\mathbf{e}^k] - \frac{h}{2}E[\wp'(\lambda^*,\tilde{\lambda}^k)\mathbf{e}^k] - hE[\tilde{\mathbf{F}}(\lambda^*)]\|_2 \\
&\leq \|\nabla\mathbf{T}'(\lambda^*)E[\mathbf{e}^k]\|_2 + \frac{h}{2}\|E[\wp'(\lambda^*,\tilde{\lambda}^k)\mathbf{e}^k]\|_2 \\
&\leq \|\nabla\mathbf{T}(\lambda^*)\|_2\|E[\mathbf{e}^k]\|_2 + \frac{h}{2}\|E[\wp'(\lambda^*,\tilde{\lambda}^k)\mathbf{e}^k]\|_2
\end{aligned} \tag{D.1.6}
$$

where $\nabla\mathbf{T}'(\lambda^*) = E[\nabla\tilde{\mathbf{T}}'(\lambda^*)]$. We note from Theorem 4.4.1 that the step-size h satisfying $0 < h < \frac{2}{\eta_{max}}$ can be chosen such that the spectral norm of the matrix $\nabla\mathbf{T}(\lambda^*)$ is less than

one, i.e, $\|\nabla \mathbf{T}(\lambda^*)\|_2 = \rho < 1$, where ρ is the spectral radius of $\nabla \mathbf{T}(\lambda^*)$ and η_{max} is the largest eigenvalue of the Jacobian matrix $\nabla \mathbf{F}(\lambda^*)$.

Let $\mathbf{T}(\tilde{\lambda}^k) - \lambda^* \triangleq \mathbf{e}^{k+1}$. Accordingly, (D.1.6) may be written as:

$$\|E[\mathbf{e}^{k+1}]\|_2 \leq \rho \|E[\mathbf{e}^k]\|_2 + \frac{h}{2}\|E[\wp'(\lambda^*, \tilde{\lambda}^k)\mathbf{e}^k]\|_2. \tag{D.1.7}$$

Thus, the square norm of the second term of (D.1.7) can be expanded as:

$$\begin{aligned} \|E[\wp'(\lambda^*, \tilde{\lambda}^k)\mathbf{e}^k]\|_2^2 &= \frac{1}{4}\left\| \begin{bmatrix} E\left[\mathbf{e}^{k'}\widehat{\mathbf{P}}_1\mathbf{e}^k\right] \\ \vdots \\ E\left[\mathbf{e}^{k'}\widehat{\mathbf{P}}_{2N}\mathbf{e}^k\right] \end{bmatrix} \right\|_2^2 = \frac{1}{4}\sum_{i=1}^{2N} |E[\mathbf{e}^{k'}\widehat{\mathbf{P}}_i\mathbf{e}^k]|_2^2 \\ &\leq \frac{1}{4}\sum_{i=1}^{2N} \|\widehat{\mathbf{P}}_i\|_2^2 (E[\|\mathbf{e}^k\|_2^2])^2 = M(E[\|\mathbf{e}^k\|_2^2])^2 \end{aligned} \tag{D.1.8}$$

where the constant $M = \frac{1}{4}\sum_{i=1}^{2N} \|\widehat{\mathbf{P}}_i\|_2^2$ and the $2N \times 2N$ matrix $\widehat{\mathbf{P}}_i$ is given by

$$\widehat{\mathbf{P}}_i = \begin{bmatrix} 0 & \dots & 0 & \mathbf{A}_i\mathbf{A}_1' & 0 & \dots & 0 \\ \vdots & & \vdots & \vdots & \vdots & & \vdots \\ 0 & \dots & 0 & \mathbf{A}_i\mathbf{A}_{i-1}' & 0 & \dots & 0 \\ \mathbf{A}_i\mathbf{A}_1' & \dots & \mathbf{A}_i\mathbf{A}_{i-1}' & 2\mathbf{A}_i\mathbf{A}_i' & \mathbf{A}_i\mathbf{A}_{i+1}' & \dots & \mathbf{A}_i\mathbf{A}_{2N}' \\ 0 & \dots & 0 & \mathbf{A}_i\mathbf{A}_{i+1}' & 0 & \dots & 0 \\ \vdots & & \vdots & \vdots & \vdots & & \vdots \\ 0 & \dots & 0 & \mathbf{A}_i\mathbf{A}_{2N}' & 0 & \dots & 0 \end{bmatrix}.$$

Note that the matrix $\widetilde{\mathbf{H}}^k = \frac{1}{2}(\mathbf{A} + \widetilde{\mathbf{N}}_1^k)(\mathbf{A} + \widetilde{\mathbf{N}}_2^k)'$. Furthermore, $\tilde{\lambda}^k$ and hence $\mathbf{e}^k$ is independent of the input noisy matrices $\widetilde{\mathbf{N}}_1^k$ and $\widetilde{\mathbf{N}}_2^k$, while $\widetilde{\mathbf{N}}_1^k$ and $\widetilde{\mathbf{N}}_2^k$, both with zero mean, are also independent with one another. Thus, it is easy to show that $E[\widetilde{\mathbf{H}}_{i,j}^k] = \frac{1}{2}\mathbf{A}_i\mathbf{A}_j'$, where $\mathbf{A}_i$ represents the ith row of the matrix $\mathbf{A}$.

Take the square norm of (D.1.7). Then, by (D.1.8), we obtain

$$\begin{aligned} \|E[\mathbf{e}^{k+1}]\|_2^2 &\leq \rho^2\|E[\mathbf{e}^k]\|_2^2 + h\rho\|E[\mathbf{e}^k]\|_2\|E[\wp'(\lambda^*, \tilde{\lambda}^k)\mathbf{e}^k]\|_2 + \frac{h^2}{4}\|E[\wp'(\lambda^*, \tilde{\lambda}^k)\mathbf{e}^k]\|_2^2 \\ &\leq \rho^2\|E[\mathbf{e}^k]\|_2^2 + h\rho\sqrt{M}\|E[\mathbf{e}^k]\|_2 E[\|\mathbf{e}^k\|_2^2] + \frac{h^2}{4}M(E[\|\mathbf{e}^k\|_2^2])^2 \\ &\leq \rho^2\|E[\mathbf{e}^k]\|_2^2 + h\rho\sqrt{M}(E[\|\mathbf{e}^k\|_2^2])^{\frac{3}{2}} + \frac{h^2}{4}M(E[\|\mathbf{e}^k\|_2^2])^2 \\ &= \rho^2\|E[\mathbf{e}^k]\|_2^2 + hf(\mathbf{e}^k) \end{aligned} \tag{D.1.9}$$

where the function $f : \Re^{2N} \longrightarrow \Re$ is defined by

$$f(\mathbf{e}^k) = \frac{h}{4}M(E[\|\mathbf{e}^k\|_2^2])^2 + \rho\sqrt{M}(E[\|\mathbf{e}^k\|_2^2])^{\frac{3}{2}}.$$

Clearly, for each k,

$$\lim_{E[\|\mathbf{e}^k\|_2^2]\to 0} \frac{f(\mathbf{e}^k)}{E[\|\mathbf{e}^k\|_2^2]} = 0$$

Thus, for any $\epsilon > 0$, there exists a $\delta = \delta(\epsilon)$ such that, for each k,

$$\frac{f(\mathbf{e}^k)}{E[\|\mathbf{e}^k\|_2^2]} < \epsilon \quad \text{for} \quad E[\|\mathbf{e}^k\|_2^2] < \delta. \tag{D.1.10}$$

Combining (D.1.10) with (D.1.9) yields

$$\|E[\mathbf{e}^{k+1}]\|_2^2 < \rho^2 \|E[\mathbf{e}^k]\|_2^2 + h\epsilon\delta. \tag{D.1.11}$$

Since both $\epsilon > 0$ and $0 < h < \frac{2}{\eta_{max}}$ can be chosen arbitrarily small, it follows from the strict inequality (D.1.11) that

$$\|E[\mathbf{e}^{k+1}]\|_2^2 \leq \rho^2 \|E[\mathbf{e}^k]\|_2^2. \tag{D.1.12}$$

From (D.1.10), we have $\|E[\mathbf{e}^k]\|_2^2 \leq E[\|\mathbf{e}^k\|_2^2] < \delta$. By (D.1.12) and the fact that $\rho < 1$, we obtain $\|E[\mathbf{e}^{k+1}]\|_2^2 < \rho^2\delta < \delta$. Thus,

$$\|E[\mathbf{e}^{k+1}]\|_2^2 \leq \rho^{2(k+1)} \|E[\mathbf{e}^0]\|_2^2 \iff \lim_{k\to\infty} \|E[\mathbf{e}^k]\|_2^2 = 0. \tag{D.1.13}$$

Furthermore, since

$$E[\tilde{\mathbf{u}}^k|\tilde{\lambda}^k] - \mathbf{u}^* = -\frac{1}{2}\mathbf{A}'\mathbf{e}^k,$$

it is easily shown by using (D.1.13) that

$$\lim_{k\to\infty} \|E[\tilde{\mathbf{u}}^k] - \mathbf{u}^*\|_2^2 \leq \frac{1}{4}\|\mathbf{A}\|_2^2 \lim_{k\to\infty} \|E[\mathbf{e}^k]\|_2^2 \iff \lim_{k\to\infty} \|E[\tilde{\mathbf{u}}^k] - \mathbf{u}^*\|_2^2 = 0.$$

The proof is complete. ∎

D.2 Proof of Theorem 7.3.2

Consider the adaptive pulse scheme (D.1.1). Let $\mathbf{e}^k \triangleq \tilde{\lambda}^k - \lambda^*$ be the *kth* error vector about λ^*. Then, it follows from (D.1.2) that

$$\mathbf{e}^{k+1} = \nabla\tilde{\mathbf{T}}'(\lambda^*)\mathbf{e}^k - \frac{h}{2}\wp'(\lambda^*, \tilde{\lambda}^k)e^k - h\tilde{\mathbf{F}}(\lambda^*) \tag{D.2.1}$$

where the matrices $\nabla\tilde{\mathbf{T}}'(\lambda^*)$, $\wp'(\lambda^*, \tilde{\lambda}^k)$ and $\tilde{\mathbf{F}}(\lambda^*)$ are defined in the proof of Theorem 7.3.1.

Taking the square-norm and the mathematical expectations on both sides of (D.2.1), we obtain

$$
\begin{aligned}
& E[\|\mathbf{e}^{k+1}\|_2^2] = E[\|\nabla\tilde{\mathbf{T}}'(\lambda^*)\mathbf{e}^k - \frac{h}{2}\wp'(\lambda^*,\tilde{\lambda}^k)\mathbf{e}^k - h\tilde{\mathbf{F}}(\lambda^*)\|_2^2] \\
= \; & E[\|\nabla\tilde{\mathbf{T}}'(\lambda^*)\mathbf{e}^k\|_2^2] + \frac{h^2}{4}E[\|\wp'(\lambda^*,\tilde{\lambda}^k)\mathbf{e}^k\|_2^2] + h^2E[\|\tilde{\mathbf{F}}(\lambda^*)\|_2^2] \\
& -hE[\mathbf{e}^{k'}\nabla\tilde{\mathbf{T}}(\lambda^*)\wp'(\lambda^*,\tilde{\lambda}^k)\mathbf{e}^k] - 2hE[\mathbf{e}^{k'}\nabla\tilde{\mathbf{T}}(\lambda^*)\tilde{\mathbf{F}}(\lambda^*)] + h^2E[\tilde{\mathbf{F}}'(\lambda^*)\wp'(\lambda^*,\tilde{\lambda}^k)\mathbf{e}^k] \\
\leq \; & E[\|\nabla\tilde{\mathbf{T}}'(\lambda^*)\mathbf{e}^k\|_2^2] + \frac{h^2}{4}E[\|\wp'(\lambda^*,\tilde{\lambda}^k)\mathbf{e}^k\|_2^2] + h|E[\mathbf{e}^{k'}\nabla\tilde{\mathbf{T}}(\lambda^*)\wp'(\lambda^*,\tilde{\lambda}^k)\mathbf{e}^k]| \\
& +h^2E[\|\tilde{\mathbf{F}}(\lambda^*)\|_2^2] + 2h|E[\mathbf{e}^{k'}\nabla\tilde{\mathbf{T}}(\lambda^*)\tilde{\mathbf{F}}(\lambda^*)]| + h^2|E[\tilde{\mathbf{F}}'(\lambda^*)\wp'(\lambda^*,\tilde{\lambda}^k)\mathbf{e}^k]| \qquad \text{(D.2.2)}
\end{aligned}
$$

where $E[\|\mathbf{e}^k\|_2^2]$ is the variance of the adaptive weighting vector about λ^*.

Let us investigate each term on the right-hand side of (D.2.2). For the first-term, it follows from properties of the conditional expectation, the Cauchy-Schwarz inequality, and the fact that the matrix $\nabla\mathbf{T}(\lambda^*)$ is independent of $\tilde{\lambda}^k$ that

$$
\begin{aligned}
& E[\|\nabla\tilde{\mathbf{T}}'(\lambda^*)\mathbf{e}^k\|_2^2] = E[\mathbf{e}^{k'}\nabla\tilde{\mathbf{T}}(\lambda^*)\nabla\tilde{\mathbf{T}}'(\lambda^*)\mathbf{e}^k] \\
= \; & E[\mathbf{e}^{k'}E[\nabla\tilde{\mathbf{T}}(\lambda^*)\nabla\tilde{\mathbf{T}}'(\lambda^*)|\tilde{\lambda}^k]\mathbf{e}^k] \leq q(h)E[\|\mathbf{e}^k\|_2^2], \qquad \text{(D.2.3)}
\end{aligned}
$$

where $q(h)$ is a function of h and is given by

$$
\begin{aligned}
& q(h) = \|E[\nabla\tilde{\mathbf{T}}(\lambda^*)\nabla\tilde{\mathbf{T}}'(\lambda^*)]\|_2 \\
= \; & \|E[\{\mathbf{I} - h\nabla\tilde{\mathbf{F}}(\lambda^*)\}\{\mathbf{I} - h\nabla\tilde{\mathbf{F}}'(\lambda^*)\}]\|_2 \\
= \; & \|\mathbf{I} - hE[\nabla\tilde{\mathbf{F}}(\lambda^*)] - hE[\nabla\tilde{\mathbf{F}}'(\lambda^*)] + h^2E[\nabla\tilde{\mathbf{F}}(\lambda^*)\nabla\tilde{\mathbf{F}}'(\lambda^*)]\|_2 \\
\leq \; & \|\mathbf{I} - 2h\nabla\mathbf{F}(\lambda^*)\|_2 + h^2E[\|\nabla\tilde{\mathbf{F}}(\lambda^*)\|_2^2] \\
= \; & 1 - 2h\eta_{min} + h^2E[\|\nabla\tilde{\mathbf{F}}(\lambda^*)\|_2^2] = \widehat{q}(h), \qquad \text{(D.2.4)}
\end{aligned}
$$

while η_{min} is the smallest eigenvalue of the Jacobian matrix $\nabla\mathbf{F}(\lambda^*)$, the matrics $\nabla\tilde{\mathbf{T}}(\lambda^*)$ and $E[\nabla\tilde{\mathbf{F}}(\lambda^*)]$ are, respectively, given by

$$
\begin{aligned}
\nabla\tilde{\mathbf{T}}(\lambda^*) &= \mathbf{I} - h\nabla\tilde{\mathbf{F}}(\lambda^*) \\
E[\nabla\tilde{\mathbf{F}}(\lambda^*)] &= \nabla\mathbf{F}(\lambda^*) = \mathbf{D}(\frac{1}{2}\mathbf{A}\mathbf{A}'\lambda^* + \mathbf{b}) + \frac{1}{2}\mathbf{D}(\lambda^*)\mathbf{A}\mathbf{A}'.
\end{aligned}
$$

Here, all matrix norms are to be understood as the spectral norm, $\eta_{min} > 0$ denotes the smallest eigenvalue of the Jacobian matrix $\nabla\mathbf{F}(\lambda^*)$, and $E[\|\nabla\tilde{\mathbf{F}}(\lambda^*)\|_2^2] = \Theta(\sigma)$ is a function of σ, where $\Theta(\sigma) = \Theta_1(\sigma) + \Theta_2(\sigma) + \Theta_3(\sigma) + \Theta_4(\sigma)$, while

$$
\begin{aligned}
& \Theta_1(\sigma) = E[\|\mathbf{D}(\tilde{\mathbf{H}}^*\lambda^* + \mathbf{b})\|_2^2] \leq 2E[\|\mathbf{D}(\tilde{\mathbf{H}}^*\lambda^*)\|_2^2] + 2\|\mathbf{D}(\mathbf{b})\|_2^2 \\
= \; & \frac{1}{2}\left\{\|\mathbf{D}(\mathbf{A}\mathbf{A}'\lambda^*)\|_2^2 + E[\|\mathbf{D}(\mathbf{A}\tilde{\mathbf{N}}_2^{*'}\lambda^*)\|_2^2] + E[\|\mathbf{D}(\tilde{\mathbf{N}}_1^*\mathbf{A}'\lambda^*)\|_2^2]\right\}
\end{aligned}
$$

$$
\begin{aligned}
&+\frac{1}{2}E[\|\mathbf{D}(\tilde{\mathbf{N}}_1^*\tilde{\mathbf{N}}_2^{*\prime}\lambda^*)\|_2^2] + 2\|\mathbf{D}(\mathbf{b})\|_2^2 \\
\leq\ & \frac{1}{2}\left\{\|\mathbf{D}(\mathbf{A}\mathbf{A}'\lambda^*)\|_2^2 + n^2\sigma^2\|\lambda^*\|_2^2(2\|\mathbf{A}\|_2^2 + n^2\sigma^2)\right\} + 2\|\mathbf{D}(\mathbf{b})\|_2^2, \\
&\Theta_2(\sigma) = \Theta_3(\sigma) = \|E[\mathbf{D}(\mathbf{H}^*\lambda^* + \mathbf{b})\mathbf{D}(\lambda^*)\tilde{\mathbf{H}}^*]\|_2 \\
\leq\ & \sqrt{E[\|\mathbf{D}(\tilde{\mathbf{H}}^*\lambda^* + \mathbf{b})\|_2^2]}\sqrt{E[\|\mathbf{D}(\lambda^*)\tilde{\mathbf{H}}^*\|_2^2]} \\
\leq\ & \sqrt{\Theta_1(\sigma)}\|\mathbf{D}(\lambda^*)\|_2\sqrt{E[\|\tilde{\mathbf{H}}^*\|_2^2]} \\
\leq\ & \frac{1}{2}\sqrt{\Theta_1(\sigma)}\|\mathbf{D}(\lambda^*)\|_2(\|\mathbf{A}\|_2^2 + n^2\sigma^2), \\
\Theta_4(\sigma) \ =\ & E[\|\mathbf{D}(\lambda^*)\tilde{\mathbf{H}}^*\|_2^2] \leq \|\mathbf{D}(\lambda^*)\|_2^2 E[\|\tilde{\mathbf{H}}^*\|_2^2] \\
\leq\ & \frac{1}{4}\|\mathbf{D}(\lambda^*)\|_2^2(\|\mathbf{A}\|_2^2 + n^2\sigma^2)^2.
\end{aligned}
$$

These inequalities are obtained because

$$
\begin{aligned}
E[\|\tilde{\mathbf{N}}_1^*\|_2^2] \ &=\ E[\|\tilde{\mathbf{N}}_2^*\|_2^2] \leq n^2\sigma^2 \\
E[\|\tilde{\mathbf{H}}^*\|_2^2] \ &\leq\ \frac{1}{4}(\|\mathbf{A}\|_2^2 + n^2\sigma^2).
\end{aligned}
$$

For the second-term, it follows from the fact that the matrix $\tilde{\mathbf{P}}_i^k$ is independent of $\tilde{\lambda}^k$ (and hence $\mathbf{e}^k$) that

$$
\begin{aligned}
E[\|\wp'(\lambda^*, \tilde{\lambda}^k)\mathbf{e}^k\|_2^2] \ &=\ E\left[\left\|\begin{bmatrix} \mathbf{e}^{k\prime}\tilde{\mathbf{P}}_1^k\mathbf{e}^k \\ \vdots \\ \mathbf{e}^{k\prime}\tilde{\mathbf{P}}_{2N}^k\mathbf{e}^k \end{bmatrix}\right\|_2^2\right] = \sum_{i=1}^{2N} E[|\mathbf{e}^{k\prime}\tilde{\mathbf{P}}_i^k\mathbf{e}^k|^2] \\
&\leq\ \sum_{i=1}^{2N} E[\|\tilde{\mathbf{P}}_i^k\|_2^2\|\mathbf{e}^k\|_2^4] = \sum_{i=1}^{2N} E[\|\tilde{\mathbf{P}}_i^k\|_2^2]E[\|\mathbf{e}^k\|_2^4] \\
&=\ \mathcal{C}_1 E[\|\mathbf{e}^k\|_2^4] \qquad \text{(D.2.5)}
\end{aligned}
$$

where $\mathcal{C}_1 = \sum_{i=1}^{2N} E[\|\tilde{\mathbf{P}}_i^k\|_2^2]$ is a constant term. By the assumption: $E[\|\mathbf{e}^k\|_2^4] \leq \ell(E[\|\mathbf{e}^k\|_2^2])^2$, (D.2.5) is reduced to

$$
E[\|\wp'(\lambda^*, \tilde{\lambda}^k)\mathbf{e}^k\|_2^2] \ \leq\ \mathcal{C}_1\ell(E[\|\mathbf{e}^k\|_2^2])^2 \qquad \text{(D.2.6)}
$$

For the third-term, since $\mathbf{F}(\lambda^*) = \mathbf{D}(\lambda^*)(\frac{1}{2}\mathbf{A}\mathbf{A}'\lambda^* + \mathbf{b}) = 0_{2N}$, and the input noisy matrices $\tilde{\mathbf{N}}_1^*$ and $\tilde{\mathbf{N}}_2^*$ are uncorrelated with one another, we have

$$
\begin{aligned}
E[\|\tilde{\mathbf{F}}(\lambda^*)\|_2^2] \ &=\ \frac{1}{4}E[\|\mathbf{D}(\lambda^*)(\mathbf{A}\tilde{\mathbf{N}}_2^{*\prime}\lambda^* + \tilde{\mathbf{N}}_1^*(\mathbf{A} + \tilde{\mathbf{N}}_2^*)')\|_2^2] \\
&\leq\ \frac{1}{4}\|\mathbf{D}(\lambda^*)\|_2^2 E[\|\mathbf{A}\tilde{\mathbf{N}}_2^{*\prime}\lambda^* + \tilde{\mathbf{N}}_1^*(\mathbf{A} + \tilde{\mathbf{N}}_2^*)'\|_2^2] \\
&\leq\ \frac{1}{4}n^2\sigma^2\|\mathbf{D}(\lambda^*)\|_2^2\|\lambda^*\|_2^2(2\|\mathbf{A}\|_2^2 + n^2\sigma^2) = \tilde{\gamma}^*(\sigma) \qquad \text{(D.2.7)}
\end{aligned}
$$

For the fourth-term, we note that the matrices $\nabla\tilde{\mathbf{T}}(\lambda^*)$ and $\wp'(\lambda^*, \tilde{\lambda}^k)$ are mutually independent. Thus,

$$\begin{aligned} E[\mathbf{e}^{k'}\nabla\tilde{\mathbf{T}}(\lambda^*)\wp'(\lambda^*,\tilde{\lambda}^k)\mathbf{e}^k] &= E[\mathbf{e}^{k'}E[\nabla\tilde{\mathbf{T}}(\lambda^*)\wp'(\lambda^*,\tilde{\lambda}^k)\mathbf{e}^k|\tilde{\lambda}^k]] \\ &= E[\mathbf{e}^{k'}E[\nabla\tilde{\mathbf{T}}(\lambda^*)]E[\wp'(\lambda^*,\tilde{\lambda}^k)\mathbf{e}^k|\tilde{\lambda}^k]]. \end{aligned}$$

Applying the Cauchy-Schwarz inequality yields

$$\begin{aligned} |E[\mathbf{e}^{k'}\nabla\tilde{\mathbf{T}}(\lambda^*)\wp'(\lambda^*,\tilde{\lambda}^k)\mathbf{e}^k]| &\leq E[\|\mathbf{e}^k\|_2\|E[\nabla\tilde{\mathbf{T}}(\lambda^*)]\|_2\|E[\wp'(\lambda^*,\tilde{\lambda}^k)\mathbf{e}^k|\tilde{\lambda}^k]\|_2] \\ &= (1-h\eta_{min})E[\|\mathbf{e}^k\|_2\|E[\wp'(\lambda^*,\tilde{\lambda}^k)\mathbf{e}^k|\tilde{\lambda}^k]\|_2] \qquad \text{(D.2.8)} \end{aligned}$$

where $\|E[\nabla\tilde{\mathbf{T}}(\lambda^*)]\|_2 = \|\mathbf{I}-h\nabla\mathbf{F}(\lambda^*)\|_2 = 1-h\eta_{min}$ for $0 < h < \frac{2}{\eta_{max}}$, η_{max} and η_{min} are, respectively, the largest and the smallest eigenvalues of $\nabla\mathbf{F}(\lambda^*)$.

Since the matrix $\tilde{\mathbf{P}}_i^k$ is independent of $\tilde{\lambda}^k$ (and hence $\mathbf{e}^k$), it follows that

$$\begin{aligned} \|E[\wp'(\lambda^*,\tilde{\lambda}^k)\mathbf{e}^k|\tilde{\lambda}^k]\|_2 &= \sqrt{\sum_{i=1}^{2N}|E[\mathbf{e}^{k'}\tilde{\mathbf{P}}_i^k\mathbf{e}^k|\tilde{\lambda}^k]|^2} = \sqrt{\sum_{i=1}^{2N}|\mathbf{e}^{k'}E[\tilde{\mathbf{P}}_i^k]\mathbf{e}^k|^2} \\ &\leq \sqrt{\sum_{i=1}^{2N}\|\mathbf{e}^k\|_2^4\|E[\tilde{\mathbf{P}}_i^k]\|_2^2} \leq \sqrt{C_1}\|\mathbf{e}^k\|_2^2 \qquad \text{(D.2.9)} \end{aligned}$$

Combining (D.2.9) and (D.2.8), we obtain

$$|E[\mathbf{e}^{k'}\nabla\tilde{\mathbf{T}}(\lambda^*)\wp'(\lambda^*,\tilde{\lambda}^k)\mathbf{e}^k]| \leq \sqrt{C_1}(1-h\eta_{min})E[\|\mathbf{e}^k\|_2^3]. \qquad \text{(D.2.10)}$$

To analyze $E[\|\mathbf{e}^k\|_2^3]$, we make use of the Cauchy-Schwarz inequality again. This leads to

$$\begin{aligned} E[\|\mathbf{e}^k\|_2^3] &= E[\|\mathbf{e}^k\|_2\|\mathbf{e}^k\|_2^2] \leq \sqrt{E[\|\mathbf{e}^k\|_2^2]}\sqrt{E[\|\mathbf{e}^k\|_2^4]} \\ &\leq \sqrt{\ell}(E[\|\mathbf{e}^k\|_2^2])^{\frac{3}{2}} \qquad \text{(D.2.11)} \end{aligned}$$

Combining (D.2.11) with (D.2.10), we obtain the following inequality for the fourth-term

$$|E[\mathbf{e}^{k'}\nabla\tilde{\mathbf{T}}(\lambda^*)\wp'(\lambda^*,\tilde{\lambda}^k)\mathbf{e}^k]| \leq \sqrt{C_1\ell}(1-h\eta_{min})(E[\|\mathbf{e}^k\|_2^2])^{\frac{3}{2}}. \qquad \text{(D.2.12)}$$

Similarly, we can show that the fifth-term yields

$$\begin{aligned} |E[\mathbf{e}^{k'}\nabla\tilde{\mathbf{T}}(\lambda^*)\tilde{\mathbf{F}}(\lambda^*)]| &= |E[\mathbf{e}^{k'}]E[\nabla\tilde{\mathbf{T}}(\lambda^*)\tilde{\mathbf{F}}(\lambda^*)]| \leq \|E[\mathbf{e}^k]\|_2\|E[\nabla\tilde{\mathbf{T}}(\lambda^*)\tilde{\mathbf{F}}(\lambda^*)]\|_2 \\ &\leq \sqrt{E[\|\mathbf{e}^k\|^2]}\|E[\nabla\tilde{\mathbf{T}}(\lambda^*)\tilde{\mathbf{F}}(\lambda^*)]\|_2. \end{aligned}$$

Moreover, since $E[\tilde{\mathbf{F}}(\lambda^*)] = \mathbf{F}(\lambda^*) = 0$, we obtain

$$\begin{aligned} \|E[\nabla\tilde{\mathbf{T}}(\lambda^*)\tilde{\mathbf{F}}(\lambda^*)]\|_2 &= \|E\{(\mathbf{I}-h\nabla\tilde{\mathbf{F}}(\lambda^*))\tilde{\mathbf{F}}(\lambda^*)\}\|_2 \\ &= \|E[\tilde{\mathbf{F}}(\lambda^*)] - hE[\nabla\tilde{\mathbf{F}}(\lambda^*)\tilde{\mathbf{F}}(\lambda^*)]\|_2 \\ &\leq h\|E[\nabla\tilde{\mathbf{F}}(\lambda^*)\tilde{\mathbf{F}}(\lambda^*)]\|_2 = hC_2(\sigma) \end{aligned}$$

where, by (D.2.7), we obtain the following inequalities for the constant term $C_2(\sigma)$:

$$\begin{aligned} C_2(\sigma) &= \|E[\nabla\widetilde{\mathbf{F}}(\lambda^*)\widetilde{\mathbf{F}}(\lambda^*)]\|_2 \leq \sqrt{E[\|\nabla\widetilde{\mathbf{F}}(\lambda^*)\|_2^2]}\sqrt{E[\|\widetilde{\mathbf{F}}(\lambda^*)\|_2^2]} \\ &\leq \sqrt{\Theta(\sigma)}\sqrt{\widehat{\gamma}^*(\sigma)}, \end{aligned}$$

while $E[\|\nabla\widetilde{\mathbf{F}}(\lambda^*)\|_2^2] = \Theta(\sigma)$. Thus, the fifth-term is reduced to

$$|E[\mathbf{e}^{k'}\nabla\widetilde{\mathbf{T}}(\lambda^*)\widetilde{\mathbf{F}}(\lambda^*)]| \leq hC_2(\sigma)\sqrt{E[\|\mathbf{e}^k\|_2^2]}. \tag{D.2.13}$$

For the last term, we note that the matrix $\widetilde{\mathbf{F}}(\lambda^*)$ is independent of $\mathbf{e}^k$ and that $E[\widetilde{\mathbf{F}}(\lambda^*)] = 0$. Thus,

$$E[\widetilde{\mathbf{F}}'(\lambda^*)\wp'(\lambda^*, \tilde{\lambda}^k)\mathbf{e}^k] = E[\widetilde{\mathbf{F}}'(\lambda^*)]E[\wp'(\lambda^*, \tilde{\lambda}^k)\mathbf{e}^k] = 0. \tag{D.2.14}$$

Combining (D.2.3)-(D.2.14) with (D.2.2) yields

$$\begin{aligned} E[\|\mathbf{e}^{k+1}\|_2^2] &\leq \widehat{q}(h)E[\|\mathbf{e}^k\|_2^2] + \frac{h^2}{4}C_1\ell(E[\|\mathbf{e}^k\|_2^2])^2 + h\sqrt{C_1\ell}(1-h\eta_{min})(E[\|\mathbf{e}^k\|_2^2])^{\frac{3}{2}} \\ &\quad +2h^2C_2(\sigma)\sqrt{E[\|\mathbf{e}^k\|_2^2]} + h^2\widehat{\gamma}^*(\sigma) \\ &= \widehat{q}(h)E[\|\mathbf{e}^k\|_2^2] + hf(E[\|\mathbf{e}^k\|_2^2]) + h^2(2C_2(\sigma)\sqrt{E[\|\mathbf{e}^k\|_2^2]} + \widehat{\gamma}^*(\sigma)) \end{aligned} \tag{D.2.15}$$

where the function $f : \Re \longrightarrow \Re$ is defined by

$$f(E[\|\mathbf{e}^k\|_2^2]) = \frac{h}{4}C_1\ell(E[\|\mathbf{e}^k\|_2^2])^2 + \sqrt{C_1\ell}(1-h\eta_{min})(E[\|\mathbf{e}^k\|_2^2])^{\frac{3}{2}}.$$

Clearly, for each k,

$$\lim_{E[\|\mathbf{e}^k\|_2^2]\to 0} \frac{f(E[\|\mathbf{e}^k\|_2^2])}{E[\|\mathbf{e}^k\|_2^2]} = 0$$

Hence, for any $\epsilon > 0$, there exists a $\delta = \delta(\epsilon)$, such that for each k,

$$\frac{f(E[\|\mathbf{e}^k\|_2^2])}{E[\|\mathbf{e}^k\|_2^2]} < \epsilon \quad \text{for} \quad E[\|\mathbf{e}^k\|_2^2] < \delta. \tag{D.2.16}$$

Since $\epsilon > 0$ can be chosen arbitrarily small, it follows from (D.2.16) and (D.2.15) that

$$\begin{aligned} & E[\|\mathbf{e}^{k+1}\|_2^2] < (\widehat{q}(h) + \epsilon h)\, E[\|\mathbf{e}^k\|_2^2] + h^2(2C_2(\sigma)\sqrt{\delta} + \widehat{\gamma}^*(\sigma)). \\ \Longrightarrow \quad & E[\|\mathbf{e}^{k+1}\|_2^2] \leq \widehat{q}(h)E[\|\mathbf{e}^k\|_2^2] + h^2(2C_2(\sigma)\sqrt{\delta} + \widehat{\gamma}^*(\sigma)). \end{aligned} \tag{D.2.17}$$

Clearly, by (D.2.17), we have

$$\begin{aligned} E[\|\mathbf{e}^{k+1}\|_2^2] &\leq (\widehat{q}(h))^{k+1}E[\|\mathbf{e}^0\|_2^2] + \frac{h^2(2C_2(\sigma)\sqrt{\delta} + \widehat{\gamma}^*(\sigma))(1-(\widehat{q}(h))^{k+1})}{1-\widehat{q}(h)} \\ &= (\widehat{q}(h))^{k+1}\left(E[\|\mathbf{e}^0\|_2^2] - \frac{h^2(2C_2(\sigma)\sqrt{\delta} + \widehat{\gamma}^*(\sigma))}{1-\widehat{q}(h)}\right) + \frac{h^2(2C_2(\sigma)\sqrt{\delta} + \widehat{\gamma}^*(\sigma))}{1-\widehat{q}(h)}. \end{aligned}$$

If the initial error point $\mathbf{e}^0$ is such that $E[\|\mathbf{e}^0\|_2^2]$ is in a sufficiently small neighborhood of the origin, and the step-size h is chosen sufficiently small such that

$$\widehat{q}(h) = 1 - 2h\eta_{min} + h^2\|\Theta(\sigma)\|_2 < 1,$$

then it follows that $E[\|\mathbf{e}^{k+1}\|_2^2] < \bar{\delta} < \delta, \forall k$. Thus, the above inequality leads to

$$\overline{\lim_{k\to\infty}} E[\|\mathbf{e}^k\|_2^2] \leq \frac{h(2C_2(\sigma)\sqrt{\delta} + \widehat{\gamma}^*(\sigma))}{2\eta_{min}} = V(h) \tag{D.2.18}$$

where the neighborhood $V(h)$ of the step-size h satisfies $0 < V(h) < \bar{\delta}$ for $0 < h < \frac{2}{\eta_{max}}$, and

$$\lim_{h\to 0} V(h) \;=\; 0.$$

Note that if $\sigma = \sqrt{var(\mathbf{n}_i)} \longrightarrow 0$ where $\mathbf{n}$ is the noise vector, then $V(h) \longrightarrow 0$ for $0 < h < \frac{2}{\eta_{max}}$.

Since $E[\tilde{\mathbf{u}}^k|\tilde{\lambda}^k] - \mathbf{u}^* = -\frac{1}{2}\mathbf{A}'\mathbf{e}^k$, it follows from (D.2.18) that

$$\overline{\lim_{k\to\infty}} E[\|E[\tilde{\mathbf{u}}^k|\tilde{\lambda}^k] - \mathbf{u}^*\|_2^2] \;\leq\; \frac{1}{4}\|\mathbf{A}\|_2^2 V(h).$$

The proof is complete. ∎

D.3 Proof of Theorem 7.3.3

Let $\mathbf{e}^k \stackrel{\Delta}{=} \tilde{\lambda}^k - \lambda^*$ be the *kth* error vector about λ^* and consider the adaptive pulse scheme (D.1.1) with variable step-size h_k. Then, we obtain

$$\mathbf{e}^{k+1} \;=\; \nabla\widetilde{\mathbf{T}}'(\lambda^*)\mathbf{e}^k - \frac{1}{2}h_k\wp'(\lambda^*, \tilde{\lambda}^k)\mathbf{e}^k - h_k\widetilde{\mathbf{F}}(\lambda^*). \tag{D.3.1}$$

where the matrices $\nabla\widetilde{\mathbf{T}}'(\lambda^*)$, $\wp'(\lambda^*, \tilde{\lambda}^k)$ and $\widetilde{\mathbf{F}}(\lambda^*)$ are defined in Appendix D.1.

Denote by

$$\mathcal{F}_k \;=\; \sigma\{\tilde{\lambda}^1, \ldots, \tilde{\lambda}^k\}$$

the smallest σ-algebra generated by the random variables $\tilde{\lambda}^1, \ldots, \tilde{\lambda}^k$.

Taking the square-norm and the conditional expectations with respect to $\mathcal{F}_k$ on both sides of (D.3.1), we obtain

$$\begin{aligned}
& E[\|\mathbf{e}^{k+1}\|_2^2|\mathcal{F}_k] = E[\|\nabla\widetilde{\mathbf{T}}'(\lambda^*)\mathbf{e}^k - \frac{h_k}{2}\wp'(\lambda^*, \tilde{\lambda}^k)\mathbf{e}^k - h_k\widetilde{\mathbf{F}}(\lambda^*)\|_2^2|\mathcal{F}_k] \\
= \;& E[\|\nabla\widetilde{\mathbf{T}}'(\lambda^*)\mathbf{e}^k\|_2^2|\mathcal{F}_k] + \frac{1}{4}h_k^2 E[\|\wp'(\lambda^*, \tilde{\lambda}^k)\mathbf{e}^k\|_2^2|\mathcal{F}_k] + h_k^2 E[\|\widetilde{\mathbf{F}}(\lambda^*)\|_2^2|\mathcal{F}_k] \\
& -h_k E[\mathbf{e}^{k'}\nabla\widetilde{\mathbf{T}}(\lambda^*)\wp'(\lambda^*, \tilde{\lambda}^k)\mathbf{e}^k|\mathcal{F}_k] - 2h_k E[e^{k'}\nabla\widetilde{\mathbf{T}}(\lambda^*)\widetilde{\mathbf{F}}(\lambda^*)|\mathcal{F}_k] \\
& +h_k^2 E[\widetilde{\mathbf{F}}'(\lambda^*)\wp'(\lambda^*, \tilde{\lambda}^k)\mathbf{e}^k|\mathcal{F}_k] \\
\leq \;& E[\|\nabla\widetilde{\mathbf{T}}'(\lambda^*)\mathbf{e}^k\|_2^2|\mathcal{F}_k] + \frac{1}{4}h_k^2 E[\|\wp'(\lambda^*, \tilde{\lambda}^k)\mathbf{e}^k\|_2^2|\mathcal{F}_k] + h_k^2 E[\|\widetilde{\mathbf{F}}(\lambda^*)\|_2^2|\mathcal{F}_k] \\
& +h_k|E[\mathbf{e}^{k'}\nabla\widetilde{\mathbf{T}}(\lambda^*)\wp'(\lambda^*, \tilde{\lambda}^k)\mathbf{e}^k|\mathcal{F}_k]| + 2h_k|E[\mathbf{e}^{k'}\nabla\widetilde{\mathbf{T}}(\lambda^*)\widetilde{\mathbf{F}}(\lambda^*)|\mathcal{F}_k]| \\
& +h_k^2|E[\widetilde{\mathbf{F}}'(\lambda^*)\wp'(\lambda^*, \tilde{\lambda}^k)\mathbf{e}^k|\mathcal{F}_k]|
\end{aligned} \tag{D.3.2}$$

In the sequel, we investigate each term on the right-hand side of (D.3.2).

For the first-term, we obtain

$$\begin{aligned} E[\|\nabla\tilde{\mathbf{T}}'(\lambda^*)\mathbf{e}^k|\mathcal{F}_k\|_2^2] &= \mathbf{e}^{k'}E[\nabla\tilde{\mathbf{T}}(\lambda^*)\nabla\tilde{\mathbf{T}}'(\lambda^*)|\mathcal{F}_k]\mathbf{e}^k \\ &\leq \widehat{q}(h_k)\|\mathbf{e}^k\|_2^2, \end{aligned} \tag{D.3.3}$$

where $\widehat{q}(h_k) = 1 - 2h_k\eta_{min} + h_k^2\Theta(\sigma)$ and $\Theta(\sigma)$ is given in the proof of Theorem 7.3.2.

For the second-term, we note that the matrix $\tilde{\mathbf{P}}_i^k$ is independent of $\tilde{\lambda}^k$ (and hence $\mathbf{e}^k$). Thus,

$$\begin{aligned} E[\|\wp'(\lambda^*,\tilde{\lambda}^k)\mathbf{e}^k|\mathcal{F}_k\|_2^2] &= \sum_{i=1}^{2N} E[|\mathbf{e}^{k'}\tilde{\mathbf{P}}_i^k\mathbf{e}^k|\mathcal{F}_k|^2] \\ &\leq \sum_{i=1}^{2N} E[\|\tilde{\mathbf{P}}_i^k\|_2^2]\|\mathbf{e}^k\|_2^4 = C_1\|\mathbf{e}^k\|_2^4 \end{aligned} \tag{D.3.4}$$

where $C_1 = \sum_{i=1}^{2N} E[\|\tilde{\mathbf{P}}_i^k\|_2^2]$ is a constant term. By (D.2.7), the third term is given by

$$E[\|\tilde{\mathbf{F}}(\lambda^*)\|_2^2] \leq \frac{1}{4}n^2\sigma^2\|\mathbf{D}(\lambda^*)\|_2^2\|\lambda^*\|_2^2(2\|\mathbf{A}\|_2^2 + n^2\sigma^2) = \widehat{\gamma}^*(\sigma) \tag{D.3.5}$$

For the fourth-term, we have

$$|E[\mathbf{e}^{k'}\nabla\tilde{\mathbf{T}}(\lambda^*)\wp'(\lambda^*,\tilde{\lambda}^k)\mathbf{e}^k|\mathcal{F}_k]| \leq \sqrt{C_1}(1 - h_k\eta_{min})\|\mathbf{e}^k\|_2^3. \tag{D.3.6}$$

Similarly, the fifth-term is reduced to

$$\begin{aligned} |E[\mathbf{e}^{k'}\nabla\tilde{\mathbf{T}}(\lambda^*)\tilde{\mathbf{F}}(\lambda^*)|\mathcal{F}_k]| &= |\mathbf{e}^{k'}E[\nabla\tilde{\mathbf{T}}(\lambda^*)\tilde{\mathbf{F}}(\lambda^*)]| \\ &\leq \|\mathbf{e}^k\|_2\|E[\nabla\tilde{\mathbf{T}}(\lambda^*)\tilde{\mathbf{F}}(\lambda^*)]\|_2 \\ &\leq h_kC_2(\sigma)\|\mathbf{e}^k\|_2, \end{aligned} \tag{D.3.7}$$

where the constant term $C_2(\sigma)$ satisfies $0 < C_2(\sigma) \leq \sqrt{\Theta(\sigma)}\sqrt{\widehat{\gamma}^*(\sigma)}$.

For the last term, since $E[\tilde{\mathbf{F}}(\lambda^*)] = 0$ and $\tilde{\mathbf{F}}(\lambda^*)$ is uncorrelated with $\mathbf{e}^k$ (hence, $\wp(\lambda^*,\tilde{\lambda}^k)$), we obtain

$$E[\tilde{\mathbf{F}}'(\lambda^*)\wp'(\lambda^*,\tilde{\lambda}^k)\mathbf{e}^k|\mathcal{F}_k] = E[\tilde{\mathbf{F}}'(\lambda^*)]E[\wp'(\lambda^*,\tilde{\lambda}^k)|\mathcal{F}_k]\mathbf{e}^k = 0. \tag{D.3.8}$$

Combining (D.3.3)- (D.3.8) with (D.3.2) yields

$$\begin{aligned} E[\|\mathbf{e}^{k+1}\|_2^2|\mathcal{F}_k] &\leq \widehat{q}(h_k)\|\mathbf{e}^k\|_2^2 + \frac{1}{4}h_k^2C_1\|\mathbf{e}^k\|_2^4 + h_k\sqrt{C_1}\,(1 - h_k\eta_{min})\,\|\mathbf{e}^k\|_2^3 \\ &\quad +2h_k^2C_2(\sigma)\|\mathbf{e}^k\|_2 + h_k^2\widehat{\gamma}^*(\sigma) \\ &= \widehat{q}(h_k)\|\mathbf{e}^k\|_2^2 + h_kf(\|\mathbf{e}^k\|_2^2) + h_k^2(2C_2(\sigma)\|\mathbf{e}^k\|_2 + \widehat{\gamma}^*(\sigma)) \end{aligned} \tag{D.3.9}$$

where $f(\|\mathbf{e}^k\|_2^2) \triangleq \frac{1}{4}h_kC_1\|\mathbf{e}^k\|_2^4 + \sqrt{C_1}\,(1 - h_k\eta_{min})\,\|\mathbf{e}^k\|_2^3$.

Clearly, for each k,

$$\lim_{\|\mathbf{e}^k\|_2^2 \to 0} \frac{f(\|\mathbf{e}^k\|^2)}{\|\mathbf{e}^k\|_2^2} = 0$$

Hence, for any $\epsilon > 0$, there exists a $\delta = \delta(\epsilon)$ such that, for each k,

$$\frac{f(\|\mathbf{e}^k\|_2^2)}{\|\mathbf{e}^k\|_2^2} < \epsilon \quad \text{for} \quad \|\mathbf{e}^k\|_2^2 < \delta. \tag{D.3.10}$$

Since $\epsilon > 0$ can be chosen arbitrarily small, it follows from (D.3.10) and (D.3.9) that

$$\begin{aligned} & E[\|\mathbf{e}^{k+1}\|_2^2|\mathcal{F}_k] < (\widehat{q}(h) + \epsilon h_k)\,\|\mathbf{e}^k\|_2^2 h_k^2 (2C_2(\sigma)\sqrt{\delta} + \widehat{\gamma}^*(\sigma)) \\ \Longrightarrow \quad & E[\|\mathbf{e}^{k+1}\|_2^2|\mathcal{F}_k] \le \widehat{q}(h_k) E[\|\mathbf{e}^k\|_2^2|\mathcal{F}_k] + h_k^2 C(\sigma,\delta) \end{aligned} \tag{D.3.11}$$

where $C(\sigma,\delta) = \left(2C_2(\sigma)\sqrt{\delta} + \widehat{\gamma}^*(\sigma)\right)$ is a constant term. Accordingly, it follows from (D.3.11) that

$$E[\|\mathbf{e}^{k+1}\|_2^2|\mathcal{F}_k] \le \|\mathbf{e}^0\|_2^2 \prod_{i=0}^{k} \widehat{q}(h_i) + \sum_{i=0}^{k} h_i^2 C(\sigma,\delta) \prod_{j=i+1}^{k} \widehat{q}(h_j). \tag{D.3.12}$$

(a) Mean Square Convergence

Define a real number sequence which is generated as follows:

$$z^{k+1} \triangleq \|\mathbf{e}^{k+1}\|_2^2 \prod_{i=k+1}^{\infty} \widehat{q}(h_i) + \sum_{i=k+1}^{\infty} h_i^2 C(\sigma,\delta) \prod_{j=i+1}^{\infty} \widehat{q}(h_j).$$

Taking the conditional expectations of z^{k+1} with respect to $\mathcal{F}_k$, it follows from (D.3.11) that

$$\begin{aligned} E[z^{k+1}|\mathcal{F}_k] &= E[\|\mathbf{e}^{k+1}\|_2^2|\mathcal{F}_k] \prod_{i=k+1}^{\infty} \widehat{q}(h_i) + \sum_{i=k+1}^{\infty} h_i^2 C(\sigma,\delta) \prod_{j=i+1}^{\infty} \widehat{q}(h_j) \\ &\le \left\{\widehat{q}(h_k)\|\mathbf{e}^k\|_2^2 + h_k^2 C(\sigma,\delta)\right\} \prod_{i=k+1}^{\infty} \widehat{q}(h_i) + \sum_{i=k+1}^{\infty} h_i^2 C(\sigma,\delta) \prod_{j=i+1}^{\infty} \widehat{q}(h_j) \\ &= \|\mathbf{e}^k\|_2^2 \prod_{i=k}^{\infty} \widehat{q}(h_i) + \sum_{i=k}^{\infty} h_i^2 C(\sigma,\delta) \prod_{j=i+1}^{\infty} \widehat{q}(h_j) \\ &= z^k. \end{aligned} \tag{D.3.13}$$

Let $\Gamma_k = \sigma\{z^1,\ldots,z^k\}$ denote the smallest σ-algebra generated by the random variables $z^1,\ldots,z^k$. By the definition of z^k, we note that $z^j, j = 1,\ldots,k$, are $\mathcal{F}_k$-measurable. Thus, it implies that $\Gamma_k \subset \mathcal{F}_k$. Taking conditional expectations of (D.3.13) with respect to Γ_k and following from the commutative property of conditional expectations, we have

$$\begin{aligned} E[z^{k+1}|\Gamma_k] &= E[E[z^{k+1}|\Gamma_k]|\mathcal{F}_k] = E[E[z^{k+1}|\mathcal{F}_k]|\Gamma_k] \\ &\le E[z^k|\Gamma_k] = z^k. \\ \Longrightarrow \quad E[z^{k+1}|\Gamma_k] &\le z^k. \end{aligned}$$

Thus, the stochastic process $\{z^k, k \geq 1\}$ is a super-Martingale relative to the nonincreasing family of the σ-algebra generated by $z^1, \ldots, z^k$ and

$$\ldots \leq E[z^{k+1}] \leq E[z^k] \leq \ldots E[z^1] < \infty$$

By the super-Martingale convergence theorems [8, 50], it follows that, for the stochastic process $\{z^k\}_{k=1}^{\infty}$, $\lim_{k\to\infty} z^k$ exists with probability 1 and is finite. Making use of the assumption: $\sum_{k=0}^{\infty} h_k^2 < \infty$ and the definition of z^k, the product and sum-product terms are convergent. Thus, it follows that $\lim_{k\to\infty} \|\mathbf{e}^k\|_2^2$ exists w.p.1, and $E[\|\mathbf{e}^k\|_2^2]$ is uniformly bounded. We note that the sequence of step-sizes $\{h_k\}_{k=0}^{\infty}$ which satisfies $h_k > 0$, $\sum_{k=0}^{\infty} h_k = \infty$, and $\sum_{k=0}^{\infty} h_k^2 < \infty$, ensures $h_k \to 0$ as $k \to \infty$. Therefore, for every sufficiently small $h_k, k = 0, 1, \ldots$, such that $0 < \widehat{q}(h_k) = 1 - 2h_k\eta_{min} + h_k^2\|\Theta(\sigma)\|_2 < 1$, we have

$$\prod_{k=0}^{\infty} \widehat{q}(h_k) = 0 \quad \text{and} \quad \lim_{k\to\infty} \widehat{q}(h_k) = 1. \tag{D.3.14}$$

Taking the expectations of (D.3.12) and letting $k \to \infty$, it follows from (D.3.14) that

$$\lim_{k\to\infty} E[\|\mathbf{e}^k\|_2^2] \leq E[\|\mathbf{e}^0\|_2^2] \prod_{i=0}^{\infty} \widehat{q}(h_i) + \sum_{i=0}^{\infty} h_i^2 C(\sigma, \delta) \prod_{j=i+1}^{\infty} \widehat{q}(h_j) = 0.$$

Therefore, we obtain the convergence in the mean square (ms) sense, i.e,

$$\lim_{k\to\infty} E[\|\mathbf{e}^k\|_2^2] = 0. \tag{D.3.15}$$

Since

$$E[\tilde{\mathbf{u}}^k|\tilde{\lambda}^k] - \mathbf{u}^* = -\frac{1}{2}\mathbf{A}'\mathbf{e}^k, \tag{D.3.16}$$

it follows that by taking the square norms and expectations on (D.3.16), we obtain the convergence in the mean square sense to the optimal filter $\mathbf{u}^*$, i.e,

$$\lim_{k\to\infty} E[\|E[\tilde{\mathbf{u}}^k|\tilde{\lambda}^k] - \mathbf{u}^*\|_2^2] = 0.$$

(b) With Probability 1

From part (a) of the theorem, we note that the sequence $\left\{\|\mathbf{e}^k\|_2^2\right\}_{k=0}^{\infty}$ is convergent, i.e, $\lim_{k\to\infty} \|\mathbf{e}^k\|_2^2$ exists w.p.1. By Fatous's lemma [48] and (D.3.15), we obtain

$$E\left[\lim_{k\to\infty} \|\mathbf{e}^k\|_2^2\right] \leq \underline{\lim_{k\to\infty}} E[\|\mathbf{e}^k\|_2^2] = \lim_{k\to\infty} E[\|\mathbf{e}^k\|_2^2] = 0.$$

Clearly,

$$E\left[\lim_{k\to\infty} \|\mathbf{e}^k\|_2^2\right] = 0 \Longleftrightarrow \lim_{k\to\infty} \|\mathbf{e}^k\|_2^2 = 0, \quad (w.p.1).$$

Thus,

$$Prob\left\{\lim_{k\to\infty}\|\tilde{\lambda}^k-\lambda^*\|_2=0\right\}=1.$$

Making use of (D.3.16), we obtain the convergence with probability one to the optimal filter, i.e,

$$Prob\left\{\lim_{k\to\infty}\|E[\tilde{\mathbf{u}}^k|\tilde{\lambda}^k]-\mathbf{u}^*\|_2=0\right\} \;=\; 1.$$

This completes the proof. ∎

Bibliography

[1] K. M. Ahmed and R. J. Evans, "An adaptive array processor with robustness and broadband capabilities", *IEEE Trans. Antennas Propagat.*, Vol. AP-32, pp. 944-950, 1984.

[2] M. Aoki, Introduction to Optimization Techniques: Fundamentals and Applications of Nonlinear Programming, Macmillan, New York, 1971.

[3] E. J. Anderson and P. Nash, Linear Programming in Infinite-dimensional Spaces, Theory and Applications, Wiley & Sons, New York, 1987.

[4] A. Cantoni, "Envelope-constrained filters: a practical application of optimization theory and algorithms", *International Conference on Optimization Techniques and Applications* (ICOTA), Vol. 1, pp. 35-52, 1998.

[5] CCITT, "Physical/Electrical characteristics of hierarchical digital interfaces", G.703, Fascicle III, 1984.

[6] G. J. Clowes, Choice of the time-scaling factor for linear system approximations using orthonormal Laguerre functions", *I*EEE Trans. Automatic Control, Vol. 10, pp. 487-489, 1965.

[7] E-K. P. Chong and S.H.Żak, An Introduction to Optimization, Wiley & Sons, New York, 1995.

[8] J. Doob, Stochastic Processes, New York: Wiley, 1953.

[9] P. S. Diniz, Adaptive Filtering: Algorithms and Practical Implementation, Kluwer Academic Publishers, London, 1997.

[10] H. H. Dam, K. L. Teo, Y. Liu, and S. Nordebo, "Optimum pole position for digital Laguerre network with least square error criterion", to appeared in *Optimization Methods and Applications Kluwer Academic.*

[11] R. J. Evans, A. Cantoni, and K. M. Ahmed, "Envelope-constrained filter with uncertain input," *Circuits, Syst. Signal Processing*, Vol. 2, pp. 131-154, 1983.

[12] R. J. Evans, A. Cantoni, and T. E. Fortmann, "Envelope-constrained filter, part I, theory and applications; part II, adaptive structures," *IEEE* Trans. Inform., Theory, Vol. IT-23, pp.421-444, 1977.

[13] R. J. Evans, Optimal Signal Processing with Constraints, PhD thesis, The University of Newcastle, 1975.

[14] Yu. G. Evtushenko, Numerical Optimization Techniques, Optimization Software, Inc. Publications Division, New York, 1985.

[15] Yu. G. Evtushenko and V. G. Zhadan, "Stable barrier-projection and barrier-Newton methods in nonlinear programming", Optimization Methods and Software, Vol. 3, pp.237-256, 1994.

[16] Yu. G. Evtushenko and V. G. Zhadan, "Stable barrier-projection and barrier-Newton methods for linear and nonlinear programming", Advanced Study Institute on Algorithms for Continuous Optimization: The State of the Art, pp. 255-285, 1994, Netherland.

[17] T. E. Fortmann, "Optimal design of filters and signals subject to sidelobe constraints", Electronic Systems Laboratory Rreport, No. ESL-R-400, Massachusetts Institute of Technology, September 1969.

[18] T. E. Fortmann, M. Athans, "Optimal filter design subject to output sidelobe constraints: theoretical considerations", Journal of Optimization Theory and Applications, Vol. 14, No.2, pp.179-197, 1974.

[19] T. E. Fortmann, R. J. Evans, "Optimal filter design subject to output sidelobe constraints: computational algorithm and numerical results", Journal of Optimization Theory and Applications, Vol. 14, pp.271-290, 1974.

[20] A. Fiacco and G. McCormic, Nonlinear programming: Sequential unconstrained minimization techniques, Wiley & Sons, New York, 1968.

[21] L. B. Fertig, and J. H. McClellan, "Dual forms for constrained adaptive filtering", *IEEE Trans. Signal Processing*, Vol. 42, No. 1, pp. 11-23, 1994.

[22] R. Fletcher, Practical Methods of Optimization, Second Edition, Wiley & Sons, New York, 1987.

[23] A. A. Goldstein, Constructive Real Analysis, New York: Harper-Row, 1967.

[24] A. Gersho, "Adaptive equalization of highly dispersive channels for data transmission", Bell System Tech. J., Vol. 48, pp. 55-70, 1969.

[25] M. A. Goberna, and M. A. López, Linear Semi-infinite Optimization, Wiley & Sons, New York, 1998.

[26] L. J. Griffiths, "Rapid measurement of digital instantaneous frequency", *IEEE Acoustics, Speech, Signal Processing*, Vol. ASSP-23, pp. 207-222, 1975.

[27] A. Grace, Optimization Toolbox for Use with MATLAB, The MathWorks, Inc., South Natick, MA, 1993.

[28] G. J. Goh and K. L. Teo, "Alternative algorithms for solving nonlinear function and functional inequalities", Applied Mathematics and Computation, Vol. 41, pp. 159-177, 1991.

[29] S. Haykin, Adaptive Filter Theory, Englewood Cliffs, NJ: Prentice-Hall, 1991.

[30] S. Ito, Y. Liu, K. L. Teo, "A dual parametrization method for convex semi-infinite programming", (ICOTA), Vol. 1, pp. 550-557, 1998.

[31] F. John, Extremum Problems with Inequalities as Subsidiary Conditions, in K. O. Friedrichs, O. E. Neugebauer, and J. J. Stoker, editors, Studies and Essays, Courant Anniversary Volume, Wiley & Sons, New York, 1948.

[32] L. S. Jennings and K. L. Teo, "A computational algorithm for functional inequality constrained optimization problem", Automatica, Vol. 26, No. 2, pp. 371-375, 1990.

[33] W. H. Kautz, "Transient synthesis in the time domain", *IRE Trans. Circuit Theory*, Vol. 1, No. 3, pp. 29-38, 1954.

[34] D. G. Luenberger, Optimization by Vector Space Method, Wiley & Sons, New York, 1969.

[35] J. W. Lechleider, "A new interpolation theorem with application to pulse transmission", *IEEE Transactions on Communication*, Vol. COM-39, pp.1438-1444, 1991.

[36] R. Lucky, J. Salz and E. J. Weldon, Principles of Data Communications, New York: McGraw-Hill, 1968.

[37] Y. W. Lee, Statistical Theory of Communication, New York, Wiley & Sons, 1960.

[38] G. P. McCormick, Nonlinear Programming : Theory, Algorithms, and Applications, Wiley & Sons, New York, 1983.

[39] R. J. McAulay and J. R. Johnson, "Optimal mismatched filter design for radra ranging detection and resolution", *IEEE Trans. Inform. Theory*, Vol. IT-17, pp. 696-701, 1971.

[40] P. M. Mäkilä, "Laguerre series approximation of infinite dimensional systems", *Automatica*, Vol. 26, pp. 885-995, 1990.

[41] R. J. McAulay "Numerical optimization techniques applied to PPM signal design", *IEEE Trans. Information Theory*, Vol. IT-14, No. 5, pp. 708-716, 1968.

[42] R. A. Nobakt, and M. R. Civanlar, "Optimal pulse shape design for digital communication systems by projections onto convex sets", *IEEE Trans. Comm.*, Vol. 43, pp. 2874-2877, 1995.

[43] T. Oliverira e Silva, "Optimality conditions for truncated Laguerre networks", *I*EEE Trans. Signal Processing, Vol. 42, pp. 2528-2530, 1994.

[44] D. A. Pierre, Optimization Theory with Applications, Wiley & Sons, New York, 1969.

[45] J. E. Perkins, U. Helmke, and J. B. Moore, "Balanced realizations via gradient flow techniques", Systems & Control Letters, Vol. 14, pp. 369-380, 1990.

[46] J. Proakis, "Advances in equalization for intersymbol interference", in Advances in Communication Systems, Vol.4, (Eds. A.V.Balakrishnan and A.J.Viterbi). New York: Academic Press, pp.124-194, 1975.

[47] A. Ralston, A First Course in Numerical Analysis, New York: McGraw-Hill, 1965.

[48] H. L. Royden, Real Analysis, Second Edition, New York: The Macmillan Co., 1968.

[49] M. Slater, "Lagrange multipliers revisited", Cowels Commission Discussion Paper, Math. 403 November 1950.

[50] S. M. Ross, Stochastic Processes, New York: John Wiley & Sons, 1982.

[51] R. T. Rockafellar, Convex Analysis, Princeton, New Jersey, 1970.

[52] G. Szegö, "Orthogonal polynomials", *Amer. Math. Soc. Coll. Publ.*, Vol. 23, 1939.

[53] T. Oliverira e Silva, "Optimality conditions for truncated Laguerre networks", *IEEE Trans. Signal Processing*, Vol. 42, pp. 2528-2530, 1994.

[54] T. Oliverira e Silva, "On the determination of the optimal pole position of Laguerre filters", *IEEE Trans. Signal Processing*, Vol. 43, pp. 2079-2087, 1995.

[55] K. L. Teo, A. Cantoni, and X. G. Lin, "A new Approach to the optimization of envelope-constrained filters with uncertain input", *IEEE Trans. Signal Processing*, Vol. 42, No. 2, 1994.

[56] K. L. Teo, G. J. Goh and K. H. Wong, A Unified Computational Approach to Optimal Control Problems, Longman Scientific and Technical, 1991.

[57] C. H. Tseng, K. L. Teo, A. Cantoni, and Z. Zang, "Iterative methods for optimal envelope-constrained filters design problem", *International Conference on Optimization Techniques and Applications* (ICOTA), Vol. 1, pp. 534-541, 1998.

[58] C. H. Tseng, K. L. Teo, A. Cantoni, and Z. Zang, "Robust envelope-constrained filter design with Laguerre bases", *IEEE International Conference on Acoustics, Speech, and Signal Processing* (ICASSP), Vol. 3, pp. 1153-1156, Phoenix, Arizona, USA, March 1999.

[59] C. H. Tseng, K. L. Teo, A. Cantoni, and Z. Zang, "A dual approach to continuous-time envelope-constrained filter design via orthonormal filters", *IEEE Trans. Circuits and Systems-I: Fundamental Theory and Applications*, Vol. 46, No. 9, pp. 1042-1054, 1999.

[60] C. H. Tseng, K. L. Teo, A. Cantoni, and Z. Zang, "Envelope-constrained filters: adaptive algorithms", *IEEE Trans. Signal Processing*, Vol. 48, No. 6, pp. 1597-1608, 2000.

[61] C. H. Tseng, K. L. Teo, and A. Cantoni, "Gradient flow approach to discrete-time envelope-constrained filter design via orthonormal filters", *IEE Proceedings-Vision, Image and Signal Processing*, to be published.

[62] C. H. Tseng, K. L. Teo, A. Cantoni, and Z. Zang, "Design of Robust envelope-constrained filter with orthonormal bases", *IEEE Trans. Signal Processing*, to be published.

[63] C. H. Tseng, K. L. Teo, and A. Cantoni, "Adaptive envelope-constrained filter design", *IEEE International Symposium on Circuits and Systems* (ISCAS), Vol. 4, pp. IV85-IV88, Geneva, Switzerland, May 2000.

[64] C. H. Tseng, K. L. Teo, and A. Cantoni, "Mean square convergence of adaptive envelope-constrained filtering", submitted to *IEEE Trans. Signal Processing*.

[65] B. Vo, A. Cantoni and K. L. Teo, "A penalty approach to iterative algorithms for envelope constrained filter design", *IEEE Trans. Signal Processing*, Vol. 45, No. 7, pp. 1869-1872, 1997.

[66] B. Vo, Z. Zang, A. Cantoni and K. L. Teo, "Continuous-time envelope-constrained filter design via orthonormal filters", *IEE Proc.-Vis. Image Signal Process.*, Vol. 142, No. 6, pp. 389-394, 1995.

[67] B. Wahlberg, "System identification using Laguerre models", *IEEE Trans. Automatic Control*, Vol. 36, No. 5, 1991.

[68] B. Widrow, P. Mantey, L. J. Griffiths, and B. B. Goode, "Adaptive antenna systems", *Proc. IEEE*, Vol. 55, No. 12, pp. 2143-2159, 1967.

[69] B. Widrow and S. D. Stearns, Adaptive Signal Processing, Englewood Cliffs, NJ: Prentice-Hall, 1985.

[70] L. C. Wood and S. Treitel, "Seismic signal processing", *Proc. IEEE* (Special Issue on Digital Signal Processing), Vol. 63, pp. 649-661, 1975.

[71] T. Yoshizawa, "The Stability Theory by Lyapunov's Second Method", Math. Soc. Japan, Tokyo, 1966.

[72] W. X. Zheng, A. Cantoni and K. L. Teo, "The sensitivity of envelope-constrained filters with uncertain input", *IEEE Trans. Circuits and Systems-I: Fundamental Theory and Applications*, Vol. 42, No. 9, 1995.

[73] W. X. Zheng, A. Cantoni and K. L. Teo, "Robust design of envelope-constrained filters in the presence of input uncertainty", *IEEE Trans. Signal Processing.* Vol. 44, No. 8, 1996.

[74] Z. Zang, A. Cantoni, B. Vo, and K. L. Teo, "Continuous-time envelope-constrained filter design: Constraint robustness maximization", 4th *IMA conference on Mathematics in Signal Processing*, Warwick UK, 1996.

[75] W. X. Zheng, B. Vo, A. Cantoni, K. L. Teo, "Recursive procedure for constrained optimization problems and its application in signal processing", *IEE Proceedings Vision, Image and Signal Processing*, Vol. 142, No. 3, pp. 161-168, 1995.

[76] Z. Zang, B. Vo, A. Cantoni, K. L. Teo, "Application of discrete-Time Laguerre networks to envelope-constrained filter design", *Proc. IEEE Int. Conf. Acoustics, Speech and Signal Processing*, Atlanta Georgia, Vol. 3, pp. 1363-1366, 1996.

[77] W. X. Zheng, "Application of simplified line searches in the design of adaptive envelope-constrained filters", *IEEE Trans. Circuits and Systems-I: Fundamental Theory and Applications*, Vol. 43, No. 10, pp. 854-857, 1996.